PRECLINICAL STUDIES: TREATMENT OF MULTIPLE SCLEROSIS AND RETINAL DEGENERATIVE DISEASE USING STEM CELLS

by

CHRISTINA FRANCES CORMIER

A dissertation submitted in partial fulfillment of the
requirements for the degree of

DOCTOR OF PHILOSOPHY IN BIOLOGICAL AND BIOMEDICAL SCIENCES

2021

Oakland University
Rochester, Michigan

Doctoral Advisory Committee:

G. Rasul Chaudhry, Ph.D., Chair
Chhabi Govind, Ph.D.
David Svinarich, Ph.D.
Mick Perez-Cruet, M.D.

Dedicated to my mother, father, brother, and husband for all their love and support.

ACKNOWLEDGMENTS

I would like to thank my mentor, Dr. Rasul Chaudhry, for giving me the opportunity to work in his lab and providing encouragement throughout my graduate studies. During my time in his lab, he has exposed me to a variety of opportunities and research projects, which has allowed me to develop a wide range of skills and build a strong foundation for future job opportunities. I would also like to thank the rest of my dissertation committee, Dr. Chhabi Govind, Dr. David Svinarich, and Dr. Mick Perez-Cruet, for their great support and helpful advice. I am grateful for funding support from OU-WB Institute for Stem Cell and Regenerative Medicine and the graduate assistantship from the Department of Biological Sciences, and the Provost's graduate research award. I would be thoughtless if I did not thank my lab mates, especially Christina, Shreeya, Naimisha, Keegan, Matteo, Michael, and Albi, who have helped me complete my work throughout my time at Oakland University. It would have been much harder to go through this process without them. Most importantly, I would like to thank my friends, family, and husband for their love and support throughout this journey. I would like to thank my late Father for encouraging and inspiring me to always strive further in my studies. To my mother and brother for being supportive and loving during my time at Oakland. Lastly, my deepest appreciation to my husband for being patient, understanding and for his unconditional support. Thank you.

Christina Cormier

ABSTRACT

PRECLINICAL STUDIES: TREATMENT OF MULTIPLE SCLEROSIS AND RETINAL DEGENERATIVE DISEASE USING STEM CELLS

by

CHRISTINA FRANCES CORMIER

Adviser: G. Rasul Chaudhry, Ph.D.

Pluripotent stem cells (PSCs) isolated from an embryo or generated by ectopic expression of transcription factors can self-renew indefinitely and differentiate into all cell types found in the body. PSCs have the highest potential for cell therapies, but they face ethical concerns as well as technical and safety challenges, including teratoma formation. In contrast, mesenchymal stem cells (MSCs) isolated from adult and perinatal sources do not pose ethical and moral dilemmas. While MSCs isolated from adult sources, such as bone marrow, require invasive procedures, their use may also cause graft verse host disease. Therefore, we have focused on MSCs isolated from perinatal sources such as the umbilical cord (UC). These cells have advantages over adult MSCs in that they are highly proliferative, do not display HLA-DR markers, and thus are not likely to be immunogenic. We tested the therapeutic efficacy of UC-derived MSCs and their derivatives in preclinical studies to treat multiple sclerosis (MS) and retinal degenerative disease (RDD). The specific aims were to 1. production of MSCs for preclinical studies; 2. treatment of MS using MSCs and NSCs; and 3. treatment of RDD using MSCs and RPC. Our results showed that MSC-derived neural stem cells (NSCs) countered the

inflammatory response, provided neural protection, and induced neurogenesis in the experimental autoimmune encephalomyelitis (EAE) mouse model of MS. Likewise, MSC-derived retinal progenitor cells (RPCs) survived, integrated, and migrated into various neural layers of the retina in the rd12 mouse model of retinitis pigmentosa (RP). RPCs promoted retinal structure, function, neural protection, and regeneration of the retina resulting in vision improvement. These highly promising findings are likely to facilitate clinical studies for treating MS and RDD.

TABLE OF CONTENTS

TABLE OF CONTENTS—Continued

TABLE OF CONTENTS—Continued

TABLE OF CONTENTS—Continued

TABLE OF CONTENTS—Continued

LIST OF TABLES

LIST OF FIGURES

LIST OF ABBREVIATIONS

3-D	Three-dimensional
ABL1	Abelson murine leukemia viral oncogene homolog 1
AD	Alzheimer's disease
AF	Amniotic fluid
ALS	Amyotrophic lateral sclerosis
AMD	Age-related macular degeneration
AT	Adipose tissue
BBB	Blood-brain barrier
bFGF	Basic fibroblast growth factor
BM	Bone marrow
CCL2	C-C motif chemokine 2
CD	Cluster of differentiation
CEBPβ	CCAAT/enhancer-binding protein beta
CH	Chorion
CL	Cord lining
CNS	Central nervous system
COL1	Collagen type 1
COL2	Collagen type 2
cpd	Cycles per degree
CPJ	Cord-placenta junction
DDD	Degenerative disc disease

DDX43	DEAD-box helicase 43
DEGs	Differentially expressed genes
DIC	Differential interface contrast
EAE	Experimental autoimmune encephalitis
EGF	Epidermal growth factor
ERG	Electroretinogram
ESCs	Embryonic stem cells
FABP4	Fatty acid- binding protein 4
FAS	Fas cell surface death receptor
FBS	Fetal bovine serum
FDA	Food and Drug Administration
FDR	False discovery rate
FGF2	Fibroblast growth factor 2
FT	Fetal tissue
GM-CSF	Granulocyte-macrophage colony-stimulating factor
GMP	Good manufacturing practices
GO	Gene ontology
GvHD	Graft-vs-host disease
h	Human
H&E	Hematoxylin and eosin
Hif1α	Hypoxia-inducible factor 1α

HOXA6	Homeobox A6
HOXD10	Homeobox D10
HP	High passage
HSCs	Hematopoietic stem cells
i.p.	Intraperitoneally
IACUC	Institutional Animal Care and Use Committee
IBC	Institutional Biosafety Committee
IFNγ	Interferon gamma
IGF1	Insulin growth factor 1
IGV	Integrative Genomics Viewer
IL-13	Interleukin 13
IL-6	Interleukin 6
INL	Inner nuclear layer
iPSC	Induced pluripotent stem cell
ISCT	International Society for Cellular Therapy
IVD	Intervertebral disc
KLF4	Kruppel like factor 4
LFB	Luxol fast blue
LP	Low passage
M1	Medium composition one
M2	Medium composition two

MHC	Major histocompatibility complex
MOG	Myelin oligodendrocyte glycoprotein
MS	Multiple sclerosis
MSCs	Mesenchymal stem cells
MT	Muscle tissue
NFKBIA	NF-kappa-B inhibitor alpha
NG2	Neuron glia antigen-2
NP	Nucleus pulpous
NPCs	Nucleus pulpous-like cells
NSCs	Neural stem cells
OCN	Osteocalcin
OCT4	Octamer-binding transcription factor 4
ODCs	Oligodendrocytes cells
OKR	Optokinetic reflex
ONL	Outer nuclear layer
OPN	Osteopontin
PB	Peripheral blood
PBS	Phosphate-buffered saline
PC	Placenta
PD	Parkinson’s disease
PPARγ	Peroxisome proliferator-activated receptors

PSC	Pluripotent stem cells
qRT-PCR	Quantitative reverse transcriptase-polymerase chain reaction
RCS	Royal College of Surgeons
RDD	Retinal degenerative disease
RGCs	Retinal ganglion cells
RP	Retinitis pigmentosa
RPCs	Retinal progenitor cells
RPE	Retinal pigment epithelium
RPKM	Reads per kilobase per million
SCID	Severe combined immunodeficiency
SEM	Standard error of the mean
SOX9	Sex determining region Y-box 9
TBST	TBS 1X containing 0.1% Tween-20
TGFβ1	Transforming growth factor-beta 1
TNFAIP6	TNF alpha-induced protein 6
TNFSF10	TNF superfamily member 10
UC	Umbilical cord tissue
UCB	Cord blood
WJ	Wharton's jelly

CHAPTER ONE

INTRODUCTION

The results for this section are from the published data available at (Brown et al., 2019)

1.1 Stem cells

The discovery of pluripotent embryonic stem cells (ESCs) (Martin, 1981) that can self-renew indefinitely and differentiate towards the ectoderm, mesoderm, and endoderm germ layers (Amit & Itskovitz-Eldor, 2002; Carpenter et al., 2003; Hoffman & Carpenter, 2005), were found to have ethical and technical concerns as well as the potential for teratoma formation *in vivo* (Goldring et al., 2011). This led researchers to search for alternative multipotent stem cells from adult sources. Multipotent human adult stem cells such as hematopoietic stem cells (HSCs) and mesenchymal stem cells (MSCs) are less likely to pose moral, ethical, or safety dilemmas as compared to ESCs (Lo & Parham, 2009; Prockop et al., 2010; Ren, G. et al., 2012). HSCs can differentiate into all blood, and immune lineages and have been used to treat leukemia and other blood disorders (Helg et al., 1998). Despite the isolation of MSCs from a wide range of adult sources as well as reports of differentiation of these cells into various lineages such as adipogenic, chondrogenic, osteogenic, and neurogenic cells (Hemmingsen et al., 2013; Moghadam et al., 2014; Tropel et al., 2006; Wang, J. et al., 2009), therapeutic use of MSCs has been hampered due to several reasons. First, isolation of MSCs from adult sources involves invasive and often painful procedures with possible donor site morbidity (Hass et al., 2011). Second, adult MSCs have variable proliferation and differentiation capabilities, which are further reduced upon passaging *in vitro* (Russell et al., 2018). Third, the self-renewal and differentiation potential of MSCs is severely affected by donor age, genetics,

and exposure to environmental stress (D'Ippolito et al., 1999; Malgieri et al., 2010; Mattiucci, D. et al., 2018). This led our lab to search for alternative sources for the isolation of MSCs.

1.2 Mesenchymal stem cells

Our lab attempted to search for alternative sources, which led to the isolation of MSCs from perinatal sources such as umbilical cord blood (UCB), umbilical cord (UC), and placenta (PC) (Beeravolu et al., 2016; Beeravolu et al., 2017; Maurice et al., 2006; Miao et al., 2006) as well as fetal sources such as fetal tissue (FT) and amniotic fluid (AF) (Gucciardo et al., 2009; Wouters et al., 2007), which are considered to be more desirable than adult sources. The cells derived from these tissues were found to also differentiate towards adipogenic, chondrogenic, osteogenic, and neurogenic cell lineages (Figure 1). However, similar to the adult sources, MSCs derived from perinatal and fetal sources also display variation in the self-renewal and differentiation potential. Recently, we have isolated cells from the human UC and PC (Beeravolu et al., 2016; Beeravolu et al., 2017). Irrespective of the niche, the isolated cells were all identified as MSCs following criteria established by the Mesenchymal and Tissue Stem Cell Committee of the International Society for Cellular Therapy (ISCT) (Dominici et al., 2006; Robey, 2017). They were adherent, exhibited fibroblastoid morphology, expressed MSC-specific cluster of differentiation (CD) markers, CD73, CD90, and CD105, and lacked CD14, CD19, CD34, and CD45. They also differentiated towards the adipogenic, chondrogenic, and osteogenic lineages *in vitro* (Beeravolu et al., 2016; Beeravolu et al., 2017). One of the niches, cord-placenta junction (CPJ), harbored highly proliferative MSCs, suggesting that they are more primitive than MSCs reported from other sources

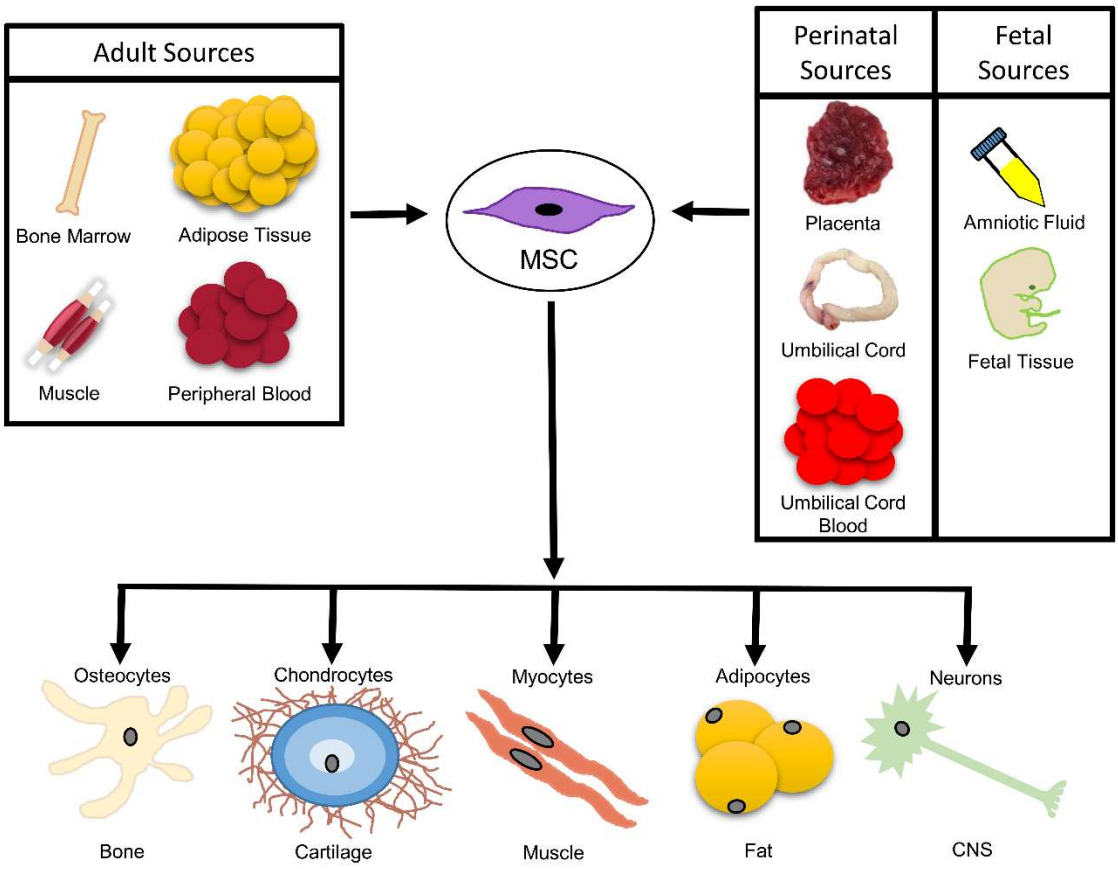

Figure 1: Sources of MSCs and their potential of differentiation into various lineages

(Beeravolu et al., 2016; Beeravolu et al., 2017). In addition, MSCs have a paracrine effect that promotes immunomodulation as well as anti-apoptotic and anti-oxidative effects, which can help treat neuromuscular pains (van Buul et al., 2014) and many other diseases (de Witte et al., 2018; Francois et al., 2013; Khubutiya et al., 2014). MSCs are also being investigated for their therapeutic potential to treat degenerative diseases and disorders such as Parkinson's disease (PD) (Jamali et al., 2018; Kim, H. W. et al., 2018), Alzheimer's disease (AD) (Cui et al., 2017; Han et al., 2018), amyotrophic lateral sclerosis (ALS) (Bonafede & Mariotti, 2017), multiple sclerosis (MS) (Harris et al., 2018; Nasri et al., 2018), degenerative disc disease (DDD) (Ahn et al., 2015; Beeravolu et al., 2018; Perez-Cruet et al., 2018), RDD (Wang, Y. et al., 2018; Zhang, M. et al., 2017), myocardial infarction (Chen, X. Q. et al., 2014), and type 1 diabetes mellitus (Evangelista et al., 2018). It has also been shown that the use of chemokines and cytokines derived from MSCs improved the treatment efficacy for autoimmune disease (Wang, M. et al., 2018; Xu, 2018; Zhang, W. et al., 2018). The interaction between MSCs and the inflammatory niche can be used to treat many different diseases (Harris et al., 2018; Xu, 2018; Zhang, H. et al., 2018).

Even with the typical morphological characteristics and expression of cell surface markers, differences in the proliferation and differentiation capacity of isolated cells have led to the questioning of the rationale for naming them as MSCs. In fact, several names have been coined and interchangeably used with MSCs, such as osteogenic stem cells (Friedenstein et al., 1970; Friedenstein et al., 1968), skeletal stem/progenitor cells (Bianco & Robey, 2000), mesodermal stem cells (Caplan, Arnold I., 2017), mesenchymal progenitor cells (Dennis, J. E. & Caplan, 2004), mesenchymal stromal cells (Caplan,

Arnold I., 2017; Horwitz et al., 2005; Owen, 1988), medicinal signaling cells (Bianco & Robey, 2000; Caplan, A. I., 2010; Caplan, Arnold I., 2017), multipotent stromal cells (Caplan, Arnold I., 2017; Skoloudik et al., 2016), and pericytes mesenchymal stem cells (Caplan, Arnold I., 2017; Kumar et al., 2017). These names are often used for convenience or as a more descriptive term for the type of activities being investigated. Cells isolated from various sources display a difference in their potential to proliferate and differentiate *in vitro* and *in vivo,* as shown in Table 1 (Caplan, A. I., 2010). Therefore, even though MSCs have been used in over 1300 clinical trials, comparing results is often impossible.

1.3 Adult MSCs

Bone marrow (BM) MSCs were first discovered in 1976 by Friedenstein and his colleagues (Friedenstein et al., 1976). BM-MSCs have been investigated and used for tissue regeneration and cell-based therapies (Alhadlaq & Mao, 2004; Samsonraj et al., 2017). However, the quantity of MSCs found in the BM is very low and ranges from 1/10,000 to 1/100,000 of cells in the BM tissue (Nasef et al., 2007). BM-MSCs have the potential risk of graft-vs-host disease (GvHD) (Amorin et al., 2014). This variation is due to the donor's health, age, and exposure to environmental stresses, altering MSC proliferation and differentiation potential *in vitro* (Mattiucci, D. et al., 2018). The BM niche is also thought to be progressively and functionally changed over a lifetime and could lead to bone diseases such as fibrous dysplasia (Chen Kevin et al., 2017). Furthermore, the processing of BM after collection could also affect the quality and quantity of isolated MSCs. In a comparative study, BM-MSCs isolated from different GMP (good manufacturing practices) centers yielded MSCs with different properties,

Table 1: Major sources and characteristics of MSCs

	Self-Renewal Potential	Population Doubling Time	Colony Forming Efficiency	Reference
AT	Up to P21	45h	60%	(Choudhery et al., 2014; Im et al., 2005; Jin, Hye Jin et al., 2013; Van Harmelen et al., 2004; Vishnubalaji et al., 2012; Xiuying et al., 2014)
BM	Up to P14	80h	52%	(Batsali et al., 2017; Beeravolu et al., 2017; Im et al., 2005; Jin, Hye Jin et al., 2013; Vishnubalaji et al., 2012)
PB	Up to P5	27h	50%	(Kim, J. et al., 2012)
UCB	Up to P18	40h	24%	(Heo et al., 2016; Jin, Hye Jin et al., 2013; Pievani et al., 2014)
CL	Up to P22	54h	59%	(Araujo et al., 2017; Beeravolu et al., 2016; Beeravolu et al., 2017)
WJ	Up to P20	43h	80%	(Batsali et al., 2017; Beeravolu et al., 2016; Beeravolu et al., 2017; Chen, G. et al., 2015; Trivanovic et al., 2013)
CPJ	> P40	16h	92%	(Bakshi et al., 2018; Beeravolu et al., 2016; Beeravolu et al., 2017)
PC	Up to P10	51h	16%	(Araujo et al., 2017; Beeravolu et al., 2016; Beeravolu et al., 2017; Chen, G. et al., 2015; Heo et al., 2016)

Table 1: Major sources and characteristics of MSCs Continued

	Self-Renewal Potential	Population Doubling Time	Colony Forming Efficiency	Reference
FT-Blood	Up to P20	50h	Not Determined	(Campagnoli et al., 2001; In't Anker et al., 2004)
FT-BM	Up to P20	33h	34%	(Brady et al., 2014; Campagnoli et al., 2001; Shin, K.-S. et al., 2009; Wang, Q. et al., 2016)
FT-Heart	Up to P15	80h	Not Determined	(Garikipati et al., 2018)
FT-Liver	Up to P20	52h	Not Determined	(Campagnoli et al., 2001; In't Anker et al., 2004)
FT-Pancreas	Up to P30	30h	Not Determined	(Hu et al., 2003)
AF	Up to P7	39h	15%	(Moraghebi et al., 2017)

such as supporting the hematopoiesis microenvironment and bone formation *in vivo* (Liu, S. et al., 2017). Such discrepancies in behavior can limit the autologous and allogenic use of BM-MSCs.

Unlike BM, adipose tissue (AT) is a more abundant source and can yield hundreds of thousands of MSCs per gram of tissue (Baer & Geiger, 2012). AT-MSCs have been investigated to repair myocardial infarction, allergic rhinitis, and muscular dystrophy using many animal models (Baek et al., 2011). AT-MSCs display a higher rate of proliferation as compared to BM-MSCs (Hass et al., 2011). However, the proliferation rate of AT-MSCs is heavily dependent upon the region of the body from which the AT was derived. AT-MSCs proliferate faster when derived from the subcutaneous fat region

than the omental fat region (Van Harmelen et al., 2004). Therefore, variation in the sources of AT-MSCs can cause inconsistencies with the results. AT-MSCs also differ in their differentiation potential when compared with BM-MSCs. AT-MSCs were able to differentiate towards the osteogenic lineage, but not to the same extent as BM-MSCs (Brennan et al., 2017; Im et al., 2005). However, in another study, there was no significant difference in the osteogenic potential of MSCs derived from BM and AT (De Ugarte et al., 2003). Media composition and source of cells could also influence the differentiation of MSCs. For example, chondrogenic differentiation of AT-MSCs requires a more complex medium, including growth factors, than BM-MSCs (Bosetti et al., 2011). AT-MSCs showed greater adipogenic potential than BM-MSCs, suggesting that the original niche of MSCs could influence the differentiation potential for each tissue source (Vishnubalaji et al., 2012).

Muscle tissue (MT) MSCs are typically found as a small population under the basal lamina, which is responsible for post-natal muscle regeneration (Farup et al., 2015). Reports have shown that MSCs derived from MT are comparable to BM-MSCs and AT-MSCs (Meligy et al., 2012; Owston et al., 2016). For instance, MT-MSCs were positive for the surface markers CD90 and CD44; however, BM-MSCs and AT-MSCs displayed a 5-7% higher expression of these markers (Meligy et al., 2012). Moreover, MT-MSCs displayed a lower proliferation rate than BM-MSCs and AT-MSCs (Giai Via et al., 2012; Meligy et al., 2012). Furthermore, AT- and BM-MSCs exhibited greater differentiation potential towards the adipogenic and osteogenic lineages than MT-MSCs (Jackson, W. et al., 2011; Sakaguchi et al., 2005). However, MT-MSCs exhibited the highest rate of

myogenic differentiation potential and expression of myoblastic markers than any other adult source (Meligy et al., 2012).

Even though there are differences in proliferation and differentiation potential of all the adult sources, each cell type could play a role in the future of regenerative medicine. Yet MSCs derived from various adult sources following invasive procedures cause discomfort to the patient/donor. This has led scientists to search for non-invasive and more promising sources of MSCs.

1.4 Perinatal and Fetal MSCs

Investigations of non-invasive sources have led to the isolation of MSCs from multiple perinatal sources, such as the UCB, UC, and PC (Beeravolu et al., 2016; Beeravolu et al., 2017; Maurice et al., 2006; Miao et al., 2006). Researchers have also investigated isolation of MSCs from fetal sources, AF (Wouters et al., 2007) and FT such as blood, bone marrow, and liver, are typically collected after terminated pregnancies during the first- and second-trimester (Campagnoli et al., 2001; Gucciardo et al., 2009; In't Anker et al., 2004) as well as heart and pancreas (Garikipati et al., 2018; Hu et al., 2003). However, there are ethical and moral concerns regarding the medical use of FT from elective abortions (Ishii & Eto, 2014). In contrast, perinatal tissues are routinely discarded after delivery as biological waste, making them a more desirable source for MSCs (O'Brien et al., 2006; Zhang, H. et al., 2018). Perinatal tissues can also yield an abundant number of cells, has an immune-privileged nature, and display potential for trilineage differentiation to the adipogenic, chondrogenic, and osteogenic lineages (Beeravolu et al., 2017; Mennan et al., 2013). Unlike adult MSCs, perinatal MSCs are less likely to be affected by environmental stresses and cause GvHD, making them the

optimal source of MSCs for cell-based therapies. Furthermore, studies have shown that numerous obstetric parameters including gestational age, route of delivery, maternal age, gestational diabetes and preeclampsia affected MSC proliferation and differentiation potential (Avercenc-Léger et al., 2017; Mazzoccoli et al., 2016).

UCB is comprised of HSCs, endothelial progenitor cells, and MSCs. Similar to BM, the amount of MSCs in UCB is extremely low, making it challenging to isolate MSCs from UCB (Bieback & Netsch, 2016). Also, the proliferation potential of UCB-MSCs has been shown to be dependent on the gestational age, and that the growth rate of UCB-MSCs is significantly lower at full term (Ma et al., 2012). However, UCB-MSCs have shown to be positive for CD73, CD90, and CD105 and can differentiate towards the adipogenic, chondrogenic, and osteogenic lineages. In a recent study, UCB-MSCs showed greater chondrogenic and osteogenic differentiation potential when compared to adult derived MSCs (Zhang, X. et al., 2011). Aside from the UCB, the UC has also been extensively studied for MSC isolation.

The UC and PC are anatomically complex tissues with different niches harboring MSCs that display variation in the proliferation and differentiation potential. Our studies showed that cells isolated from five distinct regions, cord lining (CL), Wharton's jelly (WJ), CPJ, chorion (CH), and PC (Beeravolu et al., 2016; Beeravolu et al., 2017). As depicted in Figure 2, the jelly-like tissue (WJ) surrounding the blood vessels within the UC was collected using a scalpel, and the remaining tissue was considered CL. The CPJ tissue is the region joining the whole UC with the CH/PC (Beeravolu et al., 2016; Beeravolu et al., 2017), and CH was then separated from the PC. The dissected tissues from the five distinct regions of the UC and PC were then explanted in culture flasks to

isolate cells. MSCs isolated from each segment were adherent to plastic, had fibroblastoid morphology, and were positive for CD73, CD90, and CD105 (Beeravolu et al., 2016; Beeravolu et al., 2017). In addition, integrin α6, also known as CD49f, which is upregulated in highly proliferative cells (Krebsbach & Villa-Diaz, 2017) , displays

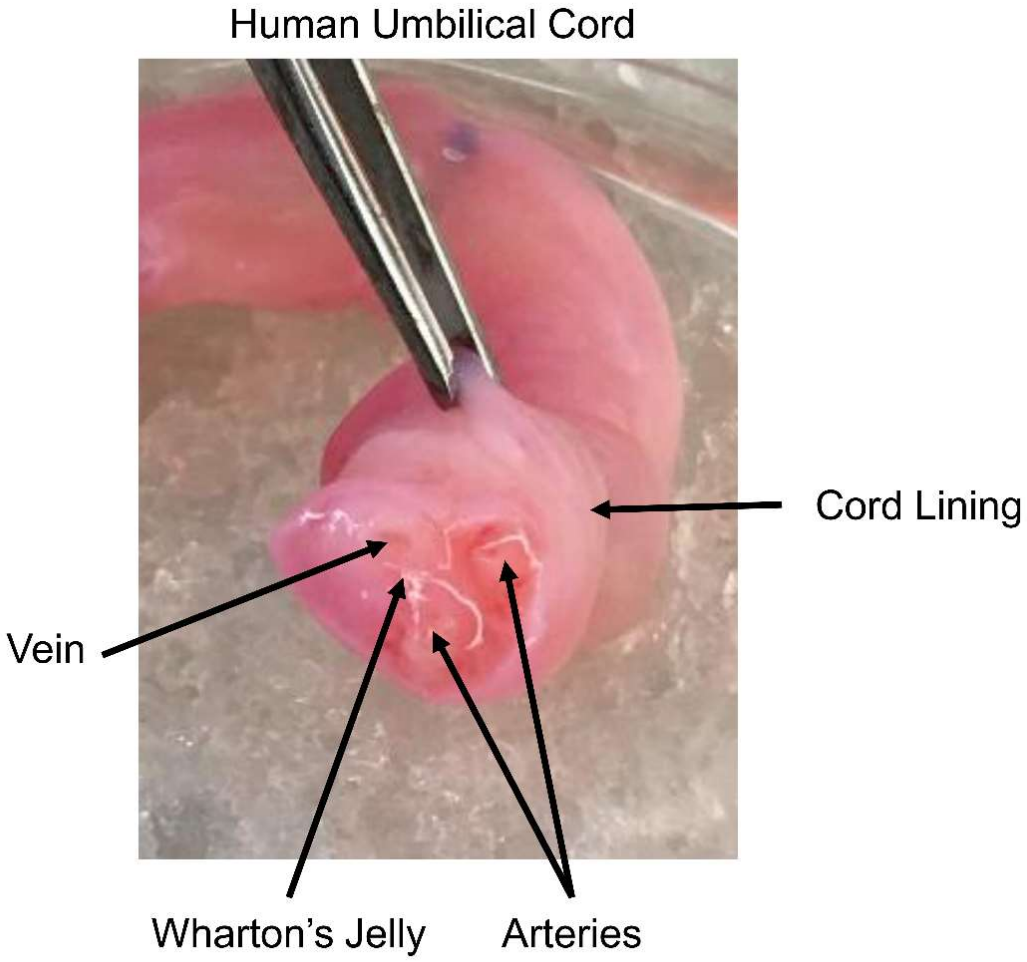

Figure 2: Anatomical sites of the human UC: arteries, vein, CL, and WJ.

variable expression between each segment. As depicted in Figure 3, cells isolated from the CH and PC displayed a decreased expression of CD49f, while CPJ remained highly expressive of CD49f, suggesting that CPJ-MSCs are more proliferative and have higher self-renewal potential than the other segments. Furthermore, when comparing proliferation rate to BM-MSCs, CPJ-MSCs showed a significantly faster doubling time and higher passaging capacity (Beeravolu et al., 2016). Whereas CPJ-MSCs showed the highest osteogenic differentiation potential with a 2-fold increase in the expression of the osteogenic genes, *collagen type 1 (COL1), osteopontin (OPN),* and *osteocalcin (OCN)* compared to BM-MSCs as determined by transcriptional analysis (Beeravolu et al., 2016). Similarly, CPJ-MSCs showed a 50-fold higher expression of the chondrogenic genes *sex-determining region Y-box 9 (SOX9)* and *collagen type 2 (COL2)* compared to BM-MSCs (Beeravolu et al., 2016). However, when analyzing the adipogenic differentiation potential, WJ-MSCs displayed the highest expression of the adipogenic genes, *CCAAT/enhancer-binding protein beta (CEBPβ), fatty acid-binding protein 4 (FABP4)*, and *peroxisome proliferator-activated receptors* (*PPARγ)*, followed by CPJ-MSCs (Beeravolu et al., 2016; Beeravolu et al., 2017). Interestingly, examination of the transcriptome revealed that two genes *(annexin A3* and *DEAD-box helicase 43 (DDX43))*, which are biomarkers for various cancer lines, were expressed significantly higher in CPJ-MSCs when compared to CL-MSCs and WJ-MSCs. Additionally, *homeobox A6* (*HOXA6)* and *homeobox D10* (*HOXD10),* genes that are involved in the regulation of cell differentiation, were expressed at a lower rate in CPJ-MSCs than CL-MSCs and WJ-MSCs. These findings could explain the long-term maintainability and proliferation potential found in CPJ-MSCs (Beeravolu et al., 2016; Beeravolu et al., 2017).Unlike

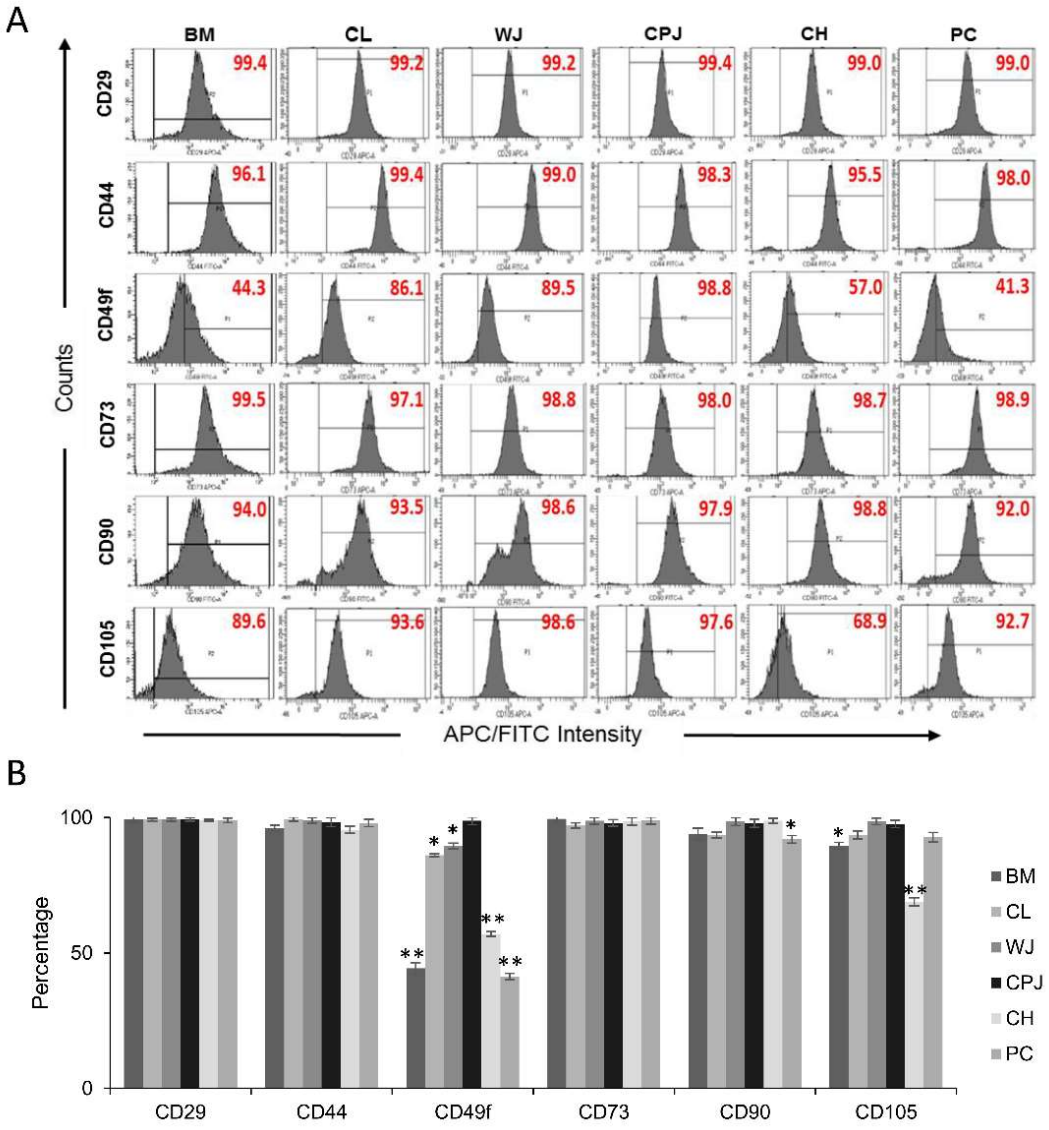

Figure 3: Characterization of MSCs derived from the BM and various perinatal segments, including CL, WJ, CPJ, CH, and PC. A and B. Histograms and graphical representation of the expression of mesenchymal markers in MSCs as determined by flow cytometry, respectively. All experiments were carried out in triplicates. Data are presented as the mean ± standard error of the mean (SEM) triplicates per analysis. Results with *$p \leq 0.05$, **$p \leq 0.01$ were considered statistically significant.

adult MSCs (i.e. BM-MSCs), perinatal MSCs do not display major histocompatibility complex class II antigens (Anastasiu et al., 2016; Fariha et al., 2011; Kim, J. et al., 2018; Liu, S. et al., 2012; Maleki et al., 2014; Shin, K.-S. et al., 2009; Tancharoen et al., 2017), making them more suitable for cell therapy.

1.5 Promising Applications of MSCs

Stem cell-based therapies can significantly impact the field of regenerative medicine. MSCs have been used in preclinical and clinical studies to treat degenerative diseases such as AD (Cui et al., 2017; Han et al., 2018; Shin, J. Y. et al., 2014; Wang, X. et al., 2018), DDD (Ahn et al., 2015; Beeravolu et al., 2018; Pereira et al., 2016; Perez-Cruet et al., 2018), RDD (Mead et al., 2018), MS (Harris et al., 2018; Nasri et al., 2018; Planchon et al., 2018), and PD (Jamali et al., 2018; Kim, H. W. et al., 2018) as summarized in Table 2. The regenerative mechanisms of transplanted MSCs for these diseases are still unclear; however, our lab has investigated the potential regenerative mechanism of MSCs and their derivatives for the treatment of RDD and MS.

1.5.1 Retinal Degenerative Diseases

RDD, including age-related macular degeneration (AMD) and retinitis pigmentosa (RP), causes progressive and incurable vision loss (Hao, X. et al., 2018; O'Neal & Luther, 2020). AMD leads to the loss of sharp and central vision due to damage to the macula that affects the main area of the retina and choroid (Surendran et al., 2018). Whereas RP is characterized by progressive degeneration of the photoreceptors, leading to night blindness followed by progressive loss of the visual field in daylight and ultimately blindness (Hamel, 2006). RP affects 1 in every 4000 people in the United

Table 2: Potential use of MSC-based therapies

Promising Applications	**Reference**
Alzheimer's Disease	(Cui et al., 2017; Han et al., 2018; Wang, X. et al., 2018)
Bone and Cartilage Diseases	(Jo et al., 2014; Kastrinaki et al., 2013)
Autoimmune Diseases	(Xu, 2018; Zhang, W. et al., 2018)
Amyotrophic lateral sclerosis	(Bonafede & Mariotti, 2017)
Diabetes	(Evangelista et al., 2018; Gabr et al., 2018)
Glaucoma	(Manuguerra-Gagne et al., 2013; Osborne et al., 2018; Roubeix et al., 2015)
Graft vs Host Disease	(Jurado et al., 2017; Zhao, K. et al., 2015)
Intervertebral Disc Disease	(Ahn et al., 2015; Beeravolu et al., 2018; Pereira et al., 2016; Perez-Cruet et al., 2018)
Multiple Sclerosis	(Harris et al., 2018; Nasri et al., 2018; Planchon et al., 2018)
Myocardial Infarction	(Baek et al., 2011; Chen, X. Q. et al., 2014)
Pain	(van Buul et al., 2014)
Parkinson's Disease	(Jamali et al., 2018; Kim, H. W. et al., 2018)
Retinal Diseases	(Wang, Y. et al., 2018; Zhang, M. et al., 2017)
Spinal Cord Injuries	(Stewart et al., 2017; Yang, C. et al., 2018)

States and 1 in every 5000 people worldwide (O'Neal & Luther, 2020). In RP, mutations in the gene, *RPE65*, result in the disruption of the RPE65 protein production in the retinal pigment epithelium (RPE) (Marlhens et al., 1998), leading to worsened vision, night blindness, and decreased peripheral vision (Prem Senthil et al., 2017). A mouse model, rd12, represents RP and Leber congenital amaurosis in humans, which causes blindness or severely impaired vision in adults and children, respectively (Pang, J. J. et al., 2005). The mutation responsible for vision loss in the rd12 model is a nonsense mutation within the *Rpe65* gene (Cai et al., 2009). Using this animal model, we have previously demonstrated the therapeutic potential of ESCs derived neuroprogenitors (Chaudhry et al., 2009). Transplantation of pluripotent stem cells, ESC- and induced pluripotent stem cell (iPSC-) derived retinal progenitors have also been reported to preserve visual function upon injection into Royal College of Surgeons (RCS) rats as well as rd1 and rd12 mice, respectively (Li, Yao, et al., 2012; Sun et al., 2015; Zou et al., 2019). Because pluripotent cells can cause teratomas and pose moral and ethical concerns, growing interest has been shown to explore other options such as MSCs for cell therapy.

MSCs exert their therapeutic effect in part by secreting trophic factors that protect cells or promote their survival and transplantation of mouse BM-MSCs delayed retinal degeneration in an animal model of RDD (Inoue, Y. et al., 2007). Mouse BM-MSCs transplanted into rhodopsin knock-out mice integrated into the RPE and the neuroretina, which lead to prolonged photoreceptor survival (Arnhold et al., 2007). Human (h) BM-MSCs injected into the subretinal space of a retinal dystrophy rat model showed significant and extensive photoreceptor rescue in transplanted eyes (Tzameret et al., 2014). On the other hand, tail vein injection of rat MSCs preserved visual function in a

rat model of RP (Wang, S. et al., 2010). Interestingly, transplantation of the combination of hBM-MSCs and fetal retinal progenitor cells (RPCs) into the subretinal space of a rat model of RP maintained retinal function based on the electroretinogram (ERG) results much better than when they were individually transplanted (Qu et al., 2017). However, these findings are difficult to translate in humans, mainly because of the invasive procedures required to isolate these cells. In addition, adult MSCs have limited proliferation and differentiation potential (Beeravolu et al., 2017). Furthermore, adult MSCs undergo genetic changes depending on donor age and environmental stress exposure (Mattiucci, D. et al., 2018). Recently, hUC-MSCs have been investigated for treating retinal degeneration. hWJ-MSCs provided neuroprotection for retinal ganglion cells (RGCs) and promoted axonal regeneration along the optic nerve in adult rats (Harvey et al., 2006). hWJ-MSCs also delayed loss of RGC in axotomy-induced rats (Millán-Rivero et al., 2018), outer nuclear layer (ONL) in RCS rats (Leow et al., 2015), and improved the thickness of the retina and upregulated pro-survival genes (Koh et al., 2021). hUCB-MSCs were suggested to improve the retinal morphological structure (Mohamed et al., 2017), exert a neuroprotective effect and rescue a significant percentage of axotomized RGCs (Zwart et al., 2009).

The potential therapeutic effects of hBM-MSCs or adipose MSCs on retinal defects have been investigated in 30 clinical trials (Labrador-Velandia et al., 2016; Oner et al., 2016; Satarian et al., 2017; Tuekprakhon et al., 2021). In some MSC transplantation studies, vision loss was halted, macular thickness increased, and/or visual acuity was improved (WeissBenes et al., 2016; WeissLevy et al., 2016; Weiss et al., 2017). Human RPC transplantation in RP patients led to moderate vision recovery and

maintenance of the ONL thickness or improved visual acuity (Liu, Y. et al., 2017). It is important to note that most clinical trials are limited to phase I/II studies (Labrador-Velandia et al., 2016; Zhao, T. et al., 2020) due to the lack of cells required for extensive clinical studies.

The current study investigated human primitive MSCs isolated from perinatal tissue, which exhibited superior characteristics compared to adult MSCs and differentiated into RPCs. When MSC-derived RPCs were transplanted in the rd12 mice, they improved retinal structure and function. They also survived, dispersed, and integrated into various neural layers, while MSCs homed to the RPE layer of the retina. These findings provide evidence that MSC-derived RPCs are a promising source for cell therapy to treat RDD.

1.5.2 Multiple Sclerosis

MS is a chronic autoimmune inflammatory disease of the central nervous system (CNS) (Dulamea, 2017). MS affects approximately 400,000 individuals in the United States and 2.5 million people worldwide. As a result, it inflicts a substantial economic and societal burden due to the early age of disease onset and recurrent relapses (Owens, 2016). In MS, inflammatory responses are elicited by the intrinsic immune system and parenchymal glial cells, contributing to oligodendrocyte damage, demyelination, axonal damage, and impaired or reduced neuronal signaling (Dulamea, 2017). Multiple factors, including genetics and environmental agents, seem to be involved with the onset of MS (Dulamea, 2017). Although drug treatments help reduce disease progression or minimize disability in patients, they cause severe side effects and do not reverse the symptoms of MS (Villoslada & Steinman, 2020). Therefore, it is imperative to design therapeutic

strategies that stop disease progression and repair the damage to the CNS without severe side effects to MS patients. With the advent of recent progress in stem cell research, cell therapy is considered a more promising alternative to drug therapy (Genc et al., 2019). MSCs have shown paracrine effects by secreting immunomodulatory cytokines and trophic factors (Fontaine et al., 2016). MSCs are known to home towards the injury site and participate in the healing and repair processes throughout life (Brown et al., 2019). Therefore, there is tremendous interest in MSCs due to their medicinal properties. However, MSCs isolated from adult sources have poor growth and limited self-renewal and differentiation potential and pose a significant risk of GvHD (Brown et al., 2019). On the other hand, MSCs isolated from perinatal sources are more naïve, exhibiting a low risk of host immune response due to the lack of expression of the major histocompatibility complex (MHC) class II antigens and thus do not cause GvHD (Brown et al., 2019). Recently, we have isolated highly proliferative primitive MSCs, which can be rapidly amplified to large numbers, and differentiated into functional derivatives, for large-scale animal and clinical studies (Beeravolu et al., 2016; Beeravolu et al., 2017; Brown et al., 2019). MSCs are known to have homing capabilities to the site of injury and the ability to secrete cytokines and growth factors that may indirectly promote endogenous tissue regeneration (Fontaine et al., 2016). However, the ability of transplanted MSCs to cross the blood-brain barrier (BBB) to repair the damaged CNS is not well established (Liu et al., 2013). Several reports describe the ability of neural stem cells (NSCs) to migrate to the area of pathology in experimental models of CNS diseases (Aboody et al., 2000; Imitola et al., 2004). In addition, resident NSCs that produce new neurons throughout life continuously decrease in MS patients (Zhang, H. et al., 2020).

Therefore, stem cell-based therapies that promote endogenous neural regeneration to repair the damage in the CNS (Wu et al., 2008; Zhu, S.-Z. et al., 2018) may prove ideal for the treatment of MS. In this study, we applied a novel cell therapy approach whereby highly proliferative and naïve primitive MSCs were first differentiated into NSCs that were transplanted into an experimental autoimmune encephalitis (EAE) mouse model, which is known to share similar characteristics and pathological features with MS (Glatigny & Bettelli, 2018). Our results demonstrated that EAE disease symptoms were reduced or reversed and significant improvements were observed in the pathology of the CNS in animals transplanted with MSCs and NSCs, with the latter being the more effective. The transplanted cells survived and migrated to the CNS where they promoted myelination and neural protection by modulating immune response and inhibiting astrogliosis as well as induced endogenous neurogenesis, thereby leading to functional recovery. Despite being highly proliferative, neither MSCs nor their derivatives, NSCs, caused immune rejection or teratoma formation. These studies demonstrate that NSCs derived from primitive MSCs have therapeutic potential to treat MS and other neurodegenerative diseases.

1.5.3 Other Degenerative Diseases

Our recent preclinical studies showed that nucleus pulpous-like cells (NPCs) derived from MSCs were more efficacious than MSCs in a rabbit model of DDD (Beeravolu et al., 2018; Perez-Cruet et al., 2018). The transplanted MSC-derived NPCs survived, migrated, and integrated in the nucleus pulpous (NP) of the intervertebral discs (IVDs). NPC transplantation also improved the water and glycosaminoglycan content of the NP, increasing disc height suggesting regeneration of rabbit NP (Perez-Cruet et al.,

2018). In a Parkinson's study, MSCs were differentiated to dopaminergic neuron cells in a hypoxic environment *in vitro*. These dopaminergic neuron cells survived when transplanted into a rat model of PD and displayed more significant improvement of behavioral impairments (Wang, Y. et al., 2013). Studies have shown promising results with MSC-based therapies for treating chronic pain using an osteoarthritis rat model (van Buul et al., 2014). Recently, MSCs have gained attention for their paracrine effects *in vivo*. MSCs have been shown to secrete various cytokines and chemokines such as fibroblast growth factor 2 (FGF2), insulin growth factor 1 (IGF1), and transforming growth factor-beta 1 (TGFβ1) (Hocking & Gibran, 2010; Kim, I. et al., 2013). These paracrine effects can greatly benefit the resident cells by promoting immunomodulation, anti-apoptotic, and anti-oxidative effects. When evaluating the global gene expression of MSCs, a few immune response genes such as *C-C motif chemokine 2* (*CCL2), TNF alpha-induced protein 6 (TNFAIP6), TNF superfamily member 10 (TNFSF10), NF-kappa-B inhibitor alpha (NFKBIA),* and *Fas cell surface death receptor (FAS),* which are part of the interferon-gamma (IFNγ) response pathway, were highly expressed (Ren, J. et al., 2018). In a recent report, MSCs were intratracheally administrated into mice with an acute lung injury that caused inflammation. These MSCs demonstrated an inhibition of the inflammatory response of the macrophages by secreting prostaglandin-E2, granulocyte-macrophage colony-stimulating factor (GM-CSF), interleukin 6 (IL-6), and interleukin 13 (IL-13), and showed improvement in the diseased lungs (Zhu, H. et al., 2017). Together these new developments in the field of regenerative medicine have provided stimulus for the use of MSCs in clinical studies.

Currently, there are over 1,300 MSC-based clinical trials in the US (ClinicalTrials.gov, 2021). Some of these studies include bone and cartilage diseases, diabetes, and osteoarthritis (Figure 4). A recent clinical study showed alleviation of pain and functional improvement when human UC-MSCs were injected in the IVDs of two DDD patients with chronic discogenic low back pain (Pang, X. et al., 2014). In another similar study, MSCs injected intradiscally into the IVD of the patients resulted in a quick and significant improvement in functionality, experienced less pain, and exhibited less IVD degeneration than the control group (Noriega et al., 2017). (Noriega et al., 2017). Additionally, a phase 1 study showed promising therapeutic effects of MSCs for the treatment of MS (Harris et al., 2018; Planchon et al., 2018). When MSC-derived, neural progenitor cells were administered intrathecally in three separate doses over the span of three months, improvements in muscle strength and functional motor skills were observed (Harris et al., 2018). Lastly, MSCs have also been investigated for the treatment of chronic tissue ulcers caused by diabetes. Patients administered with MSCs for skin healing showed an improvement in microvascularization structure (Kirana et al., 2012). Although still in infancy, an increasing number of clinical studies prefer the use of perinatal MSCs. Nevertheless, more research is needed to fully understand the capabilities of MSCs both in laboratory and clinical settings.

1.6 Potential Problems

Even though MSCs isolated from various sources have been widely studied, a number of problems warrant further investigation and are summarized in Table 3. For example, tissue sources and isolation methods can influence MSC proliferation and differentiation potential. In addition, microenvironment, donor age, and environmental

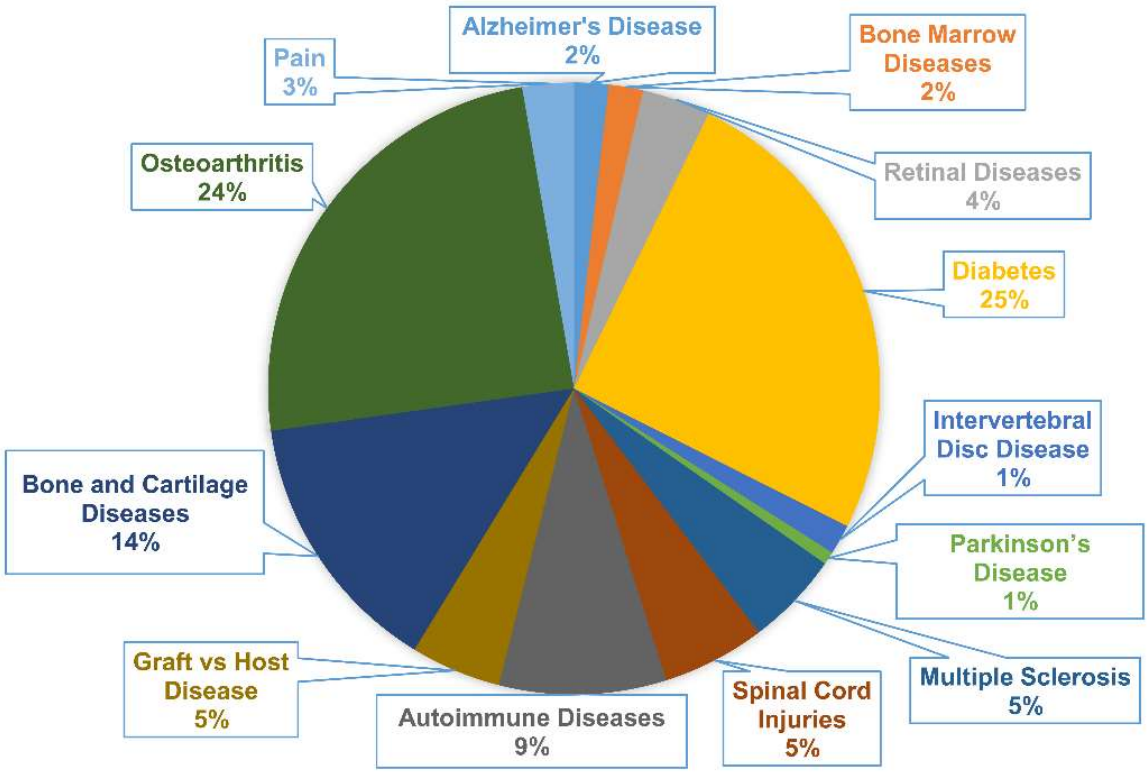

Figure 4: Ongoing MSC-based clinical trials. (ClinicalTrials.gov, 2021).

Table 3: Potential problems of MSCs associated with tissue source and isolation methods

Description	**Reference**
Isolation methods influence MSC proliferation and differentiation potential	(Liu, S. et al., 2017; Van Harmelen et al., 2004)
Source of isolation effects MSC properties	(Beeravolu et al., 2016; Beeravolu et al., 2017; De Ugarte et al., 2003; Im et al., 2005; Legzdina et al., 2016)
Media composition influences proliferation and differentiation capacity of MSCs	(Araujo et al., 2017; Beeravolu et al., 2016; Beeravolu et al., 2017; Jin, Hye Jin et al., 2013)
Microenvironment effects cell growth and differentiation of MSCs	(Alimperti, Lei et al., 2014; Li, Y. et al., 2015; Shekaran et al., 2015)
Donor age and environmental factors effect genetic stability of MSCs	(D'Ippolito et al., 1999; Malgieri et al., 2010; Mattiucci, Domenico et al., 2018; Stultz et al., 2016)
Promotion of tumor growth by MSCs	(Lacerda et al., 2015; Ridge et al., 2017)

factors affect the genetic stability of MSCs, as well as promote tumor growth by MSCs *in vivo*. No consensus on the standard properties (i.e., phenotype, differentiation potential, physiological functions, and biological properties) of MSCs have been developed (Sacchetti et al., 2016). One group of researchers argues that MSCs are only found in BM, clonogenic, multipotent, and self-renewing progenitors of only skeletal tissue (Robey, 2017). These cells are also part of the HSC niche found within the BM (Robey, 2017; Sacchetti et al., 2016). Conversely, others believe that MSCs can be derived from multiple tissues and have the potential to differentiate to more than just the osteogenic lineage (da Silva Meirelles et al., 2006). Thus, a better understanding of the origin, biological properties, and function of MSCs derived from different tissues could provide insight into what truly is an "MSC." The mesenchyme originates from the mesoderm and is first developed during the epithelial mesenchymal transition in the course of embryonic development (Bellairs, 1986). MSCs originally acquired their name through the assumption that BM-MSCs could form other mesodermal tissues such as muscle, ligaments, and tendons through the mesengenic process, and subsequently, these cells were given the name "mesenchymal stem cells" (A. I. Caplan, 1991). Alternative names, such as mesenchymal stromal cells, medicinal signaling cells, and pericyte MSCs, have been suggested to replace "mesenchymal stem cells." Mesenchymal stromal cells are among the more popular alternative names for MSCs, as scientists have agreed that it does not fit the stem cell classification and functionality. However, stromal and stem are continuously used interchangeably (Caplan, Arnold I., 2017; Horwitz et al., 2005). The name medicinal signaling cells relies on the paracrine function of MSCs *in vivo* but ignores the differentiation potential that MSCs exhibit (Caplan, A. I., 2010). Pericyte

cells are found on the blood vessels in the perivascular niche. Some believe that these cells are MSCs because they can differentiate towards the adipogenic, chondrogenic, and osteogenic lineages *in vitro* and have paracrine effects *in vivo*. However, the surface markers on these cells are different (Kumar et al., 2017). Pericytes are highly positive for neural/glial antigen-2 (NG2), a neural/glial marker, whereas MSCs express this marker at low levels. Overall, the main debate with the naming of MSCs is due to the unknown origin of these cells.

The argument that MSCs are only derived from the BM fails to recognize that MSCs are derived from the mesoderm during embryonic development, which produces many different tissues such as bone, muscle, and cartilage. Furthermore, bone is more derived explicitly from the neural crest (facial bones), paraxial mesoderm (axial bones), and somatic lateral plate mesoderm (appendicular bones) that make up all the bones found in the body (Robey, 2017). Therefore, to believe that MSCs are only derived from the BM would be implausible and leads to the unanswered question: why can't MSCs be derived from different tissues? The main concern to why some reports believe that MSCs should only be derived from BM is due to inconsistencies in MSC proliferation and differentiation potentials compared to other tissues. However, the niche and age of each tissue could influence the characteristics and functionality of the cells when isolated *in vitro*. For example, when examining the gene expression profile of MSCs derived from a different tissue, BM-MSCs displayed an increase in genes expressed in the hematopoietic support system. In contrast, UCB-MSCs showed increased genes associated with proliferation and cell-cycle regulation (Sacchetti et al., 2016). This should not come as a surprise since MSCs in the BM assist in the hematopoietic niche, and UCB-MSCs are

more primitive and proliferate for much longer than the cells derived from adult sources. Even the MSCs isolated from UC and FT have been reported to vary in their differentiation into various lineages (Beeravolu et al., 2016; Beeravolu et al., 2017; Brady et al., 2014; Guillot et al., 2007; Shin, K.-S. et al., 2009). Controversy regarding the differentiation potential of MSCs may be due to the variation in the niche and unreliable *in vitro* techniques used to differentiate and characterize MSCs. The current methods used to determine *in vitro* differentiation depend on the extracellular matrix stains such as alizarin red S and safranin O, which stain for dystrophic calcification and glycosaminoglycan linked to aggrecan, respectively.

However, due to the high susceptibility of non-specific staining, false-positive results are expected. An alternative to these methods would be to examine the gene expression at a molecular level. Quantitative reverse transcriptase-polymerase chain reaction (qRT-PCR) could be used to confirm that MSCs differentiated *in vitro* (Ragni et al., 2013). Furthermore, most reports fail to include *in vivo* differentiation imperative for characterization of MSCs (Bianco et al., 2008; Quinn & Flake, 2008). When BM-MSCs and UCB-MSCs were placed in an osteoconductive material and then transplanted subcutaneously in a severe combined immunodeficiency (SCID)/beige mouse, injected BM-MSCs formed only bone, while injected UCB-MSCs formed both bone and cartilage (Sacchetti et al., 2016). Although *in vivo* differentiation could improve MSC characterization, *in vivo* testing of MSCs alone (no carriers) has yet to be realized. This has the possibility to provide better insight into the potential of these cells and how they act on their own in a clinical setting. When examining MSCs for clinical trials, one must select the correct tissue for deriving MSCs to achieve the greatest outcome for treating a

particular disease. There are major concerns when MSCs used in cell therapy for patients are not well characterized.

Therapeutic uses of so-called stem cells have recently drawn United States Food and Drug Administration (FDA) attention due to the lack of proper approval. These uses are known as "pay-to-participate treatments" (Turner, 2017). Typically, clinical trials are free of charge to participants, except for possible recovery costs, but never for profit. These "pay-to-participate treatments" businesses were found to have little to no scientific evidence to support their studies, which puts innocent patients at risk for serious injury (Hiltzik, 2017). These businesses existed due to loopholes within the regulations of the FDA, but since 2017, the FDA has instituted new regulations on the use of stem cells for human treatments. However, some clinics manipulate these FDA regulations for their benefit by claiming that their tissue source of MSCs causes minimal manipulation to the patient, which is a well-known exemption for drug regulation (Hiltzik, 2017). The FDA has clarified these regulations to prevent businesses and clinics from taking advantage of patients, but more work is still required. The FDA recently issued a warning letter to US Stem Cell Clinic for marketing unauthorized stem cell products and deviating from GMP requirements (Meyer, 2018). The warning letter included evidence of AT-MSCs being injected intravenously or directly into the spinal cords of patients for a series of diseases, including Parkinson's disease, amyotrophic lateral sclerosis, and heart disease. The FDA also found that US Stem Cell Clinic failed to promote a sterile environment to prevent microbiological contaminates, leading to infection when injected into the patients (Meyer, 2018). Unfortunately, there was an unapproved FDA case where three women were injected in the eye with stem cells for the treatment of macular degeneration and are

now legally blind. Sadly, the firm's chief scientific officer dismissed these women as "just a handful" and that thousands of other patients were successful (Hiltzik, 2017). Overall, the FDA needs to implement stricter guidelines for stem cell based clinical trials, but this could take time, which puts patients at risk for further health complications.

1.7 Challenges

Although a great deal of advancement and interest in using MSCs for therapeutic applications face many challenges, unlike ESCs, MSCs can only proliferate for a limited number of passages *in vitro* and will eventually enter a senescence state (Cheng, H. et al., 2011; Legzdina et al., 2016). In attempts to maintain an undifferentiated and self-renewal state, MSCs were exposed to a hypoxic condition to promote the hypoxia-inducible factor 1α (Hif1α), a master regulatory protein in hypoxic conditions. Hif1α stabilization led to the upregulation of the pluripotent genes, *octamer-binding transcription factor 4 (OCT4)* and *kruppel like factor 4* (*KLF4)*, and inhibition of differentiation towards the adipogenic and osteogenic lineages (Park, I. H. et al., 2013).

Transcriptional activation or repression has been shown to be tightly linked with disruption or occupancy of nucleosomes at regulatory regions, including promoters, enhancers, silencers, and insulators (Moskowitz et al., 2017; Shivaswamy et al., 2008). Altered nucleosome occupancies due to histone modifications, such as acetylation, directly or indirectly through chromatin remodelers or other epigenetic changes regulate access to regulatory regions to transcription activators or repressors. Nucleosome analysis thus could provide important insight into the changes controlling the cell fate at a chromatin level. Our results of MNase-seq analyses showed that MSCs progressively

undergo changes in nucleosome organization upon passaging. At higher passages, the occupancy of nucleosome increases at the regulatory/promoter regions of those genes which regulate proliferation or self-renewal. For example, higher nucleosome occupancy is observed at the promoter regions of genes, *CD105* and *CD49f*, which are known to be associated with CPJ-MSCs proliferation, at higher passages (P20) compared to those cells with lower passages (P6) (Figure 5). Furthermore, a senescence gene, *abelson murine leukemia viral oncogene homolog 1* (*ABL1)*, displayed a higher occupancy of nucleosomes around the transcription start site in higher passages than lower passages, suggesting that passaging of MSCs induce senescence. Progressively slow growth and lack of differentiation of high passaged MSCs have been reported in several studies (Beeravolu et al., 2016; Bonab et al., 2006; Yang, Y.-H. K. et al., 2018). Therefore, it is imperative to develop methods to maintain MSCs without losing their self-renewal and differentiation potential. Several studies have reported large scale production of MSCs for clinical and commercial usage by devising newer techniques such as three-dimensional (3-D) culture, bioreactors, hypoxic conditions, and the addition of growth factors (Choi et al., 2017; Dayment et al., 2014; Gottipamula et al., 2013; Sart & Agathos, 2016; Swamynathan et al., 2014). Using a microcarrier-based suspension system, MSCs were amplified to a 10^3-fold increase, which was significantly higher than the 200-fold increase in monolayer culture (Yuan et al., 2014). Further studies are required to fully understand the mechanisms at play in expanding these suspended cells; however, these microcarrier-based suspension systems can greatly improve the use of MSCs for clinical studies. One of the most critical challenges is the isolation and culturing of MSCs using xenofree conditions (Laitinen et al., 2016) as cells

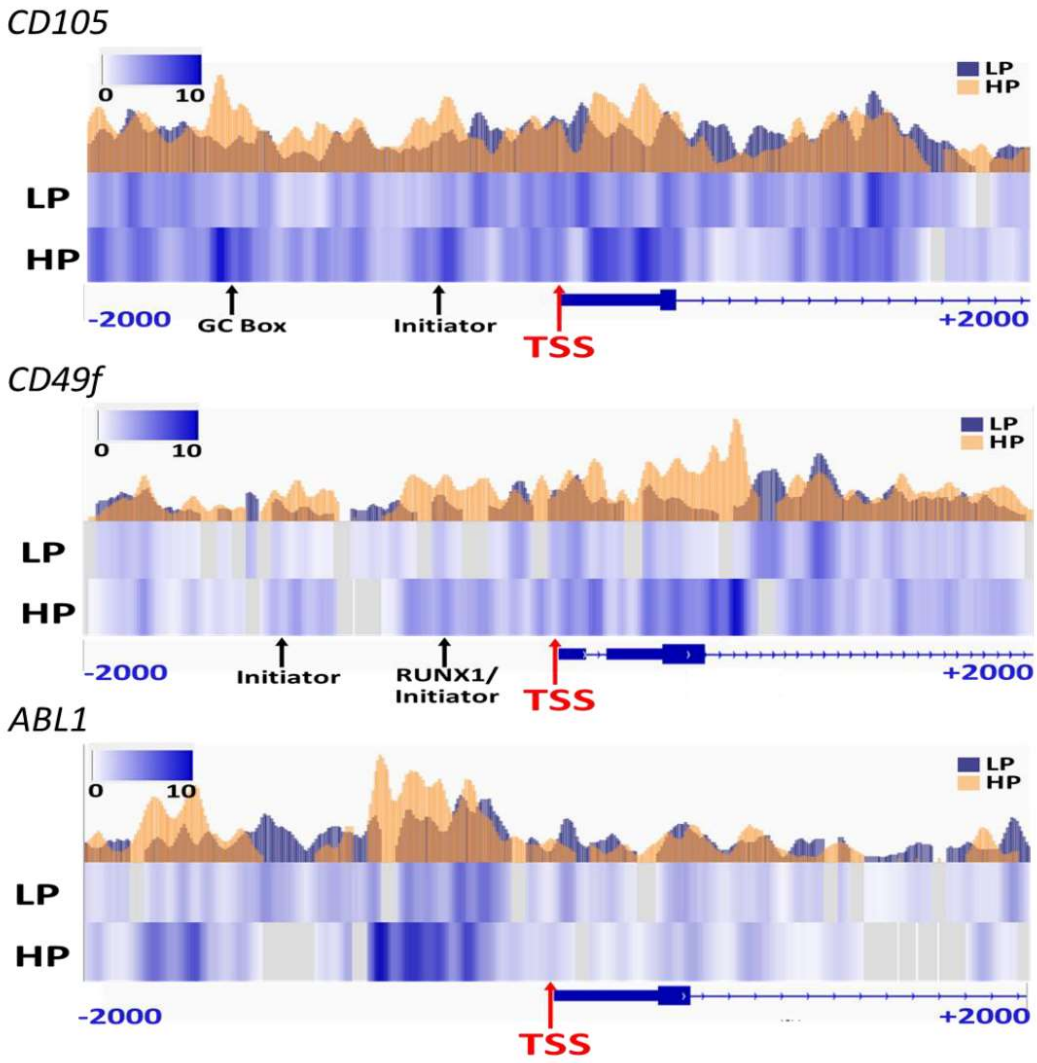

Figure 5: MNase sequencing analysis of the low passage (LP) and high passage (HP) CPJ-MSCs. Heatmaps of *CD105*, *CD49f*, and *ABL1* genes. *CD105* is an MSC specific marker, *CD49f* is expressed in highly proliferating stem cells, and *ABL1* is linked to cell senescence. Samples were sequenced using the Illumina HiSeq machine for paired-end reads. Paired-end reads were aligned to the human genome (genome assembly hg38) using Bowtie2 to map reads. Reads were counted and normalized using reads per kilobase per million (RPKM) values to determine nucleosome occupancy. Normalized values were visualized using Integrative Genomics Viewer (IGV).

grown in media containing FBS and other animal or bacterial products cannot be used for clinical purposes (Chapter 3). Additional challenges include *in vivo* survival (Moya et al., 2018) and differentiation of MSCs (Araujo et al., 2017) and are listed in Table 4. Further advancements in the culturing techniques would greatly impact the use of MSCs for regenerative medicine.

1.8 Opportunities

MSCs have shown promising outcomes in preclinical and clinical studies for treating degenerative diseases such as AD, DDD, MS, PD, RDD, pain, and providing immunomodulatory, neuroprotective, and anti-inflammatory responses *in vivo* (Beeravolu et al., 2018; Ding et al., 2017; Gugliandolo et al., 2017; Nasri et al., 2018; Osborne et al., 2018; Perez-Cruet et al., 2018; Turgeman, 2015; van Buul et al., 2014; Zhang, R. et al., 2013). Studies have shown that MSCs can be differentiated to NPCs to regenerate the nucleus pulpous in the IVD and to retinal progenitor cells to regenerate the retina within the eye (Beeravolu et al., 2018; Ding et al., 2017; Perez-Cruet et al., 2018).

Furthermore, MSCs can exert an anti-inflammatory and immunomodulatory response (Zhang, R. et al., 2013). They can also regenerate mesenchymal tissues such as bone, cartilage, muscle, ligaments, tendons, and adipose and can be utilized for many beneficial purposes. For instance, MSCs have been shown to have therapeutic effects by supporting the hematopoietic niche and hematopoietic reconstruction in the bone marrow (Isern et al., 2014). MSCs interact with HSCs within the bone marrow by secreting chemokines that promote the long-term growth of HSCs and can be used to treat different hematopoietic diseases (Li, T. & Wu, 2011). In the clinical trial setting, MSCs are known to have differentiation, homing, and immunomodulatory properties. Currently, many

Table 4: Challenges for *in vitro* expansions and clinical applications of MSCs

Description	**Reference**
Maintenance and self-renewal	(Jackson, K. A. et al., 2001; Law & Chaudhuri, 2013)
Large scale production for clinical and commercial usage	(Choi et al., 2017; Gottipamula et al., 2013; Sart & Agathos, 2016; Swamynathan et al., 2014)
Standardization of criteria for characterization	(Robey, 2017; Sacchetti et al., 2016)
Differentiation of MSCs *in vitro and in vivo*	(Alimperti, You et al., 2014; Jackson, K. A. et al., 2001)
Homing and localization to the sight of injury	(Fiumana et al., 2013; Young et al., 2018)
Cell survival and integration *in vivo*	(Cheng, J. et al., 2015; Liu, X. B. et al., 2012; Moya et al., 2018; Zhang, J. et al., 2013)
Xenofree isolation and culturing	(Bakopoulou et al., 2017; Gottipamula et al., 2013; Laitinen et al., 2016; Trivanovic et al., 2013)

studies are underway to determine the immunomodulatory properties of MSCs for the treatment of many diseases, such as colitis, immune thrombocytopenia, and encephalomyelitis (Gao, F. et al., 2016; Zappia et al., 2005; Zhang, Q. et al., 2009). Novel therapies for GvHD and other autoimmune disorders may be possible using MSCs due to suppressive effects on activated immune cells (Hao, L. et al., 2012). In addition, the use of MSCs for revitalization and renovation purposes has gained increasing interest. In a recent study, MSC-derived extracellular vesicles were found to contain various growth factors such as Collagen I and Elastin that are associated with skin rejuvenation (Kim, Y. J. et al., 2017). MSCs have also shown the potential to boost the body's natural ability to heal itself. For example, a study demonstrated that rat MSCs could enhance the recruitment of endogenous progenitors during skin wound healing (Al-Shaibani et al., 2017; Formigli et al., 2015). MSCs also demonstrated the potential in regenerative medicine by providing improvement in behavioral assays and paracrine effects. They directed cell to cell interactions that resulted in protection against neurovascular damage in a stroke (Ryu et al., 2019). Moreover, stem cells and/or their derivatives have the potential to regenerate cartilage, bone, heart, and liver (Chetty et al., 2019; Hong et al., 2018; Ishiguro et al., 2019; Kuraitis et al., 2011). Clearly, stem cells have tremendous potential that can be harnessed to treat many diseases and structural damages using cell therapy and regenerative medicine strategies.

1.9 Hypothesis and significance

Perinatal MSCs have the potential to greatly impact the field of regenerative medicines using stem cell-based therapies. MSCs can differentiate into multiple lineages, such as the chondrogenic, osteogenic, and neurological lineages. However, these cells

must be cultured *in vitro* in a xenofree environment to test the feasibility and efficiency of these cells in human clinical trials. The proposed studies will allow for the growth of xenofree MSCs *in vitro* and investigate the efficacy, feasibility, and safety of these MSCs to regenerate cells and tissues in RDD and MS disease animal models.

1.10 Specific aims

The specific aims of the study will be to:

1. Examine the efficacy of xenofree medium for the isolation, culture, and characterization of perinatal MSCs. We hypothesize that MSCs can be isolated from perinatal tissues, such as the umbilical cord and placenta, and cultured in a xenofree environment that could potentially grow as well as MSCs cultured in animal-derived chemicals. To test this hypothesis, perinatal tissues will be subjected to a xenofree medium to promote the outgrowth of MSCs. The morphological and proliferation properties of the isolated MSCs will be determined by phase-contrast microscopy and calculating generation time for each passage. MSCs grown in the xenofree medium will be compared to MSCs grown in animal-based serum and will be investigated by biochemical, molecular, and immunological assays.
2. Investigate the therapeutic potential of MSCs and their derivatives for the treatment of RDD. We hypothesize that MSC derived RPCs may be more effective in the treatment of retina degeneration of an rd12 mouse model. To test this hypothesis, rd12 mice transplanted with cells will be subjected to behavioral and functionality tests for a total of 8 weeks. Animals will then be sacrificed, and the harvested retinae will be subjected to histological assays to analyze the

structure. Specific gene and protein analysis will be analyzed via qRT-PCR, RNAseq analysis, and immunohistochemical staining, respectively. The regulatory mechanism of neuroprotection and regeneration of the retina will be investigated.

3. Determine the feasibility of MSCs and their neural derivatives for the treatment of MS. We hypothesize that MSC-derived NSCs may be more effective in reducing inflammation and gliosis as well as promoting neuroprotection and neurogenesis in the EAE mouse model that mimics the pathologies of MS. To test this hypothesize, MSCs will be differentiated towards the neural lineage and transplanted in an EAE mouse model of MS. EAE mice transplanted with cells will be subjected to neurobehavioral analysis twice daily. After 17 days, EAE mice will be sacrificed, and the lungs, lymphoid, and CNS tissues will be harvested. Animal tissues will be examined via biochemical, molecular, and immunological techniques. Specific gene and protein analysis will be analyzed via qRT-PCR and immunohistochemical staining, respectively.

CHAPTER TWO

MATERIALS AND METHODS

2.1 Medium compositions used during the duration of all projects

2.1.1 Medium composition one (M1)

Medium composition one is made of DMEM nutrient mix F12 medium (DMEM/F12; Life Technologies, Carlsbad, CA, USA), supplemented with 10% fetal bovine serum (VWR, Radnor, PA, USA), and 5.6% of antibiotic solution (0.1% gentamicin, 0.2% streptomycin, and 0.12% penicillin) (Sigma, St Louis, MO, USA).

2.1.2 Medium composition two (M2)

Medium composition two is comprised of MSC NutriStem® XF Medium supplemented with MSC NutriStem® XF Supplement Mix (Sartorius, Goettingen, Germany) and 5.6% of antibiotic solution as described in 2.1.1.

2.2 Isolation of MSCs from perinatal tissues

The tissue sample was placed on large Petri dishes, which were kept on ice in a biosafety cabinet. We then rinsed the sample multiple times with ice-cold autoclaved phosphate-buffered saline (PBS) with the help of forceps. Once the outer layer of the blood was removed, the blood vessels in the cord were rinsed multiple times with ice cold PBS using a needle and syringe to remove the blood clots. The tissue was then dissected into separate sections: CL, WJ, CPJ, CH, and PC. Cleaned samples were then carefully minced into 1- to 2-mm pieces using scissors and forceps in the presence of a commercial TrypLE (Invitrogen, Carlsbad, CA, USA) solution. Minced tissue samples were then incubated at 37°C for 30 minutes in a 5.0% CO_2 incubator to digest the samples. After

the incubation period, samples were then observed under the phase-contrast microscope to confirm the partial digestion by visualization of the released cells. Equal volumes of the M1 were added to the partially digested samples to neutralize the commercial TrypLE solution. The contents from each petri dish were transferred into 50 ml centrifuge tubes. The centrifuge tubes were then centrifuged for 2 minutes at 3000 RPM to let the digested tissue pieces settle. The supernatant was then aspirated to remove the excess TrypLE. The tissue was then resuspended and plated into a 75cm^2 tissue culture flask with 9 mL of a selected culturing medium.

The explants plated culture flasks were incubated at 37°C and were not disturbed for 2-3 days to allow for the adherence of tissue pieces. After 3 days of incubation, the medium in the flask was changed with 9 ml of fresh selected culturing medium. The tissue was observed for the appearance of the outgrowth of cells from the explants and was monitored daily. When the cell outgrowth from the tissue explants reaches 70% confluence, they are split and sub-cultured. To sub-culture the outgrown cells from the explants, the cells were dissociated by adding 1 ml of commercial TrypLE solution per 75 cm^2 culture flask. The TrypLE was spread evenly throughout the flask and incubated at 37°C for 3 minutes. The trypsinized cells were neutralized with 1-2 ml of general medium and centrifuged 3000 RPM for 3 minutes. The supernatant was removed, and the cells were resuspended in 2 ml of a selected culturing medium. Cells were then counted using a hemocytometer and plated according to the cell count (104 cells/cm^2) amplification, characterization, and cryopreservation and considered to be P1.

2.3 Maintenance and culturing of MSCs *in vitro*

Primitive MSCs were maintained using M1 or M2 growth medium and incubated at 37ºC in an atmosphere of 5% CO_2 in a humidified incubator. Light microscopy images were taken daily to track growth and changes in morphology. The medium was changed daily, and cells were passaged once the cells reached 70% confluency, as described in section 2.2. Generation time was calculated using the following equation: Doubling time= duration * log(2) / (log(final concentration) – log(initial concentration)) for every passage. Using this technique produced primitive MSCs that were maintained and expanded into large numbers without losing their self-renewal and differentiation potential.

2.4 Characterization of MSCs

2.4.1 Flow cytometry analysis

Cells were grown to 70% confluency and harvested for analysis. The cells were washed with PBS and trypsinized, followed by incubation for 3 minutes. Dissociated cells were neutralized with equal volumes of selected culturing medium and were centrifuged at 3000 RPM for 3 minutes. Carefully, the supernatants were aspirated, and the pellets were re-suspended in 2 ml of PBS for the wash step to remove any of the remaining media. The cells were again centrifuged at 3000 RPM for 3 minutes. The supernatant was aspirated, and the cells were re-suspended in FACs buffer (0.1% sodium azide in 2% FBS containing PBS). Cells (100k/tube) suspended in 100 µl of FACs buffer are stained with FITC conjugated antibodies against CD44, CD49f, CD90, and APC conjugated antibodies against CD73, CD29, CD105, and RCVRN (Becton Dickinson, Franklin Lakes, NJ, USA). The cells were then incubated for 30 minutes at 4ºC in the

dark. After the incubation period, cells were centrifuged at 2000 RPM for 8 minutes at 4ºC. The supernatant was carefully removed and placed into an eppendrof to save the antibodies. The washed cell pellets were re-suspended in 200 µl of FACs buffer, transferred into the FACs tubes, placed in an ice bucket, and closed. The cells were immediately analyzed on a FACS Canto II (Becton Dickinson) using Diva Software (Becton Dickinson). The percentages of the positive cells and negative cells, representing the cell population expressing the selected MSC surface markers were analyzed.

2.4.2 Colony forming efficient assay

Cells were analyzed for the colony-forming efficiency assay to determine the self-renewal capacity and the clonal growth of the isolated cells. Cells were seeded at a concentration of 1.63 cells/cm^2 in a 100 mm petri dish. The next day, plated cells were observed under the phase-contrast microscope and counted to confirm if the number of sticking cells were equal to the number of plated cells. The selected culturing medium was changed every 3 days for 10-14 days until colonies had formed. Cell growth was monitored every other day to monitor the clonal cell growth in colonies, which was determined by the colony size/diameter increase. After 10-14 days of cell culture, cells were harvested for crystal violet staining. For crystal violet staining, cells were washed twice with PBS, fixed in 4% paraformaldehyde (Thermo Fisher Scientific, Waltham, MA, USA) for 10 minutes, and stained with 0.1% crystal violet for 1 hour. The cells in the petri dishes were the rinsed with tap water, dried and then the numbers of colonies stained with purple color were counted. Colonies were further observed under phase-contrast microscope and images were captured. Colonies consisting of a minimal cell

number of 50 cells were considered as a colony and counted. Data was recorded as total colony number per number of plated/sticking cells.

2.4.3 Trilineage differentiation of MSCs

2.4.3.1 Chondrogenic differentiation

For chondrogenic differentiation, cells were grown on a monolayer and analyzed. Cells were plated at a concentration of 10^5 cells/ 6 well in 2 ml of selected culturing medium and grown overnight. The following day, the cells were induced towards chondrogenic differentiation by replacing the selected culturing medium with the chondrogenic induction medium containing 20 ng TGFβ1 (PeproTech, Rocky Hill, NJ, USA), 10 ng insulin (Peprotech), 100 nM dexamethasone (Thermo Fisher Scientific), and 100 µM ascorbic acid (Thermo Fisher Scientific). The cells were cultured for 3 weeks and the medium was changed every 2 days or as needed. The morphology of the cells were monitored using phase-contrast microscopy and the microscopic images were taken on the medium change day. After 3 weeks of culture, the differentiated cells were harvested for analysis.

2.4.3.2 Osteogenic differentiation

Cells were plated at a concentration of 10^5 cells / well of 6-well plate with 2 ml of selected culturing medium and grown overnight. The following day, cells were induced towards osteogenic differentiation by replacing the selected culturing medium with the osteogenic induction medium containing, 0.1 µM dexamethasone (Sigma, St Louis, MO, USA), 10 µM β-glycerophosphate (Sigma), and 50 µM ascorbate-phosphate (Thermo Fisher Scientific). The cells were cultured for 3 weeks, and the medium was changed every 2 days or as needed. The morphology of the cells was monitored using phase-

contrast microscopy, and the microscopic images were taken on the medium change day for changes in morphology. After 3 weeks of culture, the differentiated cells were harvested for analysis.

2.4.3.3 Adipogenic differentiation

Cells are plated at a concentration of 10^5cells/ 6 well of a 6-well plate with 2 ml of selected culturing medium and allowed to adhere overnight. The following day, the cells were induced towards adipogenic differentiation by replacing the selected culturing medium with the adipogenic induction medium containing, 0.5 µM isobutyl-methylxanthine (Sigma), 1 µM dexamethasone (Sigma), 10 µM insulin (PeproTech), 200 µM indomethacin (Sigma). The cells were cultured for 3 weeks and the medium is changed every 2 days or as needed. The morphology of the cells was monitored using phase-contrast microscopy and the microscopic images were taken on the medium change day for changes in morphology. After 3 weeks of culture, the differentiated cells were harvested for analysis.

2.4.4 Trilineage characterization via histological analysis

2.4.4.1 Toluidine blue staining

MSCs differentiated into the chondrogenic lineage were harvested for staining, washed three times with PBS. Cells were fixed in 4% paraformaldehyde for 10 minutes at room temperature then washed three times with PBS. Cells were then stained with 1% Toluidine Blue (Sigma) solution in the dark for 1 hour at room temperature. Cells were then washed with distilled water. Cells were then counterstained with nuclear fast red stain for 10 minutes and washed with distilled water. Cells were then mounted using Fluoromount (Thermo Fisher Scientific), and visualized under a light microscope. Blue

staining indicated synthesis of proteoglycans by chondrocytes and red stain indicated the nuclei of the cells.

2.4.4.2 Alizarin red staining

MSCs differentiated into osteogenic lineage were harvested, washed three times with PBS, and fixed with 4% paraformaldehyde for 10 minutes at room temperature. After fixation, cells were washed with PBS three times. Cells were then stained with 2% Alizarin red solution (Sigma) in the dark for 1 hour at room temperature. After the staining, the cells were washed three times with distilled water. Cells were then mounted using Fluoromount (Thermo Fisher Scientific) and visualized under a light microscope. The red color indicated bone mineralization and formation of bone nodules by the differentiated derivatives.

2.4.4.3 Oil red O staining

MSCs differentiated into adipogenic lineages were harvested for staining, washed three times with PBS, and fixed in 4% paraformaldehyde for 10 minutes at room temperature. Cells were then washed with distilled water three times and incubated with 60% isopropanol for 5 minutes. After the incubation period, the isopropanol was removed, and cells were stained with 0.3% of oil red o stain (diluted 3 parts with 2 parts of distilled water) for 15-30 minutes at room temperature. The stain was carefully removed and washed three times with distilled water. Cells were then mounted using Fluoromount (Thermo Fisher Scientific), and visualized under a light microscope. Red color-stained areas of the cell represented the lipid droplets produced by the differentiated derivatives.

2.5 Differentiation of MSCs for animal studies

2.5.1 Differentiation of primitive MSCs into RPCs

MSCs were induced to differentiate towards the retinal lineage by culturing them in neurobasal media (Thermo Fisher Scientific) containing 50 ng epidermal growth factor (EGF; PeproTech), 1 µM retinoic acid (Sigma), 100 µM taurine (PeproTech), 2 mM glutamine (Sigma), 1x B27 supplement (Thermo Fisher Scientific), and 2% FBS for 2 weeks. The differentiated cells were then characterized by flow cytometry, qRT-PCR, and immunocytochemical staining analyses.

2.5.2 Differentiation of primitive MSCs into NSCs and oligodendrocytes cells (ODCs)

Primitive MSCs were induced towards the neural lineage by culturing the cells in induction media containing 10 µg EGF (PeproTech) in DMEM/F12 basal medium supplemented with 5.6% antibiotic solution for 3 days and then replaced with neural media containing 20 µg EGF, 20 ng basic fibroblast growth factor (bFGF), 2 mM Glutamine (Sigma), 1x B27 supplement (Thermo Fisher Scientific), in the neurobasal medium for 2 weeks. NSCs were differentiated into ODCs by culturing in neurobasal medium containing 2% B27, 10 ng bFGF, 10 ng PDGF-AA (PeproTech), and 100 ng SHH (PeproTech) for 2 weeks and then 0.5% FBS, 2% B27, 1x N2, and 30 ng T3 (Thermo Fisher Scientific) for an additional 10 days. Characterization of NSCs and ODCs for the expression of neural and ODC markers was performed by flow cytometry, qRT-PCR, immunocytochemical staining, and western blot analyses.

2.6 Animal models

2.6.1 Experimental animal model for RDD

All animal experiments were approved by the Institutional Animal Care and Use Committee (IACUC), Providence Hospital, Southfield, Michigan (IACUC #101-16) and Oakland University, Rochester, Michigan (IACUC #19082), as well as the Institutional Biosafety Committee (IBC), Oakland University, Rochester, Michigan (IBC #2858). A total of 84 rd12 mutant mice from Jackson Laboratory (Bar Harbor, ME, USA) were used for this study. The rd12 mice were set up in breeding triads with one male and two females and received 7-9 pups per litter. C57BL/6J mice were used as controls. All mice were maintained at the Providence Hospital Animal Facility and Oakland University Animal Facility under a 12/12-hour light and dark cycle.

2.6.2 Induction of EAE in a mouse model of MS

All animal experiments were approved by the IACUC, Oakland University, Rochester, Michigan (IACUC #18081) and the IBC, Oakland University, Rochester, Michigan (IBC #2858). 6 week old C57BL/6J mice were obtained from Jackson Laboratory (Bar Harbor), and EAE was induced by subcutaneous immunization with 200 µg of myelin oligodendrocyte glycoprotein $(MOG)_{33–35}$ peptide in complete Freud's adjuvant containing 2-5 mg killed mycobacterium tuberculosis H37Ra/mL emulsion (Hooke Laboratories, Lawrence, MA, USA). Mice were also injected intraperitoneally (i.p.) with pertussis toxin (100 ng, Hooke Laboratories) at the day of immunization and 24 hours later following the published protocol (Dupree & Feinstein, 2018). Clinical score was blindly registered according to the following scale: 0: no clinical signs, 0.5: partial limp tail, 1: limp tail, 1.5: mild impaired righting, 2: severe impaired righting, 2.5:

mild paresis of one hind limb, 3: severe paresis of one hind limb, 3.5: severe paresis of one hind limb and mild paresis of the second hind limb, 4: paresis of two hind limbs, 4.5: paresis of both hind limb and partial fore limb, and 5: severe paralysis or death (Dupree & Feinstein, 2018). Non-injected C57BL/6J mice were used as controls. All mice were monitored and assessed for clinical score twice a day and maintained at the Oakland University Animal Facility under a 12/12-hour light and dark cycle.

2.7 Labeling and Transplantation of MSCs and their derivatives in animal models

2.7.1 Fluorochrome labeling of the cells to be transplanted

Cells are labeled with long-term cell membrane labeling dye PKH26 following the instructions of the supplier. Cells are washed with PBS, trypsinized with TrypLE, neutralized, and centrifuged for 3 minutes at 3000 RPM. Cells are then further washed with DMEM without FBS and centrifuged at 2000 RPM for 5 minutes. Meanwhile, the 2X cell suspension was prepared by adding 1 ml of Diluent C to the cell pellet. Immediately, the 2X dye solution is prepared in Diluent C by adding 4-5 µl of the dye in 1 ml of the Diluent C in a centrifuge tube and mixed well. Both the solutions, cell suspension, and the dye solutions, were rapidly mixed by pipetting. Cell and dye suspension was incubated at 37°C for 5 minutes, with frequent tube mixing. The reaction was stopped by adding an equal volume of FBS and incubated at 37°C for 1 minute. The cells were then centrifuged at 2000 RPM for 10 minutes at room temperature. The supernatant was carefully removed, and cells were washed with 10 ml of selected culturing medium, then centrifuged at 2000 RPM for 10 minutes. The wash step was repeated with selected culturing medium once again, and then the labeled cells were used

for analysis. Flow cytometry and confocal microscopy were used to confirm the efficiency of fluorescent labeling of the cells before transplantation.

2.7.2 Cell transplantation in an rd12 mouse model

Cells were labeled with cell membrane labeling dye PKH26 (Sigma) as described in 2.7.1. Confocal microscopy was used to confirm the efficiency of the fluorescently labeled cells prior to transplantation. Six-week-old rd12 mice were anesthetized by intraperitoneally injecting 0.1mL/10g mixture of ketamine/xylazine (ketamine (50 mg/kg) and xylazine (7 mg/kg)). A drop of topical anesthesia (Proparacaine Hydrochloride, Ophthalmic Solution, Alcaine, Acon, Canada) was applied to the eye before transplantation, and pupils were dilated with 1% atropine and 2.5% phenylephrine hydrochloride (Ophthalmic Solution). Using a 27 G sharp disposal needle, the eye was punctured to create a hole by a blunt needle. The animals were intravitreally injected with 1 μL of DMEM containing PKH26 labeled MSCs (2×10^5) or RPCs (2×10^5) through a 32 G needle, using a 10 μL Hamilton syringe. The experiments were performed in triplicates. The animals were monitored regularly for 4 or 8 weeks after cell transplantation.

2.7.3 Cell transplantation in EAE mice

Cells were labeled with cell membrane labeling dye PKH26 (Sigma) as described in 2.7.1. Confocal microscopy and flow cytometry analyses were used to confirm the efficiency of fluorescently labeling cells before transplantation. There were eight treatments (n=6 each), 1. Untreated healthy control, 2, healthy control+MSCs, 3. healthy control+NSCs, 4. Untreated EAE, 5. EAE score 1+MSCs, 6. EAE score 1+NSCs, 7. EAE score 2+MSCs, and 8. EAE score 2+NSCs. The experiments were performed in

triplicates. The mice were restrained in a rodent restrainer for cell transplantation. 10^6 primitive MSCs or NSCs were injected intravenously via the tail vein at either clinical score 1 or 2. The mice were monitored for 15 days following cell transplantation and then euthanized humanly to collect CNS, lymphoid tissues (spleen, brain, and spinal cord), and blood for analysis.

2.8 Functional and neurobehavioral assays

2.8.1 Electroretinography

To investigate the therapeutic effect of transplanted cells on the retina function, ERG analysis was performed 1 week before the transplantation of cells in all mice and every other week thereafter. Full-field ERGs were recorded with an Espion-III system (Diagnosys LLC, Lowell, MA, USA) connected to a computer-based system. ERGs of age-matched non-transplanted rd12 eyes were used as negative controls, and C57BL/6J mice were used as positive controls. All testing was performed in a climate-controlled, electrically isolated dark room under dim red light illumination. Mice were dark-adapted for 4 hours and anesthetized with ketamine (50 mg/kg) and xylazine (7 mg/kg). Body temperature was maintained on a 37°C warming pad. Proparacaine hydrochloride droplets were used to anesthetize the eyes, and pupils were dilated with 1% atropine and 2.5% phenylephrine hydrochloride. Methylcellulose gel (Ophthalmic Solution) was applied to the eyes, and the wire loop electrodes were placed on the cornea. Needle reference and ground electrodes were inserted into the cheek and tail, respectively. Dark-adapted mice were tested with a series of dim light flashes (0.001- 25 cd.s/m^2). Eyes were then light-adapted to a constant background light for 10 minutes. Then the ERG response

traces were averaged from a series of rapidly flickering bright light flashes (15 to 30 flashes per second at an intensity of 3 cd.s/m^2) over several seconds.

2.8.2 Visual function analysis

All visual function analyses were performed the day of transplantation and every two weeks following cell transplantation. To measure visual recovery, mice were placed in a small cage for 5 minutes prior to testing. A long Q-tip was then placed in front of the eye and the reaction time of the mouse moving its head away or recognizing the Q-tip was recorded. A score from 0-4 was given to each test (0: No head movement, 1: >1 second delay for head movement, 2: 1 second delay for head movement. 3: <1 second delay for head movement, and 4: Immediate head movement). The non-transplanted rd12 mice were used as a negative control. The C57BL/6J mice were used as positive controls. The visual recovery scale is found in Table 5. For the visual acuity assay, optokinetic reflex (OKR) was used. The mice were placed onto a small cylinder in the center of the apparatus to allow full movement. Monitors were attached to the walls of the apparatus. A video that displayed vertical alternating black and white lines moved from left to right of the screen at a constant speed. The movement of the mouse was recorded. To obtain the visual acuity of each condition, the cycles per degree (cpd= 1/[2arctan(h/2a)]) was calculated. The non-transplanted rd12 mice were used as a negative control. The C57BL/6J mice were used as positive controls.

2.9 Cell tracking

2.9.1 Harvesting retina for cell tracking

The animals were sacrificed by CO_2 overdose, and the eyes were harvested after 4 weeks or 8 weeks post-transplantation. For OCT embedding, eyes were fixed in 4%

Table 5. Visual recovery scale

Score	Description
0	No Head Movement
1	More than 1 second delay of head movement
2	1 second delay of head movement
3	Less than 1 second delay of head movement
4	Immediate Head Movement

paraformaldehyde for 10 minutes, placed in 10% sucrose for 30 minutes, and then in 30% sucrose overnight at 4^{o}C. The eyes were then embedded in OCT medium (Thermo Fisher Scientific) and sectioned (6–10 μm thick) using a cryostat. The sections were observed under confocal microscopy for presences of PKH26 dye (Cy3) labeled cells throughout the retina. To mount for cell tracking, the retinas were flattened with 4-5 relaxing cuts, fixed in 4% paraformaldehyde, stained with anti-mouse RCVRN primary antibody, followed by staining of Alexa flour 488 secondary antibodies (Thermo Fisher Scientific) and analyzed by fluorescent images captured using a confocal microscope (NIKON Instruments Inc, Melville, NY, USA

2.9.2 Harvesting CNS, lymphoid tissues, and blood for cell tracking

Blood and tissue samples were placed in red blood cell lysis buffer for 5 minutes and then homogenized, except blood samples, in a centrifuge tube. Cell culture medium

was then added to the tube, inverted, and centrifuged at 1300 rpm for 5 minutes at 4°C. The supernatant was discarded, and cells were resuspended in PBS. The cells were then filtered through a cell strainer. Labeled cells in each sample were determined using the FACS Canto II (Becton Dickinson) and Diva Software (Becton Dickinson).

2.10 Histological analysis

2.10.1 Paraffin sectioning

The animals were sacrificed by CO_2 overdose and the eyes were harvested after 4 weeks or 8 weeks post-transplantation. For paraffin embedding, eyes were fixed in 97% methanol and 3% acetic acid for 48 hours at -80°C. Eyes were then transferred to -20°C for 4 hours and then 48 hours at room temperature. Eyes were then dehydrated in 100% ethanol for 15 minutes and repeated thrice, and then transferred to xylene for 15 minutes and repeated twice. Eyes were then imbedded in paraffin and sectioned (5-10 μm thick) using a microtome.

For paraffin embedding of the brain and spinal cord tissue, samples were fixed with 4% paraformaldehyde for 24 hours. They were then dehydrated in 70% ethanol for 1 hour, 95% ethanol for 1 hour, 100% ethanol for 4 hours, xylene for 2 hours, and paraffin for 3 days. Tissue samples were then imbedded in paraffin and sectioned (5-10 μm thick) using a microtome.

2.10.2 Hematoxylin and Eosin (H&E) staining

Retina tissue sections were dehydrated with xylene for 4 minutes, followed by 100% ethanol, 95% ethanol, 70% ethanol for 2 minutes each. The sections were then washed with distilled water for 1 minute, then stained with hematoxylin (Sigma) for 45 seconds. The sections were then rinsed with 95% ethanol for 1 minute and counterstained

with eosin (Sigma) for 45 seconds. The sections were then washed with 95% ethanol for 1 minute and 100% ethanol for another minute. The sections were then cleaned with xylene for 2 minutes. The sections were then mounted with Permount (Thermo Fisher Scientific).

Brain, spinal cord, and spleen tissues were dehydrated with xylene for 5 minutes twice, followed by 100% ethanol, 95% ethanol, 70% ethanol, 50% ethanol for 2 minutes each. The sections were then washed with distilled water for 2 minute, then stained with hematoxylin (Sigma) for 15 minutes. Sections were then washed with tap water for 5 minutes. The sections were then rinsed with 95% ethanol for 30 seconds and counterstained with eosin (Sigma) for 30 seconds. The sections were then washed with 95% ethanol for 1 minute and 100% ethanol for another minute. The sections were then cleaned with xylene for 2 minutes. The sections were then mounted with Permount (Thermo Fisher Scientific).

2.10.3 Luxol fast blue (LFB) staining

Brain and spinal cord tissues were dehydrated with xylene for 5 minutes twice followed by 100% ethanol and 95% ethanol and 2 minutes each. The sections were then stained with Luxol fast blue solution (Sigma) for 24 hours at 57ºC, followed by an additional 2 hours at 60ºC. The sections were then washed with 95% ethanol for 1 minute, then distilled water for an extra minute. The stained sections were then differentiated with lithium carbonate solution (Thermo Fisher Scientific) for 30 seconds and then continued to differentiate with 70% ethanol for 20 seconds. The sections were washed with distilled water for 1 minute. Sections were then stained with cresyl violet solution (Sigma) for 5 minutes at 57ºC. Sections were then differentiated again with 95%

ethanol, then dehydrated with 100% ethanol and xylene for minutes each. The sections were then mounted with Permount (Thermo Fisher Scientific).

2.11 Analysis of retina thickness

The retina embedded in paraffin was sectioned at 5-10 μm and stained with H&E. The same location of the retina was selected for each eye, and the thickness of the whole retina, ONL, INL, and RGC was measured by Image J (NIH, Bethesda, MD, USA).

2.12 Quantification of Treg and Th17 cells in the blood, spleen, and CNS tissues

For flow cytometry analysis, the tissue samples were processed as stated above for cell tracking. Isolated cells (10^6) from each tissue were stained with CD25, IL-17A (FITC labeled antibodies), or CD4 (APC labeled antibodies) (Becton Dickinson). Labeled cells were analyzed on a FACS Canto II (Becton Dickinson) using Diva Software (Becton Dickinson).

2.13 T cell proliferation assay

Splenocytes isolated from control and EAE mice were cultured in 96-well plates (2×105 cells/well) using RPMI1640 medium (Gibco, Waltham, MA, USA) supplemented with 10% FBS and 5.6% of the antibiotic solution in the presence or absence of MOG peptide (10 μg/ml) at 37°C in 5% CO2 for 72 hours. Then MSCs or NSCs (1×103 cells/well) were added and incubated for an additional 24 hours. Measurement of T cell proliferation was performed using BrdU proliferation kit (Novus Biologicals, Centennial, CO, USA), according to the manufacturer's instructions.

2.14 Immunocytochemical and immunohistological staining

Cells were fixed with 4% paraformaldehyde for 10 minutes at room temperature, permeabilized with 0.5% Triton X-100 (Sigma) and blocked with 2% bovine serum

albumin (Sigma) for 1 hour. Cells were then stained with primary antibodies at 1:100 dilution at 4ºC overnight, followed by staining secondary antibodies at 1:200 dilution at room temperature for 2 hours (Table 6). Cells were counterstained with DAPI at 1:100 dilution for 5 minutes at room temperature. Fluorescent images were captured using a confocal microscope (NIKON Instruments Inc.). Fluorescent intensity was calculated using ImageJ software (NIH). To quantify the fluorescent intensity the following equation was used, fluorescent intensity = integrated density – (area of selected cell x mean fluorescence of background readings).

To detect the expression of human neural and inflammatory markers expressed by mouse retina, brain and spinal cord tissue, the sections were stained with primary antibodies 1:100 dilution at 4ºC overnight followed by staining of secondary antibodies at 1:200 dilution at room temperature for 2 hours (Table 6). They were counterstained with DAPI at 1:100 dilution for 5 minutes at room temperature. Representative fluorescent images/sections of the randomly selected stained areas were captured using a confocal microscope (NIKON Instruments Inc.).

2.15 qRT-PCR analysis

Isolation of the total cellular mRNA from cells and tissue was done using the GeneJET RNA purification kit (Thermo Fisher Scientific) following the manufacturer's instructions. Total RNA was purified with DNase and incubated at 37ºC for 30 minutes using a thermocycler (Bio-Rad, Hercules, CA, USA). cDNA was synthesized using iScript kit (Bio-Rad). qRT-PCR was performed by using Sso-Advanced Universal SYBR Green Supermix Kit (Bio-Rad) on CFX96 Real-Time System (Bio-Rad). A 10 µL reaction was used which included 5 µL Sybr green, 3 µL of distilled water, 0.5 µL of

Table 6. List of primary and secondary antibodies used in immunocytochemical analysis

Antibody	Primary	Secondary
ACAN	Rabbit Polyclonal	Anti-Rabbit- Alexa Fluor 488
SOX9	Goat Polyclonal	Anti-Goat- Alexa Fluor 564
COL2	Goat Polyclonal	Anti-Goat- FITC
COL1	Goat Polyclonal	Anti-Goat- FITC
OCN	Rabbit Polyclonal	Anti-Rabbit- Alexa Fluor 488
TUJ1	Mouse Polyclonal	Anti-Mouse- Alexa Fluor 488; Anti-Mouse-Cy3
NESTIN	Mouse Polyclonal	Anti-Mouse-Cy3
PAX6	Rabbit Polyclonal	Anti-Rabbit- Alexa Fluor 488
RCVRN	Mouse Polyclonal	Anti-Mouse- Alexa Fluor 488; Anti-Mouse-Cy3
CRX	Rabbit Polyclonal	Anti-Rabbit- Alexa Fluor 488
RHO	Mouse Polyclonal	Anti-Mouse-Cy3
CD90	Mouse Polyclonal	Anti-Mouse- Alexa Fluor 488
RPE65	Mouse Polyclonal	Anti-Mouse- Alexa Fluor 488
VIMENTIN	Rabbit Polyclonal	Anti-Rabbit- Alexa Fluor 488
OLIG2	Rabbit Polyclonal	Anti-Rabbit- Alexa Fluor 488
SOX10	Rabbit Polyclonal	Anti-Rabbit- Alexa Fluor 488
O4	Mouse Polyclonal	Anti-Mouse- Alexa Fluor 488; Anti-Mouse-Cy3
MBP	Mouse Polyclonal	Anti-Mouse-Cy3
MOG	Mouse Polyclonal	Anti-Mouse-Cy3

Table 6. List of primary and secondary antibodies used in immunocytochemical analysis continued

Antibody	Primary	Secondary
CD45	Rabbit Polyclonal	Anti-Rabbit- Alexa Fluor 488
CD68	Mouse Polyclonal	Anti-Mouse-Cy3
CD3E	Mouse Polyclonal	Anti-Mouse-Cy3
GFAP	Rabbit Polyclonal	Anti-Rabbit- Alexa Fluor 488
MOG	Rabbit Polyclonal	Anti-Rabbit- Alexa Fluor 488
MBP	Mouse Polyclonal	Anti-Mouse-Cy3
HNA	Mouse Polyclonal	Anti-Mouse-Cy3

forward primer, 0.5 µL of reverse primer, and 1 µL of 1:10 diluted cDNA. Each reaction was exposed to the following conditions: 98°C for 10 minutes, followed by 30 seconds of 98°C, 20 seconds of 60°C, and 30 seconds of 72°C for 44 cycles in 96-well optical reaction plates (Bio-Rad). The reference genes, *GAPDH* and *β-ACTIN*, were used to normalize the targeted genes. Each reaction was performed in triplicate. Primer sequences are listed in Table 7.

2.16 Western blot analysis

Cells were lysed using RIPA buffer (Sigma) and protein was quantified using the PierceTM 660 nm protein assay kit and NanoDrop 1000 spectrophotometer (Thermo Fisher Scientific). The cell lysate (30 µg of total proteins) was resolved using SDS-PAGE with 12% resolving gel and 6% stacking gel and transferred to a nitrocellulose membrane (Bio-Rad) at a continuous current of 100V for 90 minutes. For antibody staining, the membrane was blocked with 5% nonfat dry milk dissolved in TBS 1X containing 0.1% Tween-20 (TBST) for 30 minutes and incubated with primary antibodies at a 1:500 dilution (Table 8) in the blocking solution overnight at 4°C. The membrane was then

Table 7. List of primer sequences used in qRT-PCR

Gene	Primer Sequence	Product Length (bp)
hABCG2	F-CTGAGCTCGTCCCCTGGAT	182
	R-CTTTTGAGTGGGCACAGCAC	
hACAN	F-AGCCTGCGCTCCAATGACT	103
	R-GGAACACGATGCCTTTCACC	
hATP1B1	F-CCCAAATGTCCTTCCCGTTCA	137
	R-GCAGGAGTTTGCCATAGTACG	
hBDNF	F-TGGCTGACACTTTCGAACAC	200
	R-CCTCATGGACATGTTTGCAG	
hBDNF	F-AAGCCTTTTCCTCCTGCTGT	80
	R-ATCCGTTGGCTCTGTCCAAG	
hBEST1	F-TGCCAACCTGTCAATGAAGG	125
	R-TCCAGTCGTAGGCATACAGG	
hBMP2	F-TGTATCGCAGGCACTCAGGT	133
	R-CCACTCGTTTCTGGTAGTTCTTC	
hCALBINDIN	F-ATTTCGACGCTGACGGAAGT	99
	R-GAGCCAACAATCCAGCCTTCT	
hCALRETININ	F-AAACTCCTCTGAGGTCAGCTT	99
	R-CCGCTTCTATCCGGGACATC	
hCCL2	F-GATCTCAGTGCAGAGGCTCG	155
	R-TTTGCTTGTCCAGGTGGTCC	
hCD24	F-CACGCAGATTTATTCCAGTGAAAC	150
	R-ACCACGAAGAGACTGGCTGT	

Gene	Primer Sequence	Product Length (bp)
hCD3E	F-TCCCAACCCAGACTATGAGC	158
	R-CAAGACTAGCCCAGGAAACAG	
hCD90	F-GAAGGTCCTCTACTTATCCGCC	143
	R-TGATGCCCTCACACTTGACC	
hCEBPβ	F-TATAGGCTGGGCTTCCCCTT	94
	R-AGCTTTCTGGTGTGACTCGG	
hCNTF	F-AGGAAGATTCGTTCAGACCT	156
	R-GTTCTCTTGGAGTCGCTCTG	
hCNTF	F-CTGTAGCCGCTCTATCTGGC	112
	R-CGCAGAGTCCAGGTTGATGT	
hCOL1	F-AAGGTCATGCTGGTCTTGCT	114
	R-GACCCTGTTCACCTTTTCCA	
hCOL2	F-CTCGTGGCAGAGATGGAGAA	252
	R-CACCAGGTTCACCAGGATTG	
hCRX	F-CCTTCTGACAGCTCGGTGTT	173
	R-CCACTTTCTGAAGCCTGGAG	
hDACH1	F-TGGAGCAGACTCTGAAAACGG	137
	R-GGTGGTTCATCTGGCTCATTG	
hDHRS3	F-GGCACTGAGTGCCATTACTTC	114
	R-GGCATTGTTCACCAGGATGGT	
hEBF1	F-ATGTCTCCGAGGCATCACAAG	127
	R-ATGCTCGTGGTGACGGAGTT	
hEGF	F-AAGAATGGGGGTCAACCAGT	69

Gene	Primer Sequence	Product Length (bp)
	R-TGAAGTTGGTTGCATTGACC	
hFABP4	F-TTAGATGGGGGTGTCCTGGT	158
	R-GGTCAACGTCCCTTGGCTTA	
hFABP7	F-AGAAACTGTAAGTCTGTTGTTAGCC	255
	R-AAAGAACCTTGCCAGTGATGT	
hFGF	F-GCTTCTTCCTGCGCATCCA	353
	R-GCTCTTAGCAGACATTGGAAGA	
hFGF	F-TCCACCTATAATTGGTCAAAGTGGT	121
	R-CATCAGTTACCAGCTCCCCC	
hFZD5	F-GAACGCTTCCGCTATCCTGA	144
	R-GGTCTCGTAGTGGATGTGGTTG	
hGAPDH	F-GAAGGTGAAGGTCGGAGTC	226
	R-GAAGATGGTGATGGGATTTC	
hGDNF	F-CCAGAGGAAAAGGTCGGAGA	96
	R-CATAGCCCAGACCCAAGTCA	
hGDNF	F-TTCGGATCTCCAGGCAAGAC	361
	R-CAGGTCAGGGGCAAGAGTTC	
hGJA1	F-GGAGATGAGCAGTCTGCCTTT	149
	R-TGAGCCAGGTACAAGAGTGTG	
hGLUL	F-CTGCCATACCAACTTCAGCAC	112
	R-ATAGGCACGGATGTGGTACTG	
hGNAT2	F-GGAGTCAGGAAAGAGCACCATC	128
	R-TGATAGCCAGGATGGACTGCA	

Gene	Primer Sequence	Product Length (bp)
hGNL3	F-CTTTCCCAGGCTGATGCTCG	149
	R-AGCAGTTTGGCAGCACCTTC	
hGPNMB	F-GTGCTCAATGGAACCTTCAGC	150
	R-AGGAATCCTACTCAGCTCCAGG	
hHES1	F-GGAAATGACAGTGAAGCACCTC	129
	R-AAGCGGGTCACCTCGTTCAT	
hIGF	F-CCAAGACCCAGAAGGAAGTACA	109
	R-TGGCATGTCACTCTTCACTCC	
hIGFBP5	F-GTGCTGTGTACCTGCCCAA	104
	R-CTTGTCCACGCACCAGCAG	
hIL-10	F-TCTCCGAGATGCCTTCAGC	126
	R-TCAGACAAGGCTTGGCAAC	
hIL-1β	F-CCACAGACCTTCCAGGAGAATG	131
	R-GTGCAGTTCAGTGATCGTACAG	
hIL-2	F-AGAACTCAAACCTCTGGAGGAAG	153
	R-GCTGTCTCATCAGCATATTCACAC	
hIL-4	F-CCGTAACAGACATCTTTGCTGC	208
	R-AGTGTCCTTCTCATGGTGGCT	
hIL-6	F-AGACAGCCACTCACCTCTTCAG	132
	R-TTCTGCCAGTGCCTCTTTGCTG	
hLHX2	F-GACAGACTTGACTAGCCCCAC	312
	R-TCCAAGTTGTTCCTCGGTCC	
hMBP	F-AGGATTTGGCTACGGAGGCAGA	150

Gene	Primer Sequence	Product Length (bp)
	R-GGTTTTCAGCGTCTAGCCATGG	
hMIS18BP1	F-ACGAGAAAACCAAACAGATACTGC	111
	R-TCTGTAGCTCCTGGTGACTCA	
hMITF	F-GGCTTGATGGATCCTGCTTTG	130
	R-GAAGGTTGGCTGGACAGGAG	
hMKI67	F-GAAAGAGTGGCAACCTGCCTT	151
	R-GCACCAAGTTTTACTACATCTGCC	
hMOG	F-GAGCCTGATAGTGGAACTTCTCG	131
	R-TGAGAGGCTGAACAGACTCCAC	
hNDRG1	F-ATCACCCAGCACTTTGCCG	123
	R-GACTCCAGGAAGCATTTCAGC	
hNESTIN	F-GAAACAGCCATAGAGGGCAAA	168
	R-TGGTTTTCCAGAGTCTTCAGTGA	
hNF200	F-TGTGCTCCTGGCTTCTTACG	72
	R-TGTGCTCCTGGCTTCTTACG	
hNOTCH1	F-GGTGAACTGCTCTGAGGAGATC	150
	R-GGATTGCAGTCGTCCACGTT	
hNRL	F-ATTGGGGCTGAGTCCTGAAGA	141
	R-TCGGAAAACCGCTCTGCCA	
hO4	F-ACTGCTGCTGACTGTTCTTC	283
	R-GTAGAAACGGTTTTCACCAA	
hOCN	F-TAAACAGTGCTGGAGGCTGG	191
	R-CTTGGACACAAAGGCTGCAC	

Gene	Primer Sequence	Product Length (bp)
hOLIG2	F-CCAGAGCCCGATGACCTTTTT	178
	R-CACTGCCTCCTAGCTTGTCC	
hOPN	F-CATACAAGGCCATCCCCGTT	112
	R-TGGGTTTCAGCACTCTGGTC	
hOTX2	F-AAATCTCCCTGAGAGCGGGA	98
	R-GTAGATGTGGCGAGTGAGGG	
hPAX6	F-AATAACCTGCCTATGCAACC	206
	R-ACTTGAACTGGAACTGACAC	
hPAX6	F-TCAAGCAACAACAGCAGCAC	239
	R-TCACTCCGCTGTGACTGTTC	
hPCNA	F-CAAGTAATGTCGATAAAGAGGAGG	126
	R-GTGTCACCGTTGAAGAGAGTG	
hPDGF	F-AAAGAAGTTCCAGACCATCCC	119
	R-AGGTGACCACAATCGTTTCC	
hPLPP3	F-GTATCAGACCACAAGCACCA	122
	R-AGGGAGAGCGTCGTCTTAGT	
hPMEL	F-GGTGAGGGGGATGCATTTGA	258
	R-CCCAGGCACAGGCATGATAA	
hPMEPA1	F-CTGAGCCACTACAAGCTGTCTG	128
	R-ATTCCGTTGCCTGACACTGT	
hPPARγ	F-GGCTTCATGACAAGGGAGTTTC	74
	R-AACTCAAACTTGGGCTCCATAAAG	
hPROX1	F-GAGGGTGGGAAAGGGGTTTT	204

Gene	Primer Sequence	Product Length (bp)
	R-TCAAACGGCACTGAGCTTGT	
hPTK7	F-GTCTGAGCCGAGAGTTTGCT	95
	R-TGCGGATGGTCTTTTCTCCC	
hRCVRN	F-TTCAAGGAGTACGTCATCGCC	105
	R-GATGGTCCCGTTACCGTCC	
hRHO	F-CTTCGCAGCATTCTTGGGTG	79
	R-GTTAGGGCCTTCTGTGCCAT	
hRPE65	F-TACCACCTGTTTGATGGGCAA	360
	R-GGCCCCATTGACAGAGACAT	
hRPS27A	F-AGAGACTCGGCGGTTGAAAG	227
	R-TCCCCGTAAGGGTTTTCACG	
hRUNX2	F-TGCTTCATTCGCCTCACAAA	111
	R-AGTGACCTGCGGAGATTAAC	
hS100A11	F-CCAGAAGTATGCTGGAAAGGATG	130
	R-CATCATGCGGTCAAGGACAC	
hSERPINF1	F-TGAAGGCGAAGTCACCAAGTC	141
	R-CCATCCTCGTTCCACTCAAAG	
hSIX3	F-TGATGTTGCGGGCAGAAAAC	195
	R-GTCCTCGTGGTGGTGATTGA	
hSIX6	F-TACGCAGGTGGGCAACTG	100
	R-CCCGGAACCCTGTGACAG	
hSOX9	F-AGCGAACGCACATCAAGAC	85
	R-CTGTAGGCGATCTGTTGGGG	

Gene	Primer Sequence	Product Length (bp)
hSOX10	F-ATGAACGCCTTCATGGTGTGGG	131
	R-CGCTTGTCACTTTCGTTCAGCAG	
hSPON1	F-TGTAGCTGACCTGGCTCCAG	123
	R-CGCATCCTCTTGCCTTTGTC	
hSSEA4	F-GGGTTTGGATGAACTTCGAGTC	123
	R-GGTAGCCATAAGGCACAAAGAC	
hSULF2	F-CGGGACTCCTTCTTGGTGGA	130
	R-GGTACTCAGCACGCTGACAC	
hTFAP2A	F-GACCTCTCGATCCACTCCTTAC	137
	R-GAGACGGCATTGCTGTTGGA	
hTNF-α	F-CCCAGGGACCTCTCTCTAATCA	116
	R-AGCTGCCCCTCAGCTTGAG	
hTUJ1	F-GGCCAAGTTCTGGGAAGTCA	70
	R-CGAGTCGCCCACGTAGTTG	
hTYRP1	F-TCTCAATGGCGAGTGGTCTGT	145
	R-CCTGTGGTTCAGGAAGACGTT	
hVIMENTIN	F-TGTCCAAATCGATGTGGATGTTTC	117
	R-TTGTACCATTCTTCTGCCTCCTG	
hβ-ACTIN	F-AATCTGCGACCACACCTTCTAC	170
	R-ATAGCACAGCCTGGATAGCAAC	
hβ-ACTIN	F-CTCGCCTTTGCCGATCC	298
	R-TCTCCATGTCGTCCCAGTTG	
hβ-CATENIN	F-GGCCAGGAGAAGGGAGCA	107

Gene	Primer Sequence	Product Length (bp)
	R-GAGAGATGCCGACTTCCGAG	
mAbcg2	F-CACCATCCAACAGGCCTAGAAT	191
	R-CATCCTAGGAAGGCCGTTGT	
mAif1	F-TGAGGAGATTTCAACAGAAGCTGA	163
	R-CCTCAGACGCTGGTTGTCTT	
mAkt	F-ATCCCCTCAACAACTTCTCAGT	156
	R-CTTCCGTCCACTCTTCTCTTTC	
mApod	F-GGTGAAGCCAAACAGAGCAAC	127
	R-AGGAGTACACGAGGGCATAGT	
mAscl1	F-CTTAGCCCCCTGAAACTGGG	165
	R-AGAAGCAAAGACCGTGGGAG	
mAtp1b1	F-CCTTCCCGGTGACTTTCCCTC	78
	R-GCTGTAGCTGCACCACTCTG	
mBdnf	F-GGGTCACAGCGGCAGATAAA	86
	R-GCCTTTGGATACCGGGACTT	
mBest1	F-TTCAGACACAGGTGATGGGC	325
	R-ACTGTCGTGGGAACACACTC	
mBlbp	F-CAGTCAGGAAGGTGGCAAAGT	146
	R-GCTTGTCTCCATCCAACCGAA	
mBmpr	F-CGCTCCTTATCTTACGCCCG	105
	R-CTCCGGATCACGTAGCGAAA	
mCalbindin	F-CTTGCTGCTCTTTCGATGCC	104
	R-GTTCCTCGGTTTCGATGAAG	

Gene	Primer Sequence	Product Length (bp)
mCalretinin	F-ATGAACTGGACGCCCTCCT	140
	R-GAGCACAATCTCCAGGTCCTTT	
mCcl2	F-GCTACAAGAGGATCACCAGCAG	106
	R-GTCTGGACCCATTCCTTCTTGG	
mCcn1	F-AGAGGCTTCCTGTCTTTGGC	135
	R-CTCGTGTGGAGATGCCAGTT	
mCcnd1	F-AAAATGCCAGAGGCGGATGA	270
	R-GAGGGGGTCCTTGTTTAGCC	
mCd24	F-TTCGCATGGTCACACACTGA	124
	R-ACACACACAGTAGCTTCGGG	
mCd300lf	F-GATGCTGGCATTTACTGGTGT	132
	R-GGTTGTCACTGTGAAGATGGT	
mCd3e	F-GTGCCCTCTAGACAGTGACG	393
	R-GGCTCATAGTCTGGGTTGGG	
mChrnb4	F-TGCTCCTCGTCTCTCTGTTC	479
	R-GTTCTGCTGGTCGAAGGGAA	
mCmklr1	F-AGCTCTAGGGTCTGCTACCT	184
	R-GAATGTCCTCCGACTCGCTT	
mCntfrα	F-CTTGTGAAGGTCAGATGGGTCT	187
	R-CACCAAGACACAGGCCCAAA	
mCreb	F-TGTACCACCGGTATCCATGC	312
	R-TCTTCAATCCTTGGCACCCC	
mCrx	F-CTGGGCCACAGTCTCTGAAG	107

Gene	Primer Sequence	Product Length (bp)
	R-CTGGTGCATCAGGTCCACAT	
mCtsz	F-GTCAGCAACGATGGCATCGA	98
	R-TTGTAGGTGCTGGTCACGAT	
mCxcr4	F-GTGCAGCAGGTAGCAGTGAA	447
	R-ACGCTGCTGTAGAGGTTGAC	
mDcx	F-CTGACTCAGGTAACGACCAAGAC	102
	R-TTCCAGGGCTTGTGGGTGTA	
mEgfr	F-GGACTGTGTCTCCTGCCAGA	129
	R-GGCAGACATTCTGGATGGCA	
mErk1	F-ACACTGGCTTTCTGACGGAG	369
	R-TGATGCGCTTGTTTGGGTTG	
mErk2	F-CAGTGGAATTAAAAAGGGTGGCA	193
	R-AGCTCATCGTCAGCAGTAGC	
mEsm1	F-TTACCCGGAGGACCTTAGCA	190
	R-GGTTGCGCTTACATTCACGG	
mFabp7	F-TGGGAAACGTGACCAAACCA	178
	R-AGCTTGTCTCCATCCAACCG	
mFcgr2b	F-ACTGTGGACAGCCGTGCTAA	105
	R-ACCGTGTCTTCCTTGAGCAC	
mFgfr	F-ATGGAAAGTGTGGTCCCGTC	300
	R-TATCCCCGAGTGCTTCAGGA	
mFn1	F-CCCTATCTCTGATACCGTTGTCC	145
	R-TGCCGCAACTACTGTGATTC	

Gene	Primer Sequence	Product Length (bp)
mFos	F-GGGAATGGTGAAGACCGTGT	126
	R-GCAGCCATCTTATTCCGTTCC	
mGapdh	F-CCCTTAAGAGGGATGCTGCC	263
	R-ACTGTGCCGTTGAATTTGCC	
mGdnf	F-GAGCTGGCAAAGCTAGCACC	207
	R-CAGCTGTTGGGTTCGGAGAT	
mGfap	F-TGAATCGCTGGAGGAGGAGA	311
	R-AAGGGAGAGCTGGCAGG	
mGja1	F-GTGAGGGAAGTACCCAACAGC	76
	R-GGAAAAGGAGAGTTCGGGCT	
mGlul	F-TCACCTGATGGATGGCCCTA	307
	R-GCAGGGAAACCCTAAGCAGT	
mGnat2	F-CGGGTAAGGAGTCTCAAGGC	197
	R-CACTGATGCCACTCCCCATT	
mGnl3	F-GGAACTAAGACCGCTGGAGG	185
	R-ACACCAGCTTAGCAGCACTT	
mGpnmb	F-TCTCCTCAGTCACGCGAAAG	301
	R-CCACCCCACGAACAGTGTAA	
mGrik3	F-GTATGGAGTCGCCCATCGAC	124
	R-TGGTTGGAATCCAGGTCCCC	
mHes1	F-TTACTGCCTTGGCTCACTCC	160
	R-TTACGTCCTTTCGCCCTCAC	
mHes5	F-ACCCATAATGAGCCTTCCTTCAG	223

Gene	Primer Sequence	Product Length (bp)
	R-GGGCGAAGGGACAGTAGTTG	
mIfnγ	F-CGGCACAGTCATTGAAAGCC	199
	R-GTTGCTGATGGCCTGATTGTC	
mIgf	F-ATGTTCCCCCAGCTGTTTCC	272
	R-TGCTGATTTTCCCCATCGCT	
mIl-10	F-CGGGAAGACAATAACTGCACC	130
	R-CGGTTAGCAGTATGTTGTCCAG	
mIl-17a	F-ATCCCTCAAAGCTCAGCGT	170
	R-GGGTCTTCATTGCGGTGGA	
mIl-1β	F-AACCTGCTGGTGTGTGACGTTC	78
	R-CAGCACGAGGCTTTTTTGTTGT	
mIl-2	F-TGGAGCAGCTGTTGATGGAC	351
	R-AGATGATGCTTTGACAGAAGG	
mIl-4	F-ATCATCGGCATTTTGAACGAGG	125
	R-ACCTTGGAAGCCCTACAGAC	
mIl-6	F-CCGGAGAGGAGACTTCACAG	421
	R-GGAAATTGGGGTAGGAAGGAC	
mIrak3	F-CTGCAAAGTGGTGCTGGATG	143
	R-GCTTTGCAGAGAAGTTCCGAG	
mJak1	F-GACCAGGCAAGATCCAGACA	173
	R-CTACCTGCTCCCCTGTGTTG	
mJak2	F-GCTACCAGATGGAAACTGTGC	147
	R-GCCTCTGTAATGTTGGTGAGATC	

Gene	Primer Sequence	Product Length (bp)
mKrox-20	F-GACACTACTTTCCACCGTGT	212
	R-GATACGGGAGATCCAGGGGT	
mLhx2	F-CTCCACGGACCCTGATTGAT	429
	R-AGCAGGTAGTAGCGGTCAGA	
mMbp	F-TCCATCGGGCGCTTCTTTAG	90
	R-AAACCCACAGCTTCTCTACGG	
mMcm2	F-CCGTTCCAAGGATGCCATTC	127
	R-TGGAAAGCCGTTGGCGGTGT	
mMek1	F-AGCCAGTTGCTTTCCTTTAGTTA	409
	R-TTCCCTCTGGTGTGAACTGC	
mMek2	F-GCATTGCGGTTCCTGTATGG	178
	R-TGGTGCTTCTCTCGGAGGTA	
mMitf	F-TCCCCACAGAGTCTGAAGCA	312
	R-CTCTAGCCTGCATCTCCAGC	
mMki67	F-ACCATCATTGACCGCTCCTTT	209
	R-AGGCCCTTGGCATACACAAA	
mMme	F-CGGTGTGACAGGATTTGGGA	211
	R-GCATTCCTTGGACCCTCACC	
mMmp12	F-CACACTTCCCAGGAATCAAG	119
	R-TTTGGTGACACGACGGAACA	
mMog	F-AGGAAGGGACATGCAGCCG	166
	R-CTGCATAGCTGCATGACAACTG	
mMpz	F-GTCAAGTCCCCCAGTAGAA	151

Gene	Primer Sequence	Product Length (bp)
	R-AGGAGCAAGAGGAAAGCAC	
mNcam	F-GGTTCCGAGATGGTCAGTTGCT	158
	R-CAAGGACTCCTGTCCAATACGG	
mNecab2	F-TCCCCTTCTATGATGGGAAGCTGT	459
	R-TGTGGTTGGGGATGTAGGGA	
mNestin	F-CCTTCTCTAGTGCTCCACGTC	104
	R-CGTCGATTGAGCTCCCACAT	
mNeuN	F-GTGGCTGACTGTGCTGTTTGG	232
	R-ACTGTTGGGGTGTCGTCTAC	
mNfl-b	F-TGCGTGCTGCATTGGTATTG	213
	R-CCTAGGAACATCAGAGCCGC	
mNog	F-CACAGAGAAACAAGACGCCG	150
	R-GGTCGGGCATCCGAGATTAC	
mNr4a3	F-TGGCATTGTGCTAGTCAGCTT	141
	R-AGGTGTAGCCCTGTCAGGAT	
mNrl	F-CACGGGGAAAAGGGACGAC	76
	R-GAACCAGAAAGGCACAGCTTC	
mOsmr	F-CCACTTCTGGAAATGGAGCGA	114
	R-ATGCGTCTTCCATTCTCCGAC	
mOtx2	F-TGGTTGGAGAGTTTGCGTCA	99
	R-CAGTGGAGGCTGAGTTGGAG	
mp53	F-AACTGCTAGCTCCCATCACT	421
	R-GAGGGCCCAAGATAGAATCTTAC	

Gene	Primer Sequence	Product Length (bp)
mPax6	F-GCCACCAGACTCACCTGACAC	333
	R-GGACTTTTGCATCTGCATGGG	
mPcna	F-AGATGCCGTCGGGTGAATTT	126
	R-TGTTCCCATTGCCAAGCTCT	
mPi3k	F-CATCAGTGGCTCTGCGGTTT	148
	R-GTGGTCTTCTGGGAACTCACCT	
mPlpp3	F-CTGTGACGAGGAACTGCCAT	154
	R-TTGACCAGGTCTGTGCATCC	
mPmel	F-GCCACATGGTAGCACTCACT	220
	R-AACAAAAGCCCTCCCGCAAG	
mPou4f2	F-AGAAATCCCACCGCGAGAAG	126
	R-TTGGCTGGATGGCGAAGTAG	
mProx1	F-TTGGTTCCTGCTCATCTCTGG	95
	R-AGGGCCTTGGGCAAAAGTAA	
mPrss56	F-ACCTGGACGCCCTAGACCT	89
	R-TGTTGGCAACGCCTTGATGT	
mRaf	F-TGCCTTTTGTGTGAAGCGAC	254
	R-AATCCGTGAGCTTGCCATCA	
mRas	F-GGTCAGATCCGCCTACTG	230
	R-CACCACCACTGCCTTGTACT	
mRcvrn	F-ACCATGGGGAACAGCAAGAG	186
	R-GTCGGAGTCCGGGAAAAACT	
mRest	F-GAGATGTGTTCCCCCTCAGC	165

Gene	Primer Sequence	Product Length (bp)
	R-CATAACCATACCGCCCGACA	
mRho	F-ACTCTGCCAGCTTTCTTTGCT	132
	R-GTCGTCATCTCCCAGTGGA	
mRps27a	F-TCTGGCACTGCGTTAGACAG	155
	R-GGCCACAGAGCATACACTCA	
mS100a11	F-GGACCTCAACTGTGACGGG	73
	R-GCACGCTATAGCTAAGCCACCA	
mS100b	F-CATAACCATACCGCCCGACA	206
	R-AAAGGAGAAGTCTGCCGAGC	
mS100b	F-AGAGGGTGACAAGCACAAGC	160
	R-GAACTCCTGGAAGTCACACTCC	
mSix3	F-ACTTGGCGATCGAGGTTTGG	338
	R-AGCGAGTTAGAGAGAGCAAGC	
mSix6	F-CCAGCTCCATCCGAAACTCA	217
	R-GGGTGGGTGTTTCCATCTGT	
mSlc11a1	F-TTACTCACTCGGACCAGCAC	120
	R-GGGGGCTCTTGTCACTAATCA	
mSpon1	F-AAGGATCTGTCCCGCCTACT	389
	R-AGTTGTTACTCGCCAGGGTG	
mSstr2	F-CAAGCAATGGCTCCAACCAG	140
	R-CTTGGCATAGCGGAGGATGA	
mStat3a	F-GCCATCCTAAGCACAAAGCC	368
	R-GCATCAATGAATGGTGTCACACAGA	

Gene	Primer Sequence	Product Length (bp)
mSulf2	F-CCGGTGTCTGGTGGACTAAG	530
	R-GAGAATGGAGGAGCGAGACG	
mTbr2	F-CCACTGGATGAGGCAGGAGATT	145
	R-GTCCTCTGTCACTTCCACGATG	
mTfap2a	F-ACTCGGTGGTACAAGTTCGG	390
	R-AAGTCGGCATTAGGGGTGTG	
mTgfb2	F-GAGCACCTTTTTGCTCCTGC	413
	R-CAAGGTACCCACAGAGCACC	
mTlx	F-AGGTTCACAGGTCACCCCTA	220
	R-TCTGTCGCCTCCATTTCGTC	
mTnfα	F-CTGTAGCCCACGTCGTAGC	97
	R-TTGAGATCCATGCCGTTGG	
mTrkb	F-CACGGATGTTGCTGACCAAA	132
	R-CCAAACTTGGAATGTCTCGC	
mTuc-4	F-TCTCCAGCCTCTGAAGAAGAAAG	150
	R-GTACTTCTGCCGTGGGACC	
mTuj1	F-GGGCTCCCAGGTTAAAGTCC	81
	R-AAAATGGGGAGGACAGAGCC	
mVegf	F-GGGAGTCTGTGCTCTGGGAT	384
	R-GGTGTCTGTCTGTCTGTCCG	
mβ-Actin	F-GCAGGAGTACGATGAGTCCG	74
	R-ACGCAGCTCAGTAACAGTCC	

Table 8. List of primary and secondary antibodies used in western blot.

Antibody	Primary	Secondary
TUJ1	Rabbit Polyclonal	Anti-Rabbit-HRP
NESTIN	Mouse Polyclonal	Anti-Mouse-HRP
VIMENTIN	Rabbit Polyclonal	Anti-Rabbit-HRP
GAPDH	Mouse Polyclonal	Anti-Mouse-HRP

washed with TBST and incubated with the secondary antibody conjugated with HRP at a 1:10000 dilution in blocking solution for 2 hours at room temperature. After washing with TBST, the blot was stained with Bio-Rad chemiluminescence for 5 minutes and bands were visualized using a chemidoc (Bio-Rad). Band intensities were quantified using ImageJ software (NIH) and normalized to GAPDH.

2.17 MNase-seq analysis

Nucleosomes were cross-linked by adding formaldehyde and were then lysed. DNA was fragmented using MNase digestion. Samples were sequenced using Illumina HiSeq machine for paired-end reads and analysis was performed on the GALAXY platform. Paired-end reads were aligned to the human genome (genome assembly hg38) using Bowtie2 to map reads. Reads were counted and normalized using RPKM values to determine nucleosome occupancy. Normalized values were visualized using IGV.

2.18 RNA-seq analysis

RNA-seq analysis was performed as previously described (McKee et al., 2021). In brief, the total RNA of the samples was isolated using the GeneJet RNA purification kit (Thermo Fisher Scientific). cDNA library was prepared for RNA-seq using KAPA RNA HyperPrep Kit with RiboErase (Kapa Biosystems Inc.). The cDNA libraries were sequenced using Illumina HiSeq machine for paired-end reads using GENEWIZ (South

Plainfield, NJ) services, and sequencing analysis was performed on the GALAXY platform (Blankenberg & Hillman-Jackson, 2014). Raw sequencing reads were aligned to the human genome assembly hg38 and mouse genome mm10, and reads were counted and annotated using featureCounts using GENCODE GRCh38 and GRCm38 comprehensive gene annotation. DESeq2 was used to normalize counts and determine DEGs using statistical analysis. Ontology enrichment analysis of DEGs was performed using PANTHER and Enrichr software (Mi et al., 2013; Xie et al., 2021).

2.19 Statistical analysis

Statistical analysis was carried out by using a one-way analysis of variance (ANOVA) test for multiple comparisons followed by post hoc tests and ANOVA for repeated measures followed by Tukey's post-hoc analysis. Data are presented as the mean ± SEM of triplicates per analysis. Results were analyzed using SPSS version 26 (SPSS Inc. USA) and p values ≤ 0.01 were considered statistically significant. All statistical graphs were created using Microsoft Excel (Microsoft, Redmond, WA, USA).

CHAPTER THREE

PRODUCTION OF MSCS FOR PRECLINICAL STUDIES

3.1 Isolation of MSCs from perinatal tissues

MSCs are regularly isolated and cultured in animal-based products; however, these cells cannot be used for human clinical trials due to safety concerns. This has led our lab to investigate an animal-free (xenofree) based medium for the isolation and maintenance of our cells. To do this, we plated equal amounts of tissue in tissue culturing flasks with either M1 (animal products) or M2 (xenofree) culturing media. We examined the tissue daily for the outgrowth of cells. As depicted in Figure 6, cells emerged from tissue on day 8 in both M1 and M2 mediums. Cells were then passaged until they entered the senescent state and the generation time was recorded for each passage. The isolated cells grown in both medium types were then subjected for further analysis to characterize the cells as well as measure their differentiation potential.

3.2 Characterization of MSCs

3.2.1 Generation time and surface marker analysis of primitive MSCs

To test the growth rate of our MSCs, cells were passaged until they no longer were able to grow as these cells can only be passaged a limited number of times. Overall, MSCs exhibited larger morphology when cultured in M1 medium, whereas a smaller morphology was observed in MSCs cultured in M2 medium (Figure 7). Additionally, MSCs cultured in M1 were only able to be passaged for 26 passages with an average generation time of 30.0 hours, while MSCs cultured in M2 medium were able to be maintained for 40 passages with an average generation time of 18.7 hours (Figure 8).

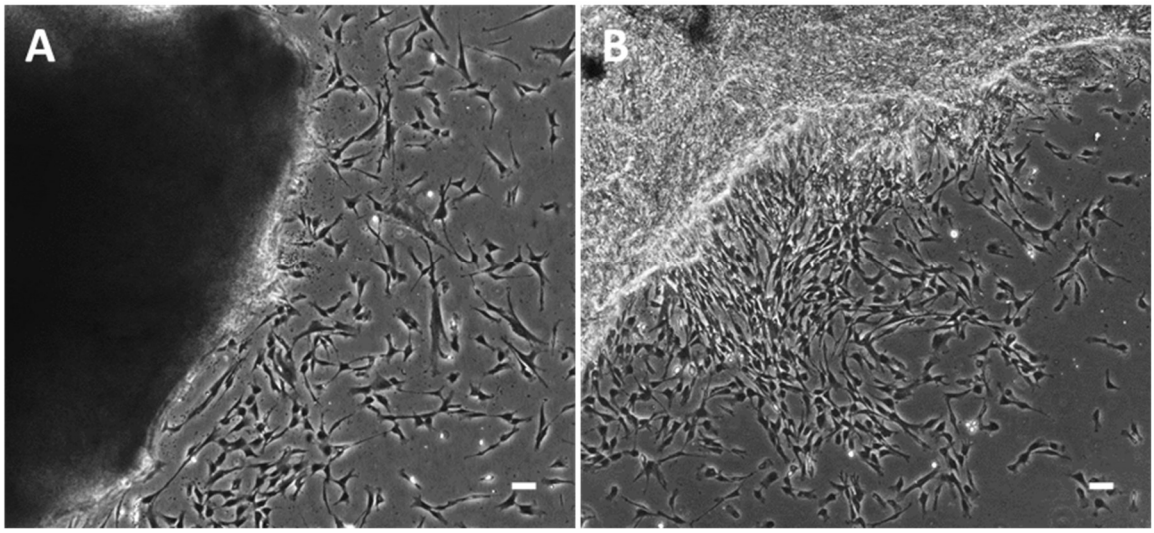

Figure 6. Phase-contrast images of (A) M1 medium and (B) M2 medium cultured cell outgrowth from explant CPJ tissue on day 8. Scale bars represent 100 μm (magnification: 4×).

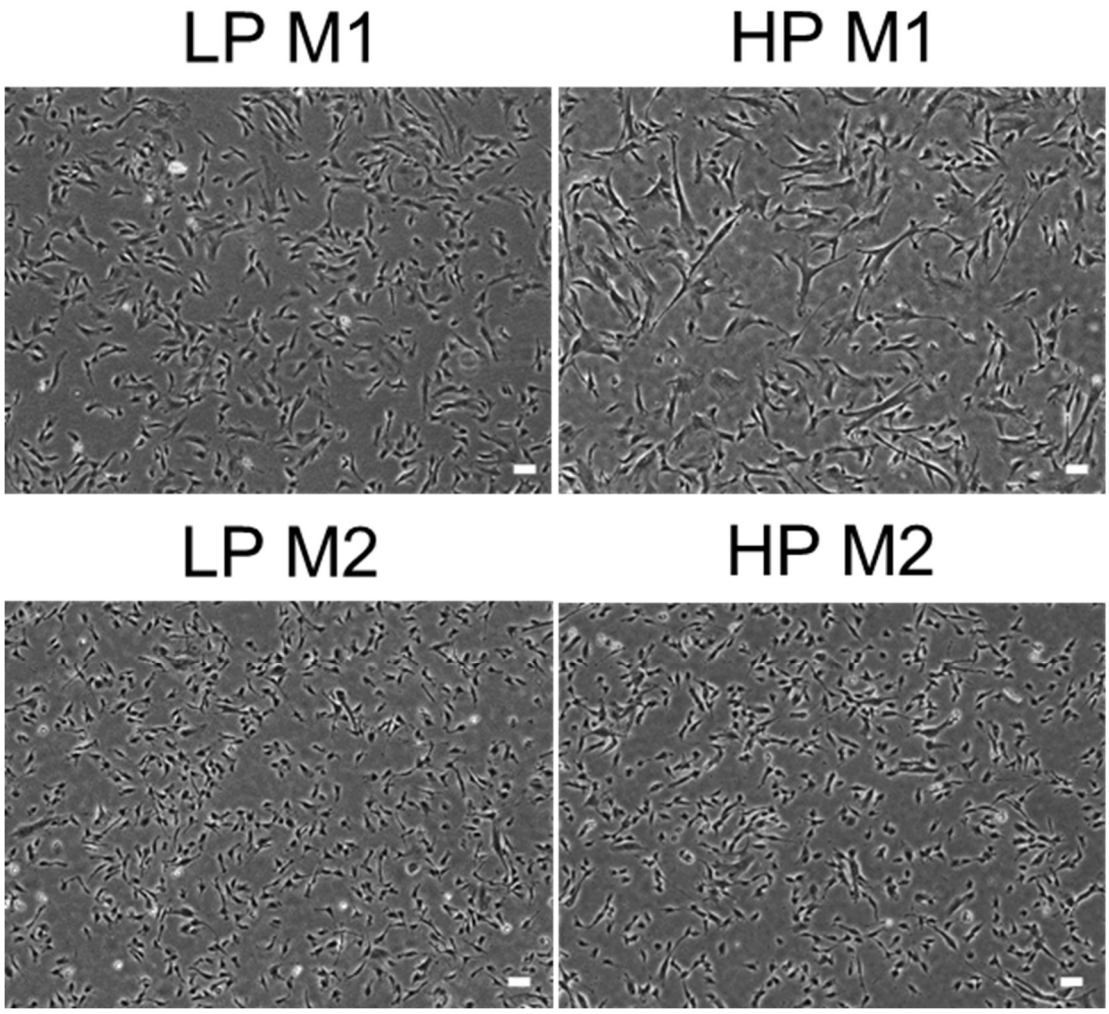

Figure 7. Phase-contrast images of low passage (P5) and high passage (P20) MSCs cultured in M1 or M2 medium. Scale bars represent 100 μm (magnification: 4×).

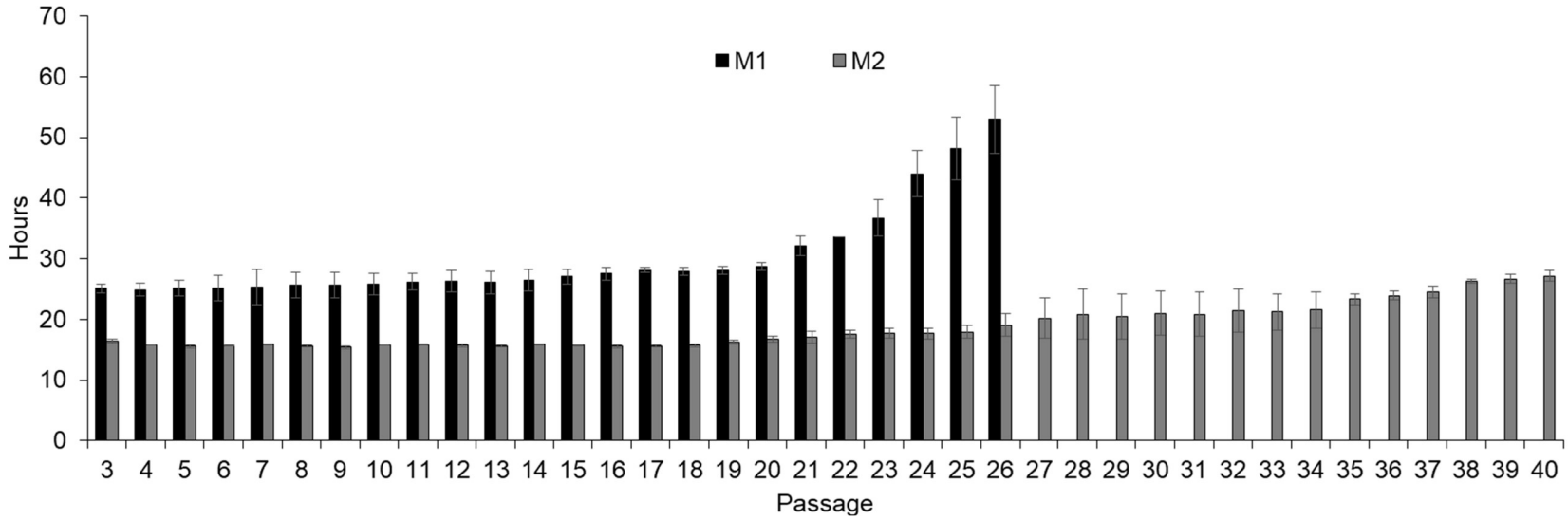

Figure 8. Generation time of MSCs cultured in M1 or M2 medium (n=3).

MSCs were further characterized via FACS analysis for the expression of MSC-specific surface markers, CD29, CD44, CD49f, CD73, CD90, and CD105 at low (P5) and high (P20) passages (Figure 9). As stated previously in chapter 1, to be considered an MSC, cells must express CD73, CD90, and CD105 (≥95%). As expected, low passage MSCs cultured in M1 medium expressed all markers above 95%. However, high passage MSCs cultured in M1 displayed a significant decrease in CD49f (1.4%) and CD90 (82.6%). In contrast, MSCs cultured in M2 medium maintained the expression of CD29, CD44, CD73, CD90 and CD105 at 95% in low and high passages, except CD49f which decreased to 86.0% in high passage M2 cells. Overall, MSCs cultured in M2 medium not only were able to be passaged longer, but maintained a smaller morphology, faster generation time, and sustained the expression levels of MSC specific surface markers when compared to MSCs cultured in M1.

3.2.2 Clonogenicity and Proliferation analysis of MSCs

Next, we examined the clonogenicity potential of the MSCs by performing CFE analysis. As depicted in Figure 10A-B, 89% of low passage MSCs cultured in M1 medium produced colonies. As anticipated, the percentage of CFE significantly decreased to 65% in high passage MSCs cultured in M1. On the other hand, MSCs cultured in M2 maintained their CFE was 99% and 95% at low and high passages, respectively. Moreover, colonies that formed in M2 medium were more confluent and produced tighter colonies. BrdU proliferation analysis displayed a similar tread to CFE analysis (Figure 10C). MSCs cultured in the M2 medium had a higher proliferation rate than MSCs cultured in the M1 medium.

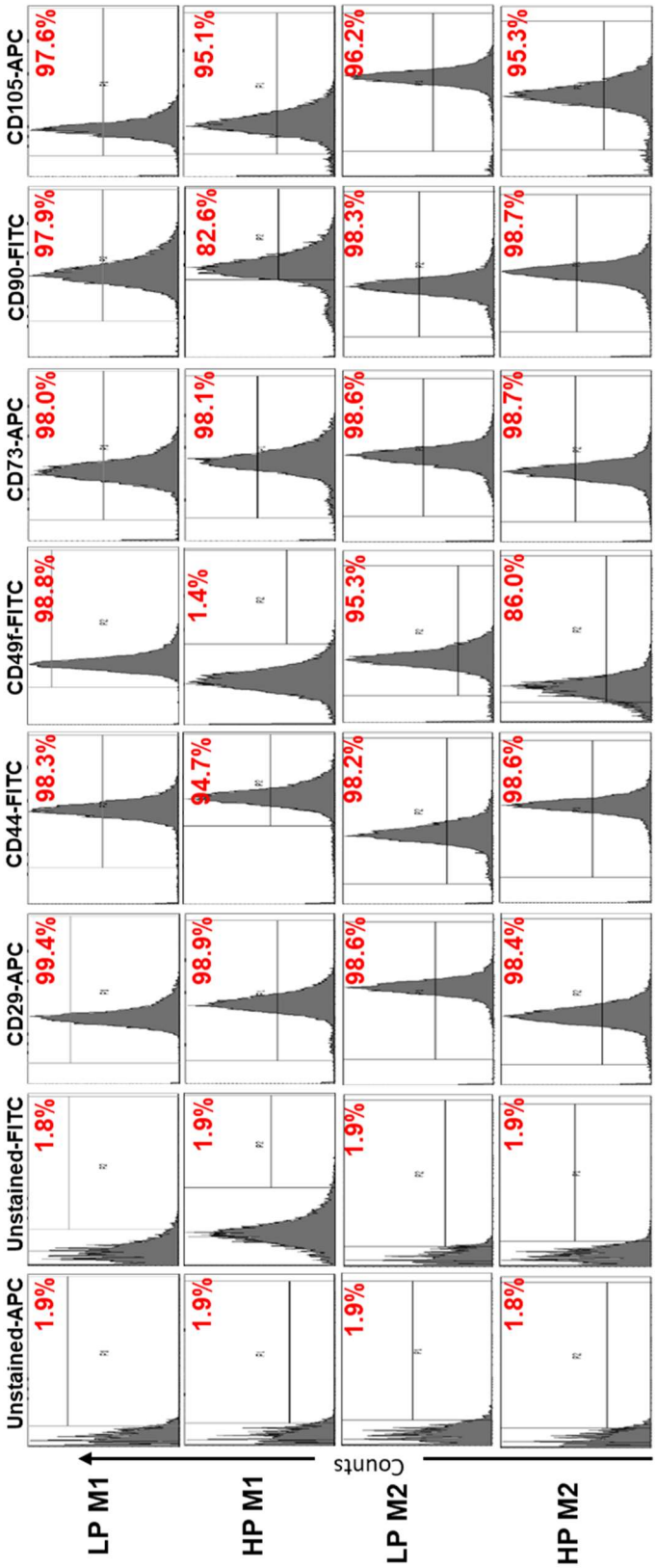

Figure 9. FACS analysis of LP and HP MSCs cultured in M1 or M2 medium.

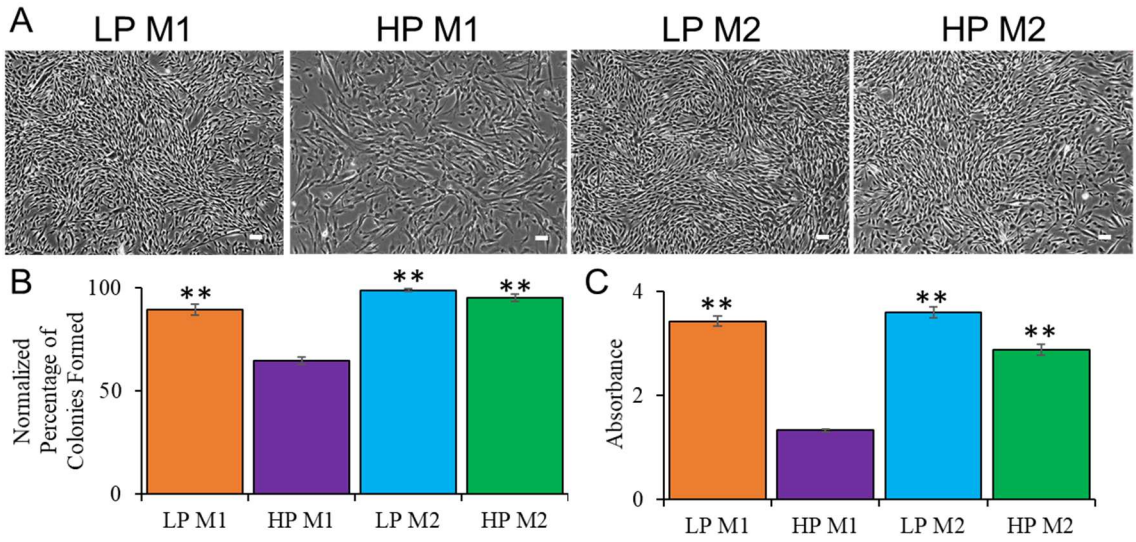

Figure 10. Proliferation analysis of MSCs cultured in M1 or M2 medium at low and high passage. (A) CFE colonies were observed under phase-contrast microscopy. Scale bars represent 100 µm (magnification: 4×). (B) Graphical representation of CFE (C) BrdU analysis of MSCs cultured in M1 and M2 medium.

3.3 Trilineage differentiation of MSCs

We next examined the ability of perinatal MSCs to differentiate towards the mesenchymal lineages (chondrogenic, osteogenic, and adipogenic cells) *in vitro* with selective differentiation media. Cells incubated in a chondrogenic medium for 3 weeks displayed altered morphology, as shown in Figure 11. To measure the chondrogenic differentiation potential of the MSCs, the cells were stained with toluidine blue for the production of polysaccharides. All cells stained positive with toluidine blue; however, the intensity was greater in MSCs cultured in M2 medium (Figure 12). The positive toluidine blue demonstrated production of GAG, suggesting that MSCs cultured in M2 medium differentiated towards the chondrogenic lineage. qRT-PCR and immunocytochemical staining confirmed that our cells differentiated into chondrogenic derivatives through the

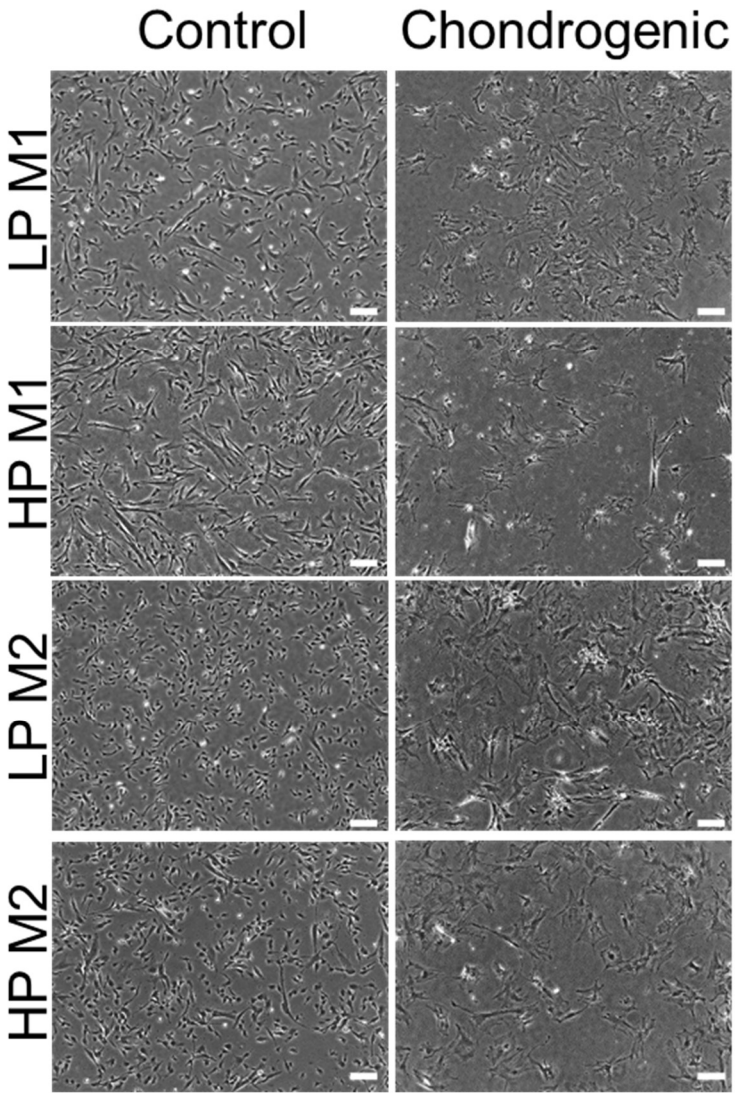

Figure 11. Phase-contrast imaging of MSC differentiation towards the chondrogenic lineage, comparing low and high passage MSCs cultured in M1 or M2 medium. Scale bars represent 100 μm (magnification: 4×).

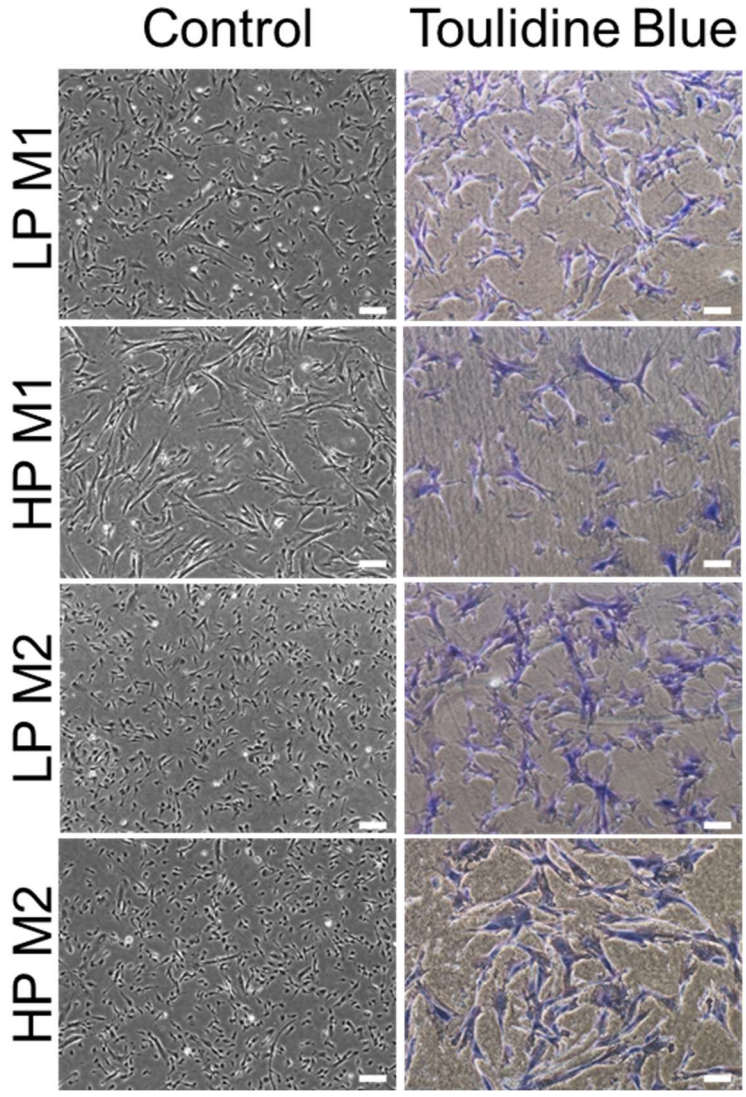

Figure 12. Phase-contrast imaging of MSC and MSC derived chondrogenic derivatives stained with toluidine blue. Scale bars represent 100 μm (magnification: 4×).

upregulation of ACAN, COL2, and SOX9 expression at the transcriptional (Figure 13) and translational levels (Figure 14). However, M2 cultured MSCs displayed greater expression of ACAN, COL2, and SOX9 when compared to M1 cultured MSCs. Taken together MSCs cultured in M2 medium demonstrated to have a greater differentiation potential towards the chondrogenic lineage.

When MSCs were cultured in an osteogenic differentiation medium for 3 weeks, they displayed a cuboidal morphology as depicted Figure 15. The osteogenic derivatives in all conditions stained positive for alizarin red, indicating the presence of calcium phosphate deposits (Figure 16). In addition, the osteogenic derivatives displayed an upregulation of the markers, COL1, OCN, RUNX2, and OPN at the gene (Figure 17) and protein level (Figure 18). Again, MSCs cultured in M2 medium displayed higher expression of these markers, specifically COL1 and OPN, when compared to M1 cultured MSCs.

Likewise, MSCs were induced towards the adipogenic lineage (Figure 19), as indicated by the production of lipid droplets positively stained with Oil Red O as presented in Figure 20. Furthermore, adipogenic derivatives showed an increased expression in the adipogenic specific genes *CEBPβ*, *FABP4*, and *PPARγ* (Figure 21). Interestingly, high passage cells cultured in M1 and M2 mediums showed greater expression of *CEBPβ*, *FABP4*, and *PPARγ* than low passage MSCs. These results support the notion that M2 cultured cells can differentiate towards the mesenchymal lineages and produce greater expression of the chondrogenic and osteogenic specific markers compared to MSCs cultured in M1.

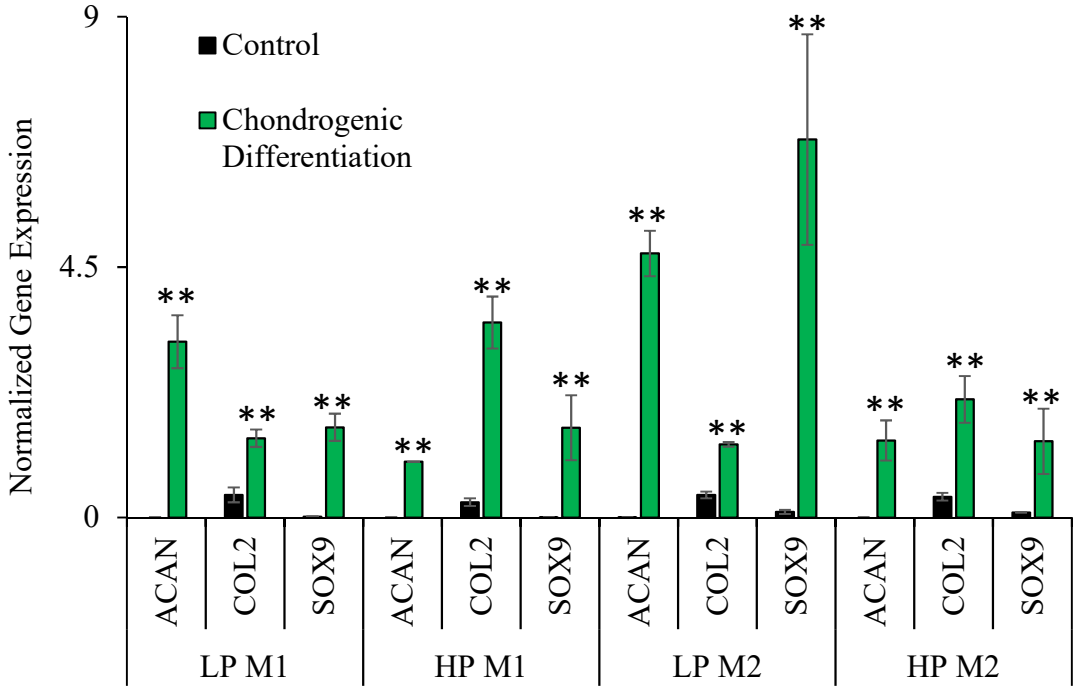

Figure 13. Transcriptional analysis of chondrogenic markers, *ACAN, COL2* and *SOX9*. Gene expression was normalized to *GAPDH* and *ACTIN*, and error bars represent the SEM of triplicate experiment. (**p≤0.01).

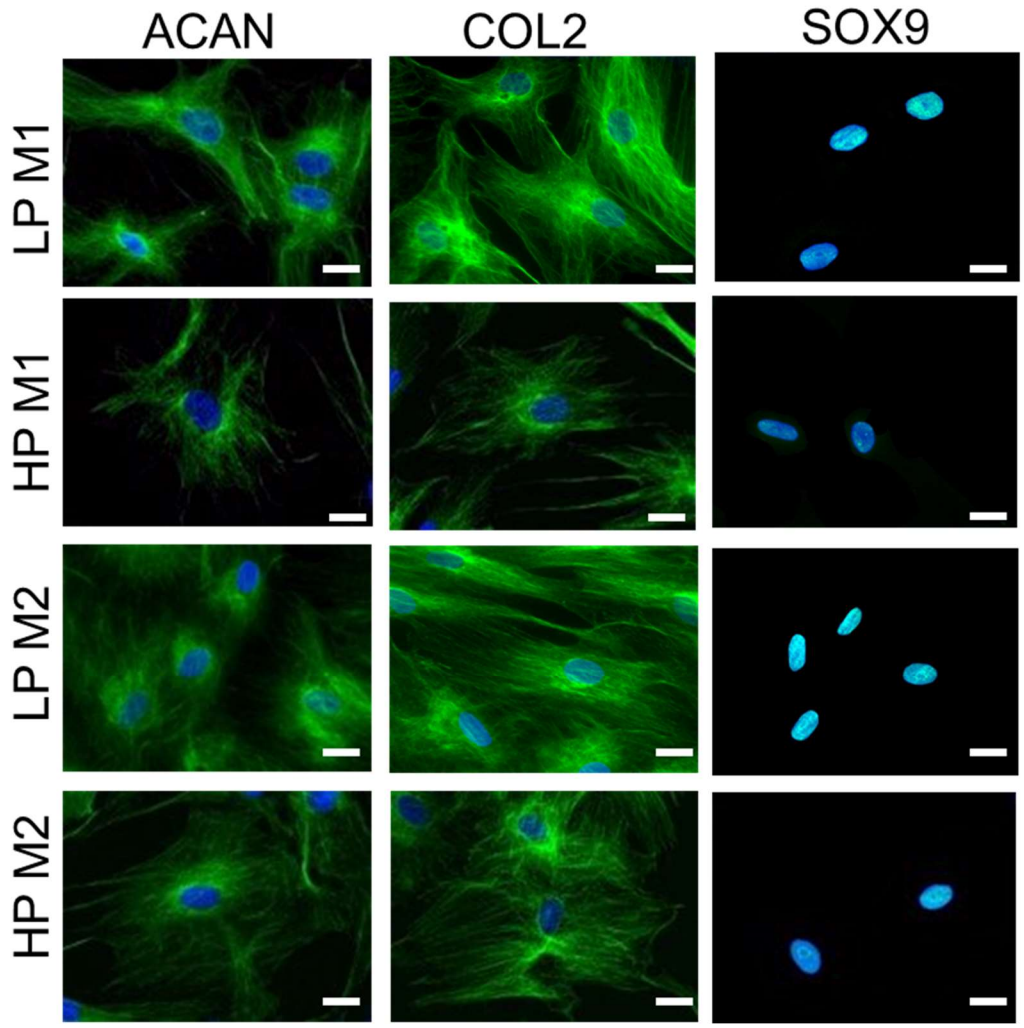

Figure 14. Translational analysis of chondrogenic markers, ACAN, COL2, and SOX9. Blue and green colors represent the DAPI staining of the nuclei and labeled antibodies against human proteins, respectively. Scale bars represent 50 µm scale bars. (Magnification: 40x).

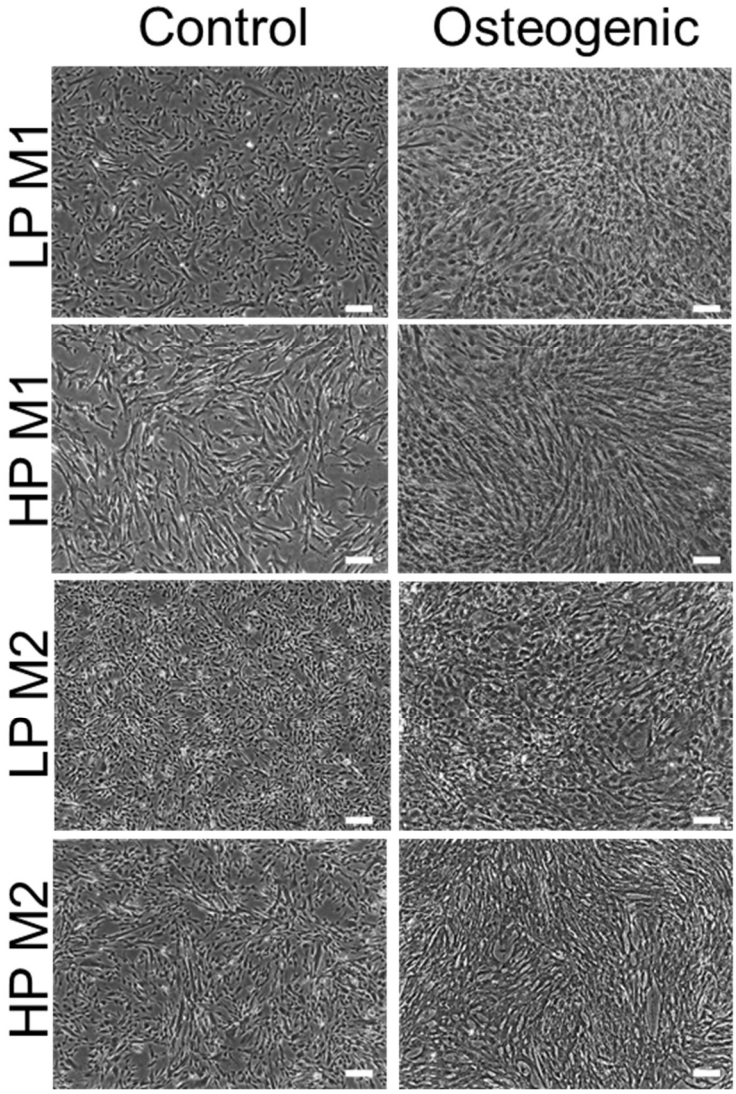

Figure 15. Phase-contrast imaging of MSC differentiation towards the osteogenic lineage, comparing low and high passage MSCs cultured in M1 or M2 medium. Scale bars represent 100 μm (magnification: 4×).

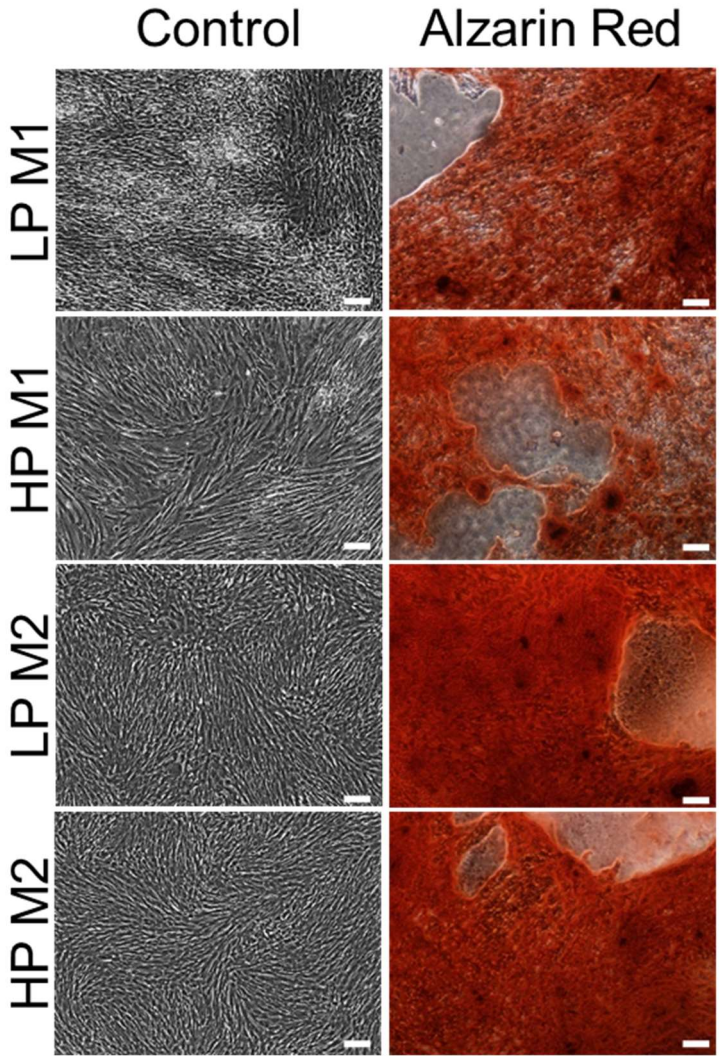

Figure 16. Phase-contrast imaging of MSC and MSC-derived osteogenic derivatives stained with alizarin red. Scale bars represent 100 μm (magnification: 4×).

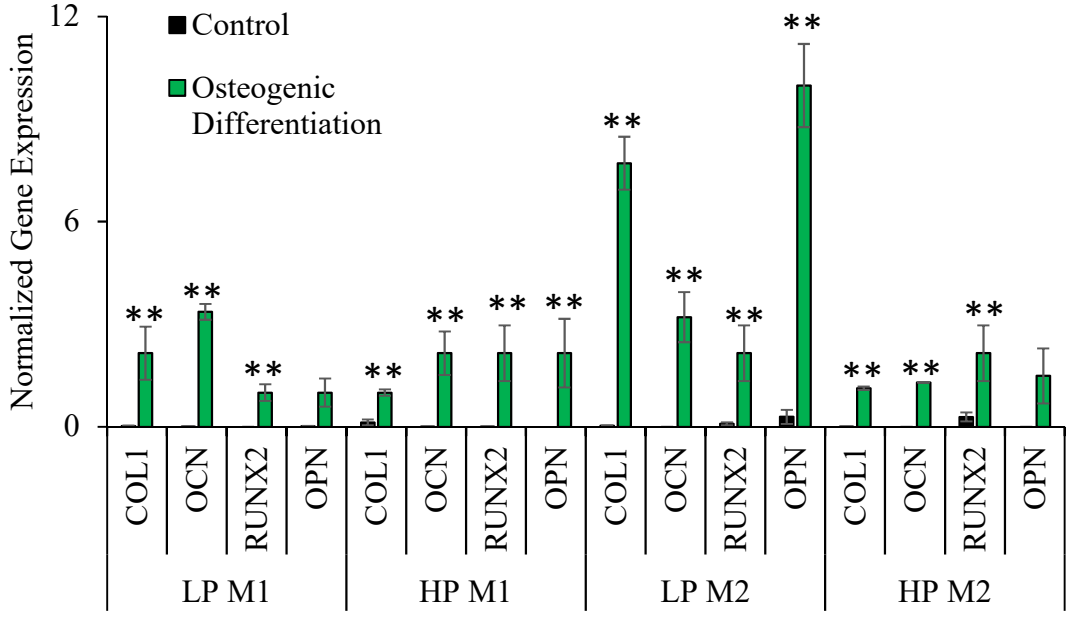

Figure 17. Transcriptional analysis of osteogenic markers, *COL1, OCN, RUNX2,* and *OPN*. Gene expression was normalized to *GAPDH* and *ACTIN*, and error bars represent the SEM of the triplicate experiment. (**p≤0.01).

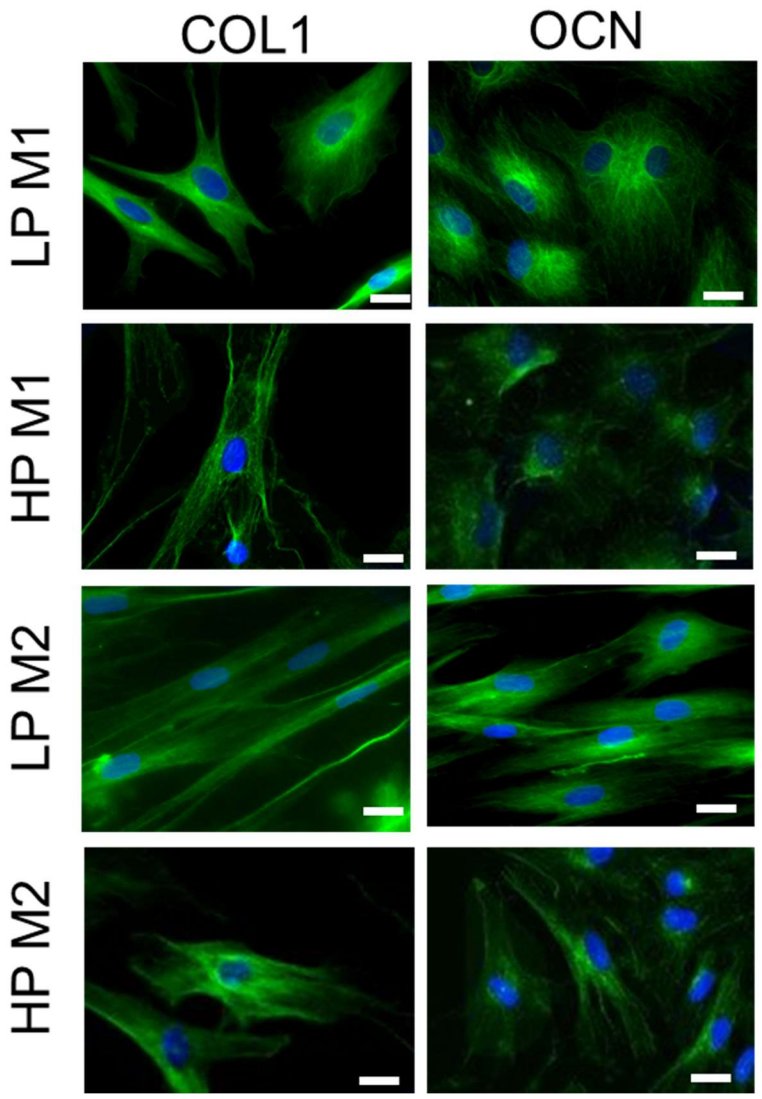

Figure 18. Translational analysis of osteogenic markers, COL1 and OCN. Blue and green colors represent the DAPI staining of the nuclei and labeled antibodies against human proteins, respectively. Scale bars represent 50 μm scale bars. (Magnification: 40x).

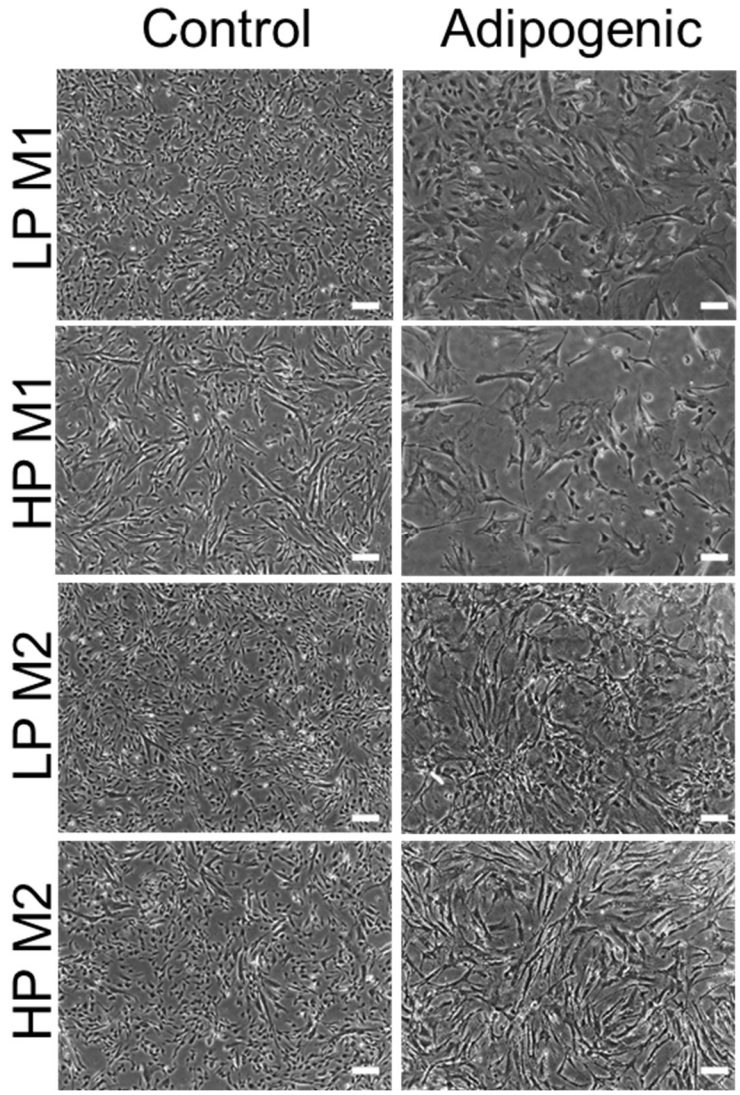

Figure 19. Phase-contrast imaging of MSC differentiation towards the adipogenic lineage, comparing low and high passage MSCs cultured in M1 or M2 medium. Scale bars represent 100 μm (magnification: 4×).

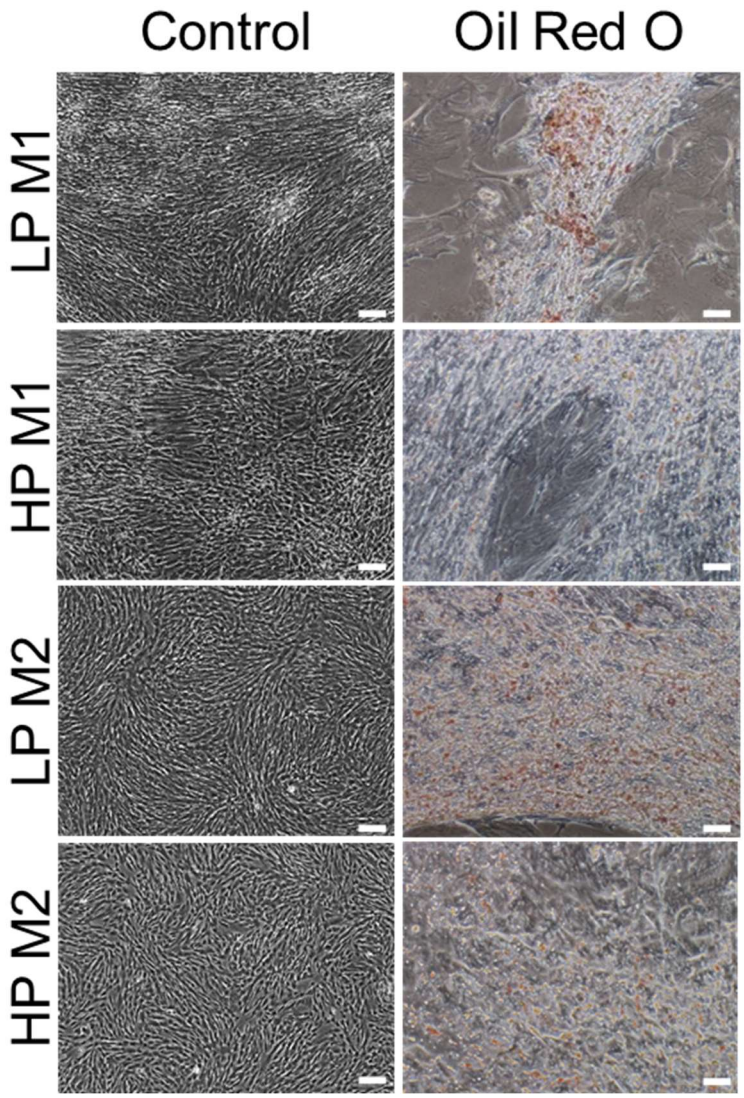

Figure 20. Phase-contrast imaging of MSC and MSC-derived adipogenic derivatives stained with oil red o. Scale bars represent 100 μm (magnification: 4×).

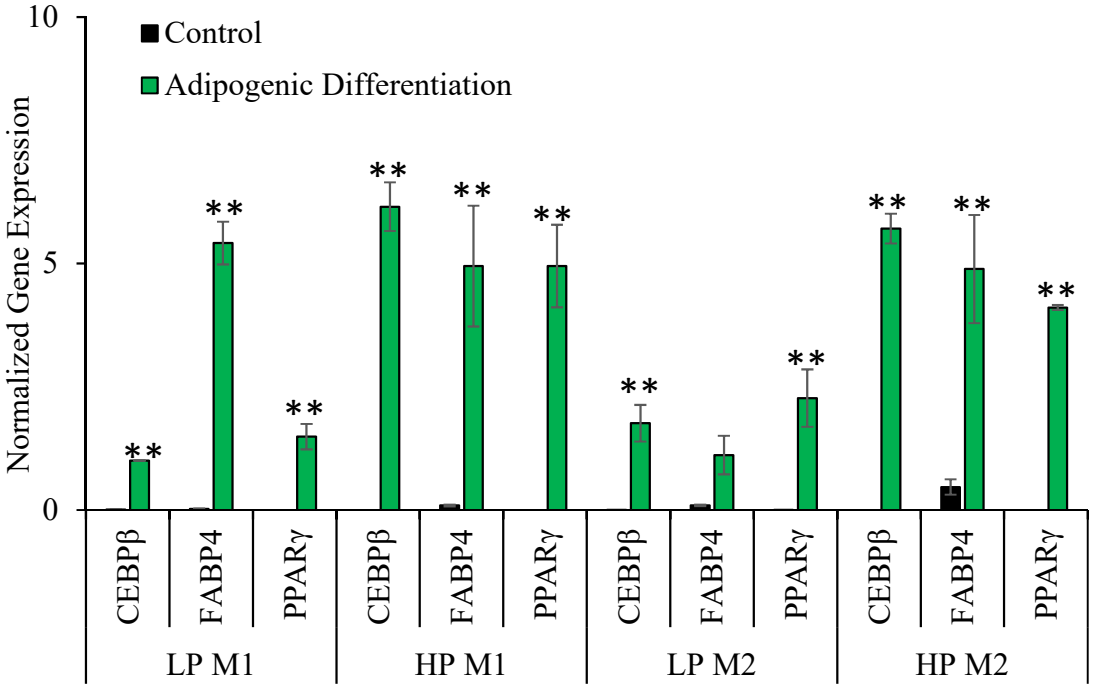

Figure 21. Transcriptional analysis of adipogenic markers, *CEBPβ, FABP4, and PPARγ*. Gene expression was normalized to *GAPDH* and *ACTIN*, and error bars represent the SEM of the triplicate experiment. (**p≤0.01).

3.4 Transcriptomic analysis of MSCs under various conditions

To investigate the molecular changes found in MSCs cultured in M1 or M2 medium, RNA-seq analysis was performed. When examining cell cycle-associated genes in low passages cells, we found that 7 genes were found to be upregulated in M1 MSCs, whereas 5 genes were upregulated in M2 MSCs (Figure 22A). Similarly, 6 genes were upregulated in both high passage M1 MSCs and M2 MSCs (Figure 22B). Likewise, when comparing low and high passage MSCs cultured in M1, we observed a similar trend where 7 genes were upregulated in low passages MSCs and 5 genes were upregulated in high passage MSCs (Figure 22C). However, when examining low passage and high passage M2 cultured cells, the distinction between the two cells is not very clear, indicating that cells preserved their stemness throughout passaging in M2 medium (Figure 22D).

We then examined the changes in senescence-associated genes by comparing the four conditions. When examining senescent associated genes on low passages cells, we found that 35 genes were found to be upregulated in M1 MSCs, whereas 33 genes were upregulated in M2 MSCs (Figure 23A). Moreover, 40 genes were upregulated in high passage M1 MSCs and only 29 genes were upregulated in M2 MSCs (Figure 23B). When comparing low and high passage MSCs cultured in M1, we observed only 24 genes were upregulated in low passages MSCs, and 43 genes were upregulated in high passage MSCs (Figure 23C). However, when comparing low and high passage MSCs cultured in M2 medium, we observed only 23 genes were upregulated in low passages MSCs and 33 genes were upregulated in high passage MSCs (Figure 23D).

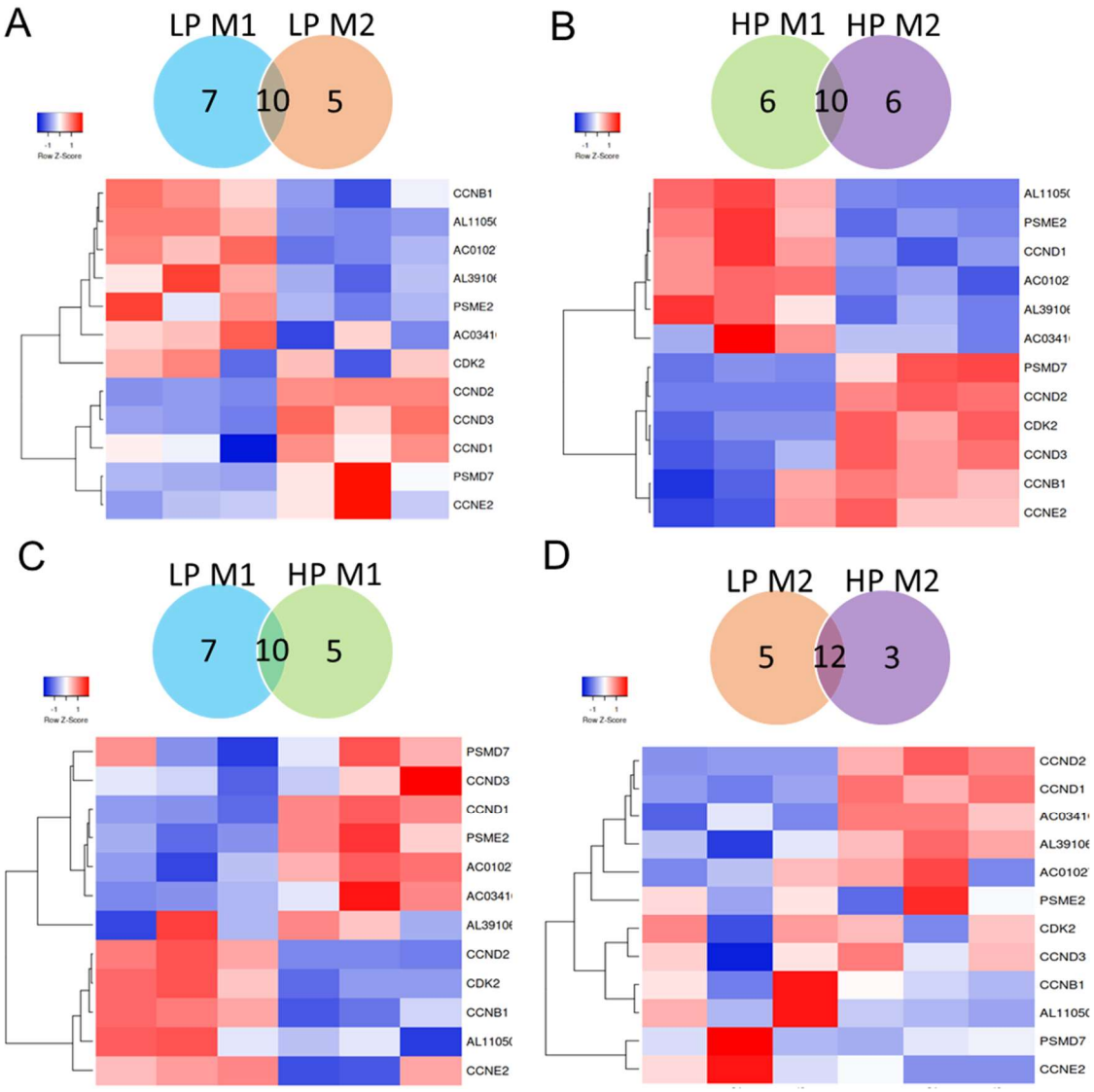

Figure 22. Transcriptome analysis of MSCs for cell cycle analysis. Heatmap showing raw z-scores of RNA-seq log2 transformed values of the differentially expressed genes involved in cell cycle pathway comparing (A) LP M1 v LP M2, (B) HP M1 v HP M2, (C) LP M1 v HP M1, and (D) LP M2 v HP M2. Up- and downregulated genes are red and blue, respectively.

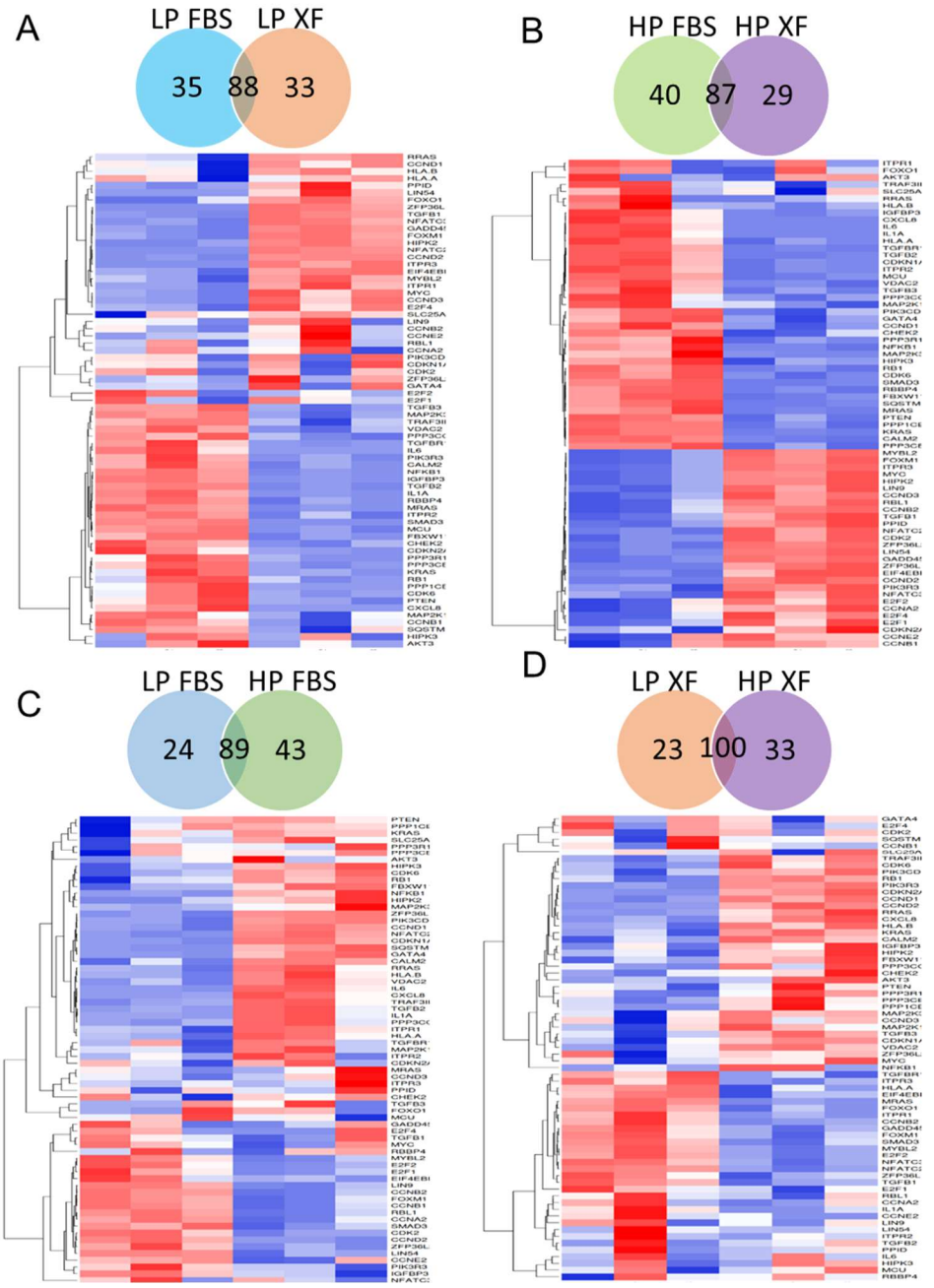

Figure 23. Transcriptome analysis of MSCs for senescence genes. Heatmap showing raw z-scores of RNA-seq log2 transformed values of the differentially expressed genes involved in senescence pathway comparing (A) LP M1 v LP M2, (B) HP M1 v HP M2, (C) LP M1 v HP M1, and (D) LP M2 v HP M2. Up- and downregulated genes are red and blue, respectively.

3.5 Discussion

MSCs are routinely cultured using animal-derived supplements and growth factors for isolation and amplification. However, the use of these animal products, such as FBS, leads to limitations and safety concerns. In addition, the components found in FBS are unknown and could carry antigens and other infectious agents that could be transferred to humans during cell transplantation (Heiskanen et al., 2007). In our lab, we have investigated alternative xenofree serums. Combined with a xenofree basal media and supplement serum, we found that MSCs cultured in M2 media were comparable, if not superior, to MSCs isolated and cultured in FBS (M1) based media.

Cells isolated from the perinatal tissue produced fibroblastoid morphology and were able to be passaged up to 40 passages and had an average generation time of 18 hours in M2 medium. Typically, MSCs are cultured for a limited number of passages with an average generation time ranging from 30 hours to 80 hours (Brown et al., 2019). This is the first report where MSCs were maintained for long-term passaging as well as preserved a steady doubling time. Additionally, the isolated cells expressed mesenchymal-specific markers such as, CD29, CD44, CD73, CD90 and CD105 at low passages in both M1 and M2 mediums. Although the percentage of the specific markers remained the same in high passage MSCs cultured in M2 medium, the expression of these markers significantly decreased in cells passaged for the long term in M1. Similarly, the CFE results showed a reduction of the growth rate in the case of M1 cultured cells when compared to M2 cultured cells. Additionally, a comparison of low and high passage MSCs cultured in M1 showed not only a reduction in cell surface markers, but displayed a large size morphology, suggesting that the cells were

undergoing gradual changes upon passaging. This theory was confirmed by the decrease of CD105, which is known to decrease when the cells undergo differentiation (Jin, H. J. et al., 2009; Levi et al., 2011). These results indicated that cells cultured in M2 medium maintained a proliferation state, whereas MSCs passaged in M1 medium had a slower proliferation rate and possibly entered the senescent state.

The MSCs derived from perinatal tissue displayed multi-lineage properties when incubated in specific differentiation media *in vitro*. The differentiated derivatives of MSCs displayed morphological and biochemical characteristics, including expression of markers for chondrogenic, osteogenic, and adipogenic lineages *in vitro*. This was confirmed through transcriptional and translation analysis and by previous reports (Beeravolu et al., 2016; Beeravolu et al., 2017). However, MSCs cultured in M2 medium produced cells with greater differentiation potential than those cultured in M1.

The transcriptome analysis revealed that low passage MSCs cultured in M2 medium showed an upregulation of the proliferative genes, *CCND2, CCND3*, and *CCND1*, compared to M1 cultured MSCs. The upregulation of these genes correlates with increased cell proliferation, and self-renewal observed in M2 cultured cells. In addition, the same genetic profile was observed in high passage MSCs cultured in M2 medium, again confirming that cells cultured in M2 medium sustained their proliferative state at higher passages. Furthermore, the gene *CCNE2*, which is essential for the control of the cell cycle at the late G1 and early S phase, was upregulated in M2 MSCs. These results validate that MSCs cultured in M2 medium are superior to cells cultured in M1 by producing cells that were able to maintain their stemness for long term passaging. This allows the possibility for the use of these cells for large scale production for human

clinical trials, as they can be continuously passaged and amplified to produce billions of cells.

We then investigated the senescent state and found that low passage M2 MSCs exhibited downregulation of the senescent genes, *KRAS, PTEN, AKT3,* and *CXCLB* when compared to MSCs cultured in M1 medium. This trend was also observed in high passage M2 MSCs. Additionally, the genetic profile between high passage MSCs in both mediums was distinctly different, demonstrating that MSCs cultured in M1 entered the senescent state upon passaging, confirming the results we obtained from the proliferation assay. However, further validation of this data via qRT-PCR is warranted.

In conclusion, our study provided a direct and relevant comparison of MSCs cultured in M1 or M2 medium. The results clearly showed that M2 medium yielded cells with higher proliferation and differentiation potential at low and high passages that can be used for clinical applications.

CHAPTER FOUR

NEURAL STEM CELLS DERIVED FROM PRIMITIVE MESENCHYMAL STEM CELLS REVERSED DISEASE SYMPTOMS AND PROMOTED NEUROGENESIS IN AN EXPERIMENTAL AUTOIMMUNE ENCEPHALOMYELITIS MOUSE MODEL OF MULTIPLE SCLEROSIS

The results for this section are from the published data available at (Brown et al., 2021)

4.1 Characterization and differentiation of primitive MSC-derived NSCs

We first differentiated the primitive MSCs into NSCs (Bakshi et al., 2018), which displayed typical neural extension morphology (Figure 24A), loss of MSC markers (Figure 24B-C), and expression of the neural genes, *NESTIN*, *TUJ1*, *VIMENTIN*, and *PAX6*, as well as neurotrophic factors, *CNTF*, *BMP2*, *PDGF*, *BDNF*, *GDNF*, *IGF*, *EGF*, and *FGF* (Figure 24D-E). Similarly, translational expression of several neural proteins, NESTIN, TUJ1, VIMENTIN, and PAX6, was displayed by NSCs (Figure 25A-B). These results were further validated by western blot analysis showing the expression of the neural proteins in NSCs (Figure 25C-D). This protocol reproducibly yielded 73% differentiation of MSCs into NSCs (Figure 25E). The ability of NSCs to differentiate to the glial linage, particular ODCs (Figure 24A), was demonstrated by the expression of *OLIG2, SOX10, O4, MBP, and MOG* at the transcriptional level (Figure 25F) and OLIG2, SOX10, O4, MBP, and MOG at the translational level (Figure 25G-H) by the NSC-derived ODCs. NSCs also differentiated into neuronal lineage (data not shown).

4.2 Improvement in the neurobehavior and reduction of disease severity in EAE mice transplanted with cells

EAE mouse model was used to investigate the effects of MSCs and NSCs on the disease process. EAE was induced in mice by MOG peptide immunization using an

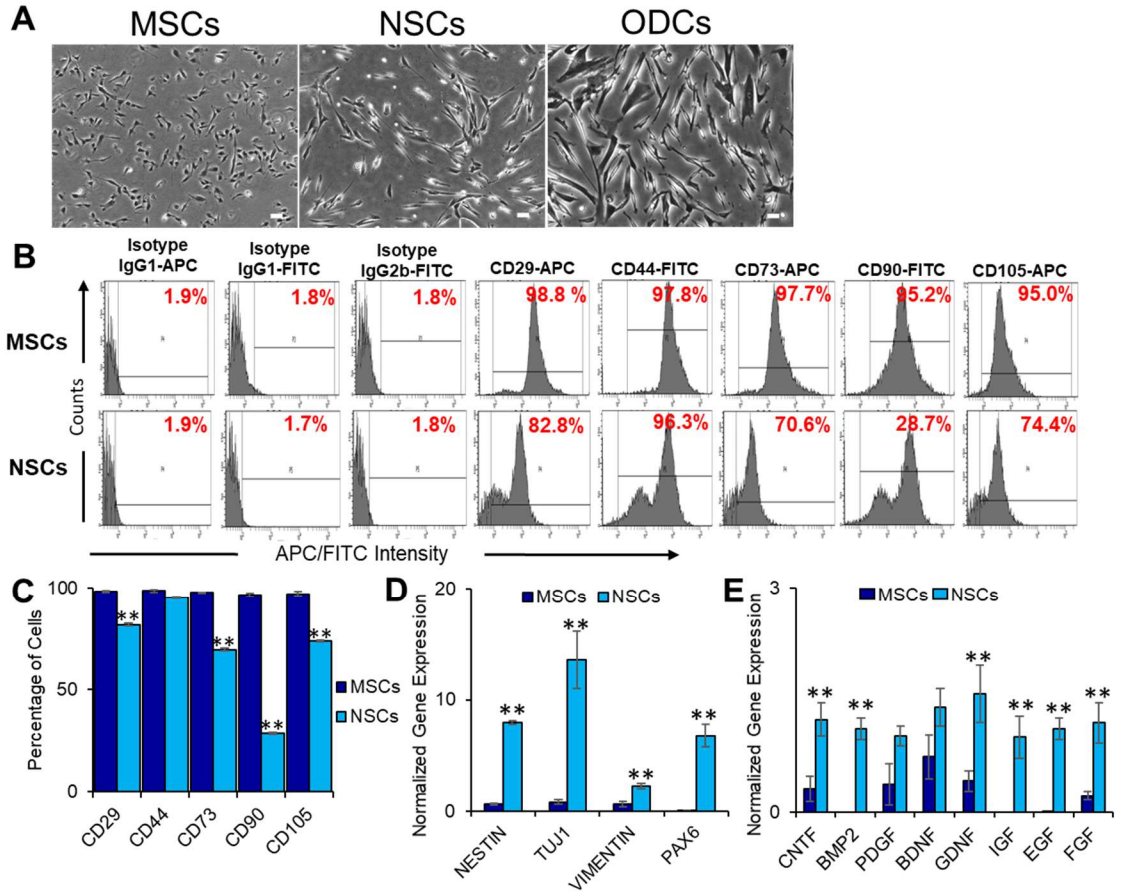

Figure 24: Characterization of NSCs and ODCs derived from primitive MSCs. (A) Phase-contrast images of the primitive MSCs, NSCs, and ODCs. Scale bars represent 100 µm (magnification: 4×). (B and C) Histograms and graphical representation of the expression of MSC markers as determined by flow cytometry, respectively. Expression of MSC markers, CD29, CD44, CD73, CD90, and CD105, was significantly reduced in NSCs (**$p \leq 0.01$). (D and E) Expression of neural and neurotrophic genes, respectively, as determined by qRT-PCR. NSCs expressed neural markers, *NESTIN, TUJ1, VIMENTIN*, and *PAX6*. NSCs also expressed neurotrophic factors, *CNTF, BMP2, PDGF, BDNF, GDNF, IGF, EGF,* and *FGF* at higher levels. Fold gene expression was normalized to *GAPDH* and *β-ACTIN,* and error bars represent the SEM of triplicate experiments (**$p \leq 0.01$).

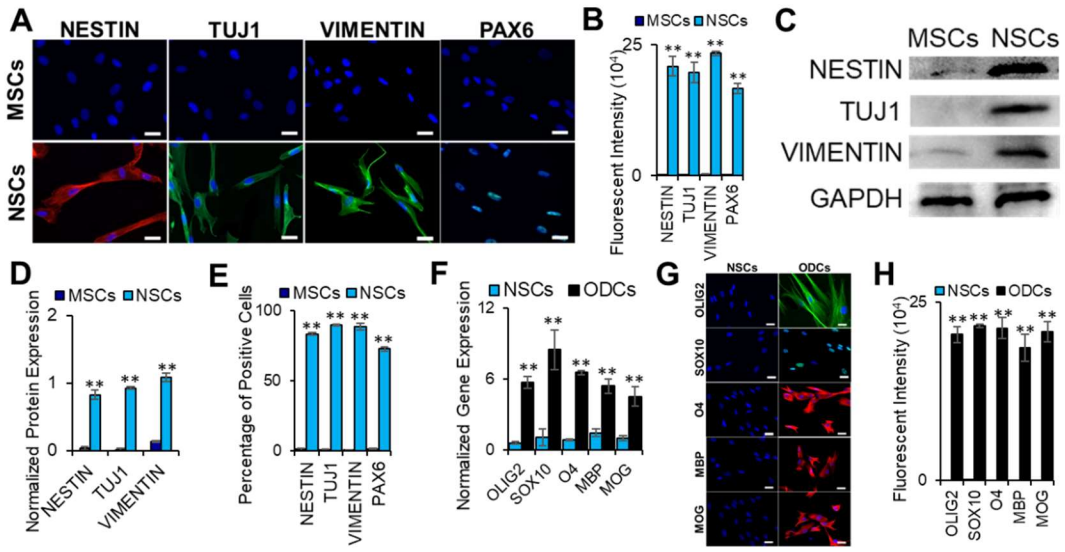

Figure 25: Protein characterization of NSCs and ODCs derived from primitive MSCs. (A) Expression of neural proteins as determined by immunocytostaining. Shown are merged images of DAPI (blue) and human antibodies (green and red). NSCs had significantly higher expression of neural proteins, NESTIN, TUJ1, VIMENTIN, and PAX6 than MSCs. (B) Quantification of fluorescent intensity of immunocytostained proteins (**p ≤ 0.01). (C and D) Western blot and quantitative analysis of normalized neural protein expression using ImageJ software, respectively (**p ≤ 0.01). All proteins were normalized to GAPDH expression. MSCs expressed low levels of NESTIN and VIMENTIN, but not TUJ1. Whereas NSCs had a significantly high level of expression of these markers. (E) Percentage of immunocytostained cells positive for NESTIN, TUJ1, VIMENTIN, and PAX6 (**p ≤ 0.01). (F) Expression of genes, *OLIG2, SOX10, O4, MBP,* and *MOG,* in ODCs, as determined by qRT-PCR. (G) Expression of proteins, OLIG2, SOX10, O4, MBP, and MOG in ODCs, as determined by immunocytostaining. Shown are merged images of DAPI (blue) and human antibodies (green and red). (H) Quantification of fluorescent intensity of immunocytostained proteins (**p ≤ 0.01). Fold gene expression (in F) was normalized to *GAPDH* and *β-ACTIN,* and error bars represent the SEM of triplicate experiments (**p ≤ 0.01). All scale bars (A and G) represent 50 μm (magnification: 40×).

established protocol (Dupree & Feinstein, 2018). Disease progression was determined by neurobehavioral analysis according to the well-established disease symptom scale (Table 9). The first signs of EAE induction in animals were noticed 11-12 days after MOG injections. Once the animals reached an EAE disease score 1 and 2, they were intravenously injected with 10^6 PKH26 labeled cells (Figure 26). The animals were evaluated for neurobehavioral changes twice a day until they were sacrificed for post-transplantation analysis. Neurobehavioral analysis results showed that the average clinical score of the EAE control (4.5±0.5) was significantly higher than the average score of mice transplanted with MSCs (1.7 ± 0.3) and NSCs (0.6 ± 0.1) at score 1 and MSCs (2.4 ± 0.2) and NSCs (2.2 ± 0.1) at score 2 (Figure 26 and Figure 27). In addition, the average weight of the untreated EAE control (13g ± 0.6g) was significantly lower than the average weights of the mice transplanted with healthy controls (Figure 26 and Figure 27), MSCs (15.7g ± 0. 7g) and NSCs (16g ± 0.4g) at score 1 and MSCs (14g ± 0.7g) and NSCs (14.6g ± 0.7g) at score 2. When MSCs were transplanted at EAE score 1, they only slowed and halted the disease progression. Whereas NSCs slowed and reversed the disease process, and animal condition was improved to near normal levels within two weeks after cell transplantation. Overall, NSCs showed greater efficacy than MSCs when transplanted at both EAE scores 1 and 2, but the results were more significant in the case of score 1. Therefore, we selected EAE score 1 transplanted animals for a detailed post-transplantation investigation. Animals were sacrificed two weeks post-transplantation, and blood, lungs, lymphatic and CNS tissues were collected for histological, biochemical, immunological and molecular analyses.

Table 9: MOG-induced EAE score scale and clinical symptoms.

Score	Symptoms
0	No clinical signs
0.5	Partial limp tail
1	Limp tail
1.5	Mild impaired righting
2	Severe impaired righting
2.5	Mild paresis of one hind limb
3	Severe paresis of one hind limb
3.5	Severe paresis of one hind limb and mild paresis of second hind limb
4	Paresis of two hind limbs
4.5	Paresis of both hind limb and partial fore limb
5	Severe paralysis or death

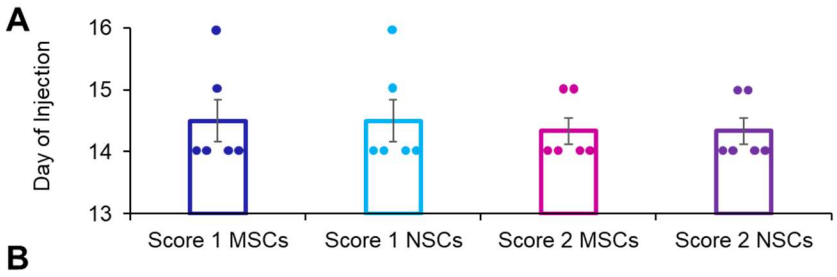

B

Conditions	Average day on onset	Average maximum disease score	Day and disease score of injected cells	Average disease score before euthanasia	Accumulated diseased score across the entire study	Average minimum weight	Average weight before euthanasia	Accumulated weight score across the entire study
Control	N/A	0	N/A	0	0	17.5g ± 0.3g	19g ± 0.3g	19.4g ± 0.4g
EAE	11.8 ± 0.6	4.6 ± 0.4	N/A	4.5 ± 0.5	3.4g ± 0.4g	13g ± 0.6g	14.7g ± .5g	14.7g ± 2.5g
MSCs	12.5 ± 0.3	2.3 ± 0.3	Day 14; Score 1	1.7 ± 0.3	1.4 ± 0.7g	15.7g ± 0.7g	19g ± 0.5g	16.8g ± 1.2g
NSCs	11.9 ± 0.2	2.5 ± 0.4	Day 14; Score 1	0.6 ± 0.1	1.1g ± 0.6g	16g ± 0.4g	18.5g ± .4g	17.0g ± 1.0g

Figure 26: Detailed analysis of cell transplantation on EAE clinical symptoms and weight. (A) Graphical representation of the day the cells were transplanted for each EAE group. (B) Clinical parameters of the EAE mice prior to and after treatment with primitive MSCs or NSCs.

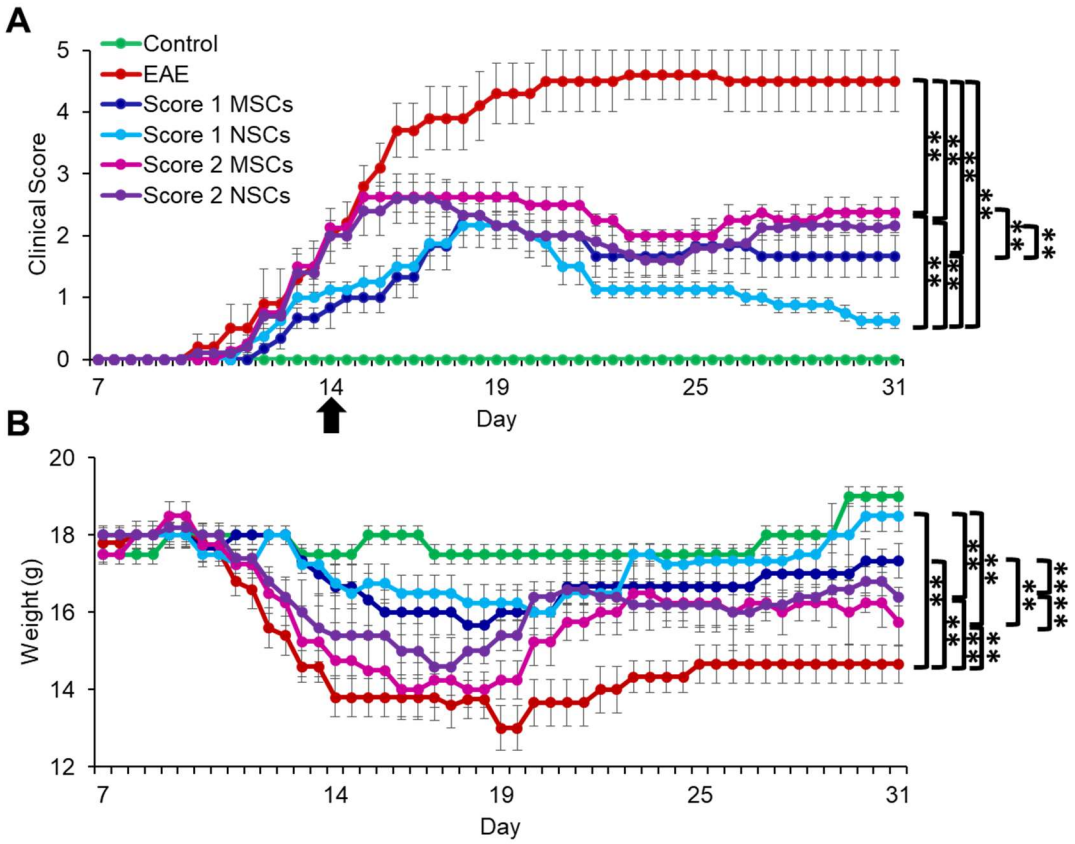

Figure 27: Effect of cell transplantation on the EAE clinical symptoms. (A and B) Changes in the clinical score of disease symptoms and weight in EAE mice (averages of n=6 each) following transplantation of cells, respectively. Primitive MSCs and NSCs were transplanted on day 14 (indicated by black arrow) at EAE score 1 and score 2 (**p ≤ 0.01). The animals were monitored, and clinical symptoms, as well as weight, were recorded daily.

4.3 Tracking of transplanted cells

The labeled transplanted cells homed to the blood, spleen, brain, and spinal cord (Figure 28). Only an insignificant number of transplanted cells were found in the lungs of all animals. Interestingly, significantly more transplanted MSCs (10.0%) than NSCs (6.7%) were observed in the blood of healthy animals, suggesting greater survivability of MSCs in the vascular system. In contrast, the number of transplanted MSCs and NSCs was 9.3% and 10.3% in the blood of EAE animals, respectively. Nearly half of the transplanted cells were found in the spleen in all animals. Notably, a significant number of transplanted cells were present in the CNS of EAE animals but not in healthy controls. A similar number of transplanted MSCs and NSCs were found in the brain (7.0% and 7.5%, respectively). Notably, NSCs (12.3%) were significantly more in the spinal cord than MSCs (10.5%). Overall, NSCs exhibited greater survivability in EAE animals than MSCs. Tissue samples were then subjected to histological analysis to investigate the effects of the transplanted cells on immune infiltrates.

4.4 Cell transplantation reduced immune infiltrates in CNS

EAE induction mediates T cell activation resulting in increased infiltrates in the CNS by permeation of the BBB and progression of disease pathogenesis (Fletcher et al., 2010). As expected, the brain and spinal cord (Figure 29A-B) showed the presence of cell infiltrates in EAE animals but not in healthy controls. The number of infiltrates in both the brain and spinal cord was significantly decreased in animals treated with MSCs and NSCs; however, NSCs exhibited a more significant reduction in infiltrates in the cortex region. Altogether, these results suggest that transplanted NSCs reduced cell infiltrates more significantly.

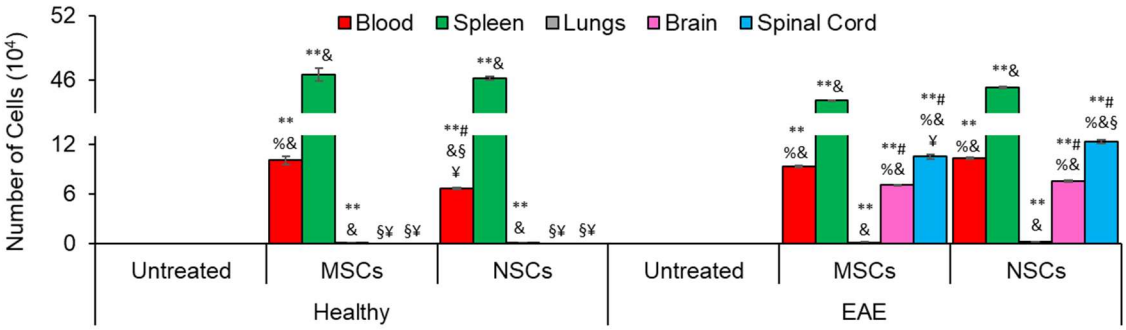

Figure 28: Transplanted cells homed to the blood, spleen, lungs, and CNS. To determine labeled cells in various organs, collected tissue samples prepared as described in the Methods and Materials were subjected to flow cytometry. Symbols, **, #, %, &, §, and ¥ indicate significant difference at $p \leq 0.01$ between all experimental conditions: healthy control, healthy control+MSCs, healthy control+NSCs, EAE, EAE+MSCs, and EAE+NSCs. A significant number of labeled cells were found in the blood and spleen, but not lungs of both healthy and EAE mice. Labeled cells were found in the CNS (both brain and spinal cord) of transplanted EAE animals.

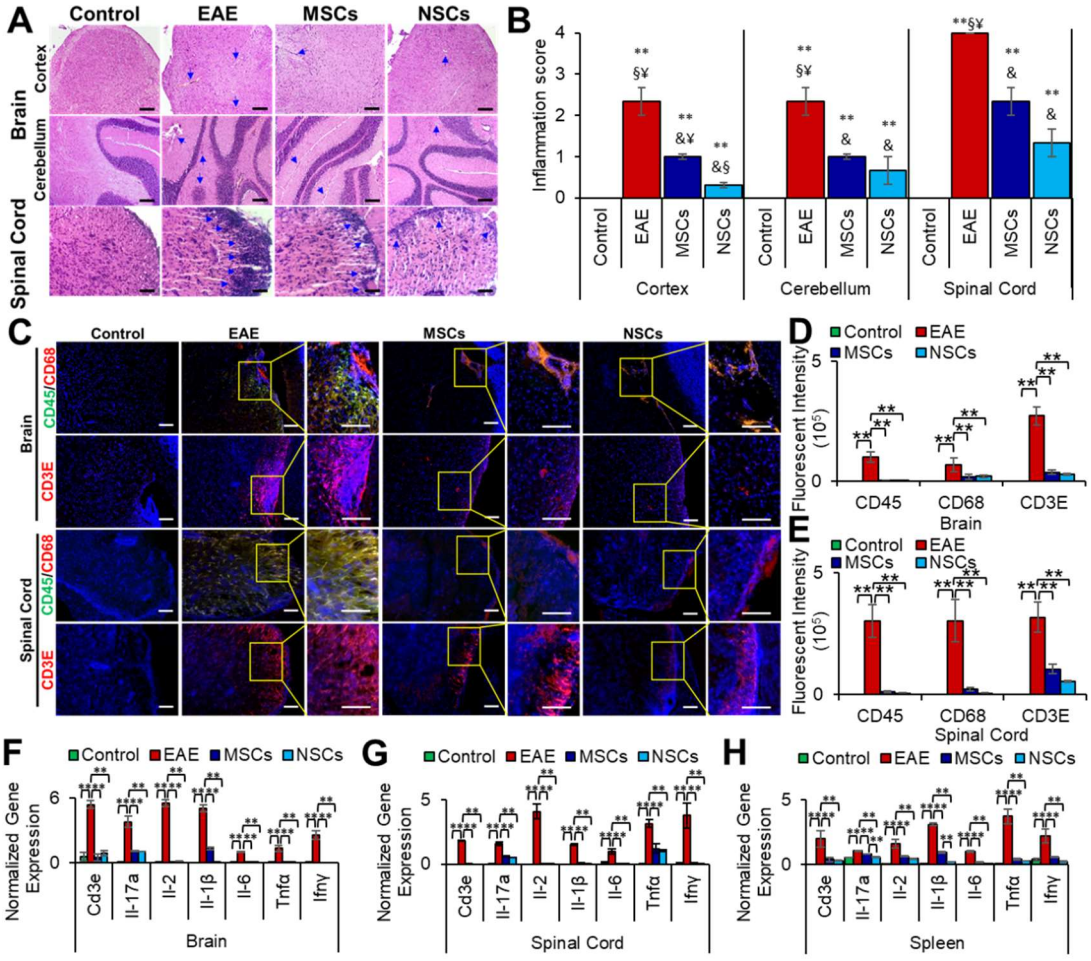

Figure 29: Reduction of inflammation in EAE animals. (A and B) Histological analysis of paraffin sections stained with H&E and brain and spinal cord inflammation scores, respectively. Cellular infiltrates reduced significantly in the CNS in EAE animals transplanted with MSCs and NSCs. Symbols, **, &, §, and ¥ indicate significant difference at $p \leq 0.01$ between all experimental conditions: healthy control, EAE, EAE+MSCs, and EAE+NSCs. All scale bars represent 50 µm (magnification: 40×). (C) Immunohistochemical staining of paraffin sections of the brain and spinal cord with cell-specific antibodies, CD45, CD68, and CD3E, representing leukocytes, macrophages, and T cells, respectively. The inserts (on the right) were magnified and overexposed to enhance contrast. All scale bars represent 50 µm (magnification: 40×). (D and E) Quantification of fluorescent intensity of brain and spinal cord sections shown in C, respectively (**$p \leq 0.01$). (F-H) Transcription of inflammation markers, *Cd3e, Il-17a, Il-2, Il-1β, Il-6, Tnfα,* and *Ifnγ*, in the brain, spinal cord, and spleen, using qRT-PCR. Fold gene expression was normalized to *Gapdh* and *β-Actin*, and error bars represent the SEM of triplicate measures (**$p \leq 0.01$).

To investigate the effect of transplanted cells on the inflammatory response in EAE mice and characterize the infiltrates observed in the H&E results, we analyzed the expression of CD45, CD68, and CD3E markers, representing leukocytes, macrophages, and T cells, respectively. The results depicted in Figure 29C-E show high expression of these markers in the brain and spinal cord of EAE animals but not in healthy controls. Importantly, NSCs were more effective in reducing the expression of all three markers in the spinal cord.

It is well known that EAE and MS are caused by an inflammatory response (Pegoretti et al., 2020). Therefore, transcriptional analysis of the brain, spinal cord, and spleen tissues was performed to determine the effects of transplanted cells on the expression of inflammatory genes. As expected, expression of the inflammatory markers, *Cd3e*, *Il-17a*, *Il-2*, *Il-1β*, *Il*-6, *Tnfα*, and *Ifnγ* was increased in the CNS and spleen in EAE animals compared to the healthy controls (Figure 29F-H). When EAE animals were transplanted with cells, the expression of inflammatory genes was significantly reduced in the CNS of MSC and NSC treated EAE animals. The expression of inflammatory genes was also reduced in the spleen (Figure 29H). In general, NSCs displayed a greater modulatory effect on inflammatory gene expression than MSCs. Overall, NSCs exerted a greater anti-inflammatory response, potentially by reducing the number of pro-inflammatory cells, macrophages, leukocytes, and T cells.

4.5 Immunomodulation of Treg and Th17 by transplanted cells

Treg (CD4+/CD25+/FOXP3+) and Th17 (CD4+/IL17A+) are the main effector cells of cell mediated immune response in EAE and MS (Fletcher et al., 2010). We investigated the levels of these cells in the blood, spleen, and CNS by flow cytometry.

Treg cells were significantly reduced to 7.7% and 8.0% in EAE animals from 34.1% and 27.5% in healthy controls in blood and spleen (Figure 30A). In contrast, Treg cells were substantially increased in EAE animals transplanted with cells in the blood and spleen. In EAE animals treated with MSCs, Treg cells were 17.4% and 22.5% in the blood and spleen, respectively. In NSC-treated animals, Treg cell levels were 27.3% and 25.4% in the blood and spleen, respectively.

In conclusion, Treg cell numbers increased in animals treated with both MSCs and NSCs; however, more significant improvements in the restoration of Treg levels in the blood were observed in the case of NSCs than MSCs. In the CNS of EAE animals, Treg levels were 10.5% and 12.0%, respectively. Although cell transplantation reduced Treg cells in the brain, they were more significantly reduced to 5.7% and 3.9% in the spinal cord of EAE animals treated with MSCs and NSCs, respectively. Taken together, NSCs showed greater efficacy than MSCs in reducing Treg cells in the spinal cord in EAE animals. It is known that Treg cells increase during the chronic late scores of EAE (Duffy et al., 2019). Therefore, it is plausible that reduced Treg levels in animals treated with cells could improve disease symptoms.

As expected, Th17 cells were significantly increased from 10.3% and 6.9% in the blood and spleen of healthy controls to 15.3% and 13.7% in EAE animals, respectively. When treated with MSCs, Th17 cell levels were not significantly affected in the blood (14.9%) but were reduced to normal levels (10.1%) in the spleen (Figure 30A). Importantly, NSC transplantation reduced Th17 to levels similar to the healthy control animals. The brain and spinal cord of EAE animals had significantly high levels of Th17 cells (22.5% and 30.5%, respectively) compared to healthy control animals (1.6% and

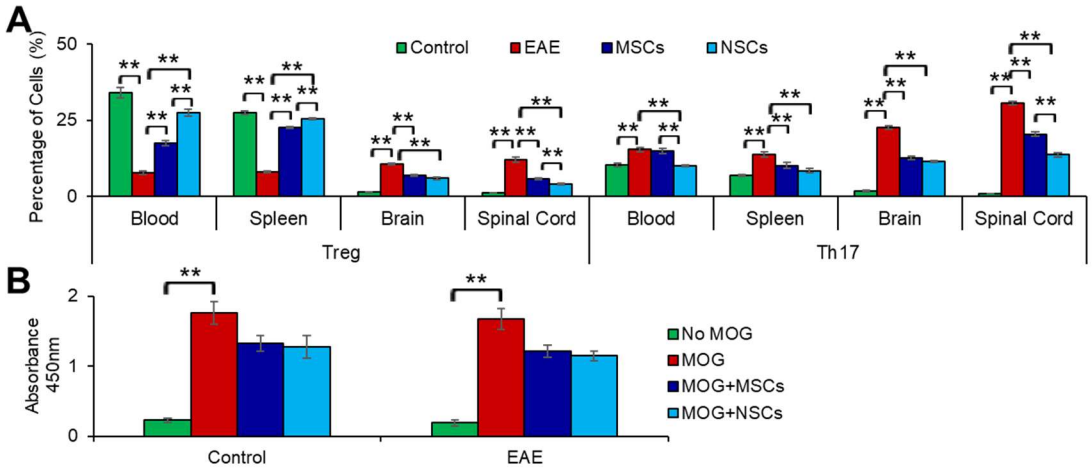

Figure 30: Modulation of Treg and Th17 cells by the transplanted cells. (A) Graphical representation of Treg (CD4+CD25+FOXP3+) and Th17 (CD4+IL-17A+) cells in the blood, spleen, brain, and spinal cord as determined by flow cytometry (**$p \leq 0.01$). Treg cell numbers went down, but Th17 went up in the blood and spleen, and both of these cells were significantly increased in the CNS of EAE animals. Transplanted cells significantly increased Treg but significantly reduced Th17 cells in the blood and spleen, and both of these cells were significantly reduced in the CNS of EAE animals. (B) Splenocytes isolated from control and EAE mice were cultured and treated with MOG35-55. After 72 hours following MOG activation, the cultures were treated with the MSCs and NSCs, and splenocyte proliferation was determined using BrdU assay.

0.9%, respectively). Upon MSC transplantation, Th17 cells were significantly reduced in the brain and spinal cord (12.6% and 20.3%, respectively). On the other hand, NSC transplantation had a more prominent effect on reducing Th17 cells in both the brain and spinal cord (11.5% and 13.7%, respectively) in EAE animals. Clearly, NSCs showed greater immunomodulatory effects in EAE mice.

It is conceivable that the transplanted cells could ablate or regulate CNS autoreactive T cells. To investigate this possibility, we evaluated MOG-activated splenocyte proliferation treated with MSCs and NSCs *ex vivo*. The BrdU analysis showed T cell proliferation stimulated with MOG in both control and EAE splenocytes but had an insignificant effect upon treatment with MSCs and NSCs (Figure 30B).

4.6 Cell transplantation reduced reactive astrocyte and gliosis in CNS

Upon induction of EAE, the expression of GFAP is increased (Figure 31A-D), due to the activation of astrocytes in response to gliosis (Moreno et al., 2013). We first examined the expression of *Cntfrα, Bmpr, Gfap, and Nfl-b* associated with astrogliosis (Abdelhak et al., 2018; Na et al., 2007) via qRT-PCR. As expected, these genes were increased in the CNS of EAE animals (Figure 5A-B). However, the expression of the gliosis-associated genes significantly decreased in the CNS tissues of EAE animals transplanted with cells. Specifically, EAE animals transplanted with NSCs displayed a greater effect in reducing these genes in the spinal cord. We then examined GFAP expression at a protein level through immunostaining of CNS tissue sections. Overall, GFAP expression was decreased in the CNS of EAE animals transplanted with cells but was only significant in the brain and not in the spinal cord (Figure 31C-D). Transplantation of NSCs promoted a greater reduction of gliosis in the EAE animals.

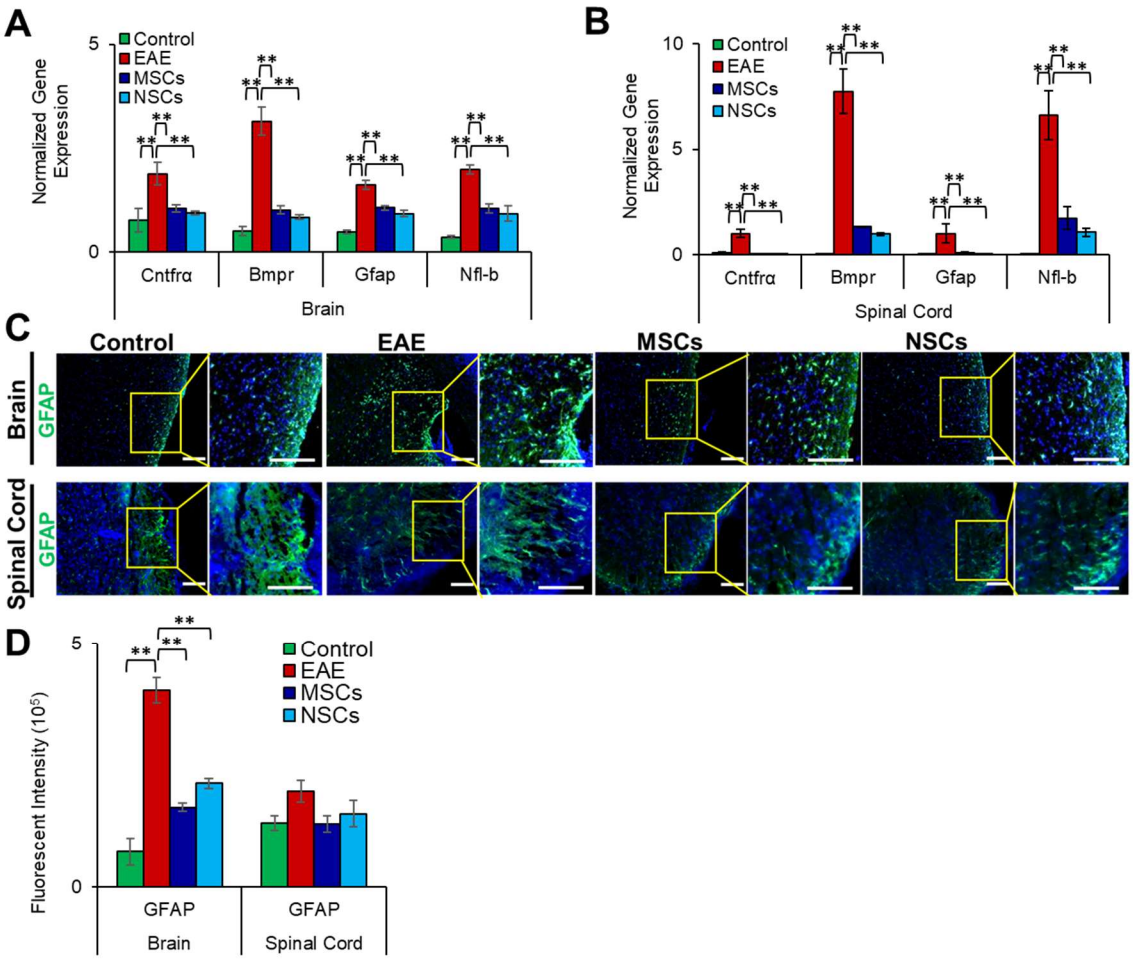

Figure 31: Suppression of gliosis by transplanted cells. (A and B) Transcription of genes, *Cntfrα, Bmpr, Gfap,* and *Nfl-b*, involved in gliosis in the brain and spinal cord, using qRT-PCR. Fold gene expression was normalized to *Gapdh* and *β-Actin* and error bars represent the SEM of triplicate measures (**p ≤ 0.01). Expression of gliosis genes was significantly upregulated in EAE mice but reduced significantly in treated animals. (C) Immunohistochemical staining of paraffin sections of the brain and spinal cord with antibody astrogliosis marker, GFAP. The inserts (on the right) were magnified and overexposed to enhance contrast. Scale bars represent 50 µm scale bars (magnification: 40×). (D) Quantification of fluorescent intensity of GFAP in the brain and spinal cord sections depicted in C, respectively (**p ≤ 0.01). GFAP levels significantly increased in EAE mice. However, they were reduced considerably in transplanted animals.

4.7 Cell treatment promoted remyelination

LFB staining of CNS tissue sections was performed to investigate the effect of transplanted cells on the degree of myelination. While LFB stain intensity was reduced in EAE mice, it was significantly improved in transplanted animals (Figure 32A-B). The staining intensity was greater in NSC-treated animals compared to those treated with MSCs. An increase in the staining intensity in the cortex and spinal cord suggests that transplanted cells induced endogenous remyelination.

To investigate the cause of increased myelin, we then examined myelin-associated gene expression in the CNS tissue by qRT-PCR. The expression of all tested myelination-associated genes, *Erk2*, *Krox-20*, *Mpz*, *Mbp*, and *Mog* was significantly upregulated in the CNS of the transplanted EAE mice (Figure 32C-D), except *Krox-20* and *Mbp* was not upregulated in the spinal cord in the case of MSCs. We validated these results by performing immunostaining of myelin-associated proteins, MBP and MOG. The expression of MBP and MOG in the brain of EAE animals (Figure 33A-B) was significantly increased upon transplantation of MSCs and NSCs. The trend in the expression of MBP and MOG in the spinal cord of EAE animals treated with cells was similar to the brain, while MBP expression was greater in EAE animals treated with NSCs in the spinal cord. These results suggest that transplanted NSCs showed increased remyelination in the CNS in EAE animals than MSCs.

4.8 Cell transplantation upregulated genes involved in neuroprotection

Neurotrophic factors support the growth, survival, and differentiation of both developing and mature neurons in the CNS (Razavi et al., 2015). It has been suggested that the neurotrophic factor BDNF plays an important role in axon protection during

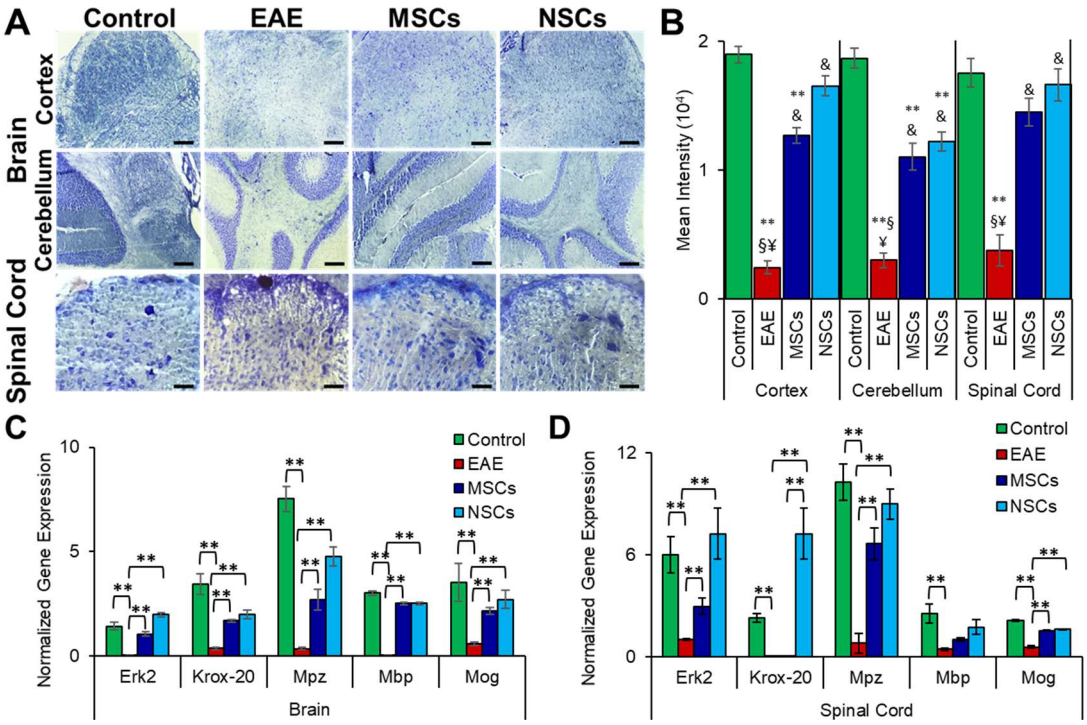

Figure 32: Cell transplantation resulted in improvement in myelination of CNS. (A) Analysis of paraffin sections of the brain and spinal cord stained with LFB to detect myelination. Scale bars represent 50 μm (magnification: 40×). (B) Quantification of LFB stain intensity of paraffin sections shown in A. Symbols, **, &, §, and ¥ indicate significant difference at $p \leq 0.01$ between all experimental conditions: healthy control, EAE, EAE + MSCs, and EAE + NSCs. LFB stain intensity was significantly improved in the cortex, cerebellum, and spinal cord in transplanted EAE animals. (C and D) Transcription of myelination markers, *Erk2, Krox-20, Mpz, Mbp*, and *Mog* in the brain and spinal cord. Fold gene expression was normalized to *Gapdh* and *β-Actin*, and error bars represent the SEM of triplicate measures (**$p \leq 0.01$).

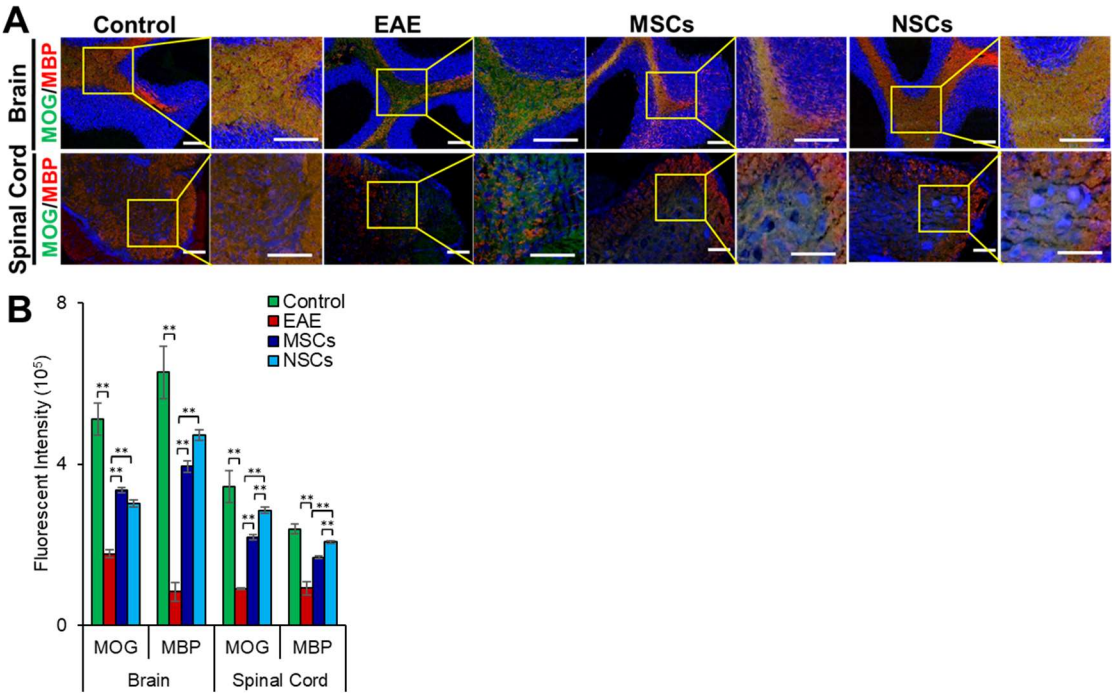

Figure 33: Cell transplantation resulted in improvement in protein myelination of CNS. (A) Immunohistochemical staining of myelin proteins, MBP and MOG, in the brain and spinal cord paraffin sections. The inserts (on the right) were magnified and overexposed to enhance contrast. Scale bars represent 50 μm scale bars (magnification: 40×). (B) Quantification of fluorescent intensity of myelin proteins in the brain and spinal cord sections depicted in A (**$p \leq 0.01$).

autoimmune demyelination of the CNS (Linker et al., 2010). Our analysis showed an extensive decrease in expression of all the tested genes, *Bdnf*, *Trkb*, *Ras, Pi3k, Akt, Creb, Fgfr, Raf, Mek1, Mek2, and Erk1,* associated with neuroprotection in EAE mice (Figure 34A-B). When EAE mice were transplanted with cells, the expression of all genes (except *Trkb* in the brain) was significantly increased, and NSCs had a greater effect than MSCs. In most cases, the expression was near or higher than the healthy control levels in both the brain and spinal cord. These results clearly show that NSCs provided greater neuroprotection than MSCs.

We next examined the effect of transplanted cells on the expression of neural proteins. We observed a significant decrease in the expression of TUJ1 and NESTIN in the brain of EAE animals (Figure 34C-D). When EAE animals were transplanted with cells, TUJ1 but not NESTIN expression was significantly improved and was near-normal levels in the brain. In contrast, the expression of both TUJ1 and NESTIN was improved significantly and was near normal levels in the spinal cord. These results suggest cell transplantation also promoted neural development.

4.9 Differentiation of transplanted cells in CNS

To investigate the fate of transplanted cells, CNS tissue sections were co-stained with cell-specific antibodies, TUJ1, OLIG2, and O4, against neural cells, oligodendrocyte progenitors, and ODCs, respectively, as well as human nuclear antigen, and visualized by fluorescent microscopy. The results depicted in Figure 35A-B, showed HNA-positive cells were found in the CNS of the transplanted EAE animals. The results in Figure 35A-D showed that while the cell-specific markers decreased in EAE animals, their expression was co-localized with HNA and significantly improved in transplanted cells. Of the

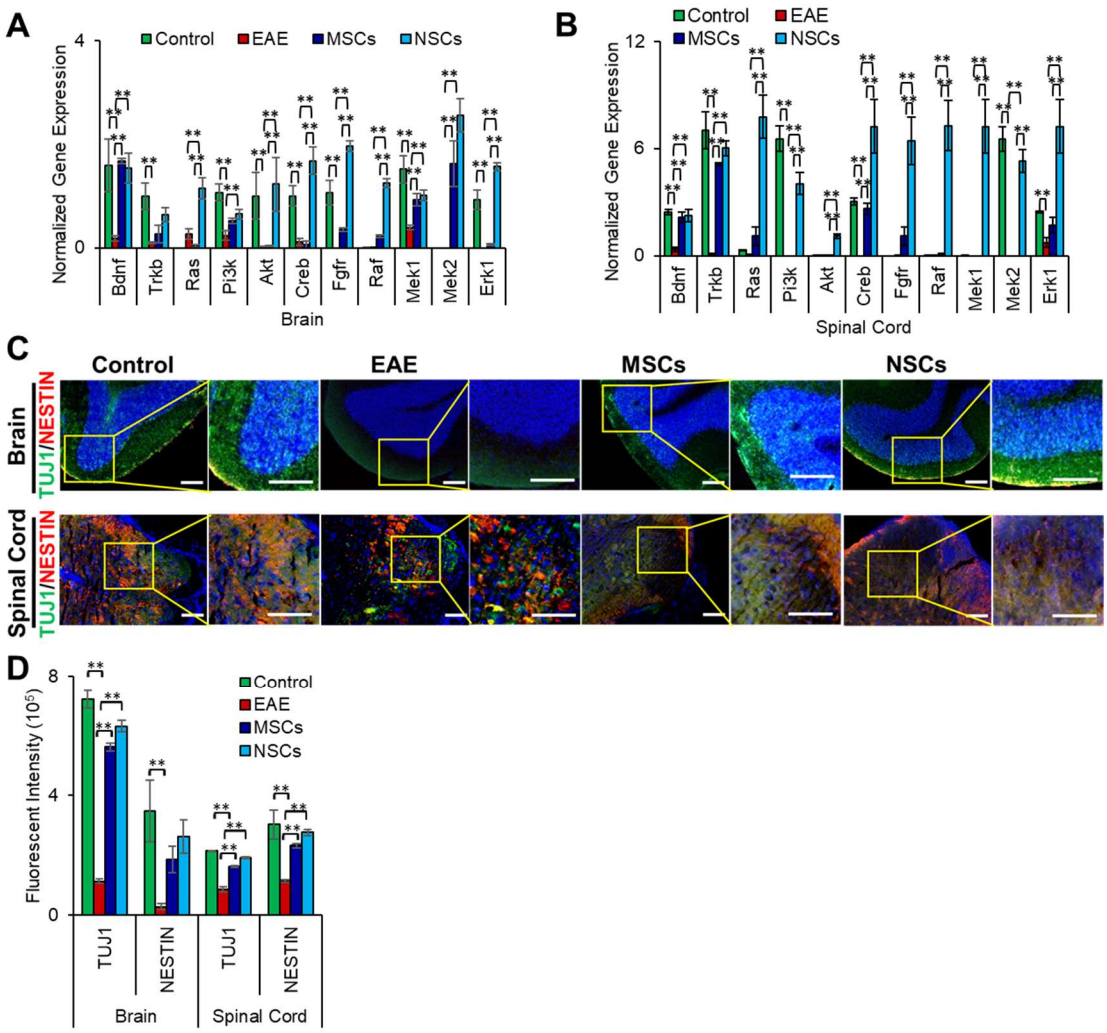

Figure 34: Cell transplantation upregulated neuroprotection markers. (A and B) Transcription of neuroprotection markers, *Bdnf, Tkrb, Ras, Pi3k, Akt, Creb, Fgfr, Raf, Mek1, Mek2, Erk1*, in the brain and spinal cord, respectively, analyzed using qRT-PCR. Fold gene expression was normalized to *Gapdh* and *β-Actin* and error bars represent the SEM of triplicate measures (**$p \leq 0.01$). All of the tested markers were increased to normal or higher levels in NSC, but not MSC transplanted animals compared to the healthy controls. (C) Immunohistochemical staining of paraffin sections of the brain and spinal cord using antibodies against neural proteins, TUJ1 and NESTIN. The inserts (on the right) were magnified and overexposed to enhance contrast. Scale bars represent 50 µm scale bars (magnification: 40×). (D) Quantification of fluorescent intensity of immunostaining in the brain and spinal cord sections depicted in C. (**$p \leq 0.01$). Expression of the neural proteins was more significantly increased in transplanted NSCs than MSCs in EAE animals.

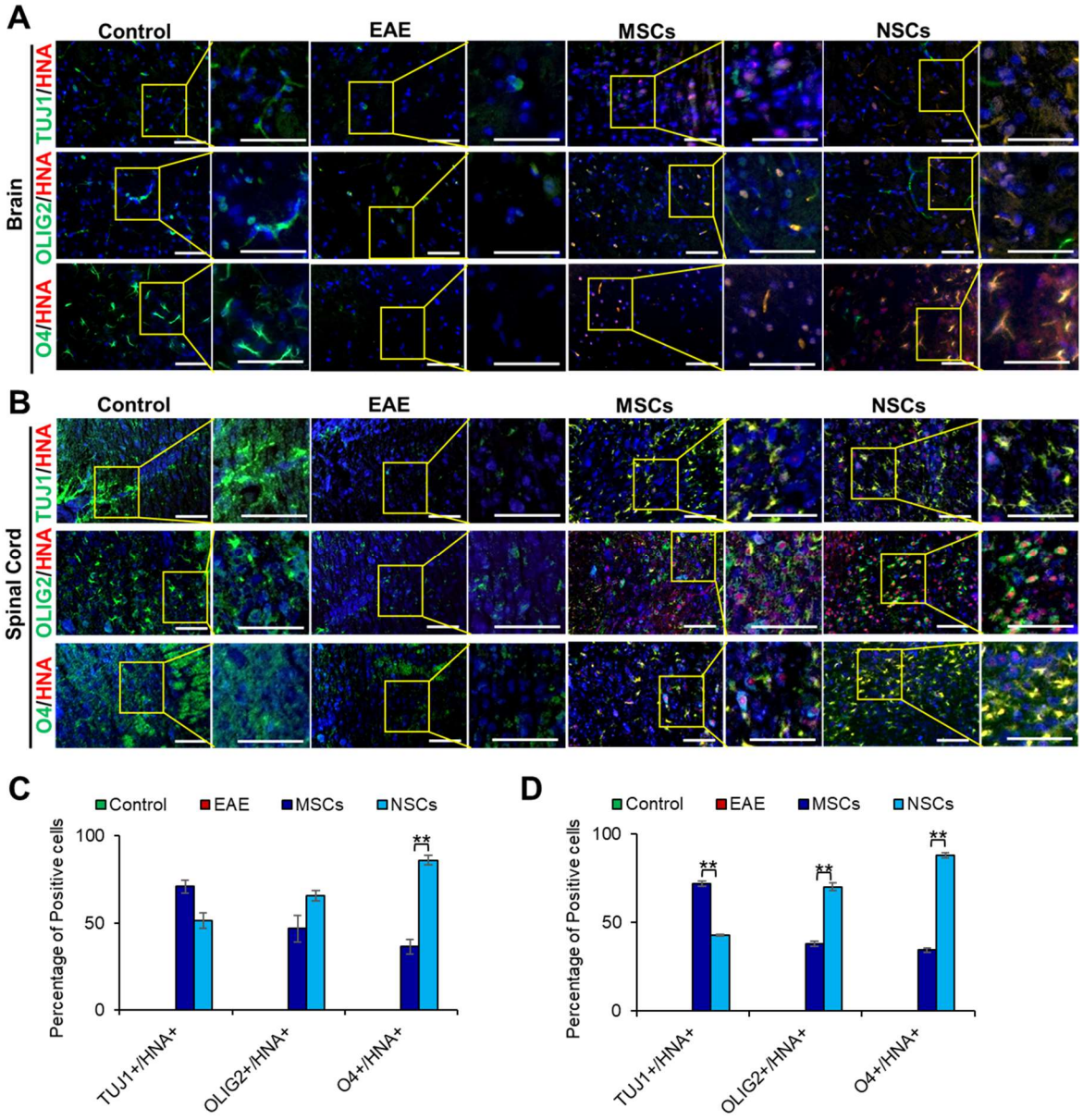

Figure 35: Transplanted cells expressed neural and oligodendrocyte proteins that co-localized with human nuclear antigen *in vivo*. (A and B) Immunohistochemical staining of paraffin sections of the brain and spinal cord with antibodies against cell specific proteins, TUJ1 (NSCs), OLIG1 (oligodendrocyte progenitor cells), and O4 (ODCs), and counterstained with antibody against HNA. The inserts (on the right) were magnified and overexposed to enhance contrast. Scale bars represent 50 µm scale bars (magnification: 40×). (C and D) Percentage of TUJ1+/HNA+, OLIG2+/HNA+, and O4+/HNA+ cells in the brain and spinal cord sections shown in A and B, respectively (**$p \leq 0.01$). TUJ1 staining intensity was greater in both the brain and spinal cord in the case of MSCs, and OLIG2 and O4 staining intensities were greater in the case of NSCs.

HNA-positive cells, 70.9%, and 72.0% cells, were positive for TUJ1 in the brain and spinal cord of MSC injected animals, respectively. In contrast, only 51.3% and 42.9% of the HNA-positive cells expressed TUJ1 in the brain and spinal cord of the NSC-treated animals, respectively. Further analysis revealed that 46.7% and 37.9% of HNA-positive cells were also OLIG2 positive while 36.5% and 34.4% of HNA-positive cells expressed O4 in the brain and spinal cord in MSC treated animals, respectively. In the case of NSC-treated animals, 65.6% and 86% of HNA-positive cells were OLIG2 positive in the brain and spinal cord. A higher number of HNA-positive cells (70.2% and 87.8%) were positive for O4 in the brain and spinal cord, respectively, in NSC-treated animals. Evidently, a significantly higher number of transplanted cells differentiated towards the ODC lineage in the case of NSCs than MSCs. These results suggest that transplanted cells promoted neural development and regeneration.

4.10 Cell transplantation results in the upregulation of neurogenesis genes

Recent studies have demonstrated that neurogenesis genes are downregulated in the CNS tissues of EAE animals (Aharoni et al., 2005). Since cell fate analysis indicated *in vivo* differentiation of transplanted cells (Figure 35), we performed the transcriptional analysis of genes known to promote neuron development and growth. As anticipated, neurogenesis genes, early (*S100b, Nestin, Blbp, Pax6,* and *Hes5)*, intermediate (*Tuj1, Ncam, Rest, Tlx, Ascl1, Tbr2, Ccnd1, Mcm2,* and *Sstr2)* and late (*Dcx, Prox1, Calretinin, NeuN. Calbindin, Pou4f2,* and *Tuc-4)* were downregulated in both the brain and spinal cord of EAE animals. However, transplanted cells rescued the expression of these genes in the CNS (Figure 36A-B). NSCs had a significantly greater expression of the neurogenesis genes in both the brain and spinal cord when compared to animals

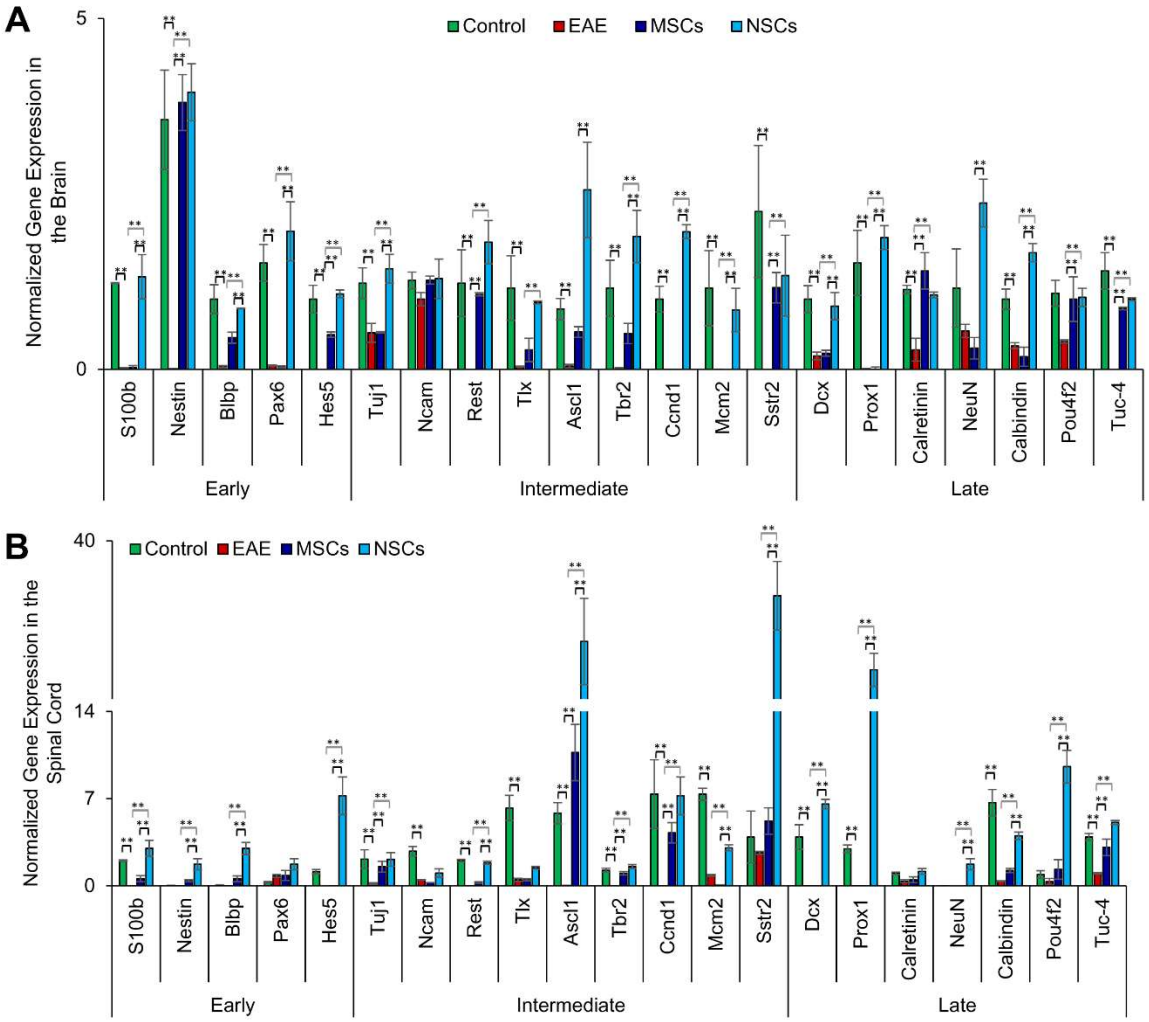

Figure 36: Cell transplantation resulted in the upregulation of neurogenesis markers in the CNS. (A and B) Determination of expression of genes associated with various stages of neurogenesis, early (*S100b, Nestin, Blbp, Pax6*, *Hes5*), intermediate (*Tuj1, Ncam, Rest, Tlx, Ascl1, Tbr2, Ccnd1, Mcm2, Sstr2*) and late (*Dcx, Prox1, Calretinin, NeuN, Calbindin, Pou4f2, Tuc-4*) using qRT-PCR. Fold gene expression was normalized to mouse *Gapdh* and *β-Actin*, and error bars represent the SEM of triplicate measures (**p ≤ 0.01). Expression of genes representing all stages of neurogenesis was greater in the case of NSCs than MSCs, but it was more pronounced in the middle and late stages of neurogenesis.

transplanted with MSCs. Taken together, NSCs resulted in a greater improvement in promoting neurogenesis via the upregulation of *Ascl1, Sstr2, Prox1, Pou4f2,* and *Dcx* in the CNS tissues.

Our results showed that *Ras, Pi3k, Akt,* and *Creb* were downregulated in EAE animals but increased in NSC transplanted animals (Figure 34). This may suggest that the BDNF-TrkB signaling pathway, which plays a crucial role in promoting cell survival and neuroprotection *in vivo* (Johnson et al., 2009; Peltier et al., 2007), is at least partially responsible for functional neural recovery in transplanted animals. Furthermore, several genes, including *Fgfr, Raf, Mek1/2, Erk1/2,* and *Olig2* as well as *Ascl1 and Prox1,* which are associated with the FGF signaling pathway and involved in neuronal and glial differentiation (Dennis, D. J. et al., 2019; Johnson et al., 2009), were down-regulated in EAE mice, but their expression was significantly increased in transplanted NSCs. Our results suggest that NSC transplantation modulated the BDNF-TrkB and FGF signaling pathways, as illustrated in Figure 37.

4.11 Discussion

In the current study, we used highly proliferative and naïve primitive MSCs isolated from a specific region of the umbilical cord tissue (Beeravolu et al., 2016; Beeravolu et al., 2017) to differentiate them into a large amount of NSCs required for animal studies. Primitive MSC-derived NSCs expressed known neural markers, including NESTIN, TUJ1, VIMENTIN, and PAX6 (Park, J. et al., 2017). Although published reports indicate expression of NESTIN (Wong et al., 2014) and VIMENTIN (Ise et al., 2019) by MSCs, our results showed that MSCs exhibited significantly lower expression of these markers. Further differentiation of NSCs yielded cells with ODC characteristics

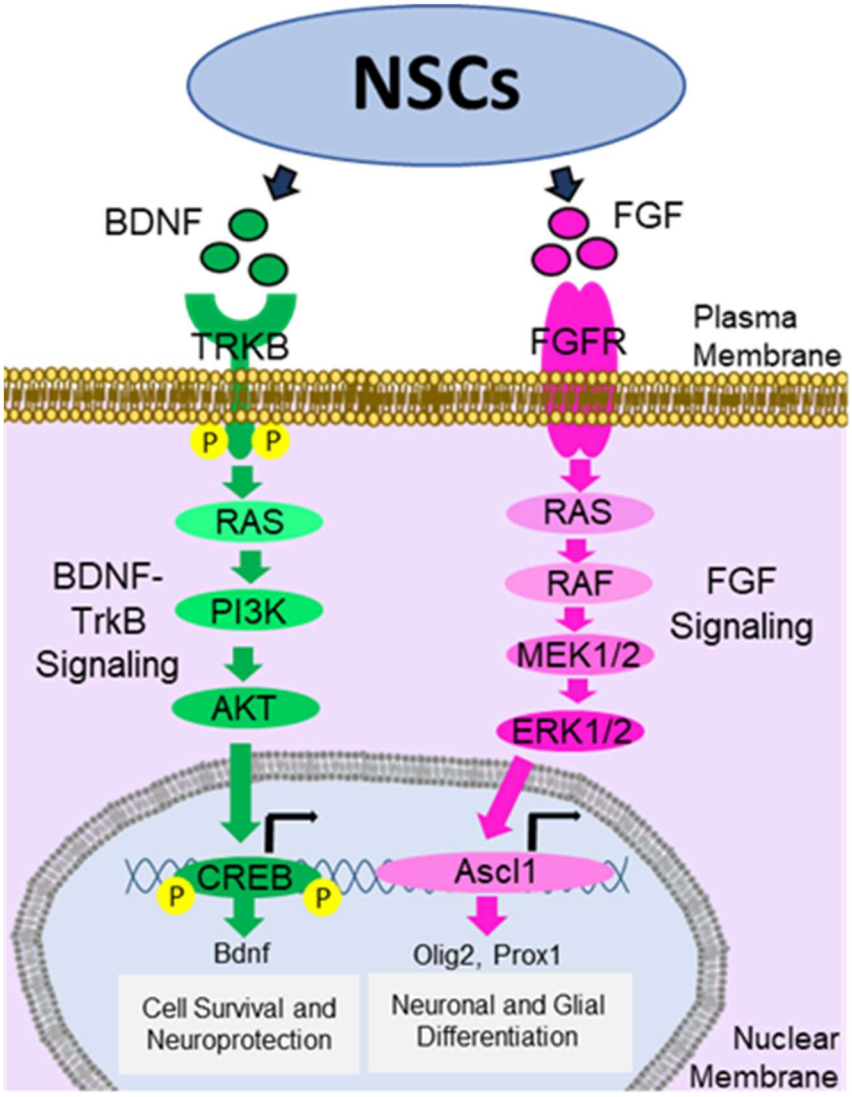

Figure 37. Proposed molecular mechanism of cell survival/neuroprotection and differentiation promoted by NSCs.

as they expressed typical markers, OLIG2, SOX10, O4, MBP, and MOG (Kuhn et al., 2019).

EAE disease progression and symptoms in the established mouse model followed a typical pattern and were scored according to published reports (Dupree & Feinstein, 2018). EAE was induced 10-11 days following MOG immunization, and clinical symptoms got progressively worse, as predicted. In addition, weight was found to be negatively correlated to disease symptoms, with an observed decrease in weight in EAE mice. Animals at score 1 and 2 of EAE were randomly transplanted with labeled MSCs and NSCs. PKH26 lipophilic tracer was used to label the cells, which has been successfully used to track cells *in vivo* for more than 8 weeks, as reported in our previous studies (Beeravolu et al., 2018; Perez-Cruet et al., 2018). Following cell transplantation, animals showed significant improvement in the clinical symptoms. The symptoms progressively and reproducibly improved in EAE disease score 1 animals than score 2 animals. Although MSCs slowed and halted the disease progression, results of NSC transplantation were even more encouraging at disease score 1. NSCs slowed and reversed the disease process as the neurobehavior of transplanted EAE animals improved to near-normal levels. In brief, NSC treatment proved to be more efficacious based on the clinical symptoms, particularly in EAE disease score 1. Therefore, post-transplantation analysis was focused on EAE disease score 1 animals.

Our cell tracking data showed that the majority of the transplanted labeled cells were localized in the blood, spleen, and CNS in EAE animals. This is consistent with previous studies where MSCs were transplanted in EAE mice and were found to home towards the spinal cord tissue (Liao et al., 2016). However, in our study, a significant

number of injected MSCs and NSCs were found in the spleen, the brain, and spinal cord, demonstrating their homing potential to migrate to multiple tissues typically affected by EAE. Interestingly, significantly more transplanted NSCs than MSCs were observed in the spinal cord. Although labeled cells transplanted in healthy animals were not found in CNS, they could permeate the BBB in diseased animals as BBB is compromised in EAE (Fletcher et al., 2010).

In EAE, activated T cells travel through the BBB, leading to increased cell infiltrates in the CNS (Fletcher et al., 2010). We also observed a significant increase of cell infiltrates in the brain and spinal cord of EAE animals. However, in EAE animals transplanted with cells, the number of infiltrates in the CNS decreased significantly. Previously, adipose MSCs have been shown to inhibit cell infiltrates in the EAE animal model (Farinazzo et al., 2018). However, in our study, NSCs displayed a greater effect than MSCs in reducing the number of infiltrates in the CNS. Although NSCs derived from various sources have modulated immune response in EAE animal models, this is the first report where NSCs derived from primitive MSCs were used and showed greater effectiveness than MSCs. As anticipated, our immunostaining results showed that infiltrates comprised leukocytes, macrophages, and T cells (Schmitt, C. et al., 2012). Since EAE induces a pro-inflammatory response, the results of this study showed that transplanted cells modulated the immune response, significantly reducing the expression of cytokines, *Cd3e*, *Il-17a*, *Il-2*, *Il-1β*, *Il*-6, *Tnfα*, and *Ifnγ*, in the CNS and spleen. In EAE, IL-6 aggravates clinical symptoms and spinal cord pathology mainly by promoting pathogenic Th17 cells, which initiate and perpetuate inflammation and demyelination (Samoilova et al., 1998; Zager et al., 2015). Our results showed that cell transplantation

effectively counters the induction of *Il-6* gene expression in the spleen and the CNS tissues. This suggests that transplanted cells exerted an anti-inflammatory response.

Studies have shown that Treg and Th17 play an important role in the development of EAE and the immune response correlated with the disease (Kleinewietfeld & Hafler, 2013; Lu et al., 2016; Zheng et al., 2015). Treg maintains cell immune tolerance, whereas Th17 mediates the inflammatory response under abnormal conditions such as during an injury (Lu et al., 2016). As expected, we observed an imbalance between Treg and Th17 in EAE animals. At the onset of EAE, the levels of Treg decreased and Th17 increased in the blood and spleen, but both increased in the CNS. However, after NSC transplantation, the imbalance was corrected, and the levels of Treg and Th17 resembled those found in the blood and spleen of the healthy controls. Whereas levels of both Treg and Th17 were reduced in the CNS of animals transplanted with cells. The underlying mechanism for restoring Treg/Th17 levels could be due to the transplanted cells modulating the function of T cells by inhibiting the production of TNFα and IFNγ as shown in our study and reported previously (Bai et al., 2009; Kurte et al., 2015; Xin et al., 2020). Although MOG induced a significant increase in the activation of splenocytes *ex vivo* (Kanakasabai et al., 2012), both MSCs and NSCs had an insignificant effect on the proliferation of splenocytes. These findings suggest that the transplanted cells did not have a tolerizing effect of ablating or regulating CNS autoreactive T cells.

In order to elucidate the mechanism that might explain the therapeutic effects of MSCs and NSCs in EAE mice, we investigated gliosis in the CNS. It is known that in chronic EAE, lesions become inactive resulting in accumulation of reactive astrocyte (GFAP+) filaments in the CNS (Brambilla, 2019). We found that astrogliosis gene, *Gfap*,

was upregulated in EAE mice as well as GFAP+ mouse cells, which were integrated into the brain and grey matter of the spinal cord. Upon cell transplantation, a significant decrease in the expression of astrogliosis genes, *Cntfrα, Bmpr, Gfap, and Nfl-b,* as well as a recession of GFAP+ cells in the grey matter was in agreement with previous reports (Bai et al., 2009; Bravo et al., 2016; Pluchino et al., 2003).

Since cell transplantation reduced infiltrates, induced anti-inflammatory response, and inhibited gliosis, they were likely to promote remyelination as reported previously (Inoue, M. et al., 2003; Maeda et al., 2019). Our approach significantly restored the lost myelin in EAE animals, particularly in the case of transplanted NSCs. Loss of ODCs and activated T cells in MS/EAE contribute to the demyelination of neurons (Wang, M.-R. et al., 2019). Our results showed significant upregulation of myelin associated genes, *Erk2, Krox-20, Mpz, Mbp, and Mog,* and proteins, MBP and MOG, suggesting restoration of ODCs resulting in significant improvement in myelination observed in animals transplanted with cells, particularly with NSCs.

Therefore, we investigated whether transplanted cells themselves differentiate into the glial lineage *in vivo*. Analysis of CNS tissues showed co-localization of expression of HNA and genes, TUJ1, as well as OLIG2 and O4, which are key factors in oligodendrogenesis (Bae et al., 2016; Jiang et al., 2020). Interestingly, MSCs displayed an upregulation of TUJ1 providing evidence that the MSCs had entered into the early stages of neural differentiation. Whereas the upregulation of OLIG2 and O4 in the case of NSC transplantation suggested that, they differentiated towards the ODC lineage. Therefore, it is plausible to suggest that NSCs have potential to differentiate *in vivo* to replace, regenerate, and repair the lost cells due to EAE.

Typically, NSCs reside in the hippocampus hilus and subventricular zone, which promote proliferation and migration in different diseases (Aharoni et al., 2005). Moreover, these cells have the potential to differentiate to produce mature astrocytes and neurons through the enhancement of neurogenesis (Picard-Riera et al., 2004). However, the therapeutic potential of self-neurogenesis in the mature CNS is very limited due to the sharp decline of this process after birth (Aharoni et al., 2005; Sorrells et al., 2018). In the current study, results showed an overall increase in the expression of neurogenesis-specific genes in the CNS tissues in NSC transplanted animals. Additionally, NSC transplanted animals displayed the greatest upregulation of *Ascl1*, *Sstr2*, and *Prox1* in the spinal cord, which promotes neuronal and ODC differentiation (Dennis, D. J. et al., 2019; Johnson et al., 2009). Presumably, these factors contributed to the greater efficacy of NSCs for neurogenesis and the reversal of EAE symptoms by preserving and regenerating the neurons. The fact that the expression of these factors is improved more significantly in animals transplanted with NSCs, and that the animals recovered to near normal conditions suggests the use of NSC therapy in MS patients would be more effective than using MSCs.

One of the possible reasons NSCs are more effective is their ability to express neurotrophins, such as BDNF, a regulator of adult neurogenesis (Numakawa et al., 2017). Studies have revealed that TrkB has the greatest relative affinity for BDNF and is expressed on a large proportion of stem cells during differentiation and maturation towards the neural lineages (Numakawa et al., 2017). When BDNF binds to TrkB, a downstream cascade effect is triggered by activating RAS, PI3K, and AKT. This activation leads to upregulation of the nuclear gene transcription of *CREB* (Peltier et al.,

2007). Studies have shown that when *CREB* is upregulated in differentiating neurons, it will enhance neuronal proliferation and cell survival (Nakagawa et al., 2002). In this study, we observed the upregulation of markers associated with BNDF-TrkB signaling, which resulted in the increased expression of *Ras*, *Pi3k*, and *Akt* as well as *Creb* and *Bdnf* in animals treated with NSCs. Although EAE animals transplanted with MSCs displayed a significant increase of *Bdnf* and *Trkb*, downstream gene expression was insignificant compared to untreated EAE animals. Therefore, NSCs displayed a greater effect in promoting proliferation and neuron maturation via activation of the BDNF-TrkB pathway through BDNF stimulation.

FGF has been found to be a potent modulator of the proliferation and differentiation of neural progenitor cells within the CNS (Woodbury & Ikezu, 2014). Additionally, FGF signaling is important for regulating neurogenesis in the CNS (Stevens et al., 2010). A study revealed that upregulation of FGF signaling led to an increase in the neural differentiation process (Kilpatrick & Bartlett, 1993). Upon FGF binding to the FGF receptor, this triggers the intracellular pathway that leads to the cascade activation of RAS, RAF, MEK1, MEK2, ERK1, and ERK2 (Li, S. et al., 2014). *Ascl1* is then transcribed due to this cascade effect leading to neuronal and ODC differentiation (Nakatani et al., 2013). Our results showed a significant upregulation of *Fgfr*, *Ras*, *Raf*, *Mek1*, *Mek2*, *Erk1*, and *Erk2,* as well as *Ascl1* and *Prox1*, particularly in NSC, transplanted animals with the greatest effect in the spinal cord. Significantly, higher expression of *Ascl1* in animals transplanted with NSCs suggests that the cells promoted neuronal differentiation as well. Altogether, our results indicate that BDNF-TrkB and

FGF signaling might play an important role in promoting proliferation, cell survival, and neuronal and glial differentiation observed when transplanted NSCs in an EAE animal.

In brief, this study demonstrated the potential of NSCs to induce anti-inflammatory responses and provide neuroprotection and promote endogenous neurogenesis resulting in the reversal of EAE clinical symptoms and repair of the damaged CNS. Although there have been a number of clinical trials utilizing autologous bone marrow MSCs and umbilical cord-derived MSCs, the results are not always conclusive (Alghwiri et al., 2020; Harris et al., 2018; Riordan et al., 2018). Furthermore, most of these studies were limited to phase I and II trials due to the limited availability of cells. Two clinical trials used human fetal-derived NSCs (ClinicalTrials.gov, 2021); however, results of these phase I/II studies have not been reported. Furthermore, NSCs were isolated from their fetal tissue, and their use could pose ethical and moral concerns (Ishii & Eto, 2014). The results of our study are highly promising in reversing the disease process and improving the EAE pathology of CNS, particularly in the case of NSCs. Significantly, since primitive MSCs used here are highly proliferative and can be maintained for many passages without losing their differentiation potential, they can be rapidly amplified and differentiated into NSCs in the amounts required for large animals and clinical studies. This has been one of the major impediments for conducting phase III and IV using MSCs or their derivatives. Further studies should be pursued to determine if higher or multiple doses of cells injected at advanced/chronic stages of EAE could also effectively reverse the EAE disease process. It would also be interesting to know if cell treatment at the time of MOG injection could block the induction of EAE in mice.

Further studies are warranted to investigate the modulation of Treg cells by NSCs. Additional studies for elucidating the cellular and molecular mechanism and associated signaling pathways for functional neuronal recovery would be helpful. Nonetheless, our study provided proof of concept and basis for investigating the efficacy of primitive MSC-derived NSCs to treat MS in clinical trials.

CHAPTER FIVE

HUMAN PRIMITIVE MESENCHYMAL STEM CELL-DERIVED RETINAL PROGENITOR CELLS PROMOTED NEUROPROTECTION AND NEUROGENESIS IN RD12 MICE

The results for this section are from the published data available at (Brown et al., 2021)

5.1 Differentiation and characterization of MSCs into RPCs

Using a differentiation medium, we used previously isolated and characterized MSCs (Beeravolu et al., 2016) to differentiate them into RPCs. The differentiated cells exhibited neural outgrowth and downregulated the mesenchymal stem cell markers, CD29, CD44, CD73, CD90, and CD105, but upregulated the protein RCVRN, neural genes *TUJ1, NESTIN,* and *PAX6,* and retinal genes, *RCVRN, CRX, RHO, SIX3*, *OTX2, SIX6, GNL3, FABP7, NF200, SSEA4, ABCG2, DACH1, PTK7, PCNA, β-CATENIN, NOTCH1,* and *RPS27A* (Figure 38A-D). The expression of neural and retinal markers was further validated by immunofluorescence staining by antibodies against TUJ1, NESTIN, PAX6, RCVRN, CRX, and RHO (Figure 39A-C). Based on these results, the differentiated derivatives of MSCs were considered to be RPCs. We estimated the rate of differentiation of MSCs into RPCs was 83%, 91%, 89%, 90%, 94%, and 81% based on the expression of TUJ1, NESTIN, PAX6, RCVRN, CRX, and RHO, respectively. RPCs also expressed high levels of neurotrophic factors, *BDNF, GDNF, IGF, CNTF, PDGF, EGF,* and *FGF* compared to MSCs (Figure 39D), suggesting that they could potentially promote neuroprotection.

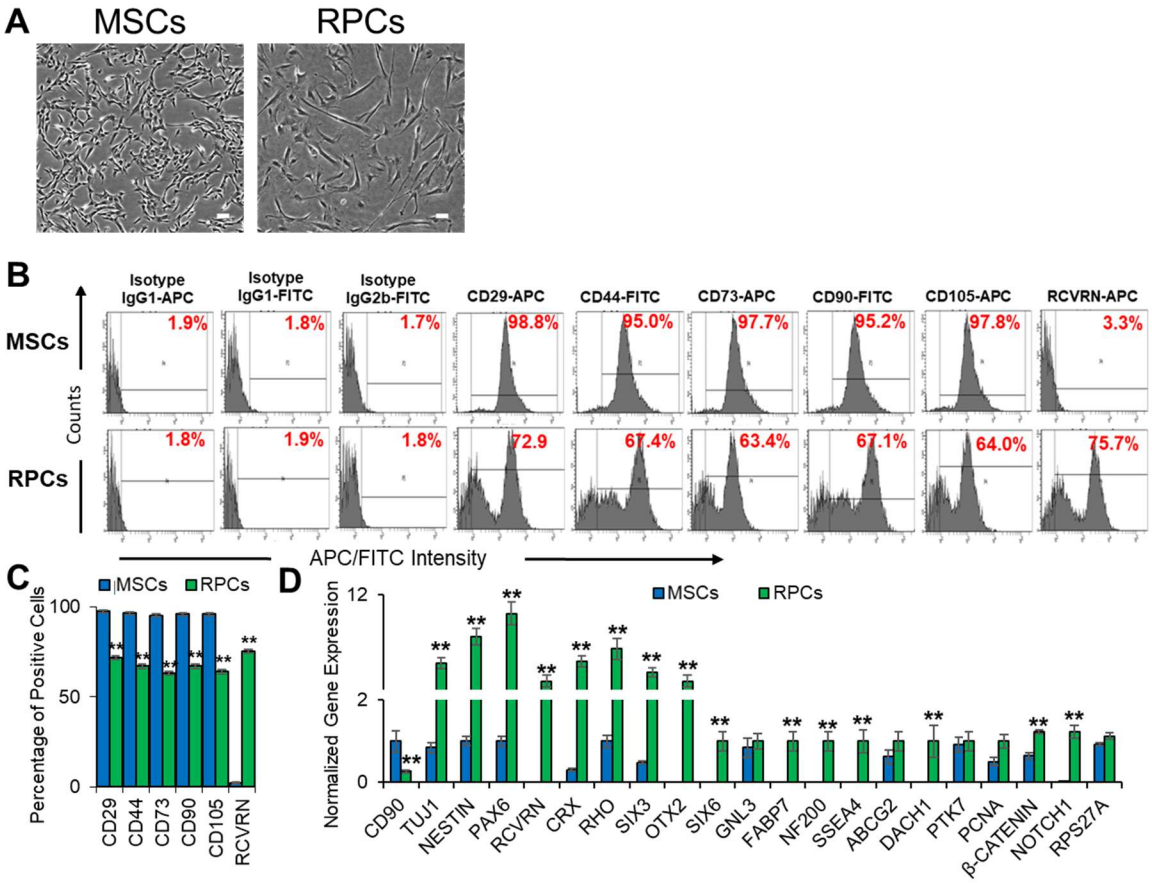

Figure 38: Characterization of RPCs derived from MSCs. (A) Phase-contrast images of MSCs and RPCs. 100 µm scale bar. (Magnification: 4x). (B and C) Histograms and graphical representation of the expression of MSC and retinal markers by MSCs and RPCs as determined by flow cytometry (**p ≤ 0.01). (D) Expression of MSC (*CD90*), neural (*TUJ1, NESTIN,* and *PAX6*), retinal (*RCVRN, CRX, RHO, SIX3, OTX2, SIX6, GNL3, FABP7, NF200, SSEA4, ABCG2, DACH1, PTK7, PCNA, β-CATENIN, NOTCH1,* and *RPS27A*) genes in MSCs and RPCs as determined by qRT-PCR. Gene expression was normalized to *GAPDH* and *β-ACTIN*. Error bars represent the SEM (**p ≤ 0.01). All experiments were carried out in triplicates.

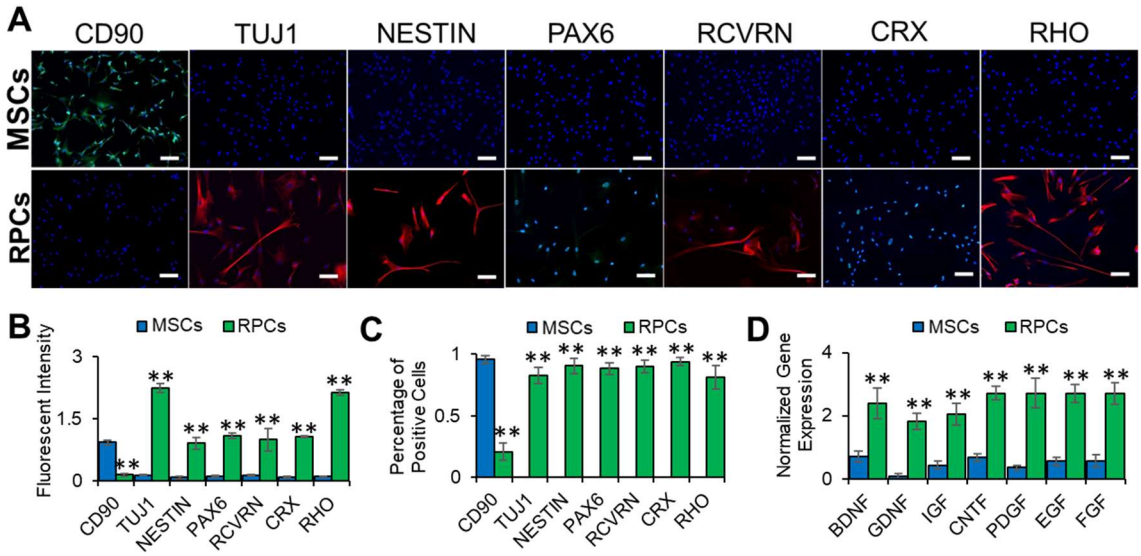

Figure 39: Neural and retinal expression of RPCs derived from MSCs (A) Expression of MSC (CD90), neural (TUJ1, NESTIN, and PAX6), and retinal (RCVRN, CRX, and RHO) proteins in MSCs and RPCs as visualized by immunocytostaining. Shown are representative merged images of DAPI (blue) and human antibodies (green and red). 100 µm scale bar (Magnification: 10x). (B) Measurement of fluorescent intensity of proteins immunocytostained using antibodies in MSCs and RPCs (**$p \leq 0.01$). (C) Percentage of positive immunocytostained cells (**$p \leq 0.01$). (D) Expression of neurotropic genes, *BDNF, GDNF, IGF, CNTF, PDGF, EGF,* and *FGF* in MSCs and RPCs. Gene expression was normalized to *GAPDH* and *β-ACTIN*, and error bars represent the SEM (**$p \leq 0.01$). Significant changes in the gene and protein expression were observed upon differentiation of MSCs into RPCs. All experiments were carried out in triplicates.

5.2 Transcriptomic analysis of MSCs and RPCs

To further characterize the RPCs, RNA-seq analysis was performed. The results depicted in Figure 40A show a distinct difference in gene expression patterns between MSCs and RPCs. This analysis revealed 2951 differentially expressed genes (DEGs) at a false discovery rate (FDR) < 0.05. Of these DEGs, 1,618 genes were upregulated in MSCs, and 1,333 genes were upregulated in RPCs. Among the top 100 DEGs (FDR < 8.3×10^{-147}), 68 and 32 genes were upregulated in MSCs and RPCs, respectively (Figure 40B-C). Notably, 8 upregulated DEGs in MSCs were specific to RPE while 18 upregulated DEGs in RPCs were specific to the neuronal layers of the retina (FDR < 0.05) (Figure 41A). The expression of selected DEGs was validated by qRT-PCR. The selected DEGs were associated with retinal cells including, photoreceptors *(SULF2, GNAT2 and NRL),* amacrine *(TFAP2A and ATP1B1),* horizontal *(NDRG1),* Müller glia *(HES1, and SPON1),* and ganglion *(EBF1)* cells (Figure 41B).

We next performed functional analysis of the DEGs using gene ontology (GO) analysis. Comparative enrichment analysis of MSCs and RPCs performed using Enrichr identified DEGs associated with biological process, molecular function, and cellular component ontologies. In the category of biological processes, MSCs were highly enriched in DNA ligation, chromosome organization, and positive regulation of cell cycle process (Figure 42A). On the other hand, RPCs were significantly enriched in regulation of axon guidance, positive regulation of stem cell differentiation, dendritic spine maintenance, astrocyte activation, negative regulation of FGF receptor signaling pathway, and regulation of regulation mesenchymal stem cell differentiation, neuron projection maintenance, and extracellular matrix organization. Next, we investigated the

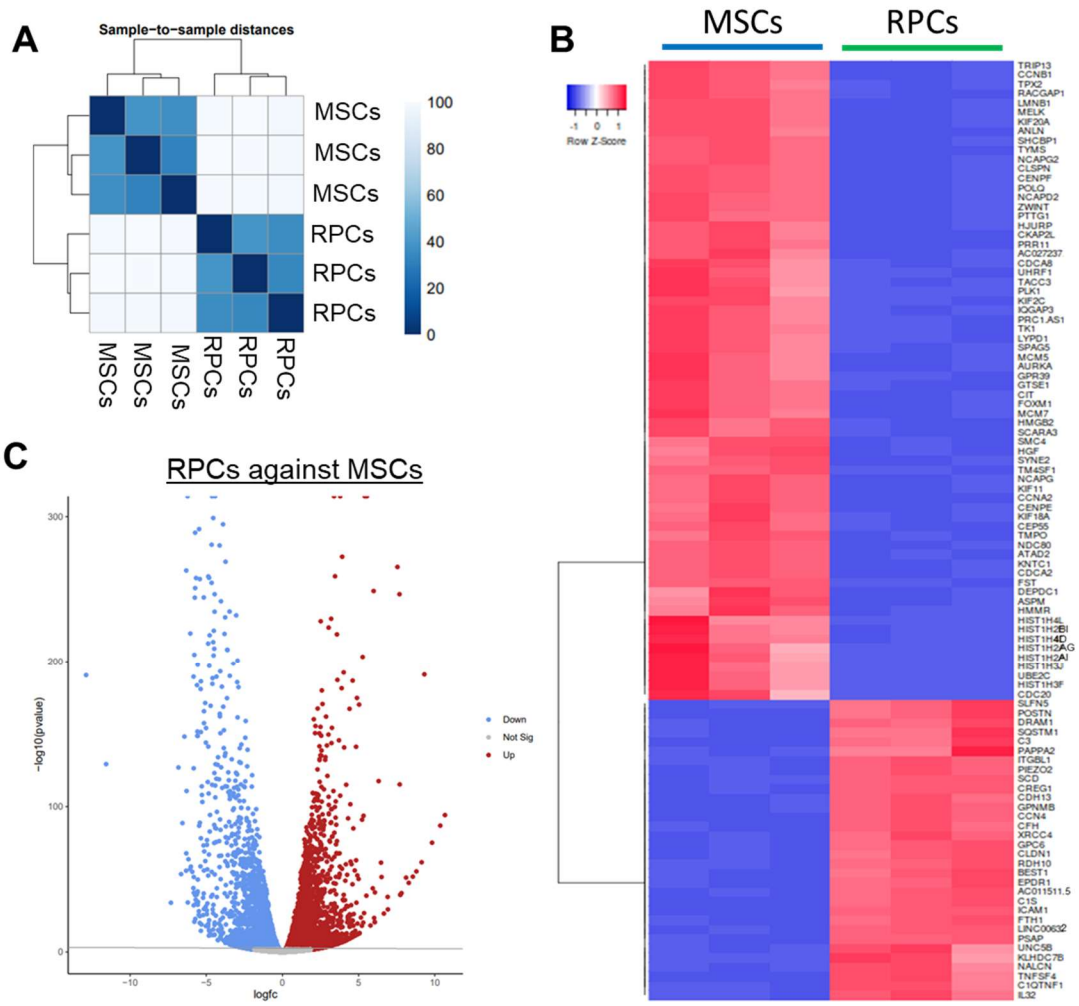

Figure 40: Transcriptome analysis of MSCs and RPCs. (A) Hierarchical clustering analysis was performed using DESeq2, and the data was plotted as a sample-to-sample heatmap. The colored indicator represents sample distances (blue signifies a high correlation). (B) Heatmap showing raw z-scores of RNA-seq log2 transformed values of the top 100 DEGs and (C) volcano plot to visualize DEGs. In the heatmap, upregulated and downregulated genes are shown in red and blue, respectively.

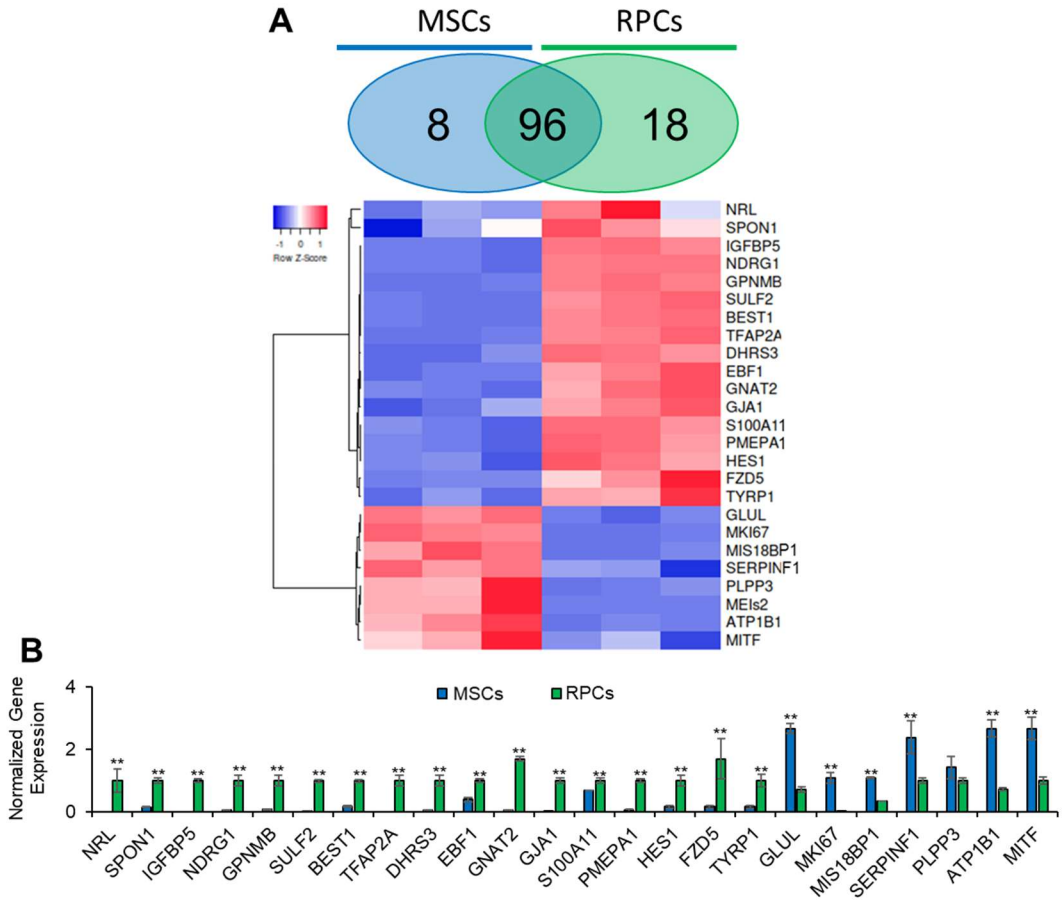

Figure 41: Transcriptome analysis of retinal specific markers (A) Heatmap showing raw z-scores of RNA-seq log2 transformed values of expression of retinal markers in MSCs and RPCs. Venn diagrams depict the total number of genes upregulated in MSCs (blue) and RPCs (green). In the heatmap, upregulated and downregulated genes are shown in red and blue, respectively. (B) Validation of selected retinal DEGs in MSCs and RPCs by qRT-PCR. Gene expression was normalized to *GAPDH* and *β-ACTIN*, and error bars represent the SEM (**p ≤ 0.01). All experiments were performed in triplicate.

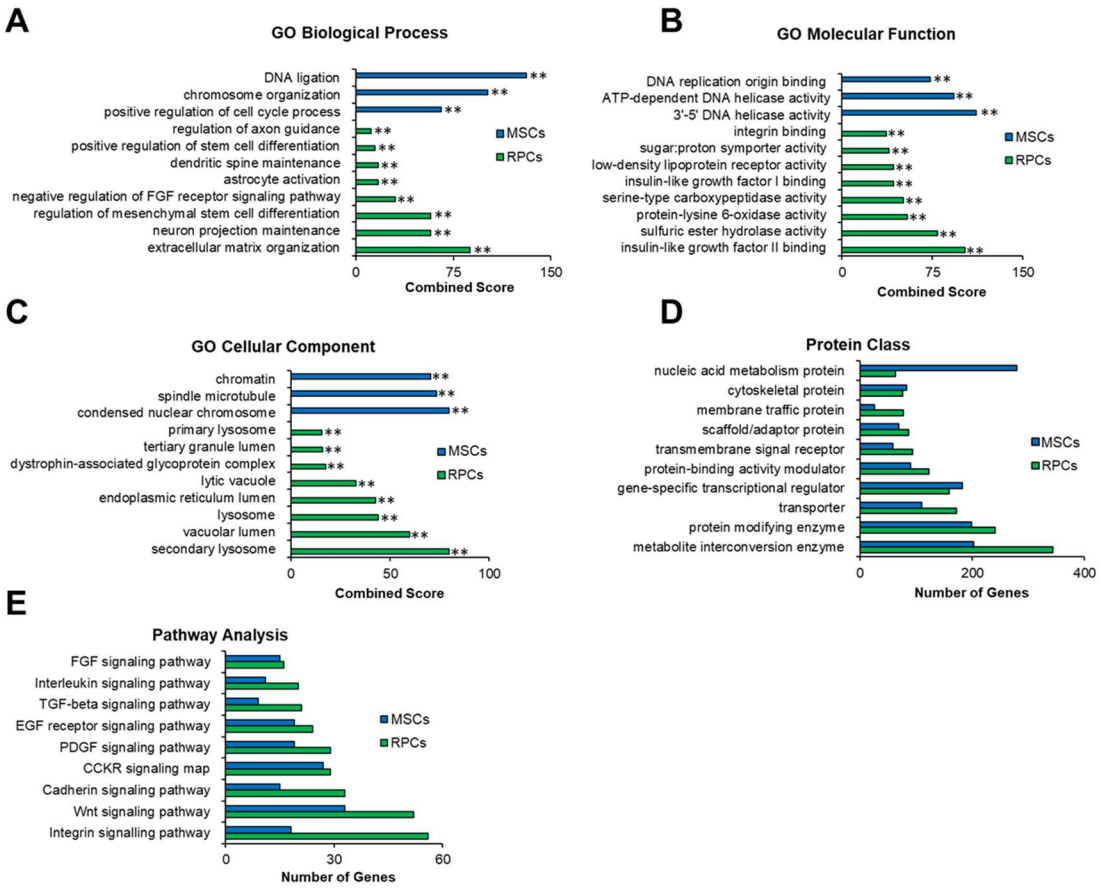

Figure 42: GO analysis of RNASeq of MSCs and RPCs. Enrichr and PANTHER analyses of DEGs was performed with Benjamini–Hochberg FDR < 0.05 using DESeq2. (A–C) GO term enrichment analysis depicting upregulated DEGs associated with biological processes, molecular function, and cellular component, respectively, and the x-axis represents the combined score generated by Enrichr (**p ≤ 0.01). (D and E) Protein classes and pathways upregulated in MSCs and RPCs, as determined by PANTHER analysis. The x-axis represents the number of genes associated with each category (**p ≤ 0.01).

category of molecular function (Figure 42B). MSCs were enriched in DNA replication origin binding, ATP-dependent DNA helicase activity, and 3'-5' DNA helicase activity. Whereas RPCs presented a significant enrichment of integrin binding, sugar:proton symporter activity, low-density lipoprotein receptor activity, insulin-like growth factor I binding, serine-type carboxypeptidase activity, protein-lysine 6-oxidase activity, sulfuric ester hydrolase activity, and insulin-like growth factor II binding. We then investigated cellular components enriched in the DEGs. GO analysis also showed that chromatin, spindle microtubule, and condensed nuclear chromosome were enriched in MSCs. While RPCs displayed significant enrichment of primary lysosome, tertiary granule lumen, dystrophin-associated glycoprotein complex, lytic vacuole, endoplasmic reticulum lumen, lysosome, vacuolar lumen, and secondary lysosome (Figure 42C).

Next, we employed PANTHER analysis to investigate differentially expressed protein classes (Figure 42D), which showed that cytoskeletal and gene-specific transcriptional regulation were enriched in MSCs and RPCs. However, nucleic acid metabolism proteins were more enriched in MSCs than RPCs. In contrast, metabolite interconversion enzyme, protein modifying enzyme, transporter, protein-binding activity modulator, transmembrane signal receptor, scaffold/adaptor protein, and membrane traffic protein classes were associated with more genes in RPCs. In signaling pathways, FGF, Interleukin, TGF-beta, EGFR, PDGF, CCKR, Cadherin, Wnt, and Integrin were more expressed in RPCs than MSCs (Figure 42E). Altogether, these results showed that RPCs derived MSCs expressed expected retinal specific genes. Interestingly, they also expressed neurotrophic genes involved in neuroprotection. Therefore, RPCs were an ideal choice to investigate their therapeutic potential.

5.3 Improvement of retinal function in rd12 mice transplanted with cells

Behavioral analysis of rd12 mice intravitreally transplanted with PKH26 labeled MSCs, and RPCs was performed for vision and acuity using visual recovery assay and OKR, respectively. We observed a significant improvement in visual recovery and acuity in transplanted animals (Figure 43A-C). These observations were followed by a quantitative functional assay using ERG. As expected, ERG analysis showed that dark- and light-adapted rd12 mice had almost a complete loss of a- and b-wave amplitudes (Figure 44). A progressively significant increase in the a- and b-wave amplitudes of the dark-adapted animals was observed in MSCs transplanted rd12 mice. Notably, an even greater increase in the a- and b-wave amplitudes was noticed in animals transplanted with RPCs (Figure 44A-C). The increase in the amplitude was greater at 8 weeks than 4 weeks after cell transplantation, indicating a progressive improvement of the vision in treated mice. In addition, the b-wave amplitude progressively improved with an increase in light intensity in rd12 mice treated with cells, but the increase was more pronounced with RPCs than MSCs (Figure 44D-F). On the other hand, in the light-adapted rd12 mice transplanted with cells, only the b-wave amplitude was progressively increased (Figure 45A-C). Again, RPCs had a more significant effect in improving the b-wave amplitude than MSCs, and the effect was more significant at 8 weeks than 4 weeks after transplantation of cells. Overall, these results showed more significant improvement in retinal function by RPCs than MSCs.

5.4 Transplanted cells improved the retinal structure

We next analyzed the structure of the retina. The results depicted in Figure 46 show that rd12 mice displayed a progressive decrease in thickness of the total retina,

A

0	No Head Movement
1	More than 1 second delay of head movement
2	1 second delay of head movement
3	Less than 1 second delay of head movement
4	Immediate Head Movement

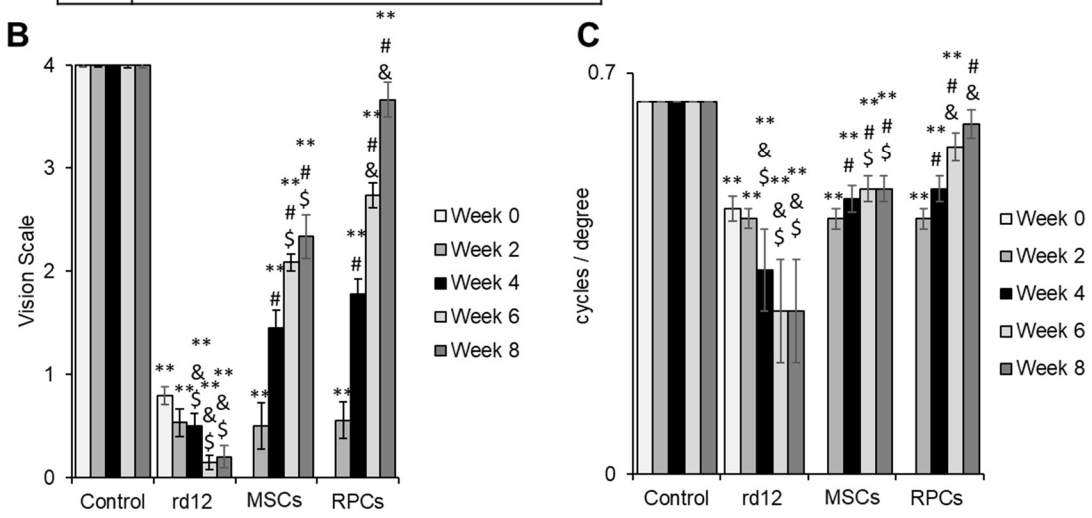

Figure 43: Behavioral analysis of mice. (A) Visual recovery scale. (B and C) Graphical representation of visual recovery and acuity assays at week 0, 2, 4, 6, 8 with WT, rd12, rd12+MSCs and rd12+RPCs (**$p \leq 0.01$). Symbols, **, #, & and $ indicate significant difference at $p \leq 0.01$ between all experimental conditions: control (wild-type), rd12, rd12+MSCs and rd12+RPCs, respectively.

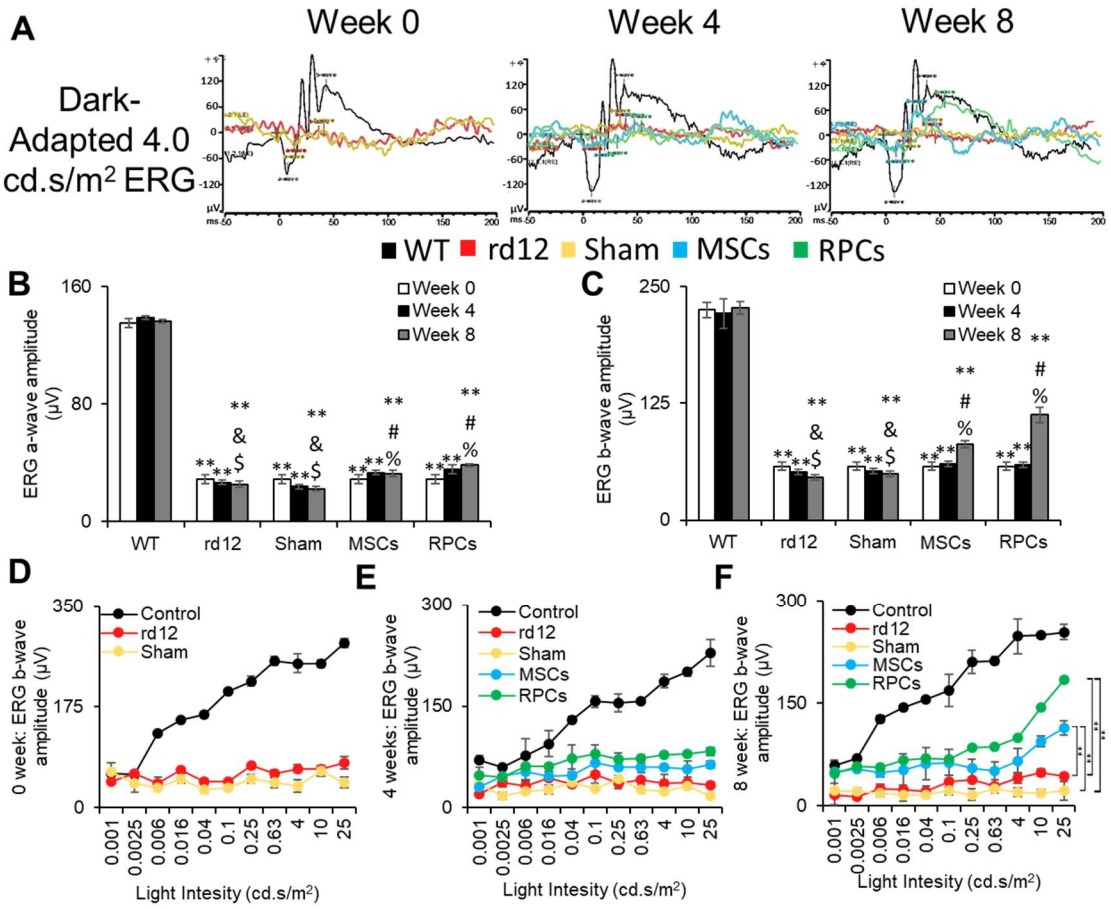

Figure 44: ERG dark-adapted analysis. (A) Representative dark-adapted ERG test of control (wild-type), rd12, sham, rd12+MSCs, and rd12+RPCs at 0, 4, and 8 weeks after transplantation of cells. (B and C) Graphical representation of the amplitude of the dark-adapted ERG a- and b-waves, respectively, from A. (D-F) Intensity-response curves of ERG b-waves at 0, 4, and 8 weeks, respectively, after transplantation of cells (**$p < 0.01$). Symbols, **, #, %, & and $ indicate significant difference at $p \leq 0.01$ between all experimental conditions: control (wild-type), rd12, sham, rd12+MSCs and rd12+RPCs, respectively.

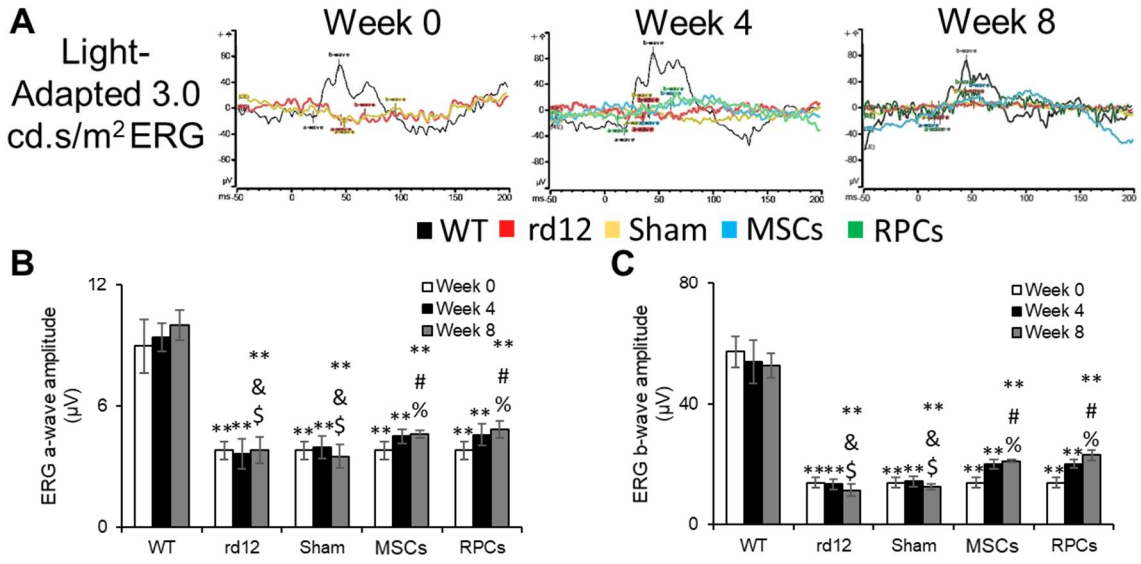

Figure 45: ERG light-adapted analysis. (A) Representative light-adapted ERG test of control (wild-type), rd12, sham, rd12+MSCs and rd12+RPCs at 0, 4, and 8 weeks after transplantation of cells. (B and C) Graphical representation of the amplitude of the light-adapted ERG a- and b-waves, respectively, from A. Symbols, **, #, %, & and $ indicate significant difference at $p \leq 0.01$ between all experimental conditions: control (wild-type), rd12, sham, rd12+MSCs, and rd12+RPCs, respectively.

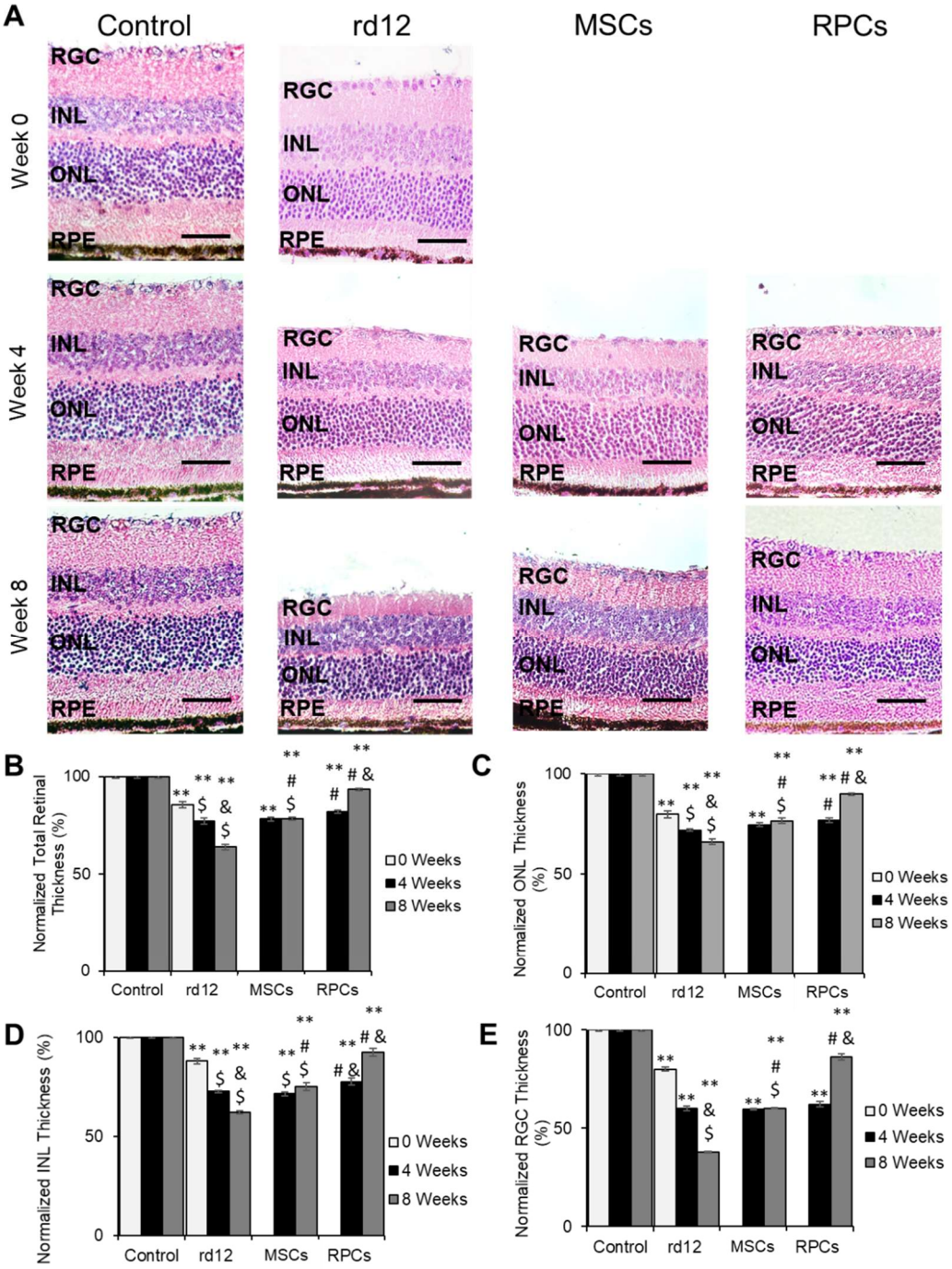

Figure 46: Histological analysis of rd12 retina transplanted with human cells. (A) H&E staining of paraffin-embedded sections of the control (wild-type), rd12, MSCs, and RPCs transplanted retina harvested at 0, 4, and 8 weeks. All scale bars represent 50 µm. (Magnification: 40x). (B-E) Graphical representation comparing the average thickness of the retina, ONL, INL, and RGC. The thickness of each retina was normalized to the control (wild-type) retina. Symbols, **, #, & and $ indicate significant difference at $p \leq 0.01$ between all experimental conditions: control (wild-type), rd12, rd12+MSCs and rd12+RPCs, respectively.

ONL, inner nuclear layer (INL), and RGC during the 8 week study signifying degeneration of the retina (Figure 46A-E). In rd12 mice transplanted with MSCs, the degeneration of the retina was halted as there was no net decrease in the retinal thickness during the 8 weeks. The thickness of the retina, ONL, INL, and RGC significantly increased (from 85.6% to 93.3%, 79.8% to 90.0%, 87.9% to 92.4%, and 80.1% to 86.3%, respectively) by 8 weeks after RPC transplantation. The transplanted cells had no adverse effects as no tumor formation was observed. Overall, MSCs halted the retinal regeneration while RPCs improved the retinal thickness.

5.5 Transplanted cells homed to the retina

Cell tracking revealed that PKH26 labeled cells were localized in the retinal whole-mount of animals transplanted with cells (Figure 47A). Differential interface contrast (DIC) microscopy confirmed the presence and dispersal of labeled cells in the retina (Figure 47B). RPCs were more dispersed than MSCs in the retina 8 weeks post-transplantation. These results suggest that transplanted cells homed to different retinal layers.

5.6 Expression of human markers in the transplanted rd12 mice retina

Since we found that the transplanted cells were localized in different retinal layers, it was conceivable that they would express various retinal markers. The expression of human markers was first investigated by transcriptional analysis. The results showed the expression of human genes associated with anti-inflammation, neuroprotection, retinal, and neurogenesis. In general, fewer human genes were expressed in animals transplanted with MSCs than RPCs. Among the anti-inflammatory genes, only expression of *IL-10* was observed 4 weeks after MSC transplantation, but *IL-4* and *IL-10*

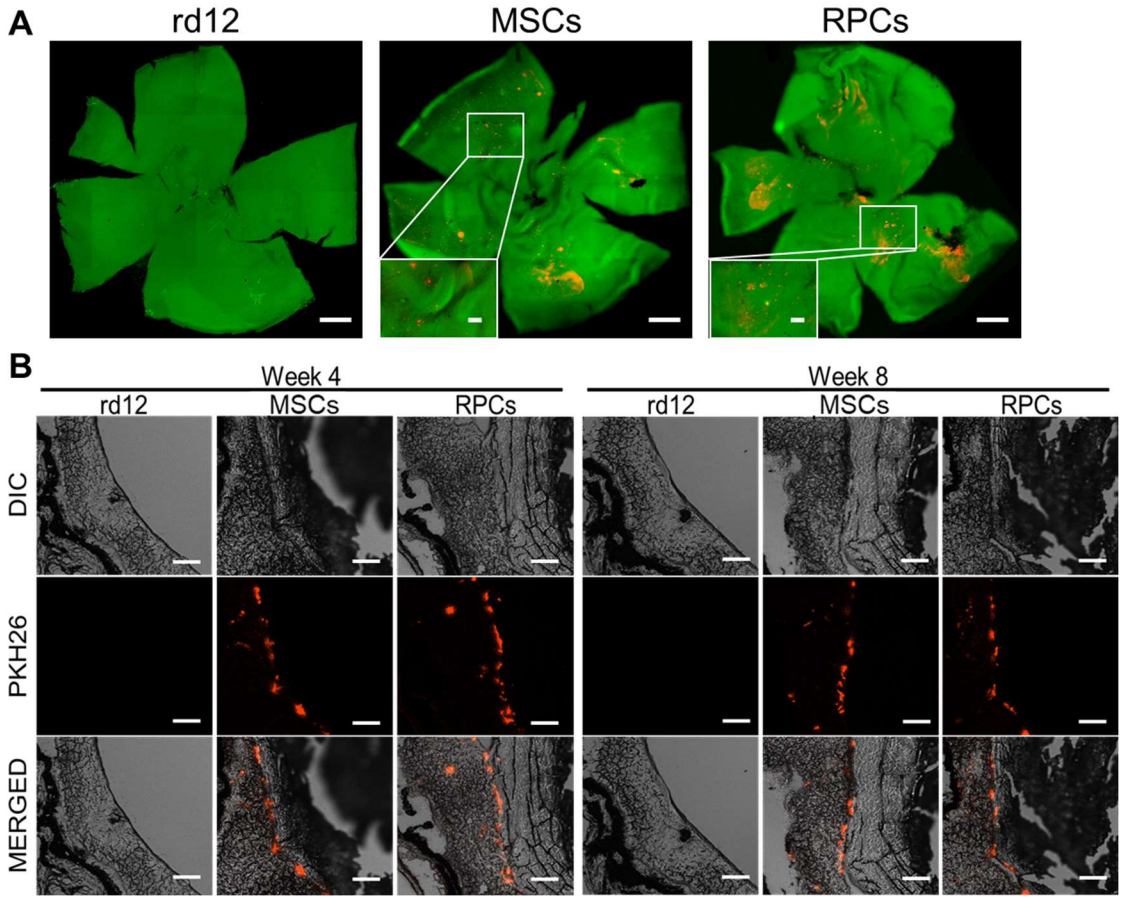

Figure 47: Tracking of cells transplanted into rd12 retina. (A) Whole-mount retina stained with RCVRN (green) 8 weeks after transplantation of PKH26-labeled (red) MSCs and RPCs. 500 µm scale bar and 20 µm scale bars (inserts). (Magnification: 5x and 40x, respectively). (B) Tracking of PKH26 (red) labeled MSCs and RPCs in the cryosections of the retina at 4 and 8 weeks. Scale bars represent 100 µm. (Magnification: 20x).

were expressed after 8 weeks in the case of RPCs (Figure 48A). No pro-inflammatory human genes were expressed in either MSC or RPC transplanted animals.

The expression of two neuroprotective genes, *BDNF,* and *CNTF* was detected only 8 weeks after transplantation of MSCs. In RPCs, some neuroprotective genes (*BDNF*, *GDNF*, and *IGF*) were expressed at 4 weeks. However, several genes, *BDNF*, *GDNF*, *IGF*, *CNTF*, *EGF*, *FGF*, and *PDGF,* were expressed 8 weeks after transplantation (Figure 48B).

As for the retinal genes, MSCs expressed human RPE genes, *PMEL, CD24, LHX2,* and *RPE65*, only at 8 weeks after transplantation. Whereas, RPC transplanted animals expressed human genes, *CRX, SIX3, OTX2, RCVRN*, *RHO, SIX6, GNL3, FABP7, NF200, ABCG2, PTK7, PCNA, β-CATENIN, NOTCH1, and RPS27A* (Figure 48C), which are predominantly associated with the neural layers (ONL, INL, and RGC) of the retina. The expression of ONL, INL, and RGC genes suggests that transplanted RPCs successfully differentiated and integrated into the neural layers of the retina. In contrast, the expression of RPE genes suggests that MSCs are differentiated and integrated into the RPE layer of the retina.

Only two neurogenesis genes, *TUJ1* and *PROX1*, were expressed at 8 weeks after transplantation of MSCs, but several neurogenesis genes, *PAX6, NESTIN, TUJ1, PROX1, CALRETININ*, and *CALBINDIN,* were expressed at 8 weeks (with only *PAX6* and *TUJ1* expressed at 4 weeks) after transplantation of RPCs (Figure 48D).

Similar to the transcriptional analysis, immunostaining studies also suggest that animals transplanted with cells expressed human neural (TUJ1) and retinal (CRX, RCVRN, and RPE65) proteins. These proteins were colocalized with human nuclear antigen (HNA). The results depicted in Figure 49A-B showed that at 4 weeks after

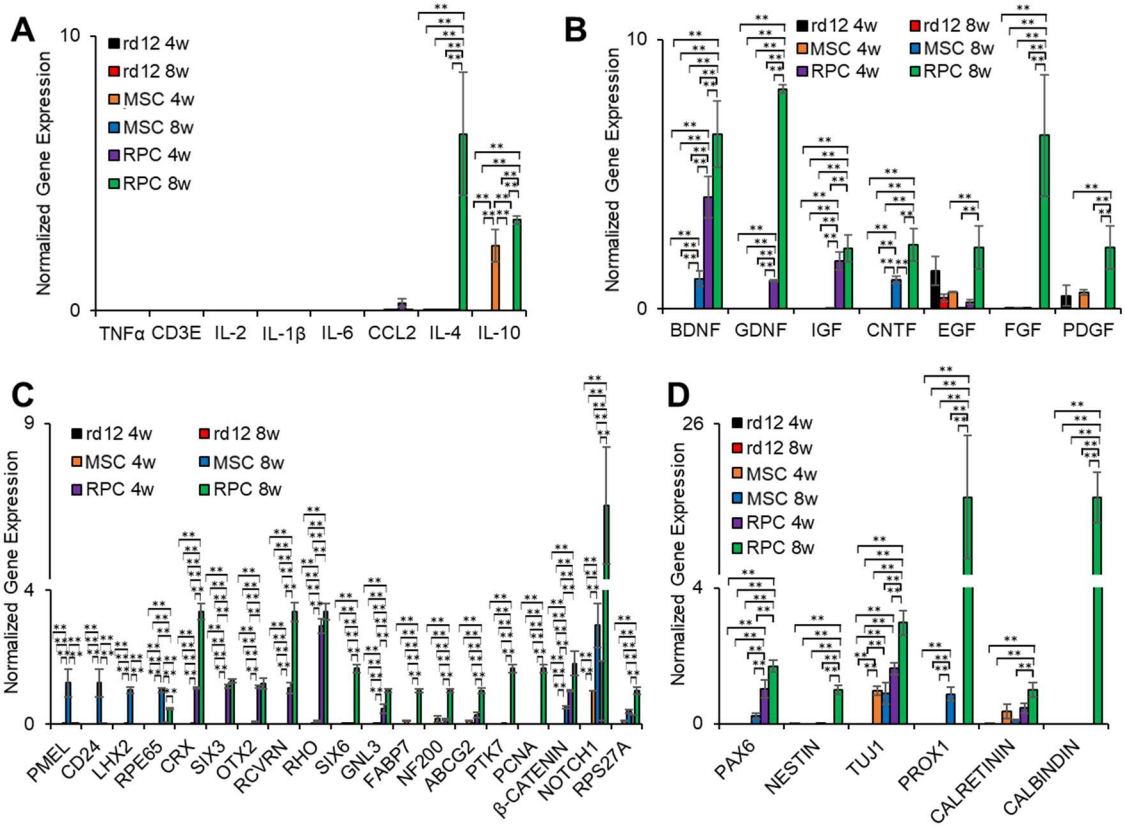

Figure 48: Post-transplantation analysis of the human genes in rd12 retina. (A) Expression of human pro- and anti-inflammatory genes, *TNFα, CD3E, IL-2, IL-1β, IL-6* and *CCL2, and IL-4* and *IL-10,* respectively, (B) neuroprotective genes, *BDNF, GDNF, IGF, CNTF, EGF, FGF, and PDGF,* (C) retinal genes, *CRX, SIX3, OTX2, RCVRN, RHO, SIX6, GNL3, FABP7, NF200, ABCG2, PTK7, PNCA, β-CATENIN, NOTCH1, RPS27A, PMEL, CD24, LHX2,* and *RPE65,* and (D) neurogenesis genes, *PAX6, NESTIN, TUJ1, PROX1, CALRETININ,* and *CALBINDIN*. All gene expression was normalized to *GAPDH* and *β-ACTIN*. Error bars represent the SEM of the triplicate experiment (**p ≤ 0.01).

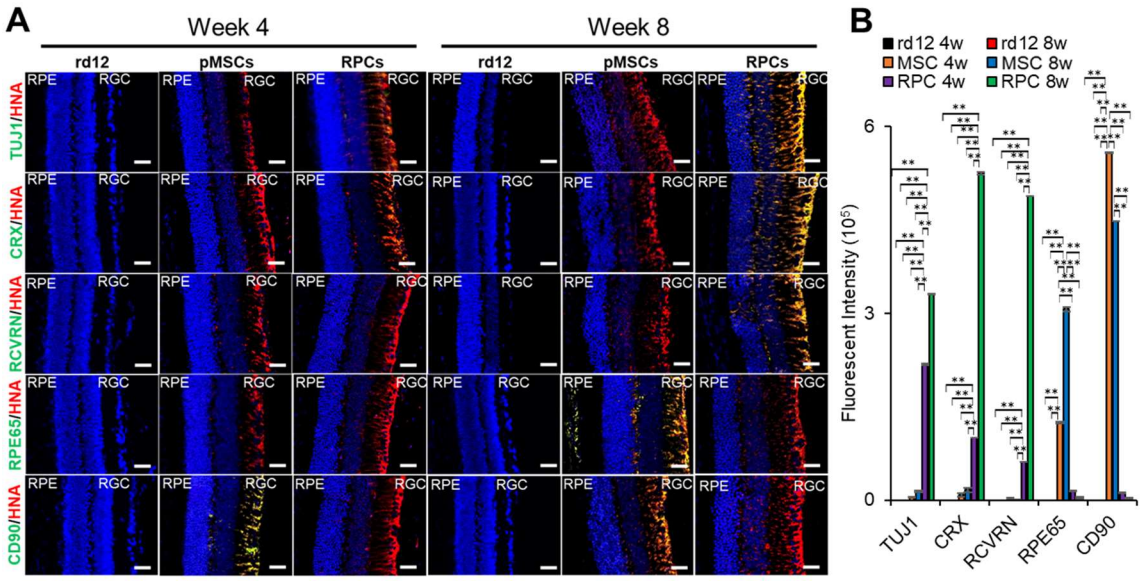

Figure 49: Post-transplantation analysis of the human proteins in rd12 retina. (A) Immunohistochemical analysis of paraffin-embedded sections of the retina showing expression of human neural (TUJ1), retinal (CRX, RCVRN, and RPE65), and MSC (CD90) proteins. The sections were countered stained with HNA (red). Blue and green colors represent the DAPI staining of the nuclei and human proteins, respectively. Scale bars represent 50 µm scale bars. (Magnification: 40x). (B) Measurement of fluorescent intensity of proteins as shown in A (**$p \leq 0.01$).

transplantation, HNA-positive cells were found in the ganglion layer and started to migrate towards the INL. However, after 8 weeks of transplantation, HNA-positive cells were more dispersed and further integrated into the retina. We then investigated the expression of cell-specific neural proteins. After 4 weeks of MSC transplantation, HNA-positive cells expressed CD90 but did not express TUJ1, CRX, RCVRN, or RPE65. However, 8 weeks after MSC transplantation, most of the HNA-positive cells were found to express RPE65 and were localized in the RPE layer. These results suggest that MSCs differentiated towards the RPE lineage.

In contrast, at 4 weeks after RPC transplantation, almost all HNA-positive cells expressed the neural marker, TUJ1, but a few also expressed the retinal markers, CRX and RCVRN. However, at 8 weeks after RPC transplantation, many HNA-positive cells expressed CRX and RCVRN in the ONL, INL, and RGC layers. RPCs demonstrated differentiation into neuronal lineages. Overall results suggest that transplanted cells differentiated into various retinal cells.

5.7 Transplanted cells promoted endogenous mouse gene expression

To evaluate the effect of the transplanted cells on the rd12 mouse retina, we investigated endogenous mouse genes associated with inflammation, neuroprotection, retina, and neurogenesis. It has been reported that pro-inflammatory genes are upregulated in rd12 mice (Gao, H. M. & Hong, 2008). Our study also found that *Tnfα, Cd3e, Il-2, Il-1β, Il-6,* and *Ccl2* were highly expressed in rd12 mice but not in the wild-type mice (Figure 50A). However, the expression of these genes was reduced to near wild-type levels in transplanted animals. Interestingly, the expression of anti-

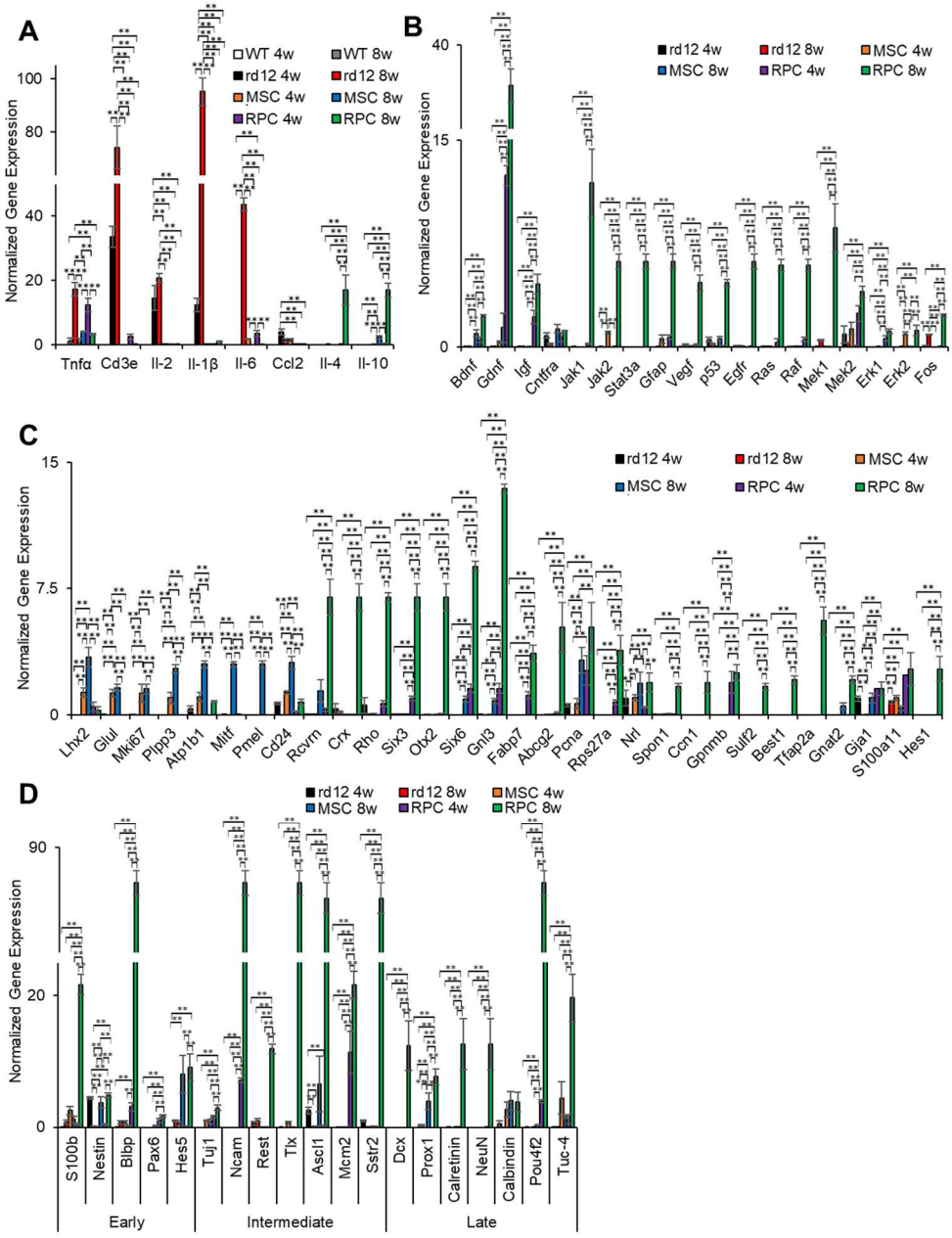

Figure 50: Effect of transplanted cells on the expression of endogenous mouse genes in rd12 retina. (A) Expression of pro-inflammatory genes (*Tnfα, Cd3e, Il-2, Il-1β, Il-6* and *Ccl2) and* anti-inflammatory genes (*Il-4* and *Il-10*), (B) neuroprotective genes *(Bdnf, Gdnf, Igf, Cntfra, Jak1, Jak2, Stat3a, Gfap, Vegf, p53, Egfr, Ras, Raf, Mek1, Mek2, Erk1, Erk2, and Fos*), (C) retinal genes (*Lhx2, Glul, Mki67, Plpp3, Atp1b1, Mitf, Pmel, Cd24, Rcvrn, Crx, Rho, Six3, Otx2, Six6, Gnl3, Fabp7, Abcg2, Pcna, Rps27a, Nrl, Spon1, Ccn1, Gpnmb, Sulf2, Best1, Tfap2a, Gnat2, Gja1, S100Aa11,* and *Hes1)* and (D) genes involved in early (*S100b, Nestin, Blbp, Pax6,* and *Hes5*), intermediate (*Tuj1, Ncam, Rest, Tlx, Ascl1, Mcm2,* and *Sstr2*) and late (*Dcx, Prox1, Calretinin, NeuN, Calbindin, Pou4f2,* and *Tuc-4*) stage of neurogenesis. All gene expression was normalized to *Gapdh* and *β-Actin*, and error bars represent the SEM of the triplicate experiment (**$p \leq 0.01$).

inflammatory genes, *ll-4* and *Il-10,* increased in rd12 mice 8 weeks after transplantation of RPCs. Only *ll-10* was expressed at a much lower level in MSCs than RPCs.

Among the neuroprotective genes, *Jak2*, *Erk2*, and *Mek2* as well as *Bdnf* and *Cntfra* were upregulated in the retina of rd12 mice 4 and 8 weeks, respectively, after MSC transplantation (Figure 50B). Whereas *Gdnf*, *Igf*, and *Mek2* and *Bdnf, Gdnf, Igf, Jak1, Jak2, Stat3a, Gfap, Vegf, p53, Egfr, Ras, Raf Mek1, Mek2, Erk1, Erk2,* and *Fos* were upregulated in the retina of animals 4 and 8 weeks, respectively, after transplantation of RPCs (Figure 50B).In addition, several RPE genes, *Lhx2, Glul, Mki67, Plpp3, Atp1b1,* and *Cd24,* were upregulated in the rd12 mice retina 4 weeks after transplantation of MSCs, and their expression was further increased by 8 weeks. In addition, *Mitf and Pmel* were expressed 8 weeks after transplantation of MSCs. In the case of RPCs, noticeable expression of *Six3*, *Six6, Gnl3, Fabp7, Pcna, Rps27A, Gpnmb, Gja1, and S100a11* was observed at 4 weeks which further increased by 8 weeks along with expression of several other retinal genes, *Crx, Otx2, Rcvrn*, *Rho, Abcg2, Nrl, Spon1, Ccn1, Sulf2, Best1, Tfap2a,* and *Hes1* (Figure 50C).

We also saw the upregulation of neurogenesis genes, which are involved in the retina's early, intermediate, and late stages. For example, the expression of *S100b, Calbindin, and Tuc-4* (after 4 weeks) and *Nestin, Hes5, Ascl1,* and *Prox1* (after 8 weeks) was increased in animals transplanted with MSCs. Whereas the expression of *Ncam*, *Mcm2*, and *Pou4f2* (after 4 weeks) and *S100b, Nestin, Blbp, Pax6*, *Hes5, Tuj1, Ncam, Rest, Tlx, Ascl1, Mcm2, Sstr2*, *Dcx, Prox1, Calretinin, NeuN, Pou4f2*, and *Tuc-4* (after 8 weeks) was increased in animals transplanted with RPCs (Figure 50D). Taken together,

RPCs were more effective in upregulating the mouse genes involved in inflammation, neuroprotection, retina, and neurogenesis.

5.8 Effect of transplanted cells on the transcriptome of rd12 mouse retina

RNA-seq analysis depicted in Figure 51A shows hierarchical clustering of rd12 mice vs. rd12 mice transplanted with cells. Expectedly, the untreated rd12 mice formed a clear cluster. In the case of the transplanted animal groups, MSCs and RPCs showed a higher gene correlation than the untreated animals. Figure 51B-C identified 39 DEGs (37 upregulated and 2 downregulated genes) at p-value < 0.05 in rd12 mice vs animals transplanted with MSCs. Whereas 36 DEGs (33 upregulated and 3 downregulated genes) at p-value < 0.05 were found in rd12 mice vs animals transplanted with RPCs (Figure 51D-E). The comparison between rd12 mice transplanted with MSCs and RPCs revealed 14 DEGs (11 and 3 upregulated genes in MSCs and RPCs, respectively) at p-value < 0.05 (Figure 51F-G).

Further analysis of the DEGs, p-value < 0.05 using GO terms identified several GO categories enriched in transplanted animals. In the biological process category, only negative regulation of T cell activation was enriched in rd12 mice transplanted with MSCs (Figure 52A). However, in RPC transplanted animals, several processes including response to axon injury, neuron remodeling, regulation of neuroinflammatory response, negative regulation of cytokine production, negative regulation of T cell activation, regulation of cell adhesion mediated by integrin, negative regulation of innate immune response, visual system development, negative regulation of leukocyte activation, positive regulation of glial cell differentiation, neural crest cell migration, regulation of axon extension involved in axon guidance, wound healing, regulation of response to

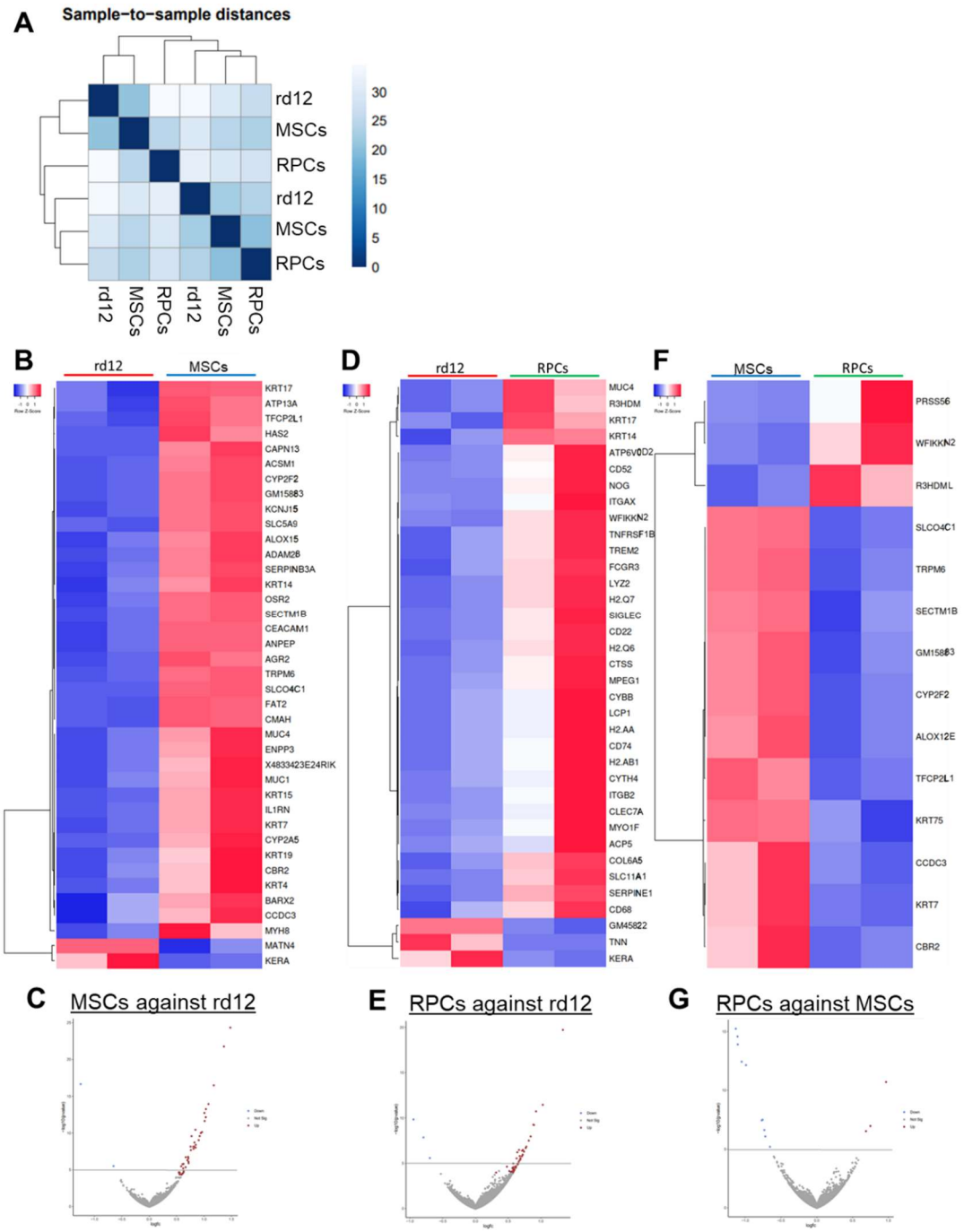

Figure 51: Transcriptome analysis of rd12 mice retina transplanted with cells. (A) RNA-seq data was analyzed to measure sample distances to evaluate for similarities. Hierarchical clustering was performed using DESeq2, and the data was plotted as a sample-to-sample heatmap. The colored indicator represents sample distances (blue signifies a high correlation). (B-G) Heatmap and volcano plots showing raw z-scores of RNA-seq log2 transformed values of the top DEGs in retina of rd12 vs rd12+MSCs (B-C), rd12 vs rd12+RPCs (D-E), and rd12+MSCs vs rd12+RPCs (F-G). Upregulated and downregulated genes are red and blue, respectively.

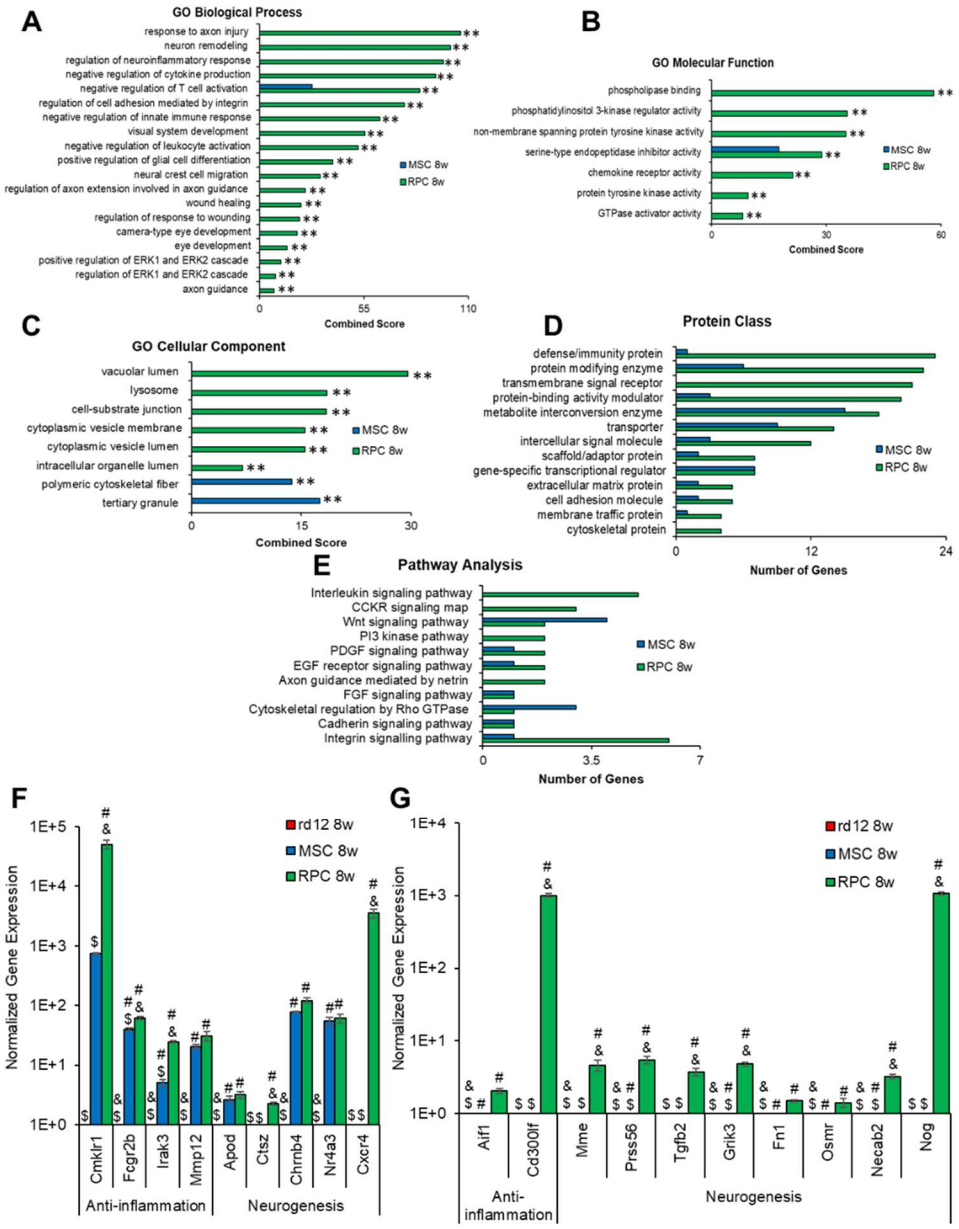

Figure 52: GO analysis of top mouse DEGs in rd12 mice retina transplanted with cells and validation by qRT-PCR. Enrichr and PANTHER analyses of DEGs were performed with $p < 0.05$ using DESeq2 after 8 week cell transplantation. (A–C) GO term enrichment analysis of upregulated DEGs associated with biological processes, molecular function, and cellular component, respectively, and the x-axis represents the combined score generated by Enrichr (**$p \leq 0.01$). (D and E) Protein classes and pathways upregulated in rd12+MSCs and rd12+RPCs, as determined by PANTHER analysis. The x-axis represents the number of genes associated with each category (**$p \leq 0.01$). (F-G) Expression of anti-inflammatory and neurogenesis genes in rd12, rd12+MSCs and rd12+RPCs and expression ± SEM normalized to rd12 and rd12+MSCs, respectively, as determined by qRT–PCR. Symbols, #, & and $ indicate significant difference at $p \leq 0.01$ between all experimental conditions: rd12, rd12+MSCs and rd12+RPCs, respectively.

wounding, camera-type eye development, eye development, positive regulation of ERK1 and ERK2 cascade, regulation of ERK1 and ERK2 cascade, and axon guidance were enriched.

In the molecular function category, again, only serine-type endopeptidase inhibitor activity was enriched in rd12 mice transplanted with MSCs. But several molecular functions include serine-type endopeptidase inhibitor activity, phospholipase binding, phosphatidylinositol 3-kinase regulator activity, non-member spanning protein tyrosine kinase activity, chemokine receptor activity, protein tyrosine kinase activity, and GTPase activator activity were enriched in rd12 mice transplanted with RPCs (Figure 52B).

In the cellular component category, polymeric cytoskeletal fiber and tertiary granule were enriched in rd12 mice transplanted with MSCs. Whereas RPCs treated animals were enriched in several cellular components, including vacuolar lumen, lysosome, cell-substrate junction, cytoplasmic vesicle membrane, cytoplasmic vesicle lumen and intracellular organelle lumen (Figure 52C).

DEGs analyzed by PANTHER revealed that protein classes, metabolite interconversion enzyme, transporter, gene-specific transcriptional regulator, extracellular matrix protein, cell adhesion molecule, and membrane traffic protein were enriched in mice transplanted with MSCs and RPCs. However, RPC transplanted animals had additional enriched protein classes, including defense/immunity protein, protein modifying enzyme, transmembrane signal receptor, protein-binding activity modulator, intercellular signal molecule, scaffold/adaptor protein, and cytoskeleton protein (Figure 52D).

For pathway analysis, we found that PDGF, EGF receptor, FGF, and cadherin signaling were enriched in rd12 transplanted MSCs and RPCs. However, Wnt signaling and cytoskeletal regulation by rho GTPase pathways were also enriched in MSCs. While interleukin, CCKR, PI3 kinase, axon guidance mediated by netrin and integrin signaling pathways were only enriched in the case of RPCs (Figure 52E).

DEGs were further validated by quantitative gene expression analysis. The results depicted in Figure 52F-G show that several log-folds significantly upregulated anti-inflammation and neurogenesis genes in transplanted animals compared to the rd12 mice. In general, anti-inflammation genes, *Cmklr1, Fcgr2b Irak3* and *Cd300lf,* and neurogenesis genes, *Ctsz, Cxcr4, Mme, Prss56, Tgfb2, Grik3, Necab2,* and *Nog,* were significantly more upregulated in rd12 mice transplanted with RPCs than MSCs. These results suggest that MSCs induced genes involved immune response and RPE regeneration. Whereas RPCs promoted the expression of genes associated with immune response, neuroprotection, various neural layers of the retina, and neurogenesis.

5.9 Discussion

This study differentiated MSCs into RPCs to treat retinal degeneration in the rd12 mice, which improved retinal function. Before transplantation, RPCs were characterized for morphological and biochemical properties. MSC-derived RPCs displayed neural extensions and expressed neural and retinal specific markers similar to published reports (Baranov et al., 2012; Schmitt, S. et al., 2009; Wang, J. et al., 2010). Transcriptomic analysis revealed that while genes associated with cell growth and proliferation (i.e. *CCNB1, CDC20,* and *CENPF* (Fu et al., 2019)) were highly expressed in MSCs, they were significantly downregulated in RPCs. In addition, several retinal specific genes

(Diehn et al., 2005), *GPNMB, BEST1,* and *TYRP1* (RPE), *TFAP2A* and *ATP1B1* (amacrine), *NDRG1* (horizontal), *HES1* and *SPON1* (Müller glia), *SULF2, GNAT2,* and *NRL* (photoreceptor), and *EBF1* (RGC) were upregulated in RPCs. GO analysis of the DEGs indicated that RPCs were enriched in biological processes associated with neuron projection and dendritic spine maintenance involved in neural differentiation (Gipson & Olive, 2017).

Following cell transplantation, the behavioral analysis showed a significant improvement in visual recovery and acuity of animals. For quantitative analysis of retinal function, the animals were examined by ERG. As expected, both a- and b-waves amplitudes were diminished in untreated animals (Zhang, Y. et al., 2013). However, there was a significant improvement in the a- and b-wave amplitudes in the dark-adapted rd12 mice transplanted with cells. Notably, a greater improvement was observed in a- and b-wave amplitudes in animals treated with RPCs than MSCs. In a previous study, a- and b-wave amplitudes were higher in dark-adapted RCS rats when treated with hBM-MSCs than untreated animals. However, the amplitudes continued to decrease over time (Tzameret et al., 2014). Another study reported a combination of hBM-MSCs and fetal RPCs was used to treat retinal degeneration and showed an increase in the a- and b-wave amplitudes of dark-adapted RCS rats compared to untreated animals (Qu et al., 2017). Again, the amplitudes progressively deteriorated even after cell transplantation. In contrast, subretinal injection of RPE-like cells derived from ESCs into rd12 mice displayed an increase in b-wave amplitude over the untreated animals but demonstrated a diminishing effect over time (Wang, N.-K. et al., 2010). Feline Müller cells injected into the vitreous of a feline ganglion cell depletion model improved retinal function (Becker

et al., 2016). Unlike these reports, our results for the first time demonstrated a temporal improvement in the a- and b-wave amplitudes, particularly in the case of RPCs, suggesting lasting effect of cell transplantation.

Post-transplantation histological analysis revealed temporal degeneration of retina in rd12 mice as previously described (Hasegawa et al., 2016). The overall retinal thickness in rd12 mice was 86%, 77%, and 64% compared to the wild-type animals at 0, 4, and 8 weeks, respectively. However, the thickness was 78% at both 4 and 8 weeks in MSC treated animals and 82% and 93% at 4 and 8 weeks, respectively, in the case of RPCs. These results suggest that while MSCs provided protection that led to retinal thickness maintenance, RPCs halted degeneration and promoted retinal regeneration. In general, the thickness of all three nuclear layers, ONL, INL, and RGC, was significantly and progressively increased in the cell transplanted animals compared with rd12 mice. However, more improvement was observed in the ONL, INL, and RGC in RPC transplanted mice. In reported studies, transplanted MSCs have improved either ONL or RGC but not both (Bakondi et al., 2017; Li, Yao et al., 2012). Therefore, our results are significant and exciting as they exhibited improvement in almost all nuclear layers, particularly in RPCs.

Previously, ESC retinal derivatives were found to survive and migrate between the ONL and RPE layers upon subretinal transplantation (Wang, N.-K. et al., 2010). Whereas fetal RPCs were found to migrate towards the INL and ONL (Liu, Y. et al., 2017). However, our cell tracking analysis showed localization of labeled cells at various sites of the retinal whole-mount, suggesting that transplanted cells dispersed from the

injection site. DIC analysis also indicated the localization of labeled cells in multiple layers of the retina.

Since MSCs are known to exert paracrine effects (Ren, G. et al., 2009), we investigated the expression of human inflammatory cytokines and neurotrophic factors in the retina of rd12 mice. Our results indicated high levels of xenogenic expression of human anti-inflammatory and neuroprotective genes in animals treated with MSCs and RPCs. No pro-inflammatory markers were expressed, suggesting that transplanted cells did not exert an immune response and were safe for cell therapy. Several human retinal and neurogenesis genes were expressed in the transplanted animals, presumably providing neural protection and regeneration. Supporting these findings, xenogeneic protein expression of retinal markers was also observed in the retina of transplanted animals. In general, xenogeneic expression was more significant in RPC than in MSC transplanted animals. Although several reports studied the effectiveness of cells in treating RDD in animal models (Bakondi et al., 2017; Li, X. X. et al., 2019; Tzameret et al., 2014), xenogenic expression of neuroprotective and neurogenesis markers has not been well-investigated. It is conceivable that retinogenesis may in part be due to the differentiation of transplanted cells.

In retinal degeneration, expression of pro-inflammatory genes has been reported to increase with a subsequent decrease in the expression of retinal genes and vision loss (Inoue, Y. et al., 2007; Kim, G. H. et al., 2019; Zou et al., 2019). We also found upregulation of several mouse pro-inflammatory genes, *Tnfα, Cd3e, Il-2, Il-1b, Il-6,* and *Ccl2*, and downregulation of several retinal genes in rd12 mice. Therefore, we investigated the effect of transplanted cells on the expression of inflammatory and retinal

genes. Our study showed that transplanted cells induced endogenous inflammatory response by suppressing pro-inflammatory genes while activating anti-inflammatory and retinal genes. RPCs were more potent than MSCs in exerting these beneficial effects. We also found that the transplanted cells, specifically RPCs, significantly upregulated several endogenous neurotrophic factors important for cell proliferation, survival, and neuronal differentiation (Das et al., 2009; Toops et al., 2012). This observation supports the results determined improvements in OKR, ERG, and retinal structure.

In contrast to birds, amphibians, and fish, *de novo* neurogenesis and regenerative capacity of the adult mammalian retina is very limited (I. Ortuño-Lizará, 2018; Xia & Ahmad, 2016). Therefore, only a few studies have investigated neurogenesis resulting from the augmentation of cells into the mammalian retina (Chaudhry et al., 2009; da Silva-Junior et al., 2021). We observed that mouse RPE and neural gene expression was increased in animals transplanted with MSCs and RPCs, respectively. In addition, we investigated neurogenesis genes in the retina of animals transplanted with cells. The expression of only a few genes, *Nestin, Hes5,* and *Prox1,* increased 8 weeks after transplantation of MSCs. Whereas the expression of several genes involved in early, intermediate, and late neurogenesis was significantly increased in animals transplanted with RPCs, and their expression was even greater 8 weeks after transplantation. Altogether, our results suggest that MSCs may be involved in the regeneration of mouse RPE. Whereas RPCs promoted regeneration of the ONL, INL, and RGC. They also validate the improvement in retinal structure and function, as stated earlier. Nevertheless, further studies would be helpful to determine the specific cell types involved in the regeneration of rd12 mice retina.

The transcriptomic analysis also revealed significant differences in the animals treated with cells compared to rd12 mice. Analysis of RNA-seq data showed that large dispersions in the sample groups did not affect differential gene expression. We found a clear and significant difference in the DEGs by analyzing the gene expression pattern affected by MSCs and RPCs. Comparative heatmap and volcano plot analyses revealed differences between animals transplanted with MSCs and RPCs in only a select number of DEGs. GO analysis indicated several biological processes enriched in the transplanted animals. In the case of MSCs, DEGs were involved in the suppression of T cell activation. Whereas RPCs not only suppressed the expression of genes involved in the immune response but also promoted the enrichment of biological processes associated with neuron remodeling, visual system, and eye development, as well as axon guidance. This pattern of enrichment suggested that the transplantation of MSCs and RPCs was effective in promoting anti-inflammatory response. RPCs promoted retinal regeneration, which led to greater improvement in visual function. These findings complement the ERG and visual recovery results as discussed earlier.

When DEGs were subjected to PANTHER analysis, activation of several pathways in the transplanted animals was revealed. Most of the signaling pathways involved in neural development were activated in both MSCs and RPCs, except that interleukin, CCKR, PI3k, and axon guidance signaling pathways were activated only in RPCs. qRT-PCR analysis of DEGs validated the activation of genes involved in anti-inflammation and neurogenesis, expressed at higher levels in RPCs than MSCs. Since qRT-PCR is a highly sensitive technique, the differences in DEG expression were many log fold higher. Some highly expressed genes in RPC transplanted animals were also

associated with anti-inflammatory response (Vitallé et al., 2020). At the same time, the other highly expressed genes are known to play a role in neuronal and retinal development. For example, *Necab2* and *Prss56*, are associated with neuronal development and ocular axial growth, respectively (Miczán et al., 2021; Paylakhi et al., 2018). Another gene, *Grik2,* acts as an excitatory neurotransmitter (Baranzini et al., 2010). Altogether, these results demonstrated that RPCs countered inflammation and induced neuroprotection and neurogenesis that improved retinal structure and physiological function.

The molecular analysis of RPC transplanted animals led us to propose a mechanism for improving retinal protection and regeneration (Figure 53). In this mechanism, upregulation of CNTF could activate the JAK/STAT pathway. RPC transplanted animals expressed high levels of CCN1 that can also activate this pathway. In addition, activated STAT3α can turn on the genes (i.e., *Gfap, Vegf* and *p53*) involved in cell proliferation and survival. In addition, EGF/FGF may activate MAPK signaling pathways, which turn on the *Ccnd1*gene, known to be involved in proliferation and neuronal differentiation. Lastly, NOG will bind to the BMPR to inhibit the BMP pathway, which can also be inhibited by FGF signaling.

In conclusion, our study demonstrated that RPCs counter inflammation provided retinal protection and promoted neurogenesis, resulting in improved retinal structure and physiological function in rd12 mice. Although several small clinical trials have utilized BM-MSCs and UC-MSCs, the results are not always conclusive

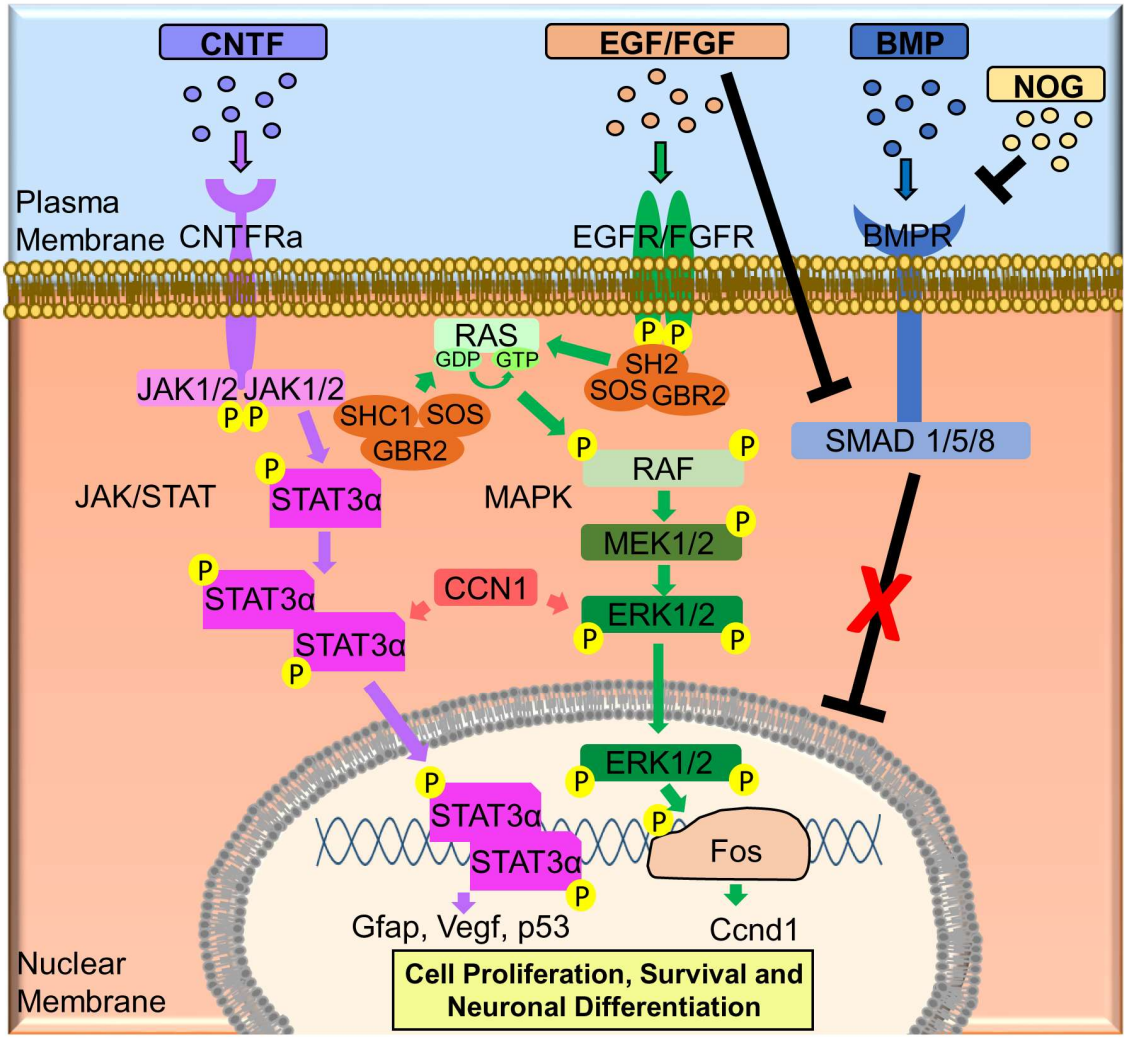

Figure 53: Proposed molecular mechanism involved the neuroprotection and retinal regeneration in rd12 mice transplanted with RPCs

(Özmert & Arslan, 2020; Tuekprakhon et al., 2021; Vilela et al., 2021). Our investigation provided proof of concept and basis for large-scale preclinical and clinical studies to treat RDD using RPCs.

APPENDIX A

IBC COMPLIANCE APPROVAL LETTER

OAKLAND UNIVERSITY

Institutional Biosafety Committee

September 28, 2017

Professor G. Rasul Chaudhry
Department of Biological Sciences

Reference: Continuing Approval of IBC Application #2858, "Isolation and Characterization of Stem Cells Derived from Cord and Peripheral Blood and Tissues for Potential Therapeutic Applications"

Dear Professor Chaudhry:

The Institutional Biosafety Committee (IBC), responsible for the review of research involving materials of human origin, recombinant DNA, and biohazardous, infectious or toxic materials, has reviewed and approved the continuing review of the project referenced above.

The proposed activities will continue to be approved at a BSL-2 for another 5 years starting, September 28, 2017 and ending September 27, 2022. The approval number 2608/2858-12 remains the same.

Any unanticipated problems, changes in, or halting of the activities proposed in the project, as described, must be promptly reported to the IBC or me at luongo@oakland.edu.

In addition, all faculty, staff and students involved in the project must be trained and qualified to conduct the project in a responsible manner. Please note, in this regard, that you, the principal investigator, are fully responsible at all times for limiting or restricting access to laboratories and for assessing, in each circumstances, who may enter or work in a laboratory when biohazardous materials are in use.

Please let me know if you have any questions. Thank you.

Sincerely,

Domenic Luongo
Biosafety Officer

DL:bk

Office of Research Administration

371 Wilson Blvd, Rochester, MI 48309-4486
(248) 370-4898 | Fax: (248) 370-2973 | oakland.edu

APPENDIX B

IACUC COMPLIANCE APPROVAL LETTERS

Oakland University
Institutional Animal Care and Use Committee
Committee Action Record

May 8, 2019	4476
Committee Review Date	RAM Number

PROJECT TITLE

Treatment of Multiple Sclerosis Using Mesenchymal Stem Cells and Their Derivatives in Animal Models

Approved [X] Disapproved [ ]

NEW PROJECT

[ ] _____ _____

IACUC Project Approval Number — Principal Investigator

REVISED PROJECT

Your Request for Revision of your Application for Use of Vertebrate Animals has been reviewed by IACUC and given full approval.

[X] **18081-R1** — **Rasul Chaudhry, Ph.D.**

New IACUC Project Approval Number* — Principal Investigator

*** Please use this new approval number, with the revision number indicated, in all future activities.**

A Cover Letter, similar to that used when addressing manuscript publications, needs to be attached to the application in RAM when submitting revisions to a previously approved IACUC application, or when submitting required modifications (in order to secure approval). Address required modifications in the same chronological order as they are listed in the Committee Action Record. Strike through the parts of the application that are being revised. (Do not use the Track Changes option to do the strike through or to make required modifications or revisions. Use the Strike Through option [abc] under the font tool bar.) The revisions need to be made in a readable typeface and of a different color of type so that anyone reviewing the modifications can easily identify where they are within the application.

Authorization for Project Commencement

Keith Williams — 5/8/2019

IACUC Chairperson: Keith Williams, PhD — Date

Approval Period:	**November 1, 2018 through October 31, 2021**
Annual Review Dates:	**November 1, 2019 and November 1, 2020**
Project Completion Summary Due Date:	**October 31, 2021**

TO: G. Rasul Chaudhry, PhD

FROM: David Svinarich, Ph.D.
Chair Animal Care Committee

SUBJECT: Project #101-16, Retinal regeneration in a mouse model using stem cells.

DATE: July 6, 2016

Your final revision has been received by The Animal Care Committee and was approved. This is to notify you that you may begin your project.

Thank You

Oakland University
Institutional Animal Care and Use Committee
Committee Action Record

September 4, 2019	4499
Committee Review Date	**RAM Number**

PROJECT TITLE

Comparison of Stem Cell Mediated Retinal Regeneration in Two Mouse Models of Retinal Degeneration

Approved [X] Disapproved [ ]

NEW PROJECT

[X] **19082** — **IACUC Project Approval Number**

Rasul Chaudhry, Ph.D. — **Principal Investigator**

REVISED PROJECT

Your Request for Revision of your Application for Use of Vertebrate Animals has been reviewed by IACUC and given full approval.

[ ] _____ — **New IACUC Project Approval Number***

_____ — **Principal Investigator**

*** Please use this new approval number, with the revision number indicated, in all future activities.**

A Cover Letter, similar to that used when addressing manuscript publications, needs to be attached to the application in RAM when submitting revisions to a previously approved IACUC application, or when submitting required modifications (in order to secure approval). Address required modifications in the same chronological order as they are listed in the Committee Action Record. Strike through the parts of the application that are being revised. (Do not use the Track Changes option to do the strike through or to make required modifications or revisions. Use the Strike Through option [abc] under the font tool bar.) The revisions need to be made in a readable typeface and of a different color of type so that anyone reviewing the modifications can easily identify where they are within the application.

Authorization for Project Commencement

Keith Williams — 9/5/2019

IACUC Chairperson: Keith Williams, PhD — **Date**

Approval Period: **October 1, 2019 through September 30, 2022**

Annual Review Dates: **October 1, 2020 and October 1, 2021**

Project Completion Summary Due Date: **September 30, 2022**

REFERENCES

Abdelhak, A., Huss, A., Kassubek, J., Tumani, H., & Otto, M. (2018). Serum GFAP as a biomarker for disease severity in multiple sclerosis. *Scientific Reports, 8*(1), 14798. doi:10.1038/s41598-018-33158-8

Aboody, K. S., Brown, A., Rainov, N. G., Bower, K. A., Liu, S., Yang, W., Small, J. E., Herrlinger, U., Ourednik, V., Black, P. M., Breakefield, X. O., & Snyder, E. Y. (2000). Neural stem cells display extensive tropism for pathology in adult brain: evidence from intracranial gliomas. *Proceedings of the National Academy of Sciences of the United States of America, 97*(23), 12846-12851. doi:10.1073/pnas.97.23.12846

Aharoni, R., Arnon, R., & Eilam, R. (2005). Neurogenesis and neuroprotection induced by peripheral immunomodulatory treatment of experimental autoimmune encephalomyelitis. *J Neurosci, 25*(36), 8217-8228. doi:10.1523/jneurosci.1859-05.2005

Ahn, J., Park, E.-m., Kim, B. J., Kim, J.-S., Choi, B., Lee, S.-H., & Han, I. (2015). Transplantation of human Wharton's jelly-derived mesenchymal stem cells highly expressing TGFβ receptors in a rabbit model of disc degeneration. *Stem Cell Res Ther, 6*, 190. doi:10.1186/s13287-015-0183-1

Al-Shaibani, M. B., Dickinson, A., Nong-Wang, X., Tulah, A. S., & Lovat, P. E. (2017). Effect of conditioned media from mesenchymal stem cells (MSC-CM) on wound healing using a prototype of a fully humanised 3D skin model. *Cytotherapy, 19*(5), e23-e24. doi:10.1016/j.jcyt.2017.03.062

Alghwiri, A. A., Jamali, F., Aldughmi, M., Khalil, H., Al-Sharman, A., Alhattab, D., Al-Radaideh, A., & Awidi, A. (2020). The effect of stem cell therapy and comprehensive physical therapy in motor and non-motor symptoms in patients with multiple sclerosis: A comparative study. *Medicine, 99*(34), e21646-e21646. doi:10.1097/MD.0000000000021646

Alhadlaq, A., & Mao, J. J. (2004). Mesenchymal stem cells: isolation and therapeutics. *Stem Cells Development, 13*(4), 436-448. doi:10.1089/scd.2004.13.436

Alimperti, S., Lei, P., Wen, Y., Tian, J., Campbell, A. M., & Andreadis, S. T. (2014). Serum-free spheroid suspension culture maintains mesenchymal stem cell proliferation and differentiation potential. *Biotechnol Prog, 30*(4), 974-983. doi:10.1002/btpr.1904

Alimperti, S., You, H., George, T., Agarwal, S. K., & Andreadis, S. T. (2014). Cadherin-11 regulates both mesenchymal stem cell differentiation into smooth muscle cells and the development of contractile function in vivo. *J Cell Sci, 127*(Pt 12), 2627-2638. doi:10.1242/jcs.134833

Amit, M., & Itskovitz-Eldor, J. (2002). Derivation and spontaneous differentiation of human embryonic stem cells. *J Anat, 200*(Pt 3), 225-232.

Amorin, B., Alegretti, A. P., Valim, V., Pezzi, A., Laureano, A. M., da Silva, M. A. L., Wieck, A., & Silla, L. (2014). Mesenchymal stem cell therapy and acute graft-versus-host disease: a review. *Human cell, 27*(4), 137-150. doi:10.1007/s13577-014-0095-x

Anastasiu, D. M., Cean, A., Bojin, M. F., Gluhovschi, A., Panaitescu, C., Paunescu, V., & Tanasie, G. (2016). Explants-isolated human placenta and umbilical cord cells share characteristics of both epithelial and mesenchymal stem cells. *Romanian Journal of Morphology and Embryology, 57*(2), 383-390.

Araujo, A. B., Salton, G. D., Furlan, J. M., Schneider, N., Angeli, M. H., Laureano, A. M., Silla, L., Passos, E. P., & Paz, A. H. (2017). Comparison of human mesenchymal stromal cells from four neonatal tissues: Amniotic membrane, chorionic membrane, placental decidua and umbilical cord. *Cytotherapy, 19*(5), 577-585. doi:10.1016/j.jcyt.2017.03.001

Arnhold, S., Absenger, Y., Klein, H., Addicks, K., & Schraermeyer, U. (2007). Transplantation of bone marrow-derived mesenchymal stem cells rescue photoreceptor cells in the dystrophic retina of the rhodopsin knockout mouse. *Graefes Arch Clin Exp Ophthalmol, 245*(3), 414-422. doi:10.1007/s00417-006-0382-7

Avercenc-Léger, L., Guerci, P., Virion, J.-M., Cauchois, G., Hupont, S., Rahouadj, R., Magdalou, J., Stoltz, J.-F., Bensoussan, D., Huselstein, C., & Reppel, L. (2017). Umbilical cord-derived mesenchymal stromal cells: predictive obstetric factors for cell proliferation and chondrogenic differentiation. *Stem Cell Res Ther, 8*(1), 161-161. doi:10.1186/s13287-017-0609-z

Bae, D. K., Park, D., Lee, S. H., Yang, G., Kyung, J., Kim, D., Shin, K., Choi, E. K., Kim, G., Hong, J. T., Kim, S. U., & Kim, Y. B. (2016). Comparative Effects of Human Neural Stem Cells and Oligodendrocyte Progenitor Cells on the Neurobehavioral Disorders of Experimental Autoimmune Encephalomyelitis Mice. *Stem Cells Int, 2016*, 4079863. doi:10.1155/2016/4079863

Baek, S. J., Kang, S. K., & Ra, J. C. (2011). In vitro migration capacity of human adipose tissue-derived mesenchymal stem cells reflects their expression of receptors for chemokines and growth factors. *Experimental & Molecular Medicine, 43*(10), 596-603. doi:10.3858/emm.2011.43.10.069

Baer, P. C., & Geiger, H. (2012). Adipose-Derived Mesenchymal Stromal/Stem Cells: Tissue Localization, Characterization, and Heterogeneity. *Stem Cells International, 2012*, 812693. doi:10.1155/2012/812693

Bai, L., Lennon, D. P., Eaton, V., Maier, K., Caplan, A. I., Miller, S. D., & Miller, R. H. (2009). Human bone marrow-derived mesenchymal stem cells induce Th2-polarized immune response and promote endogenous repair in animal models of multiple sclerosis. *Glia, 57*(11), 1192-1203. doi:10.1002/glia.20841

Bakondi, B., Girman, S., Lu, B., & Wang, S. (2017). Multimodal Delivery of Isogenic Mesenchymal Stem Cells Yields Synergistic Protection from Retinal Degeneration and Vision Loss. *Stem Cells Translational Medicine, 6*(2), 444-457. doi:10.5966/sctm.2016-0181

Bakopoulou, A., Apatzidou, D., Aggelidou, E., Gousopoulou, E., Leyhausen, G., Volk, J., Kritis, A., Koidis, P., & Geurtsen, W. (2017). Isolation and prolonged expansion of oral mesenchymal stem cells under clinical-grade, GMP-compliant conditions differentially affects "stemness" properties. *Stem Cell Res Ther, 8*(1), 247. doi:10.1186/s13287-017-0705-0

Bakshi, S., McKee, C., Walker, K., Brown, C., & Chaudhry, G. R. (2018). Toxicity of JQ1 in neuronal derivatives of human umbilical cord mesenchymal stem cells. *Oncotarget, 9*(73), 33853-33864. doi:10.18632/oncotarget.26127

Baranov, P. Y., Melo, G. B., & Young, M. J. (2012). Characterization Of Human Retinal Progenitor Cells. *Investigative ophthalmology & visual science, 53*(14), 5901-5901.

Baranzini, S. E., Srinivasan, R., Khankhanian, P., Okuda, D. T., Nelson, S. J., Matthews, P. M., Hauser, S. L., Oksenberg, J. R., & Pelletier, D. (2010). Genetic variation influences glutamate concentrations in brains of patients with multiple sclerosis. *Brain, 133*(9), 2603-2611. doi:10.1093/brain/awq192

Batsali, A. K., Pontikoglou, C., Koutroulakis, D., Pavlaki, K. I., Damianaki, A., Mavroudi, I., Alpantaki, K., Kouvidi, E., Kontakis, G., & Papadaki, H. A. (2017). Differential expression of cell cycle and WNT pathway-related genes accounts for differences in the growth and differentiation potential of Wharton's jelly and bone marrow-derived mesenchymal stem cells. *Stem Cell Res Ther, 8*, 102. doi:10.1186/s13287-017-0555-9

Becker, S., Eastlake, K., Jayaram, H., Jones, M. F., Brown, R. A., McLellan, G. J., Charteris, D. G., Khaw, P. T., & Limb, G. A. (2016). Allogeneic Transplantation of Müller-Derived Retinal Ganglion Cells Improves Retinal Function in a Feline Model of Ganglion Cell Depletion. *Stem Cells Transl Med, 5*(2), 192-205. doi:10.5966/sctm.2015-0125

Beeravolu, N., Brougham, J., Khan, I., McKee, C., Perez-Cruet, M., & Chaudhry, G. R. (2018). Human umbilical cord derivatives regenerate intervertebral disc. *Journal of Tissue Engineering and Regenerative Medicine, 12*(1), e579-e591. doi:10.1002/term.2330

Beeravolu, N., Khan, I., McKee, C., Dinda, S., Thibodeau, B., Wilson, G., Perez-Cruet, M., Bahado-Singh, R., & Chaudhry, G. R. (2016). Isolation and comparative analysis of potential stem/progenitor cells from different regions of human umbilical cord. *Stem Cell Res, 16*(3), 696-711. doi:10.1016/j.scr.2016.04.010

Beeravolu, N., McKee, C., Alamri, A., Mikhael, S., Brown, C., Perez-Cruet, M., & Chaudhry, G. R. (2017). Isolation and Characterization of Mesenchymal Stromal Cells from Human Umbilical Cord and Fetal Placenta. *J Vis Exp*(122). doi:10.3791/55224

Bianco, P., & Robey, P. (2000). Marrow stromal stem cells. *Journal of Clinical Investigations, 105*(12), 1663-1668. doi:10.1172/jci10413

Bianco, P., Robey, P. G., & Simmons, P. J. (2008). Mesenchymal stem cells: revisiting history, concepts, and assays. *Cell Stem Cell, 2*(4), 313-319. doi:10.1016/j.stem.2008.03.002

Bieback, K., & Netsch, P. (2016). Isolation, Culture, and Characterization of Human Umbilical Cord Blood-Derived Mesenchymal Stromal Cells. *Methods Mol Biol, 1416*, 245-258. doi:10.1007/978-1-4939-3584-0_14

Blankenberg, D., & Hillman-Jackson, J. (2014). Analysis of next-generation sequencing data using Galaxy. *Methods Mol Biol, 1150*, 21-43. doi:10.1007/978-1-4939-0512-6_2

Bonab, M. M., Alimoghaddam, K., Talebian, F., Ghaffari, S. H., Ghavamzadeh, A., & Nikbin, B. (2006). Aging of mesenchymal stem cell in vitro. *BMC cell biology, 7*, 14-14. doi:10.1186/1471-2121-7-14

Bonafede, R., & Mariotti, R. (2017). ALS Pathogenesis and Therapeutic Approaches: The Role of Mesenchymal Stem Cells and Extracellular Vesicles. *Frontiers in cellular neuroscience, 11*, 80-80. doi:10.3389/fncel.2017.00080

Bosetti, M., Boccafoschi, F., Leigheb, M., Bianchi Andrea, E., & Cannas, M. (2011). Chondrogenic induction of human mesenchymal stem cells using combined growth factors for cartilage tissue engineering. *Journal of Tissue Engineering and Regenerative Medicine, 6*(3), 205-213. doi:10.1002/term.416

Brady, K., Dickinson, S. C., Guillot, P. V., Polak, J., Blom, A. W., Kafienah, W., & Hollander, A. P. (2014). Human Fetal and Adult Bone Marrow-Derived Mesenchymal Stem Cells Use Different Signaling Pathways for the Initiation of Chondrogenesis. *Stem Cells Dev, 23*(5), 541-554. doi:10.1089/scd.2013.0301

Brambilla, R. (2019). The contribution of astrocytes to the neuroinflammatory response in multiple sclerosis and experimental autoimmune encephalomyelitis. *Acta neuropathologica communications, 137*(5), 757-783. doi:10.1007/s00401-019-01980-7

Bravo, B., Gallego, M. I., Flores, A. I., Bornstein, R., Puente-Bedia, A., Hernández, J., de la Torre, P., García-Zaragoza, E., Perez-Tavarez, R., Grande, J., Ballester, A., & Ballester, S. (2016). Restrained Th17 response and myeloid cell infiltration into the central nervous system by human decidua-derived mesenchymal stem cells during experimental autoimmune encephalomyelitis. *Stem Cell Res Ther, 7*, 43-43. doi:10.1186/s13287-016-0304-5

Brennan, M. A., Renaud, A., Guilloton, F., Mebarki, M., Trichet, V., Sensebé, L., Deschaseaux, F., Chevallier, N., & Layrolle, P. (2017). Inferior In Vivo Osteogenesis and Superior Angiogeneis of Human Adipose Tissue: A Comparison with Bone Marrow-Derived Stromal Stem Cells Cultured in Xeno-Free Conditions. *Stem Cells Translational Medicine, 6*(12), 2160-2172. doi:10.1002/sctm.17-0133

Brown, C., Agosta, P., McKee, C., Walker, K., Mazzella, M., Svinarich, D., & Chaudhry, G. R. (2021). Human primitive mesenchymal stem cell-derived retinal progenitor cells promoted neuroprotection and neurogenesis in rd12 mice. *bioRxiv*, 2021.2009.2020.460984. doi:10.1101/2021.09.20.460984

Brown, C., McKee, C., Bakshi, S., Walker, K., Hakman, E., Halassy, S., Svinarich, D., Dodds, R., Govind, C. K., & Chaudhry, G. R. (2019). Mesenchymal stem cells: Cell therapy and regeneration potential. *Journal of Tissue Engineering and Regenerative Medicine, 13*(9), 1738-1755. doi:10.1002/term.2914

Brown, C., McKee, C., Halassy, S., Kojan, S., Feinstein, D. L., & Chaudhry, G. R. (2021). Neural stem cells derived from primitive mesenchymal stem cells reversed disease symptoms and promoted neurogenesis in an experimental autoimmune encephalomyelitis mouse model of multiple sclerosis. *Stem Cell Res Ther, 12*(1), 499. doi:10.1186/s13287-021-02563-8

Cai, X., Conley, S. M., & Naash, M. I. (2009). RPE65: Role in the visual cycle, human retinal disease, and gene therapy. *Ophthalmic genetics, 30*(2), 57. doi:10.1080/13816810802626399

Campagnoli, C., Roberts, I. A., Kumar, S., Bennett, P. R., Bellantuono, I., & Fisk, N. M. (2001). Identification of mesenchymal stem/progenitor cells in human first-trimester fetal blood, liver, and bone marrow. *Blood, 98*(8), 2396-2402.

Caplan, A. I. (2010). What's in a name? *Tissue Eng Part A, 16*(8), 2415-2417. doi:10.1089/ten.TEA.2010.0216

Caplan, A. I. (2017). Mesenchymal Stem Cells: Time to Change the Name! *Stem Cells Translational Medicine, 6*(6), 1445-1451. doi:10.1002/sctm.17-0051

Carpenter, M. K., Rosler, E., & Rao, M. S. (2003). Characterization and differentiation of human embryonic stem cells. *Cloning Stem Cells, 5*(1), 79-88. doi:10.1089/153623003321512193

Chaudhry, G. R., Fecek, C., Lai, M. M., Wu, W.-C., Chang, M., Vasquez, A., Pasierb, M., & Trese, M. T. (2009). Fate of embryonic stem cell derivatives implanted into the vitreous of a slow retinal degenerative mouse model. *Stem Cells Dev, 18*(2), 247-258. doi:10.1089/scd.2008.0057

Chen, G., Yue, A., Ruan, Z., Yin, Y., Wang, R., Ren, Y., & Zhu, L. (2015). Comparison of biological characteristics of mesenchymal stem cells derived from maternal-origin placenta and Wharton's jelly. *Stem Cell Res Ther, 6*, 228. doi:10.1186/s13287-015-0219-6

Chen Kevin, G., Johnson Kory, R., McKay Ronald, D. G., & Robey Pamela, G. (2017). Concise Review: Conceptualizing Paralogous Stem-Cell Niches and Unfolding Bone Marrow Progenitor Cell Identities. *STEM CELLS, 36*(1), 11-21. doi:10.1002/stem.2711

Chen, X. Q., Chen, L. L., Fan, L., Fang, J., Chen, Z. Y., & Li, W. W. (2014). Stem cells with FGF4-bFGF fused gene enhances the expression of bFGF and improves myocardial repair in rats. *Biochem Biophys Res Commun, 447*(1), 145-151. doi:10.1016/j.bbrc.2014.03.131

Cheng, H., Qiu, L., Ma, J., Zhang, H., Cheng, M., Li, W., Zhao, X., & Liu, K. (2011). Replicative senescence of human bone marrow and umbilical cord derived mesenchymal stem cells and their differentiation to adipocytes and osteoblasts. *Mol Biol Rep, 38*(8), 5161-5168. doi:10.1007/s11033-010-0665-2

Cheng, J., Zhang, P., & Jiang, H. (2015). Let-7b-mediated pro-survival of transplanted mesenchymal stem cells for cardiac regeneration. *Stem Cell Res Ther, 6*, 216. doi:10.1186/s13287-015-0221-z

Chetty, S., Praneetha, S., Govarthanan, K., Verma, R., & Vadivel Murugan, A. (2019). Noninvasive Tracking and Regenerative Capabilities of Transplanted Human Umbilical Cord-Derived Mesenchymal Stem Cells Labeled with I-III-IV Semiconducting Nanocrystals in Liver-Injured Living Mice. *ACS Appl Mater Interfaces*. doi:10.1021/acsami.8b19953

Choi, W., Kwon, S. J., Jin, H. J., Jeong, S. Y., Choi, S. J., Oh, W., Yang, Y. S., Jeon, H. B., & Jeon, E. S. (2017). Optimization of culture conditions for rapid clinical-scale expansion of human umbilical cord blood-derived mesenchymal stem cells. *Clin Transl Med, 6*(1), 38. doi:10.1186/s40169-017-0168-z

Choudhery, M. S., Badowski, M., Muise, A., Pierce, J., & Harris, D. T. (2014). Donor age negatively impacts adipose tissue-derived mesenchymal stem cell expansion and differentiation. *Journal of Translational Medicine, 12*, 8-8. doi:10.1186/1479-5876-12-8

ClinicalTrials.gov. (2021). *U.S. National library of medicine*.

Cui, Y., Ma, S., Zhang, C., Cao, W., Liu, M., Li, D., Lv, P., Xing, Q., Qu, R., Yao, N., Yang, B., & Guan, F. (2017). Human umbilical cord mesenchymal stem cells transplantation improves cognitive function in Alzheimer's disease mice by decreasing oxidative stress and promoting hippocampal neurogenesis. *Behav Brain Res, 320*, 291-301. doi:10.1016/j.bbr.2016.12.021

D'Ippolito, G., Schiller, P. C., Ricordi, C., Roos, B. A., & Howard, G. A. (1999). Age-related osteogenic potential of mesenchymal stromal stem cells from human vertebral bone marrow. *J Bone Miner Res, 14*(7), 1115-1122. doi:10.1359/jbmr.1999.14.7.1115

da Silva-Junior, A. J., Mesentier-Louro, L. A., Nascimento-Dos-Santos, G., Teixeira-Pinheiro, L. C., Vasques, J. F., Chimeli-Ormonde, L., Bodart-Santos, V., de Carvalho, L. R. P., Santiago, M. F., & Mendez-Otero, R. (2021). Human mesenchymal stem cell therapy promotes retinal ganglion cell survival and target reconnection after optic nerve crush in adult rats. *Stem Cell Res Ther, 12*(1), 69. doi:10.1186/s13287-020-02130-7

da Silva Meirelles, L., Chagastelles, P. C., & Nardi, N. B. (2006). Mesenchymal stem cells reside in virtually all post-natal organs and tissues. *J Cell Sci, 119*(Pt 11), 2204-2213. doi:10.1242/jcs.02932

Das, G., Choi, Y., Sicinski, P., & Levine, E. M. (2009). Cyclin D1 fine-tunes the neurogenic output of embryonic retinal progenitor cells. *Neural Development, 4*(1), 15. doi:10.1186/1749-8104-4-15

Dayment, R. N., Taylor, C. G., Albanna, M. Z., Sarchet, K. N., Ichim, T. E., & Woods, E. J. (2014). Large-scale expansion of mesenchymal stem cells in 3D cultures using xeno-free microcarriers and human platelet lysate. *Cytotherapy, 16*(4), S110-S111. doi:10.1016/j.jcyt.2014.01.408

De Ugarte, D. A., Morizono, K., Elbarbary, A., Alfonso, Z., Zuk, P. A., Zhu, M., Dragoo, J. L., Ashjian, P., Thomas, B., Benhaim, P., Chen, I., Fraser, J., & Hedrick, M. H. (2003). Comparison of multi-lineage cells from human adipose tissue and bone marrow. *Cells Tissues Organs, 174*(3), 101-109. doi:10.1159/000071150

de Witte, S. F. H., Luk, F., Sierra Parraga, J. M., Gargesha, M., Merino, A., Korevaar, S. S., Shankar, A. S., O'Flynn, L., Elliman, S. J., Roy, D., Betjes, M. G. H., Newsome, P. N., Baan, C. C., & Hoogduijn, M. J. (2018). Immunomodulation By Therapeutic Mesenchymal Stromal Cells (MSC) Is Triggered Through Phagocytosis of MSC By Monocytic Cells. *STEM CELLS, 36*(4), 602-615. doi:10.1002/stem.2779

Dennis, D. J., Han, S., & Schuurmans, C. (2019). bHLH transcription factors in neural development, disease, and reprogramming. *Brain Res, 1705*, 48-65. doi:https://doi.org/10.1016/j.brainres.2018.03.013

Dennis, J. E., & Caplan, A. I. (2004). Advances in mesenchymal stem cell biology. *Current Opinion in Orthopaedics, 15*(5), 341-346.

Diehn, J. J., Diehn, M., Marmor, M. F., & Brown, P. O. (2005). Differential gene expression in anatomical compartments of the human eye. *Genome biology, 6*(9), R74-R74. doi:10.1186/gb-2005-6-9-r74

Ding, S. L. S., Kumar, S., & Mok, P. L. (2017). Cellular Reparative Mechanisms of Mesenchymal Stem Cells for Retinal Diseases. *International Journal of Molecular Sciences, 18*(8), 1406. doi:10.3390/ijms18081406

Dominici, M., Le Blanc, K., Mueller, I., Slaper-Cortenbach, I., Marini, F., Krause, D., Deans, R., Keating, A., Prockop, D., & Horwitz, E. (2006). Minimal criteria for defining multipotent mesenchymal stromal cells. The International Society for Cellular Therapy position statement. *Cytotherapy, 8*(4), 315-317. doi:10.1080/14653240600855905

Duffy, S. S., Keating, B. A., Perera, C. J., Lees, J. G., Tonkin, R. S., Makker, P. G. S., Carrive, P., Butovsky, O., & Moalem-Taylor, G. (2019). Regulatory T Cells and Their Derived Cytokine, Interleukin-35, Reduce Pain in Experimental Autoimmune Encephalomyelitis. *J Neurosci, 39*(12), 2326-2346. doi:10.1523/jneurosci.1815-18.2019

Dulamea, A. O. (2017). Role of Oligodendrocyte Dysfunction in Demyelination, Remyelination and Neurodegeneration in Multiple Sclerosis. *Adv Exp Med Biol, 958*, 91-127. doi:10.1007/978-3-319-47861-6_7

Dupree, J. L., & Feinstein, D. L. (2018). Influence of diet on axonal damage in the EAE mouse model of multiple sclerosis. *Journal of neuroimmunology, 322*, 9-14. doi:10.1016/j.jneuroim.2018.05.010

Evangelista, A. F., Vannier-Santos, M. A., de Assis Silva, G. S., Silva, D. N., Juiz, P. J. L., Nonaka, C. K. V., Dos Santos, R. R., Soares, M. B. P., & Villarreal, C. F. (2018). Bone marrow-derived mesenchymal stem/stromal cells reverse the sensorial diabetic neuropathy via modulation of spinal neuroinflammatory cascades. *J Neuroinflammation, 15*(1), 189. doi:10.1186/s12974-018-1224-3

Fariha, M. M., Chua, K. H., Tan, G. C., Tan, A. E., & Hayati, A. R. (2011). Human chorion-derived stem cells: changes in stem cell properties during serial passage. *Cytotherapy, 13*(5), 582-593. doi:10.3109/14653249.2010.549121

Farinazzo, A., Angiari, S., Turano, E., Bistaffa, E., Dusi, S., Ruggieri, S., Bonafede, R., Mariotti, R., Constantin, G., & Bonetti, B. (2018). Nanovesicles from adipose-derived mesenchymal stem cells inhibit T lymphocyte trafficking and ameliorate chronic experimental autoimmune encephalomyelitis. *Scientific Reports, 8*(1), 7473-7473. doi:10.1038/s41598-018-25676-2

Farup, J., Madaro, L., Puri, P. L., & Mikkelsen, U. R. (2015). Interactions between muscle stem cells, mesenchymal-derived cells and immune cells in muscle homeostasis, regeneration and disease. *Cell Death & Disease, 6*(7), e1830. doi:10.1038/cddis.2015.198

Fiumana, E., Pasquinelli, G., Foroni, L., Carboni, M., Bonafe, F., Orrico, C., Nardo, B., Tsivian, M., Neri, F., Arpesella, G., Guarnieri, C., Caldarera, C. M., & Muscari, C. (2013). Localization of mesenchymal stem cells grafted with a hyaluronan-based scaffold in the infarcted heart. *J Surg Res, 179*(1), e21-29. doi:10.1016/j.jss.2012.01.028

Fletcher, J. M., Lalor, S. J., Sweeney, C. M., Tubridy, N., & Mills, K. H. G. (2010). T cells in multiple sclerosis and experimental autoimmune encephalomyelitis. *Clinical & Experimental Immunology, 162*(1), 1-11. doi:10.1111/j.1365-2249.2010.04143.x

Fontaine, M. J., Shih, H., Schäfer, R., & Pittenger, M. F. (2016). Unraveling the Mesenchymal Stromal Cells' Paracrine Immunomodulatory Effects. *Transfus Med Rev, 30*(1), 37-43. doi:10.1016/j.tmrv.2015.11.004

Formigli, L., Paternostro, F., Tani, A., Mirabella, C., Quattrini Li, A., Nosi, D., D'Asta, F., Saccardi, R., Mazzanti, B., Lo Russo, G., & Zecchi-Orlandini, S. (2015). MSCs seeded on bioengineered scaffolds improve skin wound healing in rats. *Wound Repair Regen, 23*(1), 115-123. doi:10.1111/wrr.12251

Francois, S., Mouiseddine, M., Allenet-Lepage, B., Voswinkel, J., Douay, L., Benderitter, M., & Chapel, A. (2013). Human mesenchymal stem cells provide protection against radiation-induced liver injury by antioxidative process, vasculature protection, hepatocyte differentiation, and trophic effects. *Biomed Res Int, 2013*, 151679. doi:10.1155/2013/151679

Friedenstein, A. J., Chailakhjan, R. K., & Lalykina, K. S. (1970). The development of fibroblast colonies in monolayer cultures of guinea-pig bone marrow and spleen cells. *Cell Tissue Kinetics, 3*(4), 393-403.

Friedenstein, A. J., Gorskaja, J. F., & Kulagina, N. N. (1976). Fibroblast precursors in normal and irradiated mouse hematopoietic organs. *Exp Hematol, 4*(5), 267-274.

Friedenstein, A. J., Petrakova, K. V., Kurolesova, A. I., & Frolova, G. P. (1968). Heterotopic of bone marrow. Analysis of precursor cells for osteogenic and hematopoietic tissues. *Transplantation, 6*(2), 230-247.

Fu, L., Hu, Y., Song, M., Liu, Z., Zhang, W., Yu, F.-X., Wu, J., Wang, S., Izpisua Belmonte, J. C., Chan, P., Qu, J., Tang, F., & Liu, G.-H. (2019). Up-regulation of FOXD1 by YAP alleviates senescence and osteoarthritis. *PLoS biology, 17*(4), e3000201-e3000201. doi:10.1371/journal.pbio.3000201

Gabr, M. M., Zakaria, M. M., Refaie, A. F., Ismail, A. M., Khater, S. M., Ashamallah, S. A., Azzam, M. M., & Ghoneim, M. A. (2018). Insulin-producing Cells from Adult Human Bone Marrow Mesenchymal Stromal Cells Could Control Chemically Induced Diabetes in Dogs: A Preliminary Study. *Cell Transplant*, 963689718759913. doi:10.1177/0963689718759913

Gao, F., Chiu, S. M., Motan, D. A. L., Zhang, Z., Chen, L., Ji, H. L., Tse, H. F., Fu, Q. L., & Lian, Q. (2016). Mesenchymal stem cells and immunomodulation: current status and future prospects. *Cell Death & Disease, 7*(1), e2062. doi:10.1038/cddis.2015.327

Gao, H. M., & Hong, J. S. (2008). Why neurodegenerative diseases are progressive: uncontrolled inflammation drives disease progression. *Trends Immunol, 29*(8), 357-365. doi:10.1016/j.it.2008.05.002

Garikipati, V. N. S., Singh, S. P., Mohanram, Y., Gupta, A. K., Kapoor, D., & Nityanand, S. (2018). Isolation and characterization of mesenchymal stem cells from human fetus heart. *PLoS ONE, 13*(2), e0192244. doi:10.1371/journal.pone.0192244

Genc, B., Bozan, H. R., Genc, S., & Genc, K. (2019). Stem Cell Therapy for Multiple Sclerosis. *Adv Exp Med Biol, 1084*, 145-174. doi:10.1007/5584_2018_247

Giai Via, A., Frizziero, A., & Oliva, F. (2012). Biological properties of mesenchymal Stem Cells from different sources. *Muscles, Ligaments and Tendons Journal, 2*(3), 154-162.

Gipson, C. D., & Olive, M. F. (2017). Structural and functional plasticity of dendritic spines - root or result of behavior? *Genes, brain, and behavior, 16*(1), 101-117. doi:10.1111/gbb.12324

Glatigny, S., & Bettelli, E. (2018). Experimental Autoimmune Encephalomyelitis (EAE) as Animal Models of Multiple Sclerosis (MS). *Cold Spring Harbor perspectives in medicine, 8*(11). doi:10.1101/cshperspect.a028977

Goldring, C. E., Duffy, P. A., Benvenisty, N., Andrews, P. W., Ben-David, U., Eakins, R., French, N., Hanley, N. A., Kelly, L., Kitteringham, N. R., Kurth, J., Ladenheim, D., Laverty, H., McBlane, J., Narayanan, G., Patel, S., Reinhardt, J., Rossi, A., Sharpe, M., & Park, B. K. (2011). Assessing the safety of stem cell therapeutics. *Cell Stem Cell, 8*(6), 618-628. doi:10.1016/j.stem.2011.05.012

Gottipamula, S., Muttigi, M. S., Kolkundkar, U., & Seetharam, R. N. (2013). Serum-free media for the production of human mesenchymal stromal cells: a review. *Cell Prolif, 46*(6), 608-627. doi:10.1111/cpr.12063

Gucciardo, L., Lories, R., Ochsenbein-Kolble, N., Done, E., Zwijsen, A., & Deprest, J. (2009). Fetal mesenchymal stem cells: isolation, properties and potential use in perinatology and regenerative medicine. *Bjog, 116*(2), 166-172. doi:10.1111/j.1471-0528.2008.02005.x

Gugliandolo, A., Bramanti, P., & Mazzon, E. (2017). Mesenchymal stem cell therapy in Parkinson's disease animal models. *Current Research Translational Medicine, 65*(2), 51-60. doi:10.1016/j.retram.2016.10.007

Guillot, P. V., Gotherstrom, C., Chan, J., Kurata, H., & Fisk, N. M. (2007). Human first-trimester fetal MSC express pluripotency markers and grow faster and have longer telomeres than adult MSC. *STEM CELLS, 25*(3), 646-654. doi:10.1634/stemcells.2006-0208

Hamel, C. (2006). Retinitis pigmentosa. *Orphanet journal of rare diseases, 1*, 40-40. doi:10.1186/1750-1172-1-40

Han, L., Zhou, Y., Zhang, R., Wu, K., Lu, Y., Li, Y., Duan, R., Yao, Y., Zhu, D., & Jia, Y. (2018). MicroRNA Let-7f-5p Promotes Bone Marrow Mesenchymal Stem Cells Survival by Targeting Caspase-3 in Alzheimer Disease Model. *Front Neurosci, 12*, 333. doi:10.3389/fnins.2018.00333

Hao, L., Sun, H., Wang, J., Wang, T., Wang, M., & Zou, Z. (2012). Mesenchymal stromal cells for cell therapy: besides supporting hematopoiesis. *Interinatioal Journal of Hematology, 95*(1), 34-46. doi:10.1007/s12185-011-0991-8

Hao, X., Cheng, J., & Zhang, Z. (2018). Polymorphisms in PEDF linked with the susceptibility to age-related macular degeneration: A case-control study. *Medicine, 97*(34), e11981. doi:10.1097/md.0000000000011981

Harris, V. K., Stark, J., Vyshkina, T., Blackshear, L., Joo, G., Stefanova, V., Sara, G., & Sadiq, S. A. (2018). Phase I Trial of Intrathecal Mesenchymal Stem Cell-derived Neural Progenitors in Progressive Multiple Sclerosis. *EBioMedicine, 29*, 23-30. doi:10.1016/j.ebiom.2018.02.002

Harvey, A. R., Hu, Y., Leaver, S. G., Mellough, C. B., Park, K., Verhaagen, J., Plant, G. W., & Cui, Q. (2006). Gene therapy and transplantation in CNS repair: the visual system. *Prog Retin Eye Res, 25*(5), 449-489. doi:10.1016/j.preteyeres.2006.07.002

Hasegawa, T., Ikeda, H. O., Nakano, N., Muraoka, Y., Tsuruyama, T., Okamoto-Furuta, K., Kohda, H., & Yoshimura, N. (2016). Changes in morphology and visual function over time in mouse models of retinal degeneration: an SD-OCT, histology, and electroretinography study. *Japanese Journal of Ophthalmology, 60*(2), 111-125. doi:10.1007/s10384-015-0422-0

Hass, R., Kasper, C., Böhm, S., & Jacobs, R. (2011). Different populations and sources of human mesenchymal stem cells (MSC): A comparison of adult and neonatal tissue-derived MSC. *Cell Communication and Signaling, 9*(1), 12. doi:10.1186/1478-811X-9-12

Heiskanen, A., Satomaa, T., Tiitinen, S., Laitinen, A., Mannelin, S., Impola, U., Mikkola, M., Olsson, C., Miller-Podraza, H., Blomqvist, M., Olonen, A., Salo, H., Lehenkari, P., Tuuri, T., Otonkoski, T., Natunen, J., Saarinen, J., & Laine, J. (2007). N-glycolylneuraminic acid xenoantigen contamination of human embryonic and mesenchymal stem cells is substantially reversible. *STEM CELLS, 25*(1), 197-202. doi:10.1634/stemcells.2006-0444

Helg, C., Starobinski, M., Jeannet, M., & Chapuis, B. (1998). Donor lymphocyte infusion for the treatment of relapse after allogeneic hematopoietic stem cell transplantation. *Leuk Lymphoma, 29*(3-4), 301-313. doi:10.3109/10428199809068567

Hemmingsen, M., Vedel, S., Skafte-Pedersen, P., Sabourin, D., Collas, P., Bruus, H., & Dufva, M. (2013). The role of paracrine and autocrine signaling in the early phase of adipogenic differentiation of adipose-derived stem cells. *PLoS ONE, 8*(5), e63638-e63638. doi:10.1371/journal.pone.0063638

Heo, J. S., Choi, Y., Kim, H.-S., & Kim, H. O. (2016). Comparison of molecular profiles of human mesenchymal stem cells derived from bone marrow, umbilical cord blood, placenta and adipose tissue. *International journal of molecular medicine, 37*(1), 115-125. doi:10.3892/ijmm.2015.2413

Hiltzik, M. (2017). The FDA closes a huge loophole used by bogus stem-cell clinics, but delays serious enforcement for 3 years. *Los Angeles Times*.

Hocking, A. M., & Gibran, N. S. (2010). Mesenchymal stem cells: paracrine signaling and differentiation during cutaneous wound repair. *Exp Cell Res, 316*(14), 2213-2219. doi:10.1016/j.yexcr.2010.05.009

Hoffman, L. M., & Carpenter, M. K. (2005). Characterization and culture of human embryonic stem cells. *Nat Biotechnol, 23*(6), 699-708. doi:10.1038/nbt1102

Hong, B., Lee, S., Shin, N., Ko, Y., Kim, D., Lee, J., & Lee, W. (2018). Bone regeneration with umbilical cord blood mesenchymal stem cells in femoral defects of ovariectomized rats. *Osteoporos Sarcopenia, 4*(3), 95-101. doi:10.1016/j.afos.2018.08.003

Horwitz, E. M., Le Blanc, K., Dominici, M., Mueller, I., Slaper-Cortenbach, I., Marini, F. C., Deans, R. J., Krause, D. S., & Keating, A. (2005). Clarification of the nomenclature for MSC: The International Society for Cellular Therapy position statement. *Cytotherapy, 7*(5), 393-395. doi:10.1080/14653240500319234

Hu, Y., Liao, L., Wang, Q., Ma, L., Ma, G., Jiang, X., & Zhao, R. C. (2003). Isolation and identification of mesenchymal stem cells from human fetal pancreas. *J Lab Clin Med, 141*(5), 342-349. doi:10.1016/s0022-2143(03)00022-2

I. Ortuño-Lizará, D. A. P., N. Cuenca. (2018). Neurogenesis detection in the adult human retina. *Acta Ophthalmologica, 96*(S261), 91-91. doi:https://doi.org/10.1111/aos.13972_340

Im, G., II, Shin, Y.-W., & Lee, K.-B. (2005). Do adipose tissue-derived mesenchymal stem cells have the same osteogenic and chondrogenic potential as bone marrow-derived cells? *Osteoarthritis and Cartilage, 13*(10), 845-853. doi:https://doi.org/10.1016/j.joca.2005.05.005

Imitola, J., Raddassi, K., Park, K. I., Mueller, F. J., Nieto, M., Teng, Y. D., Frenkel, D., Li, J., Sidman, R. L., Walsh, C. A., Snyder, E. Y., & Khoury, S. J. (2004). Directed migration of neural stem cells to sites of CNS injury by the stromal cell-derived factor 1alpha/CXC chemokine receptor 4 pathway. *Proceedings of the National Academy of Sciences of the United States of America, 101*(52), 18117-18122. doi:10.1073/pnas.0408258102

In't Anker, P. S., Scherjon, S. A., Kleijburg-van der Keur, C., de Groot-Swings, G. M., Claas, F. H., Fibbe, W. E., & Kanhai, H. H. (2004). Isolation of mesenchymal stem cells of fetal or maternal origin from human placenta. *STEM CELLS, 22*(7), 1338-1345. doi:10.1634/stemcells.2004-0058

Inoue, M., Honmou, O., Oka, S., Houkin, K., Hashi, K., & Kocsis, J. D. (2003). Comparative analysis of remyelinating potential of focal and intravenous administration of autologous bone marrow cells into the rat demyelinated spinal cord. *Glia, 44*(2), 111-118. doi:10.1002/glia.10285

Inoue, Y., Iriyama, A., Ueno, S., Takahashi, H., Kondo, M., Tamaki, Y., Araie, M., & Yanagi, Y. (2007). Subretinal transplantation of bone marrow mesenchymal stem cells delays retinal degeneration in the RCS rat model of retinal degeneration. *Exp Eye Res, 85*(2), 234-241. doi:10.1016/j.exer.2007.04.007

Ise, H., Matsunaga, K., Shinohara, M., & Sakai, Y. (2019). Improved Isolation of Mesenchymal Stem Cells Based on Interactions between N-Acetylglucosamine-Bearing Polymers and Cell-Surface Vimentin. *Stem Cells Int, 2019*, 4341286. doi:10.1155/2019/4341286

Isern, J., Garcia-Garcia, A., Martin, A. M., Arranz, L., Martin-Perez, D., Torroja, C., Sanchez-Cabo, F., & Mendez-Ferrer, S. (2014). The neural crest is a source of mesenchymal stem cells with specialized hematopoietic stem cell niche function. *Elife, 3*, e03696. doi:10.7554/eLife.03696

Ishiguro, H., Kaito, T., Yarimitsu, S., Hashimoto, K., Okada, R., Kushioka, J., Chijimatsu, R., Takenaka, S., Makino, T., Sakai, Y., Moriguchi, Y., Otsuru, S., Hart, D. A., Fujie, H., Nakamura, N., & Yoshikawa, H. (2019). Intervertebral disc regeneration with an adipose mesenchymal stem cell-derived tissue-engineered construct in a rat nucleotomy model. *Acta Biomater*. doi:10.1016/j.actbio.2019.01.050

Ishii, T., & Eto, K. (2014). Fetal stem cell transplantation: Past, present, and future. *World J Stem Cells, 6*(4), 404-420. doi:10.4252/wjsc.v6.i4.404

Jackson, K. A., Majka, S. M., Wang, H., Pocius, J., Hartley, C. J., Majesky, M. W., Entman, M. L., Michael, L. H., Hirschi, K. K., & Goodell, M. A. (2001). Regeneration of ischemic cardiac muscle and vascular endothelium by adult stem cells. *J Clin Invest, 107*(11), 1395-1402. doi:10.1172/jci12150

Jackson, W., Lozito, T. P., Djouad, F., Kuhn, N. Z., Nesti, L. J., & Tuan, R. S. (2011). Differentiation and regeneration potential of mesenchymal progenitor cells derived from traumatized muscle tissue. *Journal of Cellular and Molecular Medicine, 15*(11), 2377-2388. doi:10.1111/j.1582-4934.2010.01225.x

Jamali, F., Ma Hattab, D., Amman, J., & Awidi, A. (2018). *Use of Mesenchymal Stem Cells in Parkinson Disease (PD)*. ClinicalTrials.gov.

Jiang, M., Yu, D., Xie, B., Huang, H., Lu, W., Qiu, M., & Dai, Z.-M. (2020). WNT signaling suppresses oligodendrogenesis via Ngn2-dependent direct inhibition of Olig2 expression. *Mol Brain, 13*(1), 155. doi:10.1186/s13041-020-00696-0

Jin, H. J., Bae, Y. K., Kim, M., Kwon, S.-J., Jeon, H. B., Choi, S. J., Kim, S. W., Yang, Y. S., Oh, W., & Chang, J. W. (2013). Comparative Analysis of Human Mesenchymal Stem Cells from Bone Marrow, Adipose Tissue, and Umbilical Cord Blood as Sources of Cell Therapy. *International Journal of Molecular Sciences, 14*(9), 17986-18001. doi:10.3390/ijms140917986

Jin, H. J., Park, S. K., Oh, W., Yang, Y. S., Kim, S. W., & Choi, S. J. (2009). Down-regulation of CD105 is associated with multi-lineage differentiation in human umbilical cord blood-derived mesenchymal stem cells. *Biochem Biophys Res Commun, 381*(4), 676-681. doi:10.1016/j.bbrc.2009.02.118

Jo, C. H., Lee, Y. G., Shin, W. H., Kim, H., Chai, J. W., Jeong, E. C., Kim, J. E., Shim, H., Shin, J. S., Shin, I. S., Ra, J. C., Oh, S., & Yoon, K. S. (2014). Intra-articular injection of mesenchymal stem cells for the treatment of osteoarthritis of the knee: a proof-of-concept clinical trial. *STEM CELLS, 32*(5), 1254-1266. doi:10.1002/stem.1634

Johnson, M. A., Ables, J. L., & Eisch, A. J. (2009). Cell-intrinsic signals that regulate adult neurogenesis in vivo: insights from inducible approaches. *BMB reports, 42*(5), 245-259. doi:10.5483/bmbrep.2009.42.5.245

Jurado, M., De La Mata, C., Ruiz-Garcia, A., Lopez-Fernandez, E., Espinosa, O., Remigia, M. J., Moratalla, L., Goterris, R., Garcia-Martin, P., Ruiz-Cabello, F., Garzon, S., Pascual, M. J., Espigado, I., & Solano, C. (2017). Adipose tissue-derived mesenchymal stromal cells as part of therapy for chronic graft-versus-host disease: A phase I/II study. *Cytotherapy, 19*(8), 927-936. doi:10.1016/j.jcyt.2017.05.002

Kanakasabai, S., Casalini, E., Walline, C. C., Mo, C., Chearwae, W., & Bright, J. J. (2012). Differential regulation of CD4(+) T helper cell responses by curcumin in experimental autoimmune encephalomyelitis. *J Nutr Biochem, 23*(11), 1498-1507. doi:10.1016/j.jnutbio.2011.10.002

Kastrinaki, M. C., Pavlaki, K., Batsali, A. K., Kouvidi, E., Mavroudi, I., Pontikoglou, C., & Papadaki, H. A. (2013). Mesenchymal stem cells in immune-mediated bone marrow failure syndromes. *Clin Dev Immunol, 2013*, 265608. doi:10.1155/2013/265608

Khubutiya, M. S., Vagabov, A. V., Temnov, A. A., & Sklifas, A. N. (2014). Paracrine mechanisms of proliferative, anti-apoptotic and anti-inflammatory effects of mesenchymal stromal cells in models of acute organ injury. *Cytotherapy, 16*(5), 579-585. doi:10.1016/j.jcyt.2013.07.017

Kilpatrick, T. J., & Bartlett, P. F. (1993). Cloning and growth of multipotential neural precursors: requirements for proliferation and differentiation. *Neuron, 10*(2), 255-265. doi:10.1016/0896-6273(93)90316-j

Kim, G. H., Paik, S. S., Park, Y. S., Kim, H. G., & Kim, I. B. (2019). Amelioration of Mouse Retinal Degeneration After Blue LED Exposure by Glycyrrhizic Acid-Mediated Inhibition of Inflammation. *Frontiers in cellular neuroscience, 13*, 319. doi:10.3389/fncel.2019.00319

Kim, H. W., Lee, H. S., Kang, J. M., Bae, S. H., Kim, C., Lee, S. H., Schwarz, J., Kim, G. J., Kim, J. S., Cha, D. H., Kim, J., Chang, S. W., Lee, T. H., & Moon, J. (2018). Dual Effects of Human Placenta-Derived Neural Cells on Neuroprotection and the Inhibition of Neuroinflammation in a Rodent Model of Parkinson's Disease. *Cell Transplant*, 963689718766324. doi:10.1177/0963689718766324

Kim, I., Lee, S. K., Yoon, J. I., Kim, D. E., Kim, M., & Ha, H. (2013). Fibrin glue improves the therapeutic effect of MSCs by sustaining survival and paracrine function. *Tissue Engineering Part A, 19*(21-22), 2373-2381. doi:10.1089/ten.TEA.2012.0665

Kim, J., Jo, C., Kim, H., & Hwang, Y. (2018). Comparison of Immunological Characteristics of Mesenchymal Stem Cells from the Periodontal Ligament, Umbilical Cord, and Adipose Tissue. *Stem Cells International, 2018*, 8429042. doi:10.1155/2018/8429042

Kim, J., Shin, J. M., Jeon, Y. J., Chung, H. M., & Chae, J.-I. (2012). Proteomic Validation of Multifunctional Molecules in Mesenchymal Stem Cells Derived from Human Bone Marrow, Umbilical Cord Blood and Peripheral Blood. *PLoS ONE, 7*(5), e32350. doi:10.1371/journal.pone.0032350

Kim, Y. J., Yoo, S. M., Park, H. H., Lim, H. J., Kim, Y. L., Lee, S., Seo, K. W., & Kang, K. S. (2017). Exosomes derived from human umbilical cord blood mesenchymal stem cells stimulates rejuvenation of human skin. *Biochem Biophys Res Commun, 493*(2), 1102-1108. doi:10.1016/j.bbrc.2017.09.056

Kirana, S., Stratmann, B., Prante, C., Prohaska, W., Koerperich, H., Lammers, D., Gastens, M. H., Quast, T., Negrean, M., Stirban, O. A., Nandrean, S. G., Gotting, C., Minartz, P., Kleesiek, K., & Tschoepe, D. (2012). Autologous stem cell therapy in the treatment of limb ischaemia induced chronic tissue ulcers of diabetic foot patients. *Int J Clin Pract, 66*(4), 384-393. doi:10.1111/j.1742-1241.2011.02886.x

Kleinewietfeld, M., & Hafler, D. A. (2013). The plasticity of human Treg and Th17 cells and its role in autoimmunity. *Seminars in immunology, 25*(4), 305-312. doi:10.1016/j.smim.2013.10.009

Koh, A. E.-H., Alsaeedi, H. A., Rashid, M. B. A., Lam, C., Harun, M. H. N., Ng, M. H., Mohd Isa, H., Then, K. Y., Bastion, M.-L. C., Farhana, A., Khursheed Alam, M., Subbiah, S. K., & Mok, P. L. (2021). Transplanted Erythropoietin-Expressing Mesenchymal Stem Cells Promote Pro-survival Gene Expression and Protect Photoreceptors From Sodium Iodate-Induced Cytotoxicity in a Retinal Degeneration Model. *Frontiers in Cell and Developmental Biology, 9*, 652017-652017. doi:10.3389/fcell.2021.652017

Krebsbach, P. H., & Villa-Diaz, L. G. (2017). The Role of Integrin α6 (CD49f) in Stem Cells: More than a Conserved Biomarker. *Stem Cells Dev, 26*(15), 1090-1099. doi:10.1089/scd.2016.0319

Kuhn, S., Gritti, L., Crooks, D., & Dombrowski, Y. (2019). Oligodendrocytes in Development, Myelin Generation and Beyond. *Cells, 8*(11). doi:10.3390/cells8111424

Kumar, A., D'Souza, S. S., Moskvin, O. V., Toh, H., Wang, B., Zhang, J., Swanson, S., Guo, L. W., Thomson, J. A., & Slukvin, II. (2017). Specification and Diversification of Pericytes and Smooth Muscle Cells from Mesenchymoangioblasts. *Cell Rep, 19*(9), 1902-1916. doi:10.1016/j.celrep.2017.05.019

Kuraitis, D., Ruel, M., & Suuronen, E. J. (2011). Mesenchymal stem cells for cardiovascular regeneration. *Cardiovasc Drugs Ther, 25*(4), 349-362. doi:10.1007/s10557-011-6311-y

Kurte, M., Bravo-Alegria, J., Torres, A., Carrasco, V., Ibanez, C., Vega-Letter, A. M., Fernandez-O'Ryan, C., Irarrazabal, C. E., Figueroa, F. E., Fuentealba, R. A., Riedel, C., & Carrion, F. (2015). Intravenous administration of bone marrow-derived mesenchymal stem cells induces a switch from classical to atypical symptoms in experimental autoimmune encephalomyelitis. *Stem Cells Int, 2015*, 140170. doi:10.1155/2015/140170

Labrador-Velandia, S., Alonso-Alonso, M. L., Alvarez-Sanchez, S., Gonzalez-Zamora, J., Carretero-Barrio, I., Pastor, J. C., Fernandez-Bueno, I., & Srivastava, G. K. (2016). Mesenchymal stem cell therapy in retinal and optic nerve diseases: An update of clinical trials. *World J Stem Cells, 8*(11), 376-383. doi:10.4252/wjsc.v8.i11.376

Lacerda, L., Debeb, B. G., Smith, D., Larson, R., Solley, T., Xu, W., Krishnamurthy, S., Gong, Y., Levy, L. B., Buchholz, T., Ueno, N. T., Klopp, A., & Woodward, W. A. (2015). Mesenchymal stem cells mediate the clinical phenotype of inflammatory breast cancer in a preclinical model. *Breast Cancer Res, 17*, 42. doi:10.1186/s13058-015-0549-4

Laitinen, A., Oja, S., Kilpinen, L., Kaartinen, T., Moller, J., Laitinen, S., Korhonen, M., & Nystedt, J. (2016). A robust and reproducible animal serum-free culture method for clinical-grade bone marrow-derived mesenchymal stromal cells. *Cytotechnology, 68*(4), 891-906. doi:10.1007/s10616-014-9841-x

Law, S., & Chaudhuri, S. (2013). Mesenchymal stem cell and regenerative medicine: regeneration versus immunomodulatory challenges. *Am J Stem Cells, 2*(1), 22-38.

Legzdina, D., Romanauska, A., Nikulshin, S., Kozlovska, T., & Berzins, U. (2016). Characterization of Senescence of Culture-expanded Human Adipose-derived Mesenchymal Stem Cells. *International Journal of Stem Cells, 9*(1), 124-136. doi:10.15283/ijsc.2016.9.1.124

Leow, S. N., Luu, C. D., Hairul Nizam, M. H., Mok, P. L., Ruhaslizan, R., Wong, H. S., Wan Abdul Halim, W. H., Ng, M. H., Ruszymah, B. H., Chowdhury, S. R., Bastion, M. L., & Then, K. Y. (2015). Safety and Efficacy of Human Wharton's Jelly-Derived Mesenchymal Stem Cells Therapy for Retinal Degeneration. *PLoS ONE, 10*(6), e0128973. doi:10.1371/journal.pone.0128973

Levi, B., Wan, D. C., Glotzbach, J. P., Hyun, J., Januszyk, M., Montoro, D., Sorkin, M., James, A. W., Nelson, E. R., Li, S., Quarto, N., Lee, M., Gurtner, G. C., & Longaker, M. T. (2011). CD105 protein depletion enhances human adipose-derived stromal cell osteogenesis through reduction of transforming growth factor β1 (TGF-β1) signaling. *J Biol Chem, 286*(45), 39497-39509. doi:10.1074/jbc.M111.256529

Li, S., Mattar, P., Dixit, R., Lawn, S. O., Wilkinson, G., Kinch, C., Eisenstat, D., Kurrasch, D. M., Chan, J. A., & Schuurmans, C. (2014). RAS/ERK signaling controls proneural genetic programs in cortical development and gliomagenesis. *J Neurosci, 34*(6), 2169-2190. doi:10.1523/jneurosci.4077-13.2014

Li, T., & Wu, Y. (2011). Paracrine Molecules of Mesenchymal Stem Cells for Hematopoietic Stem Cell Niche. *Bone Marrow Research, 2011*, 353878. doi:10.1155/2011/353878

Li, X. X., Yuan, X. J., Zhai, Y., Yu, S., Jia, R. X., Yang, L. P., Ma, Z. Z., Zhao, Y. M., Wang, Y. X., & Ge, L. H. (2019). Treatment with Stem Cells from Human Exfoliated Deciduous Teeth and Their Derived Conditioned Medium Improves Retinal Visual Function and Delays the Degeneration of Photoreceptors. *Stem Cells Dev, 28*(22), 1514-1526. doi:10.1089/scd.2019.0158

Li, Y., Guo, G., Li, L., Chen, F., Bao, J., Shi, Y. J., & Bu, H. (2015). Three-dimensional spheroid culture of human umbilical cord mesenchymal stem cells promotes cell yield and stemness maintenance. *Cell Tissue Res, 360*(2), 297-307. doi:10.1007/s00441-014-2055-x

Li, Y., Tsai, Y.-T., Hsu, C.-W., Erol, D., Yang, J., Wu, W.-H., Davis, R. J., Egli, D., & Tsang, S. H. (2012). Long-term safety and efficacy of human-induced pluripotent stem cell (iPS) grafts in a preclinical model of retinitis pigmentosa. *Molecular medicine (Cambridge, Mass.), 18*(1), 1312-1319. doi:10.2119/molmed.2012.00242

Liao, W., Pham, V., Liu, L., Riazifar, M., Pone, E. J., Zhang, S. X., Ma, F., Lu, M., Walsh, C. M., & Zhao, W. (2016). Mesenchymal stem cells engineered to express selectin ligands and IL-10 exert enhanced therapeutic efficacy in murine experimental autoimmune encephalomyelitis. *Biomaterials, 77*, 87-97. doi:10.1016/j.biomaterials.2015.11.005

Linker, R. A., Lee, D.-H., Demir, S., Wiese, S., Kruse, N., Siglienti, I., Gerhardt, E., Neumann, H., Sendtner, M., Lühder, F., & Gold, R. (2010). Functional role of brain-derived neurotrophic factor in neuroprotective autoimmunity: therapeutic implications in a model of multiple sclerosis. *Brain, 133*(8), 2248-2263. doi:10.1093/brain/awq179

Liu, L., Eckert, M. A., Riazifar, H., Kang, D. K., Agalliu, D., & Zhao, W. (2013). From blood to the brain: can systemically transplanted mesenchymal stem cells cross the blood-brain barrier? *Stem Cells International, 2013*, 435093. doi:10.1155/2013/435093

Liu, S., de Castro, L. F., Jin, P., Civini, S., Ren, J., Reems, J.-A., Cancelas, J., Nayak, R., Shaw, G., O'Brien, T., McKenna, D. H., Armant, M., Silberstein, L., Gee, A. P., Hei, D. J., Hematti, P., Kuznetsov, S. A., Robey, P. G., & Stroncek, D. F. (2017). Manufacturing Differences Affect Human Bone Marrow Stromal Cell Characteristics and Function: Comparison of Production Methods and Products from Multiple Centers. *Scientific Reports, 7*, 46731. doi:10.1038/srep46731

Liu, S., Yuan, M., Hou, K., Zhang, L., Zheng, X., Zhao, B., Sui, X., Xu, W., Lu, S., & Guo, Q. (2012). Immune characterization of mesenchymal stem cells in human umbilical cord Wharton's jelly and derived cartilage cells. *Cellular Immunology, 278*(1), 35-44.

Liu, X. B., Chen, H., Chen, H. Q., Zhu, M. F., Hu, X. Y., Wang, Y. P., Jiang, Z., Xu, Y. C., Xiang, M. X., & Wang, J. A. (2012). Angiopoietin-1 preconditioning enhances survival and functional recovery of mesenchymal stem cell transplantation. *J Zhejiang Univ Sci B, 13*(8), 616-623. doi:10.1631/jzus.B1201004

Liu, Y., Chen, S. J., Li, S. Y., Qu, L. H., Meng, X. H., Wang, Y., Xu, H. W., Liang, Z. Q., & Yin, Z. Q. (2017). Long-term safety of human retinal progenitor cell transplantation in retinitis pigmentosa patients. *Stem Cell Res Ther, 8*(1), 209. doi:10.1186/s13287-017-0661-8

Lo, B., & Parham, L. (2009). Ethical issues in stem cell research. *Endocr Rev, 30*(3), 204-213. doi:10.1210/er.2008-0031

Lu, P., Cao, Y., Wang, M., Zheng, P., Hou, J., Zhu, C., & Hu, J. (2016). Mature dendritic cells cause Th17/Treg imbalance by secreting TGF-β1 and IL-6 in the pathogenesis of experimental autoimmune encephalomyelitis. *Central-European journal of immunology, 41*(2), 143-152. doi:10.5114/ceji.2016.60987

Ma, L. L., Meng, F. B., Shi, P., Li, G., & Pang, X. N. (2012). Quantity and proliferation rate of mesenchymal stem cells in human cord blood during gestation. *Cell Biol Int, 36*(4), 415-418. doi:10.1042/cbi20110173

Maeda, Y., Nakagomi, N., Nakano-Doi, A., Ishikawa, H., Tatsumi, Y., Bando, Y., Yoshikawa, H., Matsuyama, T., Gomi, F., & Nakagomi, T. (2019). Potential of Adult Endogenous Neural Stem/Progenitor Cells in the Spinal Cord to Contribute to Remyelination in Experimental Autoimmune Encephalomyelitis. *Cells, 8*(9), 1025. doi:10.3390/cells8091025

Maleki, M., Ghanbarvand, F., Reza Behvarz, M., Ejtemaei, M., & Ghadirkhomi, E. (2014). Comparison of mesenchymal stem cell markers in multiple human adult stem cells. *International Journal of Stem Cells, 7*(2), 118-126. doi:10.15283/ijsc.2014.7.2.118

Malgieri, A., Kantzari, E., Patrizi, M. P., & Gambardella, S. (2010). Bone marrow and umbilical cord blood human mesenchymal stem cells: state of the art. *International Journal of Clinical and Experimental Medicine, 3*(4), 248-269.

Manuguerra-Gagne, R., Boulos, P. R., Ammar, A., Leblond, F. A., Krosl, G., Pichette, V., Lesk, M. R., & Roy, D. C. (2013). Transplantation of mesenchymal stem cells promotes tissue regeneration in a glaucoma model through laser-induced paracrine factor secretion and progenitor cell recruitment. *STEM CELLS, 31*(6), 1136-1148. doi:10.1002/stem.1364

Marlhens, F., Griffoin, J. M., Bareil, C., Arnaud, B., Claustres, M., & Hamel, C. P. (1998). Autosomal recessive retinal dystrophy associated with two novel mutations in the RPE65 gene. *Eur J Hum Genet, 6*(5), 527-531. doi:10.1038/sj.ejhg.5200205

Martin, G. R. (1981). Isolation of a pluripotent cell line from early mouse embryos cultured in medium conditioned by teratocarcinoma stem cells. *Proceedings of the National Academy of Sciences, 78*(12), 7634.

Mattiucci, D., Maurizi, G., Leoni, P., & Poloni, A. (2018). Aging- and Senescence-associated Changes of Mesenchymal Stromal Cells in Myelodysplastic Syndromes. *Cell Transplant, 27*(5), 754-764. doi:10.1177/0963689717745890

Maurice, S., Srouji, S., & Livne, E. (2006). Isolation of progenitor cells from cord blood using adhesion matrices. *Cytotechnology, 52*(2), 125-137. doi:10.1007/s10616-007-9043-x

Mazzoccoli, G., Miscio, G., Fontana, A., Copetti, M., Francavilla, M., Bosi, A., Perfetto, F., Valoriani, A., De Cata, A., Santodirocco, M., Totaro, A., Rubino, R., di Mauro, L., & Tarquini, R. (2016). Time related variations in stem cell harvesting of umbilical cord blood. *Scientific Reports, 6*, 21404-21404. doi:10.1038/srep21404

McKee, C., Brown, C., Bakshi, S., Walker, K., Govind, C. K., & Chaudhry, G. R. (2021). Transcriptomic Analysis of Naïve Human Embryonic Stem Cells Cultured in Three-Dimensional PEG Scaffolds. *Biomolecules, 11*(1). doi:10.3390/biom11010021

Mead, B., Amaral, J., & Tomarev, S. (2018). Mesenchymal Stem Cell–Derived Small Extracellular Vesicles Promote Neuroprotection in Rodent Models of Glaucoma. *Invest Ophthalmol Vis Sci, 59*(2), 702-714. doi:10.1167/iovs.17-22855

Meligy, F. Y., Shigemura, K., Behnsawy, H. M., Fujisawa, M., Kawabata, M., & Shirakawa, T. (2012). The efficiency of in vitro isolation and myogenic differentiation of MSCs derived from adipose connective tissue, bone marrow, and skeletal muscle tissue. *In Vitro Cell Dev Biol Anim, 48*(4), 203-215. doi:10.1007/s11626-012-9488-x

Mennan, C., Wright, K., Bhattacharjee, A., Balain, B., Richardson, J., & Roberts, S. (2013). Isolation and characterisation of mesenchymal stem cells from different regions of the human umbilical cord. *Biomed Res Int, 2013*, 916136-916136. doi:10.1155/2013/916136

Meyer, L. (2018). FDA seeks permanent injunctions against two stem cell clinics. *U.S. Food & Drug Administration*.

Mi, H., Muruganujan, A., Casagrande, J. T., & Thomas, P. D. (2013). Large-scale gene function analysis with the PANTHER classification system. *Nature protocols, 8*(8), 1551-1566. doi:10.1038/nprot.2013.092

Miao, Z., Jin, J., Chen, L., Zhu, J., Huang, W., Zhao, J., Qian, H., & Zhang, X. (2006). Isolation of mesenchymal stem cells from human placenta: comparison with human bone marrow mesenchymal stem cells. *Cell Biol Int, 30*(9), 681-687. doi:10.1016/j.cellbi.2006.03.009

Miczán, V., Kelemen, K., Glavinics, J. R., László, Z. I., Barti, B., Kenesei, K., Kisfali, M., & Katona, I. (2021). NECAB1 and NECAB2 are Prevalent Calcium-Binding Proteins of CB1/CCK-Positive GABAergic Interneurons. *Cerebral Cortex, 31*(3), 1786-1806. doi:10.1093/cercor/bhaa326

Millán-Rivero, J. E., Nadal-Nicolás, F. M., García-Bernal, D., Sobrado-Calvo, P., Blanquer, M., Moraleda, J. M., Vidal-Sanz, M., & Agudo-Barriuso, M. (2018). Human Wharton's jelly mesenchymal stem cells protect axotomized rat retinal ganglion cells via secretion of anti-inflammatory and neurotrophic factors. *Sci Rep, 8*(1), 16299. doi:10.1038/s41598-018-34527-z

Moghadam, F. H., Tayebi, T., Dehghan, M., Eslami, G., Nadri, H., Moradi, A., Vahedian-Ardakani, H., & Barzegar, K. (2014). Differentiation of bone marrow mesenchymal stem cells into chondrocytes after short term culture in alkaline medium. *International journal of hematology-oncology and stem cell research, 8*(4), 12-19.

Mohamed, E. M., Abdelrahman, S. A., Hussein, S., Shalaby, S. M., Mosaad, H., & Awad, A. M. (2017). Effect of human umbilical cord blood mesenchymal stem cells administered by intravenous or intravitreal routes on cryo-induced retinal injury. *IUBMB Life, 69*(3), 188-201. doi:10.1002/iub.1608

Moraghebi, R., Kirkeby, A., Chaves, P., Rönn, R. E., Sitnicka, E., Parmar, M., Larsson, M., Herbst, A., & Woods, N.-B. (2017). Term amniotic fluid: an unexploited reserve of mesenchymal stromal cells for reprogramming and potential cell therapy applications. *Stem Cell Res Ther, 8*(1), 190-190. doi:10.1186/s13287-017-0582-6

Moreno, M., Guo, F., Mills Ko, E., Bannerman, P., Soulika, A., & Pleasure, D. (2013). Origins and significance of astrogliosis in the multiple sclerosis model, MOG peptide EAE. *Journal of the neurological sciences, 333*(1-2), 55-59. doi:10.1016/j.jns.2012.12.014

Moskowitz, D. M., Zhang, D. W., Hu, B., Le Saux, S., Yanes, R. E., Ye, Z., Buenrostro, J. D., Weyand, C. M., Greenleaf, W. J., & Goronzy, J. J. (2017). Epigenomics of human CD8 T cell differentiation and aging. *Sci Immunol, 2*(8). doi:10.1126/sciimmunol.aag0192

Moya, A., Paquet, J., Deschepper, M., Larochette, N., Oudina, K., Denoeud, C., Bensidhoum, M., Logeart-Avramoglou, D., & Petite, H. (2018). Human Mesenchymal Stem Cell Failure to Adapt to Glucose Shortage and Rapidly Use Intracellular Energy Reserves Through Glycolysis Explains Poor Cell Survival After Implantation. *STEM CELLS, 36*(3), 363-376. doi:10.1002/stem.2763

Na, Y. J., Jin, J. K., Kim, J. I., Choi, E. K., Carp, R. I., & Kim, Y. S. (2007). JAK-STAT signaling pathway mediates astrogliosis in brains of scrapie-infected mice. *J Neurochem, 103*(2), 637-649. doi:10.1111/j.1471-4159.2007.04769.x

Nakagawa, S., Kim, J. E., Lee, R., Chen, J., Fujioka, T., Malberg, J., Tsuji, S., & Duman, R. S. (2002). Localization of phosphorylated cAMP response element-binding protein in immature neurons of adult hippocampus. *J Neurosci, 22*(22), 9868-9876. doi:10.1523/jneurosci.22-22-09868.2002

Nakatani, H., Martin, E., Hassani, H., Clavairoly, A., Maire, C. L., Viadieu, A., Kerninon, C., Delmasure, A., Frah, M., Weber, M., Nakafuku, M., Zalc, B., Thomas, J. L., Guillemot, F., Nait-Oumesmar, B., & Parras, C. (2013). Ascl1/Mash1 promotes brain oligodendrogenesis during myelination and remyelination. *J Neurosci, 33*(23), 9752-9768. doi:10.1523/jneurosci.0805-13.2013

Nasef, A., Fouillard, L., El-Taguri, A., & Lopez, M. (2007). Human bone marrow-derived mesenchymal stem cells. *The Libyan Journal of Medicine, 2*(4), 190-201. doi:10.4176/070705

Nasri, F., Mohtasebi, M. S., Hashemi, E., Zarrabi, M., Gholijani, N., & Sarvestani, E. K. (2018). Therapeutic Efficacy of Mesenchymal Stem Cells and Mesenchymal Stem Cells-derived Neural Progenitors in Experimental Autoimmune Encephalomyelitis. *Int J Stem Cells, 11*(1), 68-77. doi:10.15283/ijsc17052

Noriega, D. C., Ardura, F., Hernandez-Ramajo, R., Martin-Ferrero, M. A., Sanchez-Lite, I., Toribio, B., Alberca, M., Garcia, V., Moraleda, J. M., Sanchez, A., & Garcia-Sancho, J. (2017). Intervertebral Disc Repair by Allogeneic Mesenchymal Bone Marrow Cells: A Randomized Controlled Trial. *Transplantation, 101*(8), 1945-1951. doi:10.1097/tp.0000000000001484

Numakawa, T., Odaka, H., & Adachi, N. (2017). Actions of Brain-Derived Neurotrophic Factor and Glucocorticoid Stress in Neurogenesis. *International Journal of Molecular Sciences, 18*(11), 2312. doi:10.3390/ijms18112312

O'Brien, T. A., Tiedemann, K., & Vowels, M. R. (2006). No longer a biological waste product: umbilical cord blood. *Med J Aust, 184*(8), 407-410.

O'Neal, T. B., & Luther, E. E. (2020). Retinitis Pigmentosa *StatPearls*. Treasure Island (FL): StatPearls Publishing Copyright © 2020, StatPearls Publishing LLC.

Oner, A., Gonen, Z. B., Sinim, N., Cetin, M., & Ozkul, Y. (2016). Subretinal adipose tissue-derived mesenchymal stem cell implantation in advanced stage retinitis pigmentosa: a phase I clinical safety study. *Stem Cell Res Ther, 7*(1), 178-178. doi:10.1186/s13287-016-0432-y

Osborne, A., Sanderson, J., & Martin, K. R. (2018). Neuroprotective Effects of Human Mesenchymal Stem Cells and Platelet-Derived Growth Factor on Human Retinal Ganglion Cells. *STEM CELLS, 36*(1), 65-78. doi:10.1002/stem.2722

Owen, M. (1988). Marrow stromal stem cells. *J Cell Sci Suppl, 10*, 63-76.

Owens, G. M. (2016). Economic burden of multiple sclerosis and the role of managed sare organizations in multiple sclerosis management. *The American journal of managed care, 22*(6 Suppl), s151-s158.

Owston, H., Giannoudis, P. V., & Jones, E. (2016). Do skeletal muscle MSCs in humans contribute to bone repair? A systematic review. *Injury, 47*, S3-S15.

Özmert, E., & Arslan, U. (2020). Management of retinitis pigmentosa by Wharton's jelly-derived mesenchymal stem cells: prospective analysis of 1-year results. *Stem Cell Res Ther, 11*(1), 353. doi:10.1186/s13287-020-01870-w

Pang, J. J., Chang, B., Hawes, N. L., Hurd, R. E., Davisson, M. T., Li, J., Noorwez, S. M., Malhotra, R., McDowell, J. H., Kaushal, S., Hauswirth, W. W., Nusinowitz, S., Thompson, D. A., & Heckenlively, J. R. (2005). Retinal degeneration 12 (rd12): a new, spontaneously arising mouse model for human Leber congenital amaurosis (LCA). *Molecular vision, 11*, 152-162.

Pang, X., Yang, H., & Peng, B. (2014). Human umbilical cord mesenchymal stem cell transplantation for the treatment of chronic discogenic low back pain. *Pain Physician, 17*(4), E525-530.

Park, I. H., Kim, K. H., Choi, H. K., Shim, J. S., Whang, S. Y., Hahn, S. J., Kwon, O. J., & Oh, I. H. (2013). Constitutive stabilization of hypoxia-inducible factor alpha selectively promotes the self-renewal of mesenchymal progenitors and maintains mesenchymal stromal cells in an undifferentiated state. *Experimental and Molecular Medicine, 45*, e44. doi:10.1038/emm.2013.87

Park, J., Lee, N., Lee, J., Choe, E. K., Kim, M. K., Lee, J., Byun, M. S., Chon, M.-W., Kim, S. W., Lee, C. J., Kim, J. H., Kwon, J. S., & Chang, M.-S. (2017). Small molecule-based lineage switch of human adipose-derived stem cells into neural stem cells and functional GABAergic neurons. *Scientific Reports, 7*(1), 10166-10166. doi:10.1038/s41598-017-10394-y

Paylakhi, S., Labelle-Dumais, C., Tolman, N. G., Sellarole, M. A., Seymens, Y., Saunders, J., Lakosha, H., deVries, W. N., Orr, A. C., Topilko, P., John, S. W., & Nair, K. S. (2018). Müller glia-derived PRSS56 is required to sustain ocular axial growth and prevent refractive error. *PLoS genetics, 14*(3), e1007244-e1007244. doi:10.1371/journal.pgen.1007244

Pegoretti, V., Swanson, K. A., Bethea, J. R., Probert, L., Eisel, U. L. M., & Fischer, R. (2020). Inflammation and Oxidative Stress in Multiple Sclerosis: Consequences for Therapy Development. *Oxidative medicine and cellular longevity, 2020*, 7191080-7191080. doi:10.1155/2020/7191080

Peltier, J., O'Neill, A., & Schaffer, D. V. (2007). PI3K/Akt and CREB regulate adult neural hippocampal progenitor proliferation and differentiation. *Dev Neurobiol, 67*(10), 1348-1361. doi:10.1002/dneu.20506

Pereira, C. L., Teixeira, G. Q., Ribeiro-Machado, C., Caldeira, J., Costa, M., Figueiredo, F., Fernandes, R., Aguiar, P., Grad, S., Barbosa, M. A., & Gonçalves, R. M. (2016). Mesenchymal Stem/Stromal Cells seeded on cartilaginous endplates promote Intervertebral Disc Regeneration through Extracellular Matrix Remodeling. *Scientific Reports, 6*, 33836. doi:10.1038/srep33836

Perez-Cruet, M., Beeravolu, N., McKee, C., Brougham, J., Khan, I., Bakshi, S., & Chaudhry, G. R. (2018). Potential of Human Nucleus Pulposus-Like Cells Derived From Umbilical Cord to Treat Degenerative Disc Disease. *Neurosurgery*. doi:10.1093/neuros/nyy012

Picard-Riera, N., Nait-Oumesmar, B., & Baron-Van Evercooren, A. (2004). Endogenous adult neural stem cells: limits and potential to repair the injured central nervous system. *Journal of neuroscience research, 76*(2), 223-231. doi:10.1002/jnr.20040

Pievani, A., Scagliotti, V., Russo, F. M., Azario, I., Rambaldi, B., Sacchetti, B., Marzorati, S., Erba, E., Giudici, G., Riminucci, M., Biondi, A., Vergani, P., & Serafini, M. (2014). Comparative analysis of multilineage properties of mesenchymal stromal cells derived from fetal sources shows an advantage of mesenchymal stromal cells isolated from cord blood in chondrogenic differentiation potential. *Cytotherapy, 16*(7), 893-905. doi:10.1016/j.jcyt.2014.02.008

Planchon, S. M., Lingas, K. T., Reese Koc, J., Hooper, B. M., Maitra, B., Fox, R. M., Imrey, P. B., Drake, K. M., Aldred, M. A., Lazarus, H. M., & Cohen, J. A. (2018). Feasibility of mesenchymal stem cell culture expansion for a phase I clinical trial in multiple sclerosis. *Mult Scler J Exp Transl Clin, 4*(1), 2055217318765288. doi:10.1177/2055217318765288

Pluchino, S., Quattrini, A., Brambilla, E., Gritti, A., Salani, G., Dina, G., Galli, R., Del Carro, U., Amadio, S., Bergami, A., Furlan, R., Comi, G., Vescovi, A. L., & Martino, G. (2003). Injection of adult neurospheres induces recovery in a chronic model of multiple sclerosis. *Nature, 422*(6933), 688-694. doi:10.1038/nature01552

Prem Senthil, M., Khadka, J., & Pesudovs, K. (2017). Seeing through their eyes: lived experiences of people with retinitis pigmentosa. *Eye, 31*(5), 741-748. doi:10.1038/eye.2016.315

Prockop, D. J., Brenner, M., Fibbe, W. E., Horwitz, E., Le Blanc, K., Phinney, D. G., Simmons, P. J., Sensebe, L., & Keating, A. (2010). Defining the risks of mesenchymal stromal cell therapy. *Cytotherapy, 12*(5), 576-578. doi:10.3109/14653249.2010.507330

Qu, L., Gao, L., Xu, H., Duan, P., Zeng, Y., Liu, Y., & Yin, Z. Q. (2017). Combined transplantation of human mesenchymal stem cells and human retinal progenitor cells into the subretinal space of RCS rats. *Scientific Reports, 7*(1), 199. doi:10.1038/s41598-017-00241-5

Quinn, C., & Flake, A. W. (2008). In vivo Differentiation Potential of Mesenchymal Stem Cells: Prenatal and Postnatal Model Systems. *Transfusion Medicine and Hemotherapy, 35*(3), 239-247. doi:10.1159/000129129

Ragni, E., Viganò, M., Rebulla, P., Giordano, R., & Lazzari, L. (2013). What is beyond a qRT-PCR study on mesenchymal stem cell differentiation properties: how to choose the most reliable housekeeping genes. *Journal of Cellular and Molecular Medicine, 17*(1), 168-180. doi:10.1111/j.1582-4934.2012.01660.x

Razavi, S., Nazem, G., Mardani, M., Esfandiari, E., Salehi, H., & Esfahani, S. H. (2015). Neurotrophic factors and their effects in the treatment of multiple sclerosis. *Adv Biomed Res, 4*, 53. doi:10.4103/2277-9175.151570

Ren, G., Chen, X., Dong, F., Li, W., Ren, X., Zhang, Y., & Shi, Y. (2012). Concise review: mesenchymal stem cells and translational medicine: emerging issues. *Stem Cells Translational Medicine, 1*(1), 51-58. doi:10.5966/sctm.2011-0019

Ren, G., Su, J., Zhang, L., Zhao, X., Ling, W., L'Huillie, A., Zhang, J., Lu, Y., Roberts, A. I., Ji, W., Zhang, H., Rabson, A. B., & Shi, Y. (2009). Species variation in the mechanisms of mesenchymal stem cell-mediated immunosuppression. *STEM CELLS, 27*(8), 1954-1962. doi:10.1002/stem.118

Ren, J., Ward, D., Chen, S., Tran, K., Jin, P., Sabatino, M., Robey, P. G., & Stroncek, D. F. (2018). Comparison of human bone marrow stromal cells cultured in human platelet growth factors and fetal bovine serum. *Journal of Translational Medicine, 16*, 65. doi:10.1186/s12967-018-1400-3

Ridge, S. M., Sullivan, F. J., & Glynn, S. A. (2017). Mesenchymal stem cells: key players in cancer progression. *Mol Cancer, 16*(1), 31. doi:10.1186/s12943-017-0597-8

Riordan, N. H., Morales, I., Fernández, G., Allen, N., Fearnot, N. E., Leckrone, M. E., Markovich, D. J., Mansfield, D., Avila, D., Patel, A. N., Kesari, S., & Paz Rodriguez, J. (2018). Clinical feasibility of umbilical cord tissue-derived mesenchymal stem cells in the treatment of multiple sclerosis. *J Transl Med, 16*(1), 57. doi:10.1186/s12967-018-1433-7

Robey, P. (2017). "Mesenchymal stem cells": fact or fiction, and implications in their therapeutic use. *F1000Research, 6*, F1000 Faculty Rev-1524. doi:10.12688/f1000research.10955.1

Roubeix, C., Godefroy, D., Mias, C., Sapienza, A., Riancho, L., Degardin, J., Fradot, V., Ivkovic, I., Picaud, S., Sennlaub, F., Denoyer, A., Rostene, W., Sahel, J. A., Parsadaniantz, S. M., Brignole-Baudouin, F., & Baudouin, C. (2015). Intraocular pressure reduction and neuroprotection conferred by bone marrow-derived mesenchymal stem cells in an animal model of glaucoma. *Stem Cell Res Ther, 6*, 177. doi:10.1186/s13287-015-0168-0

Russell, A. L., Lefavor, R., Durand, N., Glover, L., & Zubair, A. C. (2018). Modifiers of mesenchymal stem cell quantity and quality. *Transfusion, 58*(6), 1434-1440. doi:10.1111/trf.14597

Ryu, B., Sekine, H., Homma, J., Kobayashi, T., Kobayashi, E., Kawamata, T., & Shimizu, T. (2019). Allogeneic adipose-derived mesenchymal stem cell sheet that produces neurological improvement with angiogenesis and neurogenesis in a rat stroke model. *J Neurosurg*, 1-14. doi:10.3171/2018.11.jns182331

Sacchetti, B., Funari, A., Remoli, C., Giannicola, G., Kogler, G., Liedtke, S., Cossu, G., Serafini, M., Sampaolesi, M., Tagliafico, E., Tenedini, E., Saggio, I., Robey, Pamela G., Riminucci, M., & Bianco, P. (2016). No Identical "Mesenchymal Stem Cells" at Different Times and Sites: Human Committed Progenitors of Distinct Origin and Differentiation Potential Are Incorporated as Adventitial Cells in Microvessels. *Stem Cell Reports, 6*(6), 897-913. doi:10.1016/j.stemcr.2016.05.011

Sakaguchi, Y., Sekiya, I., Yagishita, K., & Muneta, T. (2005). Comparison of human stem cells derived from various mesenchymal tissues: Superiority of synovium as a cell source. *Arthritis & Rheumatism, 52*(8), 2521-2529. doi:10.1002/art.21212

Samoilova, E. B., Horton, J. L., Hilliard, B., Liu, T. S., & Chen, Y. (1998). IL-6-deficient mice are resistant to experimental autoimmune encephalomyelitis: roles of IL-6 in the activation and differentiation of autoreactive T cells. *J Immunol, 161*(12), 6480-6486.

Samsonraj, R. M., Raghunath, M., Nurcombe, V., Hui, J. H., van Wijnen, A. J., & Cool, S. M. (2017). Concise Review: Multifaceted Characterization of Human Mesenchymal Stem Cells for Use in Regenerative Medicine. *Stem Cells Translational Medicine, 6*(12), 2173-2185. doi:10.1002/sctm.17-0129

Sart, S., & Agathos, S. N. (2016). Large-Scale Expansion and Differentiation of Mesenchymal Stem Cells in Microcarrier-Based Stirred Bioreactors. *Methods Mol Biol, 1502*, 87-102. doi:10.1007/7651_2015_314

Satarian, L., Nourinia, R., Safi, S., Kanavi, M. R., Jarughi, N., Daftarian, N., Arab, L., Aghdami, N., Ahmadieh, H., & Baharvand, H. (2017). Intravitreal Injection of Bone Marrow Mesenchymal Stem Cells in Patients with Advanced Retinitis Pigmentosa; a Safety Study. *J Ophthalmic Vis Res, 12*(1), 58-64. doi:10.4103/2008-322x.200164

Schmitt, C., Strazielle, N., & Ghersi-Egea, J.-F. (2012). Brain leukocyte infiltration initiated by peripheral inflammation or experimental autoimmune encephalomyelitis occurs through pathways connected to the CSF-filled compartments of the forebrain and midbrain. *J Neuroinflammation, 9*(1), 187. doi:10.1186/1742-2094-9-187

Schmitt, S., Aftab, U., Jiang, C., Redenti, S., Klassen, H., Miljan, E., Sinden, J., & Young, M. (2009). Molecular Characterization of Human Retinal Progenitor Cells. *Investigative ophthalmology & visual science, 50*(12), 5901-5908. doi:10.1167/iovs.08-3067

Shekaran, A., Sim, E., Tan, K. Y., Chan, J. K., Choolani, M., Reuveny, S., & Oh, S. (2015). Enhanced in vitro osteogenic differentiation of human fetal MSCs attached to 3D microcarriers versus harvested from 2D monolayers. *BMC Biotechnol, 15*, 102. doi:10.1186/s12896-015-0219-8

Shin, J. Y., Park, H. J., Kim, H. N., Oh, S. H., Bae, J. S., Ha, H. J., & Lee, P. H. (2014). Mesenchymal stem cells enhance autophagy and increase beta-amyloid clearance in Alzheimer disease models. *Autophagy, 10*(1), 32-44. doi:10.4161/auto.26508

Shin, K.-S., Na, K.-H., Lee, H.-J., Kim, D.-G., Shin, S.-J., Kim, J. K., & Kim, G. J. (2009). Characterization of Fetal Tissue-derived Mesenchymal Stem Cells. *International Journal of Stem Cells, 2*(1), 51-58.

Shivaswamy, S., Bhinge, A., Zhao, Y., Jones, S., Hirst, M., & Iyer, V. R. (2008). Dynamic remodeling of individual nucleosomes across a eukaryotic genome in response to transcriptional perturbation. *PLoS biology, 6*(3), e65-e65. doi:10.1371/journal.pbio.0060065

Skoloudik, L., Chrobok, V., Kalfert, D., Koci, Z., Sykova, E., Chumak, T., Popelar, J., Syka, J., Laco, J., Dedkova, J., Dayanithi, G., & Filip, S. (2016). Human Multipotent Mesenchymal Stromal Cells in the Treatment of Postoperative Temporal Bone Defect: An Animal Model. *Cell Transplant, 25*(7), 1405-1414. doi:10.3727/096368915x689730

Sorrells, S. F., Paredes, M. F., Cebrian-Silla, A., Sandoval, K., Qi, D., Kelley, K. W., James, D., Mayer, S., Chang, J., Auguste, K. I., Chang, E. F., Gutierrez, A. J., Kriegstein, A. R., Mathern, G. W., Oldham, M. C., Huang, E. J., Garcia-Verdugo, J. M., Yang, Z., & Alvarez-Buylla, A. (2018). Human hippocampal neurogenesis drops sharply in children to undetectable levels in adults. *Nature, 555*(7696), 377-381. doi:10.1038/nature25975

Stevens, H. E., Smith, K. M., Rash, B. G., & Vaccarino, F. M. (2010). Neural stem cell regulation, fibroblast growth factors, and the developmental origins of neuropsychiatric disorders. *Front Neurosci, 4*. doi:10.3389/fnins.2010.00059

Stewart, A. N., Kendziorski, G., Deak, Z. M., Brown, D. J., Fini, M. N., Copely, K. L., Rossignol, J., & Dunbar, G. L. (2017). Co-transplantation of mesenchymal and neural stem cells and overexpressing stromal-derived factor-1 for treating spinal cord injury. *Brain Res, 1672*, 91-105. doi:10.1016/j.brainres.2017.07.005

Stultz, B. G., McGinnis, K., Thompson, E. E., Lo Surdo, J. L., Bauer, S. R., & Hursh, D. A. (2016). Chromosomal stability of mesenchymal stromal cells during in vitro culture. *Cytotherapy, 18*(3), 336-343. doi:https://doi.org/10.1016/j.jcyt.2015.11.017

Sun, J., Mandai, M., Kamao, H., Hashiguchi, T., Shikamura, M., Kawamata, S., Sugita, S., & Takahashi, M. (2015). Protective Effects of Human iPS-Derived Retinal Pigmented Epithelial Cells in Comparison with Human Mesenchymal Stromal Cells and Human Neural Stem Cells on the Degenerating Retina in rd1 mice. *STEM CELLS, 33*(5), 1543-1553. doi:10.1002/stem.1960

Surendran, H., Rathod, R. J., & Pal, R. (2018). Generation of Transplantable Retinal Pigmented Epithelial (RPE) Cells for Treatment of Age-Related Macular Degeneration (AMD). *Methods Mol Biol*. doi:10.1007/7651_2018_140

Swamynathan, P., Venugopal, P., Kannan, S., Thej, C., Kolkundar, U., Bhagwat, S., Ta, M., Majumdar, A. S., & Balasubramanian, S. (2014). Are serum-free and xeno-free culture conditions ideal for large scale clinical grade expansion of Wharton's jelly derived mesenchymal stem cells? A comparative study. *Stem Cell Res Ther, 5*(4), 88. doi:10.1186/scrt477

Tancharoen, W., Aungsuchawan, S., Pothacharoen, P., Markmee, R., Narakornsak, S., Kieodee, J., Boonma, N., & Tasuya, W. (2017). Differentiation of mesenchymal stem cells from human amniotic fluid to vascular endothelial cells. *Acta Histochemistry, 119*(2), 113-121. doi:10.1016/j.acthis.2016.11.009

Toops, K. A., Hagemann, T. L., Messing, A., & Nickells, R. W. (2012). The effect of glial fibrillary acidic protein expression on neurite outgrowth from retinal explants in a permissive environment. *BMC Research Notes, 5*(1), 693. doi:10.1186/1756-0500-5-693

Trivanovic, D., Kocic, J., Mojsilovic, S., Krstic, A., Ilic, V., Djordjevic, I. O., Santibanez, J. F., Jovcic, G., Terzic, M., & Bugarski, D. (2013). Mesenchymal stem cells isolated from peripheral blood and umbilical cord Wharton's jelly. *Srp Arh Celok Lek, 141*(3-4), 178-186.

Tropel, P., Platet, N., Platel, J. C., Noel, D., Albrieux, M., Benabid, A. L., & Berger, F. (2006). Functional neuronal differentiation of bone marrow-derived mesenchymal stem cells. *STEM CELLS, 24*(12), 2868-2876. doi:10.1634/stemcells.2005-0636

Tuekprakhon, A., Sangkitporn, S., Trinavarat, A., Pawestri, A. R., Vamvanij, V., Ruangchainikom, M., Luksanapruksa, P., Pongpaksupasin, P., Khorchai, A., Dambua, A., Boonchu, P., Yodtup, C., Uiprasertkul, M., Sangkitporn, S., & Atchaneeyasakul, L. O. (2021). Intravitreal autologous mesenchymal stem cell transplantation: a non-randomized phase I clinical trial in patients with retinitis pigmentosa. *Stem Cell Res Ther, 12*(1), 52. doi:10.1186/s13287-020-02122-7

Turgeman, G. (2015). The therapeutic potential of mesenchymal stem cells in Alzheimer's disease: converging mechanisms. *Neural regeneration research, 10*(5), 698-699. doi:10.4103/1673-5374.156953

Turner, L. (2017). ClinicalTrials.gov, stem cells and 'pay-to-participate' clinical studies. *Regen Med, 12*(6), 705-719. doi:10.2217/rme-2017-0015

Tzameret, A., Sher, I., Belkin, M., Treves, A. J., Meir, A., Nagler, A., Levkovitch-Verbin, H., Barshack, I., Rosner, M., & Rotenstreich, Y. (2014). Transplantation of human bone marrow mesenchymal stem cells as a thin subretinal layer ameliorates retinal degeneration in a rat model of retinal dystrophy. *Exp Eye Res, 118*, 135-144. doi:https://doi.org/10.1016/j.exer.2013.10.023

van Buul, G. M., Siebelt, M., Leijs, M. J., Bos, P. K., Waarsing, J. H., Kops, N., Weinans, H., Verhaar, J. A., Bernsen, M. R., & van Osch, G. J. (2014). Mesenchymal stem cells reduce pain but not degenerative changes in a mono-iodoacetate rat model of osteoarthritis. *J Orthop Res, 32*(9), 1167-1174. doi:10.1002/jor.22650

Van Harmelen, V., Rohrig, K., & Hauner, H. (2004). Comparison of proliferation and differentiation capacity of human adipocyte precursor cells from the omental and subcutaneous adipose tissue depot of obese subjects. *Metabolism, 53*(5), 632-637.

Vilela, C. A. P., Messias, A., Calado, R. T., Siqueira, R. C., Silva, M. J. L., Covas, D. T., & Paula, J. S. (2021). Retinal function after intravitreal injection of autologous bone marrow-derived mesenchymal stromal cells in advanced glaucoma. *Doc Ophthalmol, 143*(1), 33-38. doi:10.1007/s10633-021-09817-z

Villoslada, P., & Steinman, L. (2020). New targets and therapeutics for neuroprotection, remyelination and repair in multiple sclerosis. *Expert Opin Investig Drugs, 29*(5), 443-459. doi:10.1080/13543784.2020.1757647

Vishnubalaji, R., Al-Nbaheen, M., Kadalmani, B., Aldahmash, A., & Ramesh, T. (2012). Comparative investigation of the differentiation capability of bone-marrow- and adipose-derived mesenchymal stem cells by qualitative and quantitative analysis. *Cell Tissue Res, 347*(2), 419-427. doi:10.1007/s00441-011-1306-3

Vitallé, J., Terrén, I., Orrantia, A., Bilbao, A., Gamboa, P. M., Borrego, F., & Zenarruzabeitia, O. (2020). The Expression and Function of CD300 Molecules in the Main Players of Allergic Responses: Mast Cells, Basophils and Eosinophils. *International Journal of Molecular Sciences, 21*(9). doi:10.3390/ijms21093173

Wang, J., Yang, J., Gu, P., & Klassen, H. (2010). Effects of glial cell line-derived neurotrophic factor on cultured murine retinal progenitor cells. *Molecular vision, 16*, 2850-2866.

Wang, J., Ye, F., Cheng, L.-j., Shi, Y.-j., Bao, J., Sun, H.-q., Wang, W., Zhang, P., & Bu, H. (2009). Osteogenic differentiation of mesenchymal stem cells promoted by overexpression of connective tissue growth factor. *J Zhejiang Univ Sci B, 10*(5), 355-367. doi:10.1631/jzus.B0820252

Wang, M.-R., Zhang, X.-J., Liu, H.-C., Ma, W.-D., Zhang, M.-L., Zhang, Y., Li, X., Dou, M.-M., Jing, Y.-L., Chu, Y.-J., & Zhu, L. (2019). Matrine protects oligodendrocytes by inhibiting their apoptosis and enhancing mitochondrial autophagy. *Brain Research Bulletin, 153*, 30-38. doi:https://doi.org/10.1016/j.brainresbull.2019.08.006

Wang, M., Yuan, Q., & Xie, L. (2018). Mesenchymal Stem Cell-Based Immunomodulation: Properties and Clinical Application. *Stem Cells International, 2018*, 3057624-3057624. doi:10.1155/2018/3057624

Wang, N.-K., Tosi, J., Kasanuki, J. M., Chou, C. L., Kong, J., Parmalee, N., Wert, K. J., Allikmets, R., Lai, C.-C., Chien, C.-L., Nagasaki, T., Lin, C.-S., & Tsang, S. H. (2010). Transplantation of reprogrammed embryonic stem cells improves visual function in a mouse model for retinitis pigmentosa. *Transplantation, 89*(8), 911-919. doi:10.1097/TP.0b013e3181d45a61

Wang, Q., Yang, Q., Wang, Z., Tong, H., Ma, L., Zhang, Y., Shan, F., Meng, Y., & Yuan, Z. (2016). Comparative analysis of human mesenchymal stem cells from fetal-bone marrow, adipose tissue, and Warton's jelly as sources of cell immunomodulatory therapy. *Human Vaccines & Immunotherapeutics, 12*(1), 85-96. doi:10.1080/21645515.2015.1030549

Wang, S., Lu, B., Girman, S., Duan, J., McFarland, T., Zhang, Q. S., Grompe, M., Adamus, G., Appukuttan, B., & Lund, R. (2010). Non-invasive stem cell therapy in a rat model for retinal degeneration and vascular pathology. *PLoS ONE, 5*(2), e9200. doi:10.1371/journal.pone.0009200

Wang, X., Ma, S., Yang, B., Huang, T., Meng, N., Xu, L., Xing, Q., Zhang, Y., Zhang, K., Li, Q., Zhang, T., Wu, J., Yang, G. L., Guan, F., & Wang, J. (2018). Resveratrol promotes hUC-MSCs engraftment and neural repair in a mouse model of Alzheimer's disease. *Behav Brain Res, 339*, 297-304. doi:10.1016/j.bbr.2017.10.032

Wang, Y., Yang, J., Li, H., Wang, X., Zhu, L., Fan, M., & Wang, X. (2013). Hypoxia promotes dopaminergic differentiation of mesenchymal stem cells and shows benefits for transplantation in a rat model of Parkinson's disease. *PLoS ONE, 8*(1), e54296. doi:10.1371/journal.pone.0054296

Wang, Y., Zhang, D., Shen, B., Zhang, Y., & Gu, P. (2018). Stem/Progenitor Cells and Biodegradable Scaffolds in the Treatment of Retinal Degenerative Diseases. *Curr Stem Cell Res Ther, 13*(3), 160-173. doi:10.2174/1574888x13666171227230736

Weiss, J. N., Benes, S. C., & Levy, S. (2016). Stem Cell Ophthalmology Treatment Study (SCOTS): improvement in serpiginous choroidopathy following autologous bone marrow derived stem cell treatment. *Neural Regen Res, 11*(9), 1512-1516. doi:10.4103/1673-5374.191229

Weiss, J. N., Levy, S., & Benes, S. C. (2016). Stem Cell Ophthalmology Treatment Study (SCOTS): bone marrow-derived stem cells in the treatment of Leber's hereditary optic neuropathy. *Neural Regen Res, 11*(10), 1685-1694. doi:10.4103/1673-5374.193251

Weiss, J. N., Levy, S., & Benes, S. C. (2017). Stem Cell Ophthalmology Treatment Study: bone marrow derived stem cells in the treatment of non-arteritic ischemic optic neuropathy (NAION). *Stem Cell Investig, 4*, 94. doi:10.21037/sci.2017.11.05

Wong, A., Ghassemi, E., & Yellowley, C. E. (2014). Nestin expression in mesenchymal stromal cells: regulation by hypoxia and osteogenesis. *BMC Vet Res, 10*, 173. doi:10.1186/s12917-014-0173-z

Woodbury, M. E., & Ikezu, T. (2014). Fibroblast growth factor-2 signaling in neurogenesis and neurodegeneration. *Journal of neuroimmune pharmacology : the official journal of the Society on NeuroImmune Pharmacology, 9*(2), 92-101. doi:10.1007/s11481-013-9501-5

Wouters, G., Grossi, S., Mesoraca, A., Bizzoco, D., Mobili, L., Cignini, P., & Giorlandino, C. (2007). Isolation of amniotic fluid-derived mesenchymal stem cells. *J Prenat Med, 1*(3), 39-40.

Wu, J., Sun, Z., Sun, H. S., Wu, J., Weisel, R. D., Keating, A., Li, Z. H., Feng, Z. P., & Li, R. K. (2008). Intravenously administered bone marrow cells migrate to damaged brain tissue and improve neural function in ischemic rats. *Cell Transplant, 16*(10), 993-1005.

Xia, X., & Ahmad, I. (2016). Unlocking the Neurogenic Potential of Mammalian Müller Glia. *International Journal of Stem Cells, 9*(2), 169-175. doi:10.15283/ijsc16020

Xie, Z., Bailey, A., Kuleshov, M. V., Clarke, D. J. B., Evangelista, J. E., Jenkins, S. L., Lachmann, A., Wojciechowicz, M. L., Kropiwnicki, E., Jagodnik, K. M., Jeon, M., & Ma'ayan, A. (2021). Gene Set Knowledge Discovery with Enrichr. *Curr Protoc, 1*(3), e90. doi:10.1002/cpz1.90

Xin, Y., Gao, J., Hu, R., Li, H., Li, Q., Han, F., He, Z., Lai, L., & Su, M. (2020). Changes of immune parameters of T lymphocytes and macrophages in EAE mice after BM-MSCs transplanation. *Immunol Lett*. doi:10.1016/j.imlet.2020.05.005

Xiuying, L., Jinping, B., Xiaofeng, J., Ronggui, L., Yali, X., & Yimin, W. (2014). Comprehensive characterization of four different populations of human mesenchymal stem cells as regards their immune properties, proliferation and differentiation. *International Journal of Molecular Medicine, 34*(3), 695-704. doi:10.3892/ijmm.2014.1821

Xu, J. (2018). Therapeutic Applications of Mesenchymal Stem Cells for Systemic Lupus Erythematosus. *Adv Exp Med Biol*. doi:10.1007/5584_2018_212

Yang, C., Wang, G., Ma, F., Yu, B., Chen, F., Yang, J., Feng, J., & Wang, Q. (2018). Repeated injections of human umbilical cord blood-derived mesenchymal stem cells significantly promotes functional recovery in rabbits with spinal cord injury of two noncontinuous segments. *Stem Cell Res Ther, 9*(1), 136. doi:10.1186/s13287-018-0879-0

Yang, Y.-H. K., Ogando, C. R., Wang See, C., Chang, T.-Y., & Barabino, G. A. (2018). Changes in phenotype and differentiation potential of human mesenchymal stem cells aging in vitro. *Stem Cell Res Ther, 9*(1), 131-131. doi:10.1186/s13287-018-0876-3

Young, S., Flynn, L. E., & Amsden, B. G. (2018). Adipose-derived stem cells in a resilient in situ forming hydrogel modulate macrophage phenotype. *Tissue Eng Part A*. doi:10.1089/ten.TEA.2018.0093

Yuan, Y., Kallos, M. S., Hunter, C., & Sen, A. (2014). Improved expansion of human bone marrow-derived mesenchymal stem cells in microcarrier-based suspension culture. *Journal of Tissue Engineer and Regenerative Medicine, 8*(3), 210-225. doi:10.1002/term.1515

Zager, A., Peron, J. P., Mennecier, G., Rodrigues, S. C., Aloia, T. P., & Palermo-Neto, J. (2015). Maternal immune activation in late gestation increases neuroinflammation and aggravates experimental autoimmune encephalomyelitis in the offspring. *Brain Behav Immun, 43*, 159-171. doi:10.1016/j.bbi.2014.07.021

Zappia, E., Casazza, S., Pedemonte, E., Benvenuto, F., Bonanni, I., Gerdoni, E., Giunti, D., Ceravolo, A., Cazzanti, F., Frassoni, F., Mancardi, G., & Uccelli, A. (2005). Mesenchymal stem cells ameliorate experimental autoimmune encephalomyelitis inducing T-cell anergy. *Blood, 106*(5), 1755-1761. doi:10.1182/blood-2005-04-1496

Zhang, H., Kim, Y., Ro, E. J., Ho, C., Lee, D., Trapp, B. D., & Suh, H. (2020). Hippocampal Neurogenesis and Neural Circuit Formation in a Cuprizone-Induced Multiple Sclerosis Mouse Model. *J Neurosci, 40*(2), 447-458. doi:10.1523/jneurosci.0866-19.2019

Zhang, H., Tao, Y., Ren, S., Liu, H., Zhou, H., Hu, J., Tang, Y., Zhang, B., & Chen, H. (2018). Simultaneous harvesting of endothelial progenitor cells and mesenchymal stem cells from the human umbilical cord. *Exp Ther Med, 15*(1), 806-812. doi:10.3892/etm.2017.5502

Zhang, J., Jia, X. H., Xu, Z. W., Ding, F. P., Zhou, X., Fu, H., Liu, Y., Ou, L. L., Li, Z. J., & Kong, D. L. (2013). Improved mesenchymal stem cell survival in ischemic heart through electroacupuncture. *Chin J Integr Med, 19*(8), 573-581. doi:10.1007/s11655-012-1101-3

Zhang, M., Zhang, F., Sun, J., Sun, Y., Xu, L., Zhang, D., Wang, Z., & He, W. (2017). The condition medium of mesenchymal stem cells promotes proliferation, adhesion and neuronal differentiation of retinal progenitor cells. *Neurosci Lett, 657*, 62-68. doi:10.1016/j.neulet.2017.07.053

Zhang, Q., Shi, S., Liu, Y., Uyanne, J., Shi, Y., Shi, S., & Le, A. D. (2009). Mesenchymal Stem Cells Derived from Human Gingiva Are Capable of Immunomodulatory Functions and Ameliorate Inflammation-Related Tissue Destruction in Experimental Colitis. *Journal of immunology (Baltimore, Md. : 1950), 183*(12), 7787-7798. doi:10.4049/jimmunol.0902318

Zhang, R., Liu, Y., Yan, K., Chen, L., Chen, X.-R., Li, P., Chen, F.-F., & Jiang, X.-D. (2013). Anti-inflammatory and immunomodulatory mechanisms of mesenchymal stem cell transplantation in experimental traumatic brain injury. *J Neuroinflammation, 10*(1), 871. doi:10.1186/1742-2094-10-106

Zhang, W., Feng, Y. L., Pang, C. Y., Lu, F. A., & Wang, Y. F. (2018). Transplantation of adipose tissue-derived stem cells ameliorates autoimmune pathogenesis in MRL/lpr mice : Modulation of the balance between Th17 and Treg. *Z Rheumatol*. doi:10.1007/s00393-018-0450-5

Zhang, X., Hirai, M., Cantero, S., Ciubotariu, R., Dobrila, L., Hirsh, A., Igura, K., Satoh, H., Yokomi, I., Nishimura, T., Yamaguchi, S., Yoshimura, K., Rubinstein, P., & Takahashi, T. A. (2011). Isolation and characterization of mesenchymal stem cells from human umbilical cord blood: reevaluation of critical factors for successful isolation and high ability to proliferate and differentiate to chondrocytes as compared to mesenchymal stem cells from bone marrow and adipose tissue. *J Cell Biochem, 112*(4), 1206-1218. doi:10.1002/jcb.23042

Zhang, Y., Harrison, J. M., Nateras, O. S., Chalfin, S., & Duong, T. Q. (2013). Decreased retinal-choroidal blood flow in retinitis pigmentosa as measured by MRI. *Doc Ophthalmol, 126*(3), 187-197. doi:10.1007/s10633-013-9374-1

Zhao, K., Lou, R., Huang, F., Peng, Y., Jiang, Z., Huang, K., Wu, X., Zhang, Y., Fan, Z., Zhou, H., Liu, C., Xiao, Y., Sun, J., Li, Y., Xiang, P., & Liu, Q. (2015). Immunomodulation effects of mesenchymal stromal cells on acute graft-versus-host disease after hematopoietic stem cell transplantation. *Biol Blood Marrow Transplant, 21*(1), 97-104. doi:10.1016/j.bbmt.2014.09.030

Zhao, T., Liang, Q., Meng, X., Duan, P., Wang, F., Li, S., Liu, Y., & Yin, Z. Q. (2020). Intravenous Infusion of Umbilical Cord Mesenchymal Stem Cells Maintains and Partially Improves Visual Function in Patients with Advanced Retinitis Pigmentosa. *Stem Cells Dev, 29*(16), 1029-1037. doi:10.1089/scd.2020.0037

Zheng, Q., Yang, T., Fang, L., Liu, L., Liu, H., Zhao, H., Zhao, Y., Guo, H., Fan, Y., & Wang, L. (2015). Effects of Bu Shen Yi Sui Capsule on Th17/Treg cytokines in C57BL/6 mice with experimental autoimmune encephalomyelitis. *BMC Complement Altern Med, 15*, 60. doi:10.1186/s12906-015-0572-0

Zhu, H., Xiong, Y., Xia, Y., Zhang, R., Tian, D., Wang, T., Dai, J., Wang, L., Yao, H., Jiang, H., Yang, K., Liu, E., Shi, Y., Fu, Z., Gao, L., & Zou, L. (2017). Therapeutic Effects of Human Umbilical Cord-Derived Mesenchymal Stem Cells in Acute Lung Injury Mice. *Scientific Reports, 7*, 39889. doi:10.1038/srep39889

Zhu, S.-Z., Szeto, V., Bao, M.-H., Sun, H.-S., & Feng, Z.-P. (2018). Pharmacological approaches promoting stem cell-based therapy following ischemic stroke insults. *Acta pharmacologica Sinica, 39*(5), 695-712. doi:10.1038/aps.2018.23

Zou, T., Gao, L., Zeng, Y., Li, Q., Li, Y., Chen, S., Hu, X., Chen, X., Fu, C., Xu, H., & Yin, Z. Q. (2019). Organoid-derived C-Kit(+)/SSEA4(-) human retinal progenitor cells promote a protective retinal microenvironment during transplantation in rodents. *Nat Commun, 10*(1), 1205. doi:10.1038/s41467-019-08961-0

Zwart, I., Hill, A. J., Al-Allaf, F., Shah, M., Girdlestone, J., Sanusi, A. B., Mehmet, H., Navarrete, R., Navarrete, C., & Jen, L. S. (2009). Umbilical cord blood mesenchymal stromal cells are neuroprotective and promote regeneration in a rat optic tract model. *Experimental neurology, 216*(2), 439-448. doi:10.1016/j.expneurol.2008.12.028